Investigation of glycine transporter GLYT1 in tumour cell proliferation

Christine Garcia Bierhals

Thesis submitted for the degree of Doctor of Philosophy

Epithelial Research Group

Institute for Cell and Molecular Biosciences

Newcastle University, UK

January 2018

Abstract

Rapidly proliferating cancer cells consume significantly more glycine than slow growing cancer cells and rapidly proliferative normal cells. Extracellular glycine supports high growth rates of tumour cells, being utilised in purine and glutathione synthesis. Glutathione, the major cellular antioxidant, is involved in chemotherapy resistance and cancer progression. It was observed that glycine transport via a specific glycine transporter GLYT1 is utilised to maintain adequate glutathione levels under cellular stress. Additionally, GLYT1 is regulated by the transcription factor ATF4, itself upregulated under cellular stress and also linked to cancer progression. Thus, extracellular glycine may play an essential role in tumour cell survival and proliferation and inhibiting its uptake could be a possible target in association with current cancer treatments. To address this hypothesis the work described in this thesis evaluated the role of a specific glycine transporter, GLYT1, in supporting tumour cell proliferation utilising molecular and pharmacological approaches.

A549, a non-small cell lung cancer (NSCLC) cell line, and HT29, a colorectal cancer cell line, were utilised as models of rapidly proliferating tumour cells. A498, a renal cancer cell line, and HUVEC, a human umbilical vein endothelial cell, were utilised as models of slow growing tumour cell and non-transformed fast growing cell line, respectively. Following GLYT1 knockdown (kd), tumour cells presented a significant reduction in glycine uptake and cell proliferation. When compared to control cells, rapidly proliferating GLYT1kd tumour cells showed a reduction of ~30% in cell number over time and a decrease of ~50% in DNA replication rate, whereas it had only a minor or no effect on the other cell lines. GLYT1kd downregulated expression of mRNA of other amino acid transporters able to transport glycine, PAT1 and SNAT2. GLYT1kd also reduced glutathione levels of all tumour cells. A reduction in mRNA levels of cystine transporter subunit, xCT, essential to maintain intracellular levels of cysteine, another component of glutathione, was also observed following GLYT1 downregulation. When cells were treated with a specific GLYT1 inhibitor, ALX-5407, in a pharmacological approach, a reduction in cell proliferation was observed after 96h treatment with a prolonged doubling time for the fast growing tumour cells, while A498 and HUVEC cells proliferation were not affected by the inhibitor, when compared to untreated cells. ATF4 effect on cell proliferation and glycine uptake was also evaluated. ATF4kd decreased significantly GLYT1 mRNA levels, but had only a mild influence on glycine uptake of all cell types analysed. There was a significant reduction in proliferation of ATF4kd tumour cells, ~40% for A549 and HT29 cells and 26% for A498 cell; ATF4kd in HUVEC cells increased cell proliferation by ~11%, when compared to control cells. ATF4 was also important to maintain intracellular levels of glutathione. ATF4kd dowregulated the transcription factors involved in stress response (ATF3, ATF5 and ATF6) suggesting a connection between them.

Data from this work show that glycine uptake by GLYT1 is required to maintain proliferation rates of highly proliferative cancer cells, but not slowly proliferating and non-tumour cells. This suggests that targeting GLYT1 may be a possible new approach to cancer treatment.

For my parents, Bel and Renato, and for Gus.

Acknowledgments

I would like to thank my supervisors Prof. Barry Hirst and Dr. Alison Howard for the opportunity to perform this work and for all the support, patience and teaching throughout these four years. I am grateful to Mrs. Maxine Giggie for all the help with tissue culture and in the lab, and for all her support and kindness. To Dr. Git Chung for his help with glycine uptake and western blotting experiments and for all the support and friendship. I would also like to thank my colleagues of the lab M2.019a Dr. Catherine Mowbray, Andrejus Suchenko and Ahmed Obaid for their help in the lab and friendship. I am also grateful to former colleagues from our group Dr. Livingstone Fultang, Rebecca Hall and Laura Duffield, who had previously improved some techniques utilised in this work. My many thanks to Dr. Andreas Werner and Dr. Ruth Valentine for the advice as my progression panel. To the Epithelial Reasearch group Prof. David Thwaites, Dr. Noel Edwards, Prof. Jeff Pearson, Prof. Diane Ford and Dr. Mike Gray and also to Dr. Judith Hall and Dr. Luisa Wakeling, I am grateful for all the advice, supplied materials and equipment.

My special thanks to my parents, Bel and Renato, for all encouragement and unconditional love, and to Gustavo, who is always there for me, for the emotional support and love. Finally, I would like to thank the programme Ciencias sem Fronteiras from CAPES Foundation, Ministry of Education of Brazil, for the financial support to perform this work.

Table of Contents

Chapter 6: ATF4 knockdown

List of Figure

Chapter 1

Chapter 2

Chapter 3

Chapter 4

Chapter 5

Chapter 6

Chapter 7

List of Tables

List of Abbreviations

$ATB^{0,+}$	Amino Acid Transporter $B^{0,+}$
ATCC	American Tissue Culture Collection
ATF4	Activating Transcription Factor 4
AKT	Protein Kinase B
Cdk	Cyclin-dependent kinases
CREB	Response Element-Binding Protein
cMYC	Cellular Homologue to the Viral Oncogene of the Avian Myelocytomatosis Retrovirus
DMEM	Dulbecco's Modified Eagles Medium
dNTPs	Deoxynucleotide Triphosphates
eIFα	Eukaryotic Initiation Factor 2-alpha
ER	Endoplasmic Reticulum
ERK	Extracellular Signal-Regulated Kinase
FCS	Foetal Calf Serum
GAR	Glycinamide Ribonucleotide
GCN2	General Control Non-depressible 2 (GCN2) Kinase
GCL	Glutamate Cysteine Ligase
GCLC	GCL catalytic subunit
GCLM	GCL modulator subunit
GCS	Glycine Cleavage System
GLDC	Glycine Decarboxylase
GSH	Glutathione
GSS	Glutathione Sinthetase
IARC	International Agency for Research on Cancer
FOS	FBJ Murine Osteosarcoma Viral Oncogene Homolog
LAT1	L-type Amino-acid Transporter
Formyl-THF	5,10-formyl tetrahydrofolate
meTHF	5,10-methylene tetrahydrofolate
MTHFD	Methylenetetrahydrofolate Dehydrogenase
mTOR	Mammalian Target of Rapamycin
NADPH	Nicotinamide Adenine Dinucleotide Phosphate
NSCLC	Non-Small Cell Lung Cancer
NEAA	Non-essential Amino Acid
PAT 1/2	Proton-assisted Amino Acid Transporter 1/2

PCR	Polymerase Chain Reaction
PERK	Protein Kinase-like Endoplasmic Reticulum Kinase
PHGDH	Phosphoglycerate Dehydrogenase
PI3K	Phosphatidylinositol-3-kinases
PSAT	Phosphohydroxythreonine Aminotransferase
PSPH	Phosphoserine Phosphatase
pRb	Retinoblastoma Protein
RAS	Rat Sarcoma Viral Oncogene Homologue
ROS	Reactive Oxygen Species
RTK	Receptor Tyrosine Kinases
SHMT	Serine Hydroxymethyltransferase
SNAT 1/2	System A Neutral Amino Acid Transporter 1/2
SNP	Single Nucleotide Polymorphism
TDH	Threonine Dehydrogenase
THF	Tetrahydrofolate
UPR	Unfolded Protein Response
WHO	World Health Organization

Chapter 1. Introduction

Recently it was observed that the requirement for glycine is significantly greater in rapidly proliferating cancer cells than in either slow growing cancer cells or rapidly-proliferating non-cancerous cells, suggesting that manipulation of glycine availability may allow a novel therapeutic approach to treatment of highly progressive cancers (Jain et al., 2012). Although part of the increased demand for glycine in rapidly proliferating tumour cells was met by up-regulation of mitochondrial glycine synthesis, it was demonstrated there was a requirement for extracellular glycine in maintenance of cell proliferation (Jain et al., 2012). Glycine transported into cells by the specific glycine transporter GLYT1 is used in maintaining glutathione levels during stress and the transporter is regulated by the transcription factor, activating transcription factor 4 (ATF4), which has been linked to cancer progression (Howard et al., 2010, Harding et al., 2003). Thus, it was hypothesised that glycine transport and GLYT1 are up-regulated in rapidly proliferating cancer cells by the action of ATF4, and it is the primary aim of the work described here to investigate that hypothesis.

1.1 Cell Proliferation

Some adult cells are able to proliferate when stimulated, as by injury, for example (Franks and Knowles, 2005). Somatic cells, during the cell cycle, increase their components and duplicate their genetic material throughout the synthesis phase, also known as S phase, and then the nuclear and cytosolic division (mitosis and cytokinesis) in two daughter cells occur in the mitosis phase, or M phase, resulting in cell replication (Morgan, 2007b, Franks and Knowles, 2005). Additionally, there are two gap phases, one before S phase, G1, and other before M phase, G2, where cells grow and are subject to complex regulations that allow or inhibit the transition to the next phase of the cell cycle (Morgan, 2007b, Alberts et al., 2002). The main components of cell cycle control system are cyclin-dependent kinases, or Cdks, activated by cyclins (Morgan, 2007b). Specific types of cyclins regulate different cell cycle phases and cyclin levels regulate the activity of Cdks (Morgan, 2007b). This way, Cdk-cyclin is responsible for the progression of the cell cycle at regulatory checkpoints present in G1 and G2 phases when conditions are ideal, phosphorylating proteins that are necessary to initiate S and M phases, as these proteins are related to DNA replication, mitogenic and cytokinesis

processes (Morgan, 2007b). Cell growth is then often coordinated with cell division (Morgan, 2007b). Cell type specific genetic characteristics, growth factors and mitogens are involved in growth and division regulation (Morgan, 2007b). Mitogens activate the GTPase Ras, transcription factor Myc and the Akt kinase which in turn induce cell division and, in some cells, growth (Morgan, 2007b).

Late G1 phase gene expression is controlled by E2F family members, E2F1-5, which induce expression of cyclins, that in turn activate specific Cdks responsible for the entry in S phase (Morgan, 2007b). E2F activity is inhibited by pRB interaction in non-proliferating cells (Morgan, 2007b). Mitogens activate cyclin-Cdk that phosphorylate pRB followed by dissociation from E2F proteins (Morgan, 2007b). The best-known mitogens are the platelet-derived growth factor, PDGF, and the epidermal growth factor, EGF (Morgan, 2007b). Mitogens activate mitogenic signalling pathways, involving activation of GTPase Ras that stimulates the Raf-MEK-MAP kinase cascade (Morgan, 2007b). MAP kinase delivers the mitogenic signal into the nucleus by triggering the expression of genes to mitogen stimulation (Morgan, 2007b). Induction of Fos, for example, increases the expression of AP-1, which in turn induces expression of another set of genes that codes for cyclins activating Cdks and start cell-cycle progression (Morgan, 2007b). MAP kinase also triggers the expression of Myc that interact with other proteins to form a gene regulatory complex that induces expression of cyclins, Cdk, and regulators of cell growth and metabolism (Morgan, 2007b). Ras-MAP kinase pathway also induces the formation of PIP3 that binds to Akt protein and stimulates its activity helping to stimulate cell growth and survival (Morgan, 2007b).

During normal conditions survival factors activate signalling pathways that suppress apoptosis (Alberts et al., 2002). Other signals induce cell death when required, as seen for cells with severe DNA damage or excessive levels of mitogenic signals (Alberts et al., 2002). During this process proteases and nucleases are irreversibly activated resulting in cell death (Alberts et al., 2002). For example, when cytochrome c is released from the mitochondria to the cytoplasm, this activates the protease caspase family members and Bcl-2 (Alberts et al., 2002). The release of cytochrome c is controlled by survival factors (Lain and Lane, 2005). DNA damage for example, activates p53 that also activates apoptosis (Lain and Lane, 2005). p53 is

involved in a large number of gene expression that promote cell cycle arrest, and is regulated by MDM2 that induces its degradation (Lain and Lane, 2005).

1.2 Cancer Overview

Cancer comprises a group of over 100 diseases that affect millions of people and is one of the main causes of death around the world (Stratton et al., 2009, WHO). According to the International Agency for Research on Cancer (IARC) 2012 cancer surveillance, the number of deaths attributed to cancer was 8.2 million in that year (IARC). Lung, liver, stomach, colorectal and breast cancers were the major causes of mortality (IARC). The World Health Organisation (WHO) estimates 75 million people will be diagnosed with cancer worldwide, with 21 million new cases and 13 million deaths by the year 2030 (WHO). Many tumour types have poor prognosis and the treatments available, radiotherapy, chemotherapy and surgery, are insufficient. A better understanding of the disease that leads to more effective therapies is thus needed.

Oncogenesis is caused by a combination of an individual's intrinsic genetic characteristics (e.g. efficiency of DNA repair) and environmental factors such as chemical (e.g. tobacco smoke), physical (e.g. ultraviolet radiation) and biological (e.g. viruses) carcinogens (King and Robins, 2006a, WHO). A series of somatic mutations are required for some cancer types (minimum of six to ten); others, such as prostate cancer, may require about 30 mutations, which provide growth advantages, in order for a normal cell to become a cancer cell (Hahn and Weinberg, 2002, Stratton et al., 2009, Morgan, 2007a). Epigenetic changes also contribute to cancer development, as methylation and demethylation of promoter regions repress and de-repress relevant genes (King and Robins, 2006b, King and Robins, 2006c). Similarly, hypomethylation increases chromosomal instability which can promote aberrant cell proliferation (King and Robins, 2006b, King and Robins, 2006c). Indeed, cancer cells present transcriptional profile alterations of thousands of genes which are physiologically different from normal cells (Hahn and Weinberg, 2002).

Proto-oncogene and tumour suppressor gene mutations, with gain and loss of function respectively, exert a key role in cancer induction (Pelengaris and Kan, 2006c). Oncogenes are the active forms of proto-oncogenes responsible for regulation of cell replication, growth, survival, differentiation, and mortality (Pelengaris and Kan, 2006b).

They are classified into four functional classes: transcription factors (e.g. Myc), growth factors (e.g. Sis), receptors (e.g. Rtk) and signal transducers (e.g. Ras family) (Pelengaris and Kan, 2006b). Tumour suppressor genes control and help to repair DNA damage, and are able to induce growth arrest during the two gap phases (G1 and G2) of the cell cycle (Pelengaris and Kan, 2006c, Roussel, 2006). The most studied tumour suppressors are retinoblastoma protein (pRb) and transcription factor p53 (Roussel, 2006).

Sustained chronic proliferative signalling - through somatic mutations, changes in gene expression and/or altered production of growth factors and their receptor proteins - is an important hallmark of cancer (Hanahan and Weinberg, 2011). The Ras/Raf/MEK/ERK and Ras/PI3K/PTEN/Akt/mTOR pathways (Figure 1.1), for example, control cell growth and survival (Steelman et al., 2011). Mutations that support constitutive activation of these pathways are frequently observed in many cancer types as they produce abnormal proliferative and survival signals (Steelman et al., 2011, Aksamitiene et al., 2012, De Luca et al., 2012). Active ERK can phosphorylate additional transcription factors in the nucleus, such as FOS, JUN, Elk-1 and CREB among others, that bind in the promoter regions of growth factor and cytokine genes, for example, thus promoting growth and preventing apoptosis of cells (Steelman et al., 2011). In the same way, AKT activation affects the activity of transcription factors such as murine double minute 2 (MDM2), which regulates p53 activity, and nuclear factor kappa from B cells (NF-κB) (Steelman et al., 2011). mTOR ensures that cell duplication only happens at adequate nutrient and energy levels and is responsible for the regulation of protein synthesis through phosphorylation of 4E-BP, which enables the eukaryotic initiation factor 4E (eIF4E) for translational initiation (Mendoza et al., 2011). Together, these pathways are extremely important in cell survival, proliferation, differentiation and metabolism (De Luca et al., 2012).

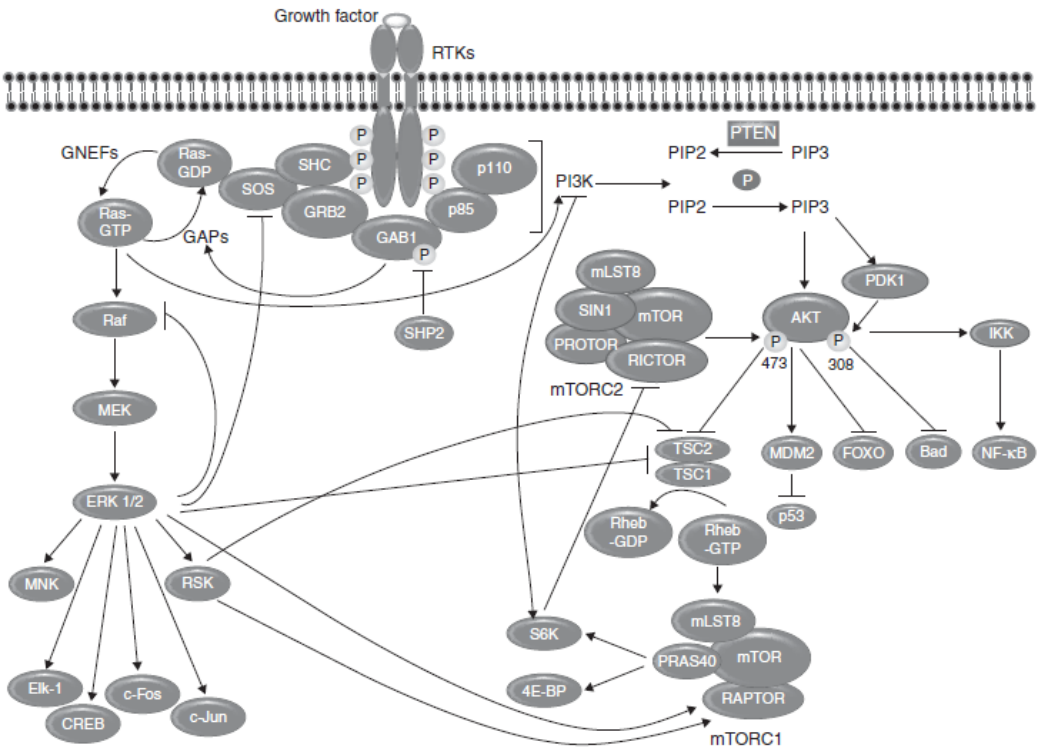

Figure 1.1: Interaction of the Ras/Raf/MEK/ERK and Ras/PI3K/PTEN/Akt/mTOR pathways. These kinase cascade signalling pathways are important to regulate and transduce proliferative signals through phosphorylation and dephosphorylation of proteins. They are able to interact with each other through positive and negative feedback. Many proteins altered in various cancer types are involved in these pathways, e.g. RAS, AKT, p53 and mTOR. (De Luca A. *et al.*, 2012)

Nutrient levels influence anabolic processes via the amino acid sensing system that regulates mTORC1 activity (Figure 1.2) (González and Hall, 2017). During amino acid availability the GTPase proteins RAGs, present in the lysosome, through interaction with the complex Ragulator, are activated and bind to Raptor protein, which in turn recruits mTORC1 to the lysosome, where Rheb activates it (González and Hall, 2017, Abrahamsen and Stenmark, 2011). Rheb is inactivated by the interaction with TSC complex, which is composed of TSC2 in association with TSC1 and TBC1D7(González and Hall, 2017). Growth factors activate Rheb via PI3K-AKT pathway; AKT phosphorylates TSC2, which is then released from the lysosome (Zoncu et al., 2011b). How amino acids influence this signalling pathway and activate mTORC1 is still being elucidated.

Amino acids in the lysosome lumen interact with the lysosomal v-ATPase, which is associated with Ragulator during amino acid starvation, and may alter its structure

leading to its dissociation from Ragulator and Rag activation (Abrahamsen and Stenmark, 2011, Zoncu et al., 2011a). It is known that arginine, glutamine and leucine play an important role in mTORC1 activity (González and Hall, 2017). Leucine binds to Sestrin2, a possible leucine sensor, in the cytoplasm resulting in its dissociation from Gator2, which inactivates Gator1, a negative regulator of Rags (González and Hall, 2017). This way leucine triggers Rag heterodimers activation, being important to mTORC1 lysosome localisation (González and Hall, 2017). Another study also showed that leucyl tRNA-synthetase act as leucine sensors and regulate mTORC1 (González and Hall, 2017). Additionally, the leucine and glutamine transporters, heterodimer SLC7A5-SLC3A2 antiporter and SLC1A5, respectively, affect mTORC1 signalling (González and Hall, 2017). SLC7A5-SLC3A2 import leucine in exchange for glutamine export; thus, the relevance of glutamine transporter SLC1A5 is to support glutamine and thus leucine uptake that activate mTORC1 (González and Hall, 2017). A study observed that SLC7A5-SLC3A2 is recruited to the lysosome where possibly leucine availability influences mTORC1 activity (Milkereit et al., 2015, González and Hall, 2017). It was also observed that Castor dimers act as an arginine sensor, and when arginine is present Castor association with Gator2 is disrupted, culminating in mTORC1 activation (González and Hall, 2017). Some glioblastoma and ovarian cancers present mutations on Gator2 and possibly some tumour may overexpress Gator1 leading to a hyperactive mTORC1 signalling (Bar-Peled and Sabatini, 2014).

Other amino acid transporters act as amino acid sensors that influence the mTORC1-signalling pathway. The lysosomal amino acid transporter SLC38A9 senses arginine levels and binds to Rag proteins (Figure 1.2) (González and Hall, 2017). Additionally, SLC36A1 (PAT1) present in the lysosome has been shown to be essential for amino acid activation of mTORC1, possibly interacting with Rag/Ragultor/vATPase when sensing intraluminal amino acid availability (Zheng et al., 2016). There is evidence that fast growing cells present an accumulation of PAT transporter in the lysosome suggesting its relevance for these cell growths (Goberdhan, 2010). Under nutrient starvation in normal cells, mTORC1 activation is downregulated and autophagy is induced in an attempt to provide cells with nutrients, that accumulate in autolysosomes (Goberdhan, 2010). In tumour cells, when autophagy is triggered, the resulting autolysosome probably express increased levels of PAT as these cells demonstrate high levels of cell proliferation (Goberdhan, 2010). Another amino acid transporter observed to act as a possible “transceptor” is SLC38A2 (SNAT2), that possibly activates signalling molecules when there is a conformational change during

amino acid transport (Zheng et al., 2016). Some studies suggest that this transporter senses extracellular amino acid levels and regulate mTORC1, but the precise mechanism remains to be elucidated (Zheng et al., 2016). Under amino acid depletion SNAT2 is upregulated and also insulin, a growth factor, induces an increase in its expression at the cell membrane (Zheng et al., 2016).

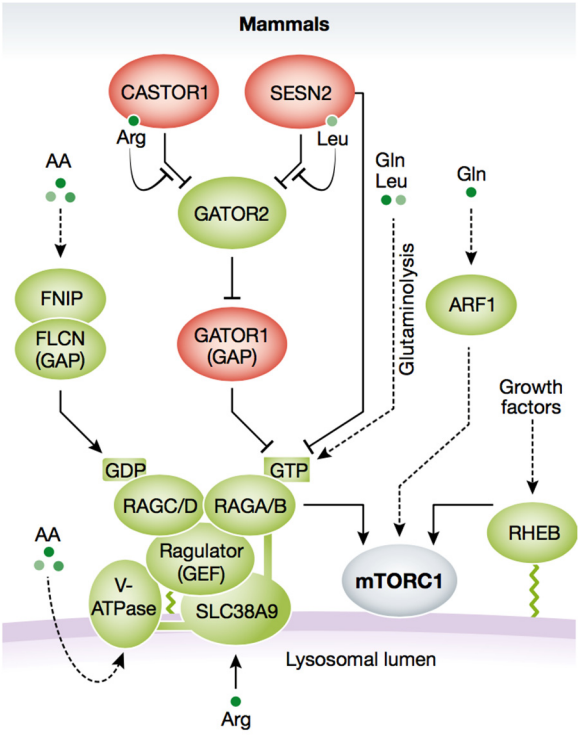

Figure 1.2: Amino acid signalling pathway. Activation of mTORC1 by arginine, leucine, glutamine and growth factors. During nutrient availability Rag proteins are activated and bind to Raptor that translocate mTORC1 to the lysosome where Rheb activates it. Rag inhibition by Castor, Sesn2 and Gator1 is present in red. Leucine and arginine activate Gator2 that inhibit Gator allowing activation of Rag. Other amino acids regulate vATPase association with Rag. SLC38A9 transporter binds to Rag in presence of arginine in the lysosomal lumen. (From González and Hall 2017)

Cancer cells also need to evade growth suppressors that inhibit cell proliferation (Hanahan and Weinberg, 2011). One mechanism that enables this capability is mutation resulting in loss of function of tumour suppressor genes such as pRb and p53 (Hanahan and Weinberg, 2011). These genes control growth arrest, apoptosis and senescence, transduce growth-inhibitory signals and receive signals of intracellular stresses (e.g. low glucose concentrations and oxygen levels) as well as genomic abnormalities (Hanahan and Weinberg, 2011). Moreover, cancer cells evade apoptosis by increasing expression of anti-apoptotic regulators such as Bcl-2, and regulating

autophagy induced by nutrient deficiency (Hanahan and Weinberg, 2011). Interestingly both mechanisms seem to be affected by the Ras/PI3K/PTEN/Akt/mTOR and Ras/Raf/MEK/ERK pathways (Hanahan and Weinberg, 2011, Steelman et al., 2011, McCubrey et al., 2011). AKT and ERK phosphorylation of transcription factors, for example, influences genes that regulate apoptosis such as those of the Bcl-2 family, and mTOR activates c-Myc (Steelman et al., 2011, McCubrey et al., 2011).

Many cancer types also depend on mutations that culminate in overproduction of mitogens and/or its receptors (Morgan, 2007a). This way, tumours are not dependent on extracellular mitogens, growth factors or survival factors to induce cell growth and proliferation (Morgan, 2007a). Additionally, upregulation of telomerase activity, related to senescence and crisis/apoptosis resistance, leads to an immortalised cell capable of replicating indefinitely and thus generating a cell mass (tumour) by cloning of its progenitor cell (Hanahan and Weinberg, 2000, Pelengaris and Kan, 2006a, B. and M.W., 2006a, Hlatky and Hahnfeldt, 2014). Consequently, the induction of angiogenesis is needed to provide oxygen and nutrients as well as to discard metabolic waste and carbon dioxide in sustaining the growth of the tumour (Hanahan and Weinberg, 2011, B. and M.W., 2006b). Eventually, a malignant tumour is able to migrate to other sites of the body, passing tissue barriers and metastasising to distant organs (Stratton et al., 2009).

Apart from the deregulation of cell proliferation controls, another emerging hallmark highlighted in recent years is the alteration of energy metabolism (Hanahan and Weinberg, 2011). Rapid proliferation and cellular growth require metabolic adaptation to sustain new physiological demands (Hanahan and Weinberg, 2011). Reprogramming energy metabolism facilitates cancer cell development and progression (Hanahan and Weinberg, 2011).

1.3 Cancer Metabolism and Glycine

In 1924, Warburg observed an abnormal metabolic behaviour of cancer cells; even with adequate oxygen supply, these cells utilised anaerobic glycolysis to produce energy, a condition known as aerobic glycolysis or the Warburg effect (Warburg, 1956, Vander Heiden et al., 2009, Vermeersch and Styczynski, 2013). Normal cells convert glucose to pyruvate through glycolysis in the cytosol, and then to carbon dioxide via oxidative phosphorylation in the mitochondria in the presence of oxygen (Figure 1.3). In anaerobic conditions, glycolysis continues in the cytosol and only a small amount of

pyruvate is sent to the mitochondria (Hanahan and Weinberg, 2011). However, in cancer cells, glucose is converted to lactate in the main pathway responsible for their energetic metabolism (Vander Heiden et al., 2009, Hanahan and Weinberg, 2011).

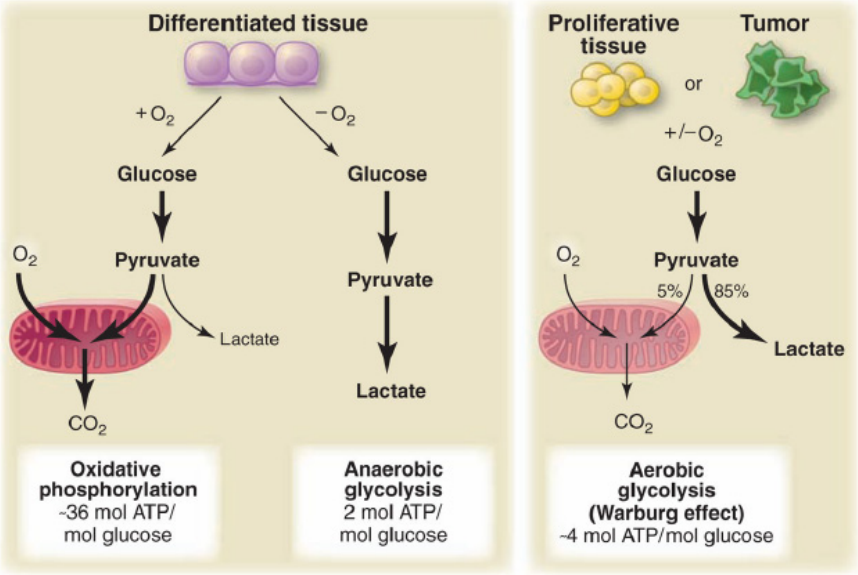

Figure 1.3: Differences between oxidative phosphorylation, anaerobic glycolysis and the Warburg effect. In the presence of oxygen normal cells direct pyruvate into the mitochondria where it is aerobically oxidised to produce energy; in the absence of oxygen and in tumour cells, pyruvate is retained in the cytoplasm, where glycolysis continues and results in lactate production. This latter process, anaerobic glycolysis, is the main source of energy for tumour cells (From Vander Heiden *et al*., 2009).

As glycolysis provides 18-fold less ATP than mitochondrial oxidative phosphorylation, cancer cells need to compensate for this energy imbalance (Hanahan and Weinberg, 2011). In order to increase ATP production, cancer cells augment glucose uptake by increasing glucose transporter GLUT1 expression, a mechanism regulated by hypoxia-inducible transcription factor-1α (HIF1α) (Hanahan and Weinberg, 2011, DeBerardinis et al., 2008, Steelman et al., 2011, Mobasheri et al., 2005). Incidentally, increased glucose intake, reduction of phosphorylative oxidation and increased lactate production are distinct characteristics of oncogene activation (Hsu and Sabatini, 2008). Recent studies demonstrated that even though glycolysis generates fewer ATPs per mole of glucose, it can provide more ATPs per mass of the related enzymes than oxidative phosphorylation, being an important mechanism in highly proliferative cells which have many metabolic pathways occurring in the cytosol (Tedeschi et al., 2013, Vazquez et al., 2010, Vazquez and Oltvai, 2011).

One of the main purposes of the Warburg effect is to provide precursors utilised in biosynthetic pathways of rapidly proliferating cells (Figure 1.4) (Hanahan and Weinberg, 2011). One example that corroborates this hypothesis is the isoform alteration of pyruvate kinase (PK), the enzyme responsible for converting phosphoenolpyruvate (PEP) to pyruvate. In cancer cells, PK isoenzyme 1 (PKM1) expression is decreased but PKM2, which usually has reduced activity, is upregulated (Eigenbrodt et al., 1992, Mazurek et al., 2005, Hsu and Sabatini, 2008, Vander Heiden et al., 2010). It was observed that c-Myc was able to regulate the nuclear RNA binding proteins that favour the production of PKM2 by alternative splicing (Ye et al., 2012),(David et al., 2010). A reduced PK activity results in accumulation of glycolytic intermediates (Mazurek et al., 2005, Hsu and Sabatini, 2008, Vander Heiden et al., 2010). Additionally, glucose transporters, hexokinase and phosphofructokinase activities are upregulated by PI3K/AKT, supporting formation of intermediates of glycolysis, which are then available to participate in anabolic pathways (Vander Heiden et al., 2009, DeBerardinis et al., 2008).

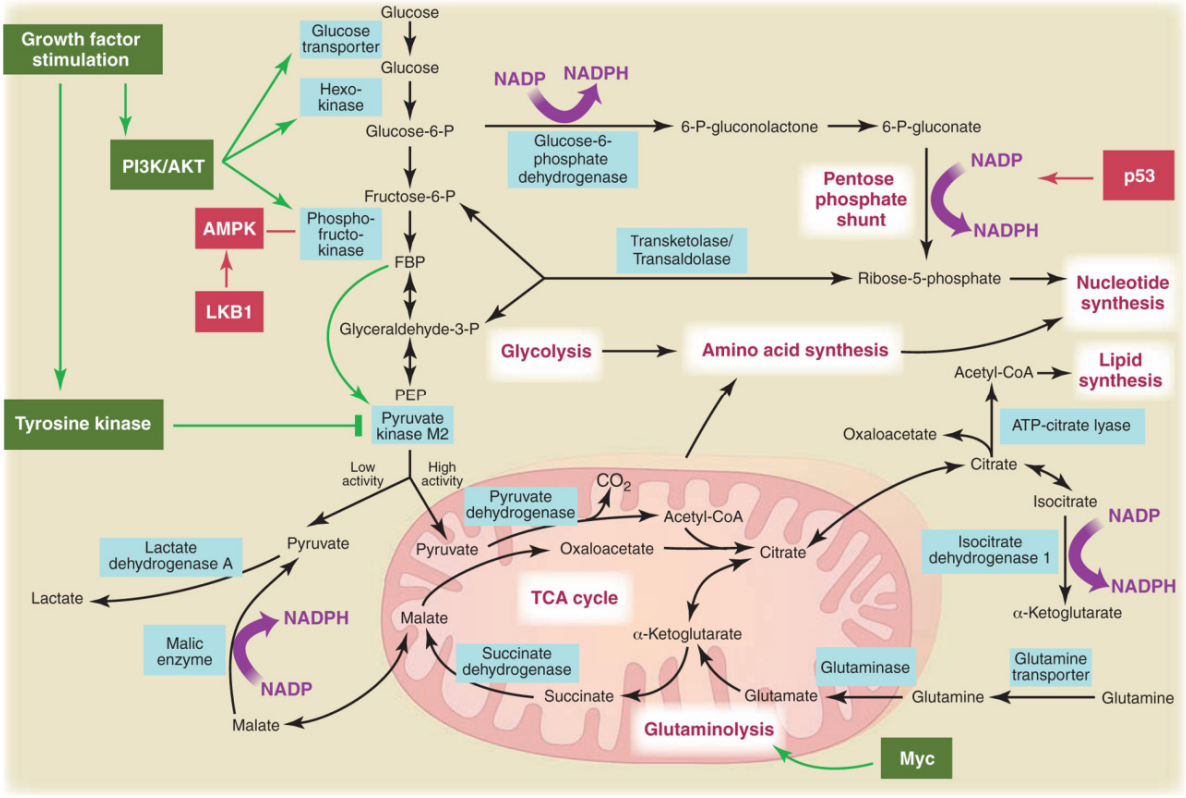

Figure 1.4: Interaction between different anabolic pathways, their connection with glycolysis intermediates and oncogene regulation. As demonstrated, glycolysis intermediates support lipid, amino acid and nucleotide synthesis (From Vander Heiden *et al*., 2009).

The glycolytic intermediates are diverted from glycolysis to other metabolic pathways. Thus, glucose-6-phosphate is utilised in the pentose phosphate pathway, which will provide ribose 5-phosphate for nucleotide synthesis and NADPH (Vander Heiden et al., 2009, Fan et al., 2014). Phosphoglycerate dehydrogenase (PHGDH), overexpressed in a large number of tumours, diverts 3-phosphoglycerate (3PG) to the *de novo* synthesis of L-serine and glycine (Figure 1.5) (Locasale et al., 2011). PSAT1, an enzyme of the serine biosynthesis pathway, is also involved in the conversion of glutamate to a-ketoglutarate (aKG), an intermediate of the tricarboxylic acid (TCA) cycle (Possemato et al., 2011). The TCA cycle provides intermediates for fatty acids synthesis (Possemato et al., 2011, DeBerardinis et al., 2007). Indeed, glutamine and glucose metabolism generate intermediates utilised in amino acid, protein, fatty acid and nucleotide biosynthetic pathways, consequently supporting high proliferative rates (Vander Heiden et al., 2009).

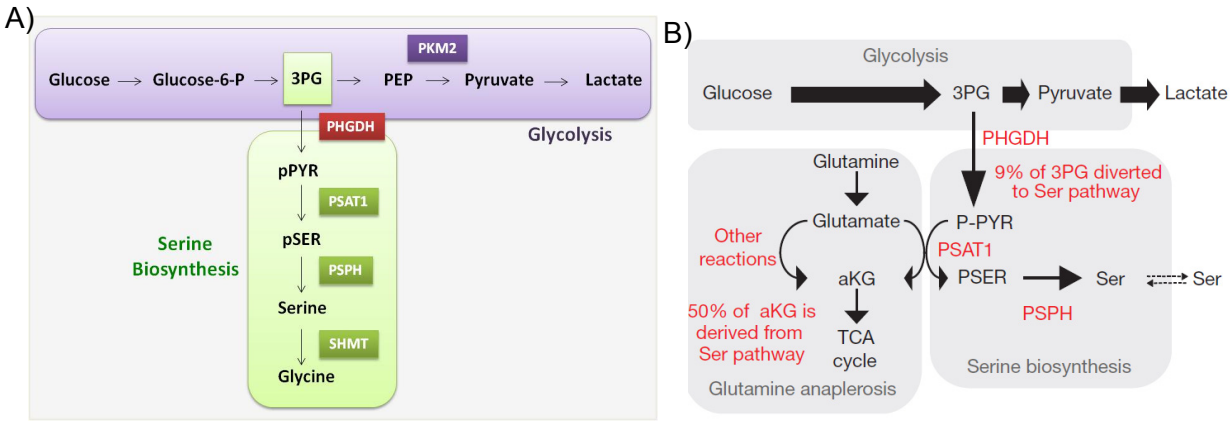

Figure 1.5: Participation of 3PG in the serine biosynthetic pathway. (A) Importance of PKM2 and PHGDH regulation to induce serine biosynthesis and (B) the influence of PSAT1 enzyme in serine and α-ketoglutarate synthesis (Figure B Adapted from Richard Possemato *et al.*, 2011).

It was observed that serine activates PKM2 (Maddocks et al., 2013, Mazurek, 2011, Eigenbrodt et al., 1983). When cells have a low concentration of serine, PKM2 activity is reduced which leads to accumulation of glycolytic intermediates, one of which is 3PG (Mazurek, 2011, Ye et al., 2012). 3PG can be used for serine biosynthesis and when serine levels are restored PKM2 activity is increased and the glycolytic flux recovered (Ye et al., 2012). Serine also regulates mTOR activity; when the intracellular concentration of serine increases, mTOR activity is enhanced, enabling cell proliferation (Ye et al., 2012). In addition, serine contributes to protein

and amino acid synthesis, as does glycine, and is a precursor for lipid, which facilitates the production of macromolecules and organelles (Nelson and Cox, 2005). Glycine participates in glutathione (GSH) and nucleotide formation (Nelson and Cox, 2005). Serine and glycine synthetic pathways are therefore extremely important in cellular proliferation (Ye et al., 2012, Mazurek, 2011, Hanahan and Weinberg, 2011).

The one-carbon units donated by glycine and/or serine, can participate in three biochemical pathways – the folate cycle, the methionine cycle and transsulphuration (Locasale, 2013). During *de novo* synthesis, serine can be converted to glycine by donating a one-carbon unit to tetrahydrofolate (THF) to form 5,10-methylene-THF (meTHF) in a reaction catalysed by two isoforms of the enzyme serine hydroxymethyl transferase 1 and 2 (SHMT1/2), which are present in cytosol and mitochondria, respectively (Figure 1.6 A) (Tibbetts and Appling, 2010). Thereafter, meTHF is reduced to 5-methyl-THF (mTHF) or converted to formyl-THF (F-THF) (Locasale, 2013). Demethylation of mTHF generates THF, completing the folate cycle and providing one carbon to generate methionine (MET) from homocysteine (hCYS), starting the methionine cycle (Locasale, 2013). Serine can also condense to hCYS initiating the transsulphuration pathway (Figure 5 B) (Locasale, 2013). Glycine cleavage by the oxidoreductase enzyme glycine decarboxylase (GLDC), known as glycine cleavage system (GCS), also produces carbon units for THF methylation, as well as NADH, CO_2 and NH_3 (Locasale, 2013, Zhang et al., 2012, Kume et al., 1991). In summary, transsulphuration is dependent on the methionine cycle that is interconnected with the folate cycle, which, in turn, depends on the one-carbon units provided by serine and glycine.

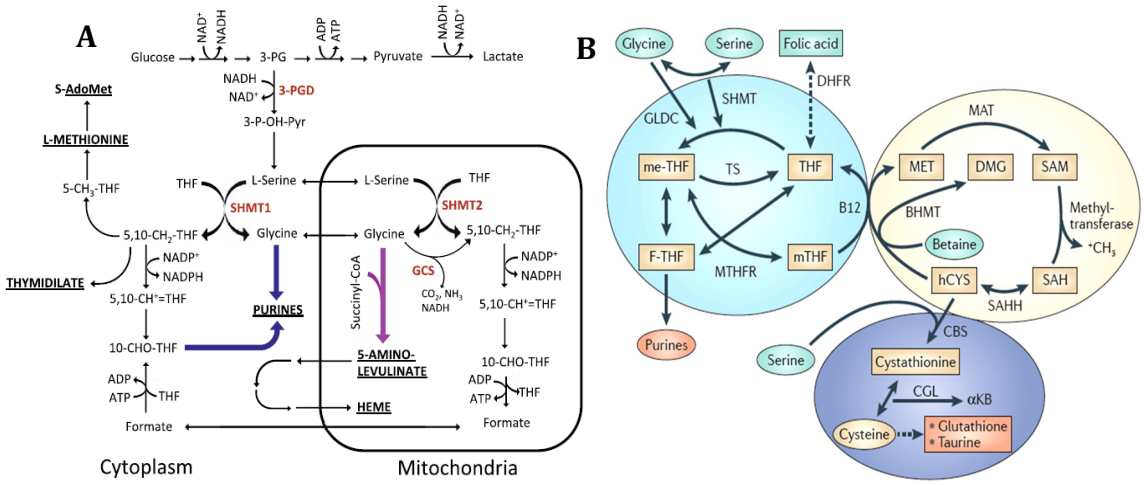

Figure 1.6: Compartmentalisation and interconnection of one-carbon metabolism. (A) Integration of cytoplasmic and mitochondrial one-carbon metabolism pathways. (B) Interconnection between the folate and methionine cycles and transsulfuration. One-carbon metabolism is involved in the synthesis of amino acids, purines and GSH (Figure A: from di Salvo *et al*., 2013; Figure B: from Locasale, 2013).

Serine and glycine metabolic pathways and one-carbon metabolism intermediates have been shown to be essential for survival of cancer cells (Kalhan and Hanson, 2012, Locasale, 2013). S-adenosylmethionine (SAM), an intermediate of the methionine cycle, donates a methyl group used in epigenetic regulation, contributing to methylation of histones, DNA and RNA (Locasale, 2013). F-THF provides formyl groups for purine formation and me-THF contributes to thymidylate synthesis; also enzymic reactions involving formation and oxidation of F-THF generate significant NADPH, thus contributing to REDOX defence and supporting biosynthesis (di Salvo et al., 2013, Di Pietro et al., 2002, Fan et al., 2014). Cysteine, a transsulphuration intermediate, can also be utilised in GSH - a tripeptide composed of cysteine, glycine and glutamate (Nelson and Cox, 2005, Locasale, 2013, Thelwall et al., 2012). Therefore, one-carbon metabolism functions as an integrator of nutritional status in cellular physiology and contributes to cellular anabolic pathways, as well as to post-translational and nucleotide pool regulation (Locasale, 2013).

Maddocks et al. (2013) observed that cancer cells lacking p53 showed reduced proliferation and viability in response to serine starvation than those harbouring p53 (Maddocks et al., 2013). They also noted that animals fed with a diet restricted in serine and glycine had reduced tumour volume, and that *in vitro* serine and glycine depletion showed a greater effect in reducing tumour growth in cells lacking p53 (Maddocks et

al., 2013). However, they did not observe a reduction in cell proliferation during glycine starvation (Maddocks et al., 2013). Moreover, during nutrient starvation, it was observed that initial depletion in GSH was less in cells harbouring p53 (Maddocks et al., 2013). Under this condition, it was suggested that cells tend to increase oxidative phosphorylation to produce energy, thus increasing O_2 consumption and consequently ROS formation (Maddocks et al., 2013, Chaneton et al., 2012). This way, p53-p21 induction of GSH synthesis observed during serine starvation is possibly an attempt to overcome the oxidative stress (Amelio et al., 2014, Maddocks et al., 2013). In a recent study it was observed that serine and glycine starvation increase survival in mice models of an intestinal cancer and lymphoma driven by APC and Myc activation, respectively, whereas the diet restriction had no effect on mice bearing pancreatic and intestinal cancer driven by Kras (Maddocks et al., 2017). Kras induced expression of serine synthesis pathway enzymes, which possibly maintained glycine and GSH levels even when serine levels were depleted (Maddocks et al., 2017). These results demonstrate the complex regulation of tumour suppressor genes and oncogenes on cellular metabolism.

Recent research highlights the relevance of glycine metabolism to cancer cell proliferation. Glycine is a versatile non-essential amino acid that can be obtained from serine, choline and threonine (Figure 1.7) (Wang et al., 2013a). The enzyme SHMT2 present in the mitochondria is mainly responsible for the conversion of serine into glycine and release of meTHF, an important reaction for tumour cells as described earlier (Wang et al., 2013a). Serine can be obtained from nutrition but also from glucose via the serine biosynthesis pathway as described before. Glycine is also the final product of threonine degradation by the enzyme threonine dehydrogenase, although this enzyme is responsible only for a small percentage (7-11%) of the threonine degradation in adult humans (Wang et al., 2013a). Additionally, choline oxidative degradation leads to glycine formation in the reaction step catalyzed by sarcosine oxidase (Wang et al., 2013a). However, since choline levels present in diet is very low, its relevance for glycine synthesis is minor (Wang et al., 2013a). In addition to its relevance for purine and GSH synthesis, glycine serves as a precursor to the phosphocreatine biosynthetic pathway, acts as an inhibitory neurotransmitter in the central nervous system and is able to condense with succinyl-CoA to form 5-aminolevulinate in mitochondria, a precursor of haem of the cytochromes (Nelson and Cox, 2005, di Salvo et al., 2013).

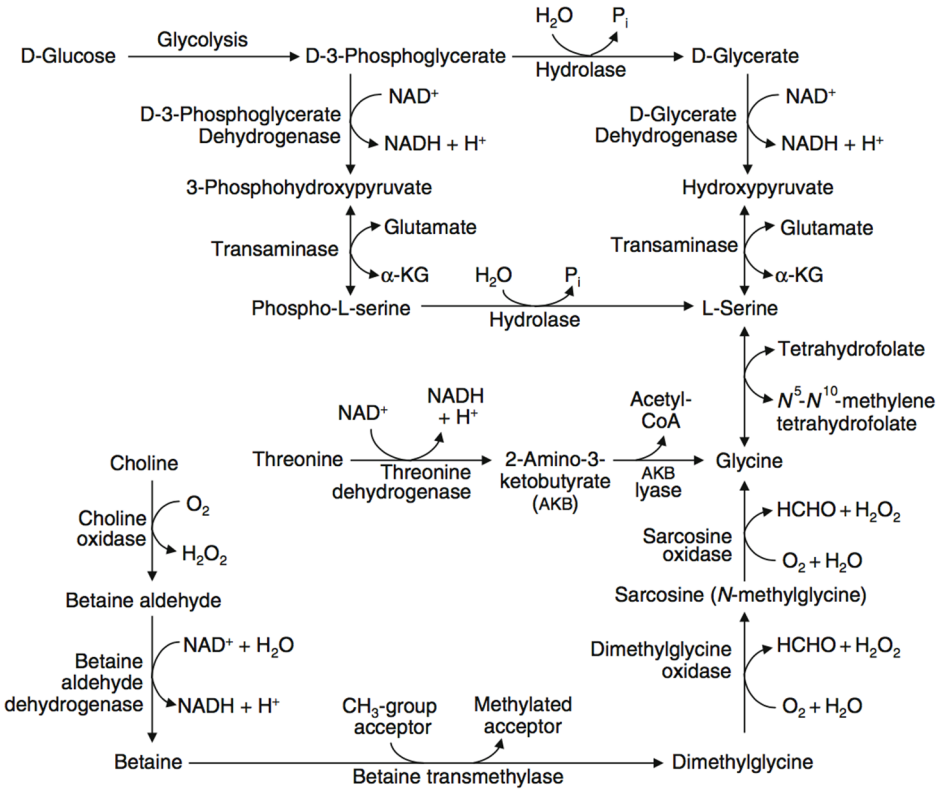

Figure 1.7: Glycine synthesis pathways. Characterisation of serine, threonine and choline metabolic pathways that generate glycine as product (From Wang et al., 2013).

The serine biosynthesis pathway enzymes are upregulated in many tumour types and confer advantages to cancer proliferation. There is a correlation of SHMT2 expression with higher mortality rates in breast cancer patients (Jain et al., 2012). Sitter et al. (2010) also observed that tissue from patients with poor prognosis presented a high concentration of glycine (Sitter et al., 2010). Other studies have associated overexpression of SHMT2 as well as other serine/glycine metabolic enzymes (such as PHGDH, PSPH, PSAT1) with breast cancer and other tumour types (Lee et al., 2014, Noh et al., 2014, Possemato et al., 2011, Pollari et al., 2011, Kim et al., 2014); and PSAT1, PSPH, and SHMT2 overexpression can also induce cell transformation (Zhang et al., 2012). Additionally, SHMT2 is overexpressed in hypoxic regions of glioma, conferring survival advantages possibly through a depletion of serine and SAICAR, an intermediate of *de novo* purine synthesis and substrate of an enzyme dependent on F-THF, both activators of PKM2 (Kim et al., 2015). This way, SHMT2 upregulation avoids using pyruvate to participate in the TCA cycle, therefore, reducing oxygen consumption by this metabolic route (Kim et al., 2015).

Glycine catabolism occurs via SHMT2 reversible reaction, but mainly via glycine cleavage system (GCS) in the mitochondria (Wang et al., 2013). GCS is a complex of

enzymes responsible for the oxidative degradation of glycine that works in three partial reactions (Figure 1.8) (Kikuchi et al., 2008, Razak et al., 2017). In the first reaction P-protein promotes glycine decarboxylation utilizing H-protein as co-substrate (Kikuchi et al., 2008). Glycine associated with H-protein is then degraded by T-protein in a reaction that requires THF as methylene acceptor yielding me-THF and ammonia (Kikuchi et al., 2008). Finally, in the last reaction L-protein catalyzes the reoxidation of the reduced lipoate associated with H-protein from previous reaction generating NADH (Kikuchi et al., 2008).

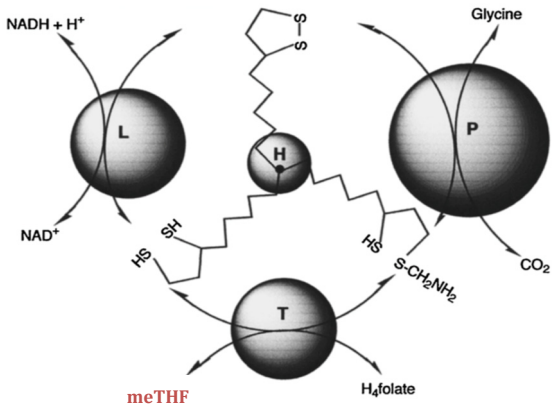

Figure 1.8 Glycine cleavage system. First, glycine is decarboxylated by P protein with H-protein as co-substrate and releasing CO2, and then the glycine dissociation from H-protein occurs via T-protein with formation of meTHF (red) in the reaction. Lastly, L-protein regenerates H-protein generating NADH in the reaction (Adapted from Kikuchi et al., 2008).

GCS is related with cellular transformation, tumorigenesis and proliferation in some cancer types. Tumour-initiating cells (TIC) of NSLC express high levels of GCS and other glycine/serine metabolic enzymes (Zhang et al., 2012). GCS is required for TIC proliferation and tumour growth, and its overexpression, together with SHMT2, is able to induce cellular transformation that leads to tumour formation (Zhang et al., 2012). GCS induces glycolysis and increases pyrimidine levels including thymidine, deoxyuridine, thymine, uracil, and cytosine (Zhang et al., 2012). Additionally, another study demonstrated that sarcosine (N-methyl derivate of glycine) is related to prostate cancer invasion and its levels are increased in urine of prostate cancer patients (Sreekumar et al., 2009). In ischemic regions of gliomas, an increased expression of SHMT2 coupled with enhanced GCS expression confers advantages to tumour growth when oxygen and nutrient levels are limited (Kim et al., 2015). It was observed that GCS inhibition led to an accumulation of glycine that is further metabolised forming

toxic products, such as aminoacetone and methyl-glyoxal, impairing tumour growth in cells with high expression of SHMT2 (Kim et al., 2015).

As described before, glycine provides C_2N directly to purine synthesis, or participates in its formation through one-carbon metabolism (Nelson and Cox, 2005). Utilising radiolabelled glycine, studies have identified the metabolic processes that employ glycine from diet. Treating A549 cells with ^{15}N-glycine Liu et al. (2015) identified the relevance of glycine for purine synthesis (Figure 1.9b) (Liu et al., 2015). Glycine was observed associated with the phosphorylated sugar ring, and then converted into xanthine/hypoxanthine and then into adenine and adenosine that is phosphorylated to form AMP, ADP and ATP (Liu et al., 2015). Analysing healthy adult humans following ingestion of ^{13}C-glycine and collecting urine to analyse the carbons in the uric acid, the final product of purine catabolism, Baggott et al. observed a major fraction of radiolabeled carbon in C5 position (Figure 1.9a) indicating a direct incorporation of glycine into purine (Baggott et al., 2007). Moreover, they also identified a small fraction of C8 labelled, suggesting a contribution via one-carbon unit through meTHF generated by GCS that is possibly utilised in *de novo* purine synthesis by the enzyme glycinamide ribonucleotide (GAR) transformylase (Baggott et al., 2007). The authors speculate that as the liver has a highly active GCS in the mitochondria, this generates increased levels of meTHF from glycine (Baggott et al., 2007). However, other studies suggest that glycine is only incorporated directly into purine (Jain et al., 2012; Fan et al., 2014). It was observed that SHMT2 inhibition led to an accumulation of AICAR and SAICAR implying that one-carbon units from serine only are incorporated into C2 position (Kim et al., 2015). In HEK293T cells, glycine was incorporated intact into purines, but not via one-carbon units, which was provided by serine-derived meTHF via SHMT2 (Fan et al., 2014). This way, glycine is mainly incorporated into purine directly, and possibly only cells in normal conditions with a highly active GCS, with a consequent increased formation of meTHF, might have a small contribution providing one-carbon units to *de novo* purine synthesis.

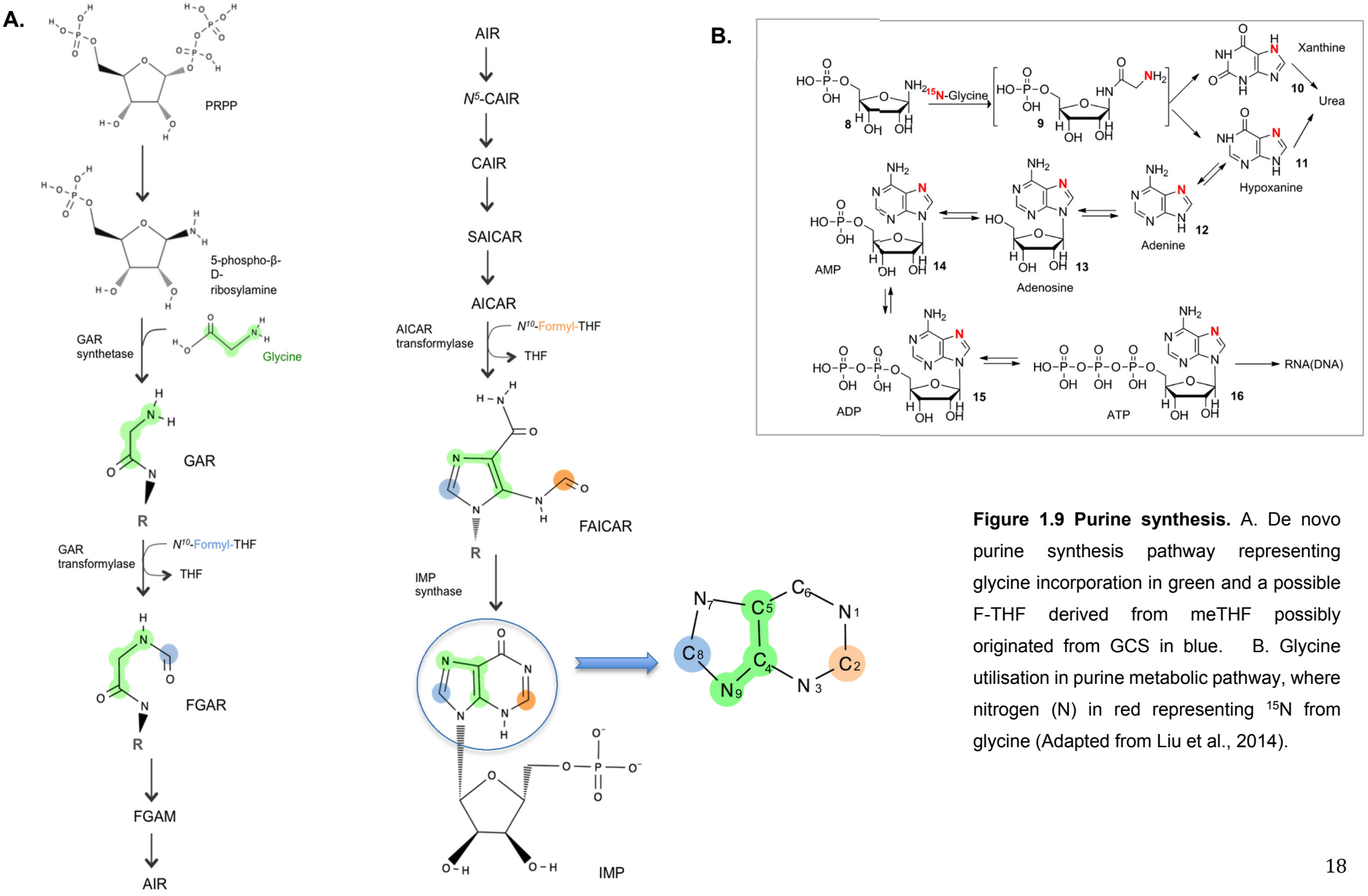

Figure 1.9 Purine synthesis. A. De novo purine synthesis pathway representing glycine incorporation in green and a possible F-THF derived from meTHF possibly originated from GCS in blue. B. Glycine utilisation in purine metabolic pathway, where nitrogen (N) in red representing ^{15}N from glycine (Adapted from Liu et al., 2014).

Extracellular glycine is also utilised in serine synthesis and contributes to NADPH formation. In healthy individuals infused with ^{13}C-glycine, about 41% of glycine intake was converted into serine via SHMT (Lamers et al., 2007). Glycine was utilised as substrate for the enzyme and also providing one-carbon units to form meTHF, generated by GCS, essential for the reaction (Lamers et al., 2007). Additionally, about 39% of the glycine ^{13}C was released as CO_2 possibly through glycine decarboxylation, primarily via GCS and further reduction of meTHF to F-THF, catalysed by the enzyme MTHFD2, and additional reduction to CO_2 and THF, a reaction catalysed by N^{10}-formylTHF dehydrogenase (Lamers et al., 2007). Fan et al verified this hypothesis utilising HEK293T cells. When ^{13}C-glycine was administered, it was observed that majority of meTHF formed in the GCS reactions was oxidised to CO_2 with an increase in NADPH production as result of the reaction (Fan et al., 2014). They also observed that knockdown of GCS impairs cancer growth (Fan et al., 2014). GCS possibly eliminates excess of glycine that can be toxic to cells and contributes to NADPH production, important to redox reactions (Fan et al., 2014).

Glycine is also required for GSH synthesis. GSH is a tripeptide composed of glutamic acid, cysteine and glycine (Traverso et al., 2013). GSH synthesis occurs in a two-step reaction (Figure 1.10) catalised by the enzymes ɣ-glutamylcysteine ligase (GCL) and glutathione synthetase (GSS) that have cysteine as a step limiting factor and GCL as the rate-limiting enzyme (Traverso et al., 2013). Rats with fibrosarcoma infused with ^{13}C-glycine showed a high concentration of radiolabelled GSH in the tumour (Thelwall et al., 2005). Studies in rat mammary tumour infused with ^{13}C-glycine observed carbon from glycine in the glycinyl and cysteinyl-residues of GSH indicating that glycine was also utilised as a precursor in cysteine synthesis (Thelwall et al., 2012). Two carbons of serine were also radiolabelled indicating that serine, synthesised from glycine, was utilised in the transsulphuration pathway to produce cysteine, which is then incorporated into GSH (Thelwall et al., 2012). During GSH synthesis nitrogen from glycine was observed in the dipeptide cysteine-glutamine (Figure 9), in A549 cells incubated with ^{15}N-glycine (Liu et al., 2015). This result corroborates the hypothesis that glycine is also utilised in the transsulphuration pathway having cysteine as product, incorporated later with glycine (a GSS substrate), to form GSH (Liu et al., 2015). Supporting these findings, a study with glioma cells showed that following depletion in GSH levels, there is an increase in the transsulphuration pathway activity to generate cysteine (Kandil et al., 2010).

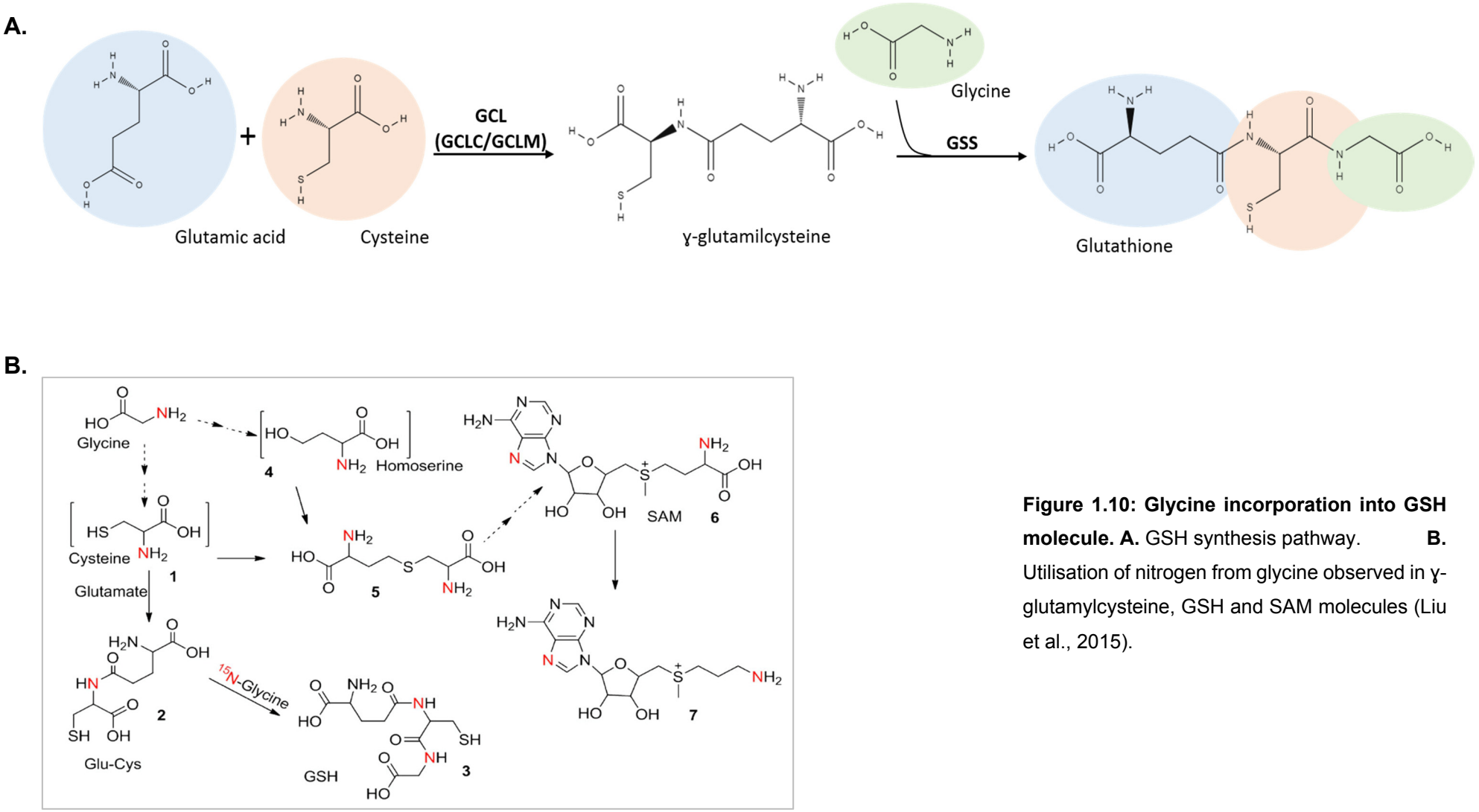

Figure 1.10: Glycine incorporation into GSH molecule. A. GSH synthesis pathway. **B.** Utilisation of nitrogen from glycine observed in ɣ-glutamylcysteine, GSH and SAM molecules (Liu et al., 2015).

GSH is the major cellular antioxidant. GSH peroxidase is responsible for the oxidation of GSH to GSSG, which has antioxidant properties reducing hydrogen and lipid peroxides (Lu, 2013). GSSG reductase then reduces GSSG to GSH and utilises NADPH as a cofactor (Lu, 2013). In many tumour and normal cells GSH supports cell proliferation being essential to cell cycle progression, where its levels increase during DNA synthesis (Lu, 2013, Traverso et al., 2013). GSH maintains glutaredoxin or thioredoxin reduced, essential to ribonucleotide reductase, the rate-limiting enzyme in the DNA synthesis (Lu, 2013). GSH levels also regulate apoptosis influencing caspase activity where its levels are decreased due the generation of ROS and reduced GCL activity (Lu, 2013). A positive link was observed between GSH levels and cancer proliferation, metastasis and drug resistance in tumour cells (Traverso et al., 2013).

Jain et al. (2012) verified that glycine has a key role in rapidly proliferative cancer cells (Jain et al., 2012). In this study, the consumption and release of metabolites of various cancer cell lineages from the National Cancer Institute for drug screening (NCI60) panel, a well-characterised human cancer cell line collection, were evaluated (Jain et al., 2012, Shoemaker, 2006). They observed high concentrations and utilisation of glycine in highly proliferative cells as well as increased SHMT2 expression (Jain et al., 2012). Interestingly, a highly proliferative melanoma lineage imported around 33% of total intracellular glycine from extracellular sources (Jain et al., 2012). Glycine deprivation and SHMT2 knockdown decreased proliferation leading to G1 phase prolongation (Jain et al., 2012). Glycine consumed by rapidly proliferative cancer cells was incorporated in purines directly and in GSH (Jain et al., 2012, Thelwall et al., 2012). Additionally, as described before, mouse models of lymphoma and intestinal tumours fed with a glycine/serine-free diet demonstrated an increase in survival rates, compared with control animals fed a normal diet, with a reduction in serine/ glycine and GSH concentration in the tumours (Maddocks et al., 2017).

Conversely, it was observed that glycine without serine is unable to rescue cell proliferation in *in vitro* experiments (Labuschagne et al., 2014). Labuschagne et al. suggested that it is serine, rather than glycine, that is important in providing one-carbon units to biosynthetic pathways and that, since tumour cells avidly consume serine, extracellular glycine uptake only becomes relevant under serine deprivation (Labuschagne et al., 2014). It was observed that serine deprivation and increased glycine abundance impaired cell growth because glycine is utilised for serine synthesis by SHMT2, which in turn depletes meTHF levels, therefore halting purine synthesis that lead to GAR accumulation (Labuschagne et al., 2014). Moreover, it was

demonstrated that tumour cells growing in medium with an adequate level of serine and glycine expelled excess glycine through passive efflux (Labuschagne et al., 2014). This way, when cells face serine starvation, glycine uptake may contribute to cell survival by restoring serine levels. Moreover, when serine levels are low, but not completely absent, glycine uptake contributes to cellular proliferation as demonstrated by Jain et al., since it is required for purine and GSH synthesis (Jain et al., 2012).

Clinical studies have also identified increased glycine concentration in tumour tissue as an adverse prognostic factor in cancer patients (Cao et al., 2012, Redalen et al., 2016). A study with advanced rectal cancer patients following treatment showed that high glycine levels in tumours were significantly related to poor progression-free survival and the authors suggested that inhibition of glycine uptake may be a possible new approach to highly proliferating and hypoxic tumours (Redalen et al., 2016). Another clinical study showed that glycine levels were increased in lung cancer tissues and decreased in plasma, when compared to tissue and plasma concentration of normal individuals (Zhao et al., 2014). In patients with glioma, elevated glycine levels can be observed more frequently in grade IV tumours (Maudsley et al., 2014). The distribution of glycine in glioma showed a correlation with choline and was frequently observed in areas near high lactate levels (Maudsley et al., 2014). Data from this clinical study also suggested that glycine synthesis was increased in areas with incomplete hypoxia (Maudsley et al., 2014).

Glycine influences endothelial cell growth and angiogenesis. *In vivo* studies of a mouse model of melanoma demonstrated that high levels of glycine supplementation in the diet inhibited tumour growth, reducing tumour size by about 77% (Rose et al., 1999). However, glycine had no direct effect on tumour proliferation, but significantly disturbed angiogenesis, reducing the number of vessels in the tumour (Rose et al., 1999). In endothelial cells, high glycine levels facilitate interaction of glycine with GlyR, increasing its activity, and inhibit cell proliferation induced by VEGF; and in hepatocellular carcinoma cells, glycine reduced VEGF expression via GlyR (Bruns et al., 2016, Bruns et al., 2014). VEGF signalling is dependent on Ca^{2+} influx, whereas glycine interaction with GlyR, a chloride channel, is activated, resulting in hyperpolarisation of the cell membrane and blocking Ca^{2+} influx (Bruns et al., 2016, Bruns et al., 2014, Yamashina et al., 2001). Thus, glycine interaction with GlyR counteracts the effects of VEGF in endothelial cells, inhibiting proliferation and migration and consequently preventing angiogenesis (Yamashina et al., 2007, Yamashina et al., 2001). Additionally, a recent study observed that VEGF induced the

specific glycine transporter GLYT1 activation leading to a higher glycine uptake in endothelial cells, which in turn participates in a signalling pathway involving mTOR that increased mitochondria function and promoted angiogenesis (Guo et al., 2017). Thus, data from these studies suggest that when glycine levels are increased about ten times the normal plasma level (250-500μM) in the extracellular environment, interaction of glycine with GlyR is facilitated resulting in angiogenesis inhibition, whereas in normal conditions extracellular glycine uptake by GLYT1 seems to contribute to VEGF signalling and support angiogenesis.

Recent studies have highlighted a link between glycine and mTOR. Analysing the inhibition of mTORC1 in osteosarcoma cells, Wang et al. observed that there was an inhibition of cell proliferation and also a reduction of about 50% in serine and glycine levels (Wang et al., 2017). Furthermore, mTORC1 inhibition reduced serine biosynthesis enzymes PHGDH, PSAT and PSPH mRNA expression (Wang et al., 2017). According to this study, additional supplementation with glycine and serine may rescue cell proliferation when mTORC1 was inhibited (Wang et al., 2017). Moreover, cell proliferation was increased 2.5 and 1.5 times when osteosarcoma cells were treated with 0.4mM of serine or glycine, respectively, in comparison to untreated cells, and also the GSH levels were increased following the amino acid supplementation (Wang et al., 2017). In a mouse myoblast cells glycine supplementation increased DNA replication and activated mTORC1 via Akt enhancing protein synthesis (Sun et al., 2016). It was also suggested that mTORC1 activation by amino acid occurs in two steps: priming and activation (Dyachok et al., 2016). In the first step, one or more hydrophilic amino acids, such as glycine, sensitize mTORC1 for further activation, mainly promoted by leucine as discussed earlier in this chapter (Dyachok et al., 2016).

In summary, extracellular glycine seems to play an important role in cell growth of rapidly proliferating tumour cells. This small versatile amino acid contributes to purine and GSH synthesis, is involved in mTOR signalling and angiogenesis. Thus, inhibition of glycine transport may increase plasma levels of glycine and reduce intracellular abundance, which, in association with serine starvation, may lead to a reduction in cell proliferation.

1.4 Glycine transporters

The solute carriers (SLCs) of the families SLC6A - SLC6A9 (GLYT1), SLC6A5 (GLYT2), SLC6A14 ($ATB^{0,+}$), SLC36A - SLC36A1(PAT1), SLC36A2 (PAT2) and SLC38 - SLC38A2 (SNAT2) and SLC38A4 (SNAT4) are amino acid transporters involved in glycine transport. Considering that rapidly proliferative cells require extracellular glycine for purine and GSH production (Jain et al., 2012), these transporters may play an important role in supporting growth and proliferation.

1.4.1 GLYT

GLYT1 and GLYT2 belong to the Na^+ - and Cl^- - dependent neurotransmitter family SLC6 and they have high affinity for glycine (Howard and Hirst, 2011). GLYT2 only transports glycine and GLYT1 is able to transport glycine and sarcosine (Howard and Hirst, 2011). Both proteins are present in plasma membrane having 12 transmembrane domains, six extracellular and five intracellular loops (figure 1.11a), and N-glycosylation specific sites (Betz et al., 2006, Olivares et al., 1995). In intestinal cells, GLYT1 is located in both basal and apical membrane surfaces (Christie et al., 2001). Glycine uptake through GLYTs is dependent on transmembrane sodium gradient which is generated by Na^+/K^+-ATPase (Betz et al., 2006). GLYT2 co-transports $3Na^+/Cl^-$/glycine and GLYT1 co-transports $2Na^+/Cl^-$/glycine (figure 1.11b), thus the electrochemical driving force if more favourable for GLYT2-mediated transport of glycine into cells (Gomeza et al., 2006, Betz et al., 2006). In contrast, the lower Na^+ requirement enables GLYT1 to be reversed, allowing cellular release of glycine to the extracellular environment when physiological changes occur such as modification in membrane potential and in Na^+ and glycine concentrations (Roux and Supplisson, 2000, Betz et al., 2006).

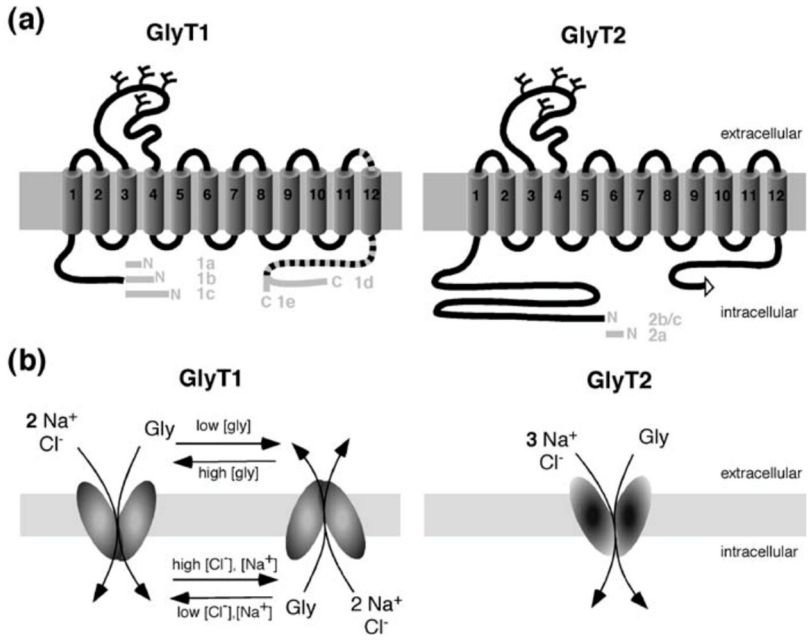

Figure 1.11 GLYT1 and GLYT2 transporters. (a) Membrane topology of GLYTs transporters with 12 transmembrane domains. (b) Differences in stochiometry of GLYT1 and GLYT1 transporters indicating the co-transport of Na^+ and Cl^- (Gomeza et al., 2006).

GLYT1 and GLYT2 demonstrate different tissue distributions (Howard and Hirst, 2011). GLYT2 is expressed in neurons of the medulla, cerebellum and spinal cord as well as in mast cells and macrophages (Howard and Hirst, 2011, Borowsky et al., 1993). The human GLYT1 gene, located on chromosome 1, encodes for at least three protein isoforms wherein variants 1 (GLYT1b) and 3 (GLYT1a) are the best characterised (Howard and Hirst, 2011, Borowsky and Hoffman, 1998). GLYT1a and GLYT1b utilise alternative promoters and only differ in the NH_2 terminal region, but with identical glycine specificity (Borowsky and Hoffman, 1998, Howard and Hirst, 2011, Durkin et al., 2011, Christie et al., 2001). These isoforms demonstrate different tissue distribution. GLYT1a (NCBI number: NM_001024845) is found in neuronal tissues and several peripheral organs (intestine, kidney, uterus, lung, among others) and GLYT1B is present in brain and spinal cord (Howard and Hirst, 2011, Borowsky et al., 1993, Borowsky and Hoffman, 1998).

Although progress has been made in elucidating epigenetic and post-translational regulation of GLYT1, still little is known about these mechanisms. The N-glycosylation of GLYT1 seems to drive the transporter to the plasma membrane, being an important post-translational modification (Olivares et al., 1995). In Caco-2 cells, protein kinase C (PKC) is involved in GLYT1 downregulation (Howard and Hirst, 2011, Christie et al., 2001). Additionally, Zn^{2+} was reported to inhibit GLYT1 in central nervous system, impairing conformational changes essential to glycine transport (Ju et al., 2004).

Another study has identified HMGN3a, a nucleosome binding protein, as a potential upregulator of the GLYT1 gene through its capacity of unfolding chromatin and enabling access to the GLYT1 promoter (West et al., 2004). Furthermore, it was observed that GLYT1 is a target of the stress response system and is upregulated by activating transcriptional factor 4 (ATF4), known to be a central factor in several stress response pathways including oxidative and endoplasmic reticulum (ER) stress (discussed in details in section 1.6) (Harding et al., 2003).

Glycine acts as inhibitory and excitatory neurotransmitter in the central nervous system (CNS) (Harvey and Yee, 2013). It binds to glycine receptors (GlyR) activating chloride ion influx via an anion channel resulting in hyperpolarisation of post synaptic membranes in inhibitory synapses (Harvey and Yee, 2013). Glycine also acts as an agonist of NMDA receptors being essential for its activation by L-glutamate in excitatory synapses (Harvey and Yee, 2013). Studies have shown that the abundance of glycine in the neuronal cleft is controlled by specific glycine transporters, GLYT1 and GLYT2, Na^+,Cl^- -dependent transporters, responsible for glycine reuptake, GLYT1 being the major regulator near NMDA receptors (Harvey and Yee, 2013). Consequently, pharmacological approaches involving GLYT1 transporter have been analysed in recent years as a possible treatment for schizophrenia, pain control, alcohol dependence and epilepsy among other disorders involving the CNS (Harvey and Yee, 2013).

The most extensive studies about pharmacological inhibition of GLYT1 transporters are focused on schizophrenia treatment and some GLYT1 inhibitors have been tested in clinical trials phase one and two (Harvey and Yee, 2013). It is hypothesized that reduction in glutamatergic synapses involving NMDA receptors is responsible for the negative and cognitive symptoms of schizophrenia; therefore increasing glycine in the synaptic cleft via GLYT1 inhibitors is highlighted as a possible treatment (Harvey and Yee, 2013). However, these inhibitors have also been showing positive effects in other disorder involving the CNS. ALX5407 has also shown anti-nociceptive action and anxiolytic effect in rats; continuous administration of this inhibitor did not change GLYT1 protein expression in the rat spinal cord (Barthel et al., 2014, Komatsu et al., 2015). When ischemia was induced in rats, administration of high doses of ALX5407 reduced infarct volume, neuronal injury, expression of caspase-3, and increase in Bcl-2/Bax, via increased glycine interaction with GlyR (Huang et al., 2016).

ALX-5407 is a potent, selective and irreversible GLYT1 inhibitor, for all GLYT1 variants, that presents IC_{50} of 3-30nM, which may vary depending on the experiment, being noncompetitive for sarcosine or glycine binding sites (Núñez et al., 2005, Atkinson et al., 2001). In an experiment utilising QT6-1C cells transfected with GLYT1 or cell aggregates prepared from rat brain or spinal cord the IC_{50} for ALX5407 was 3nM and the inhibitor completely impaired glycine uptake in these cells (Atkinson et al., 2001). QT6-1C cells treated with 60nM ALX-5407 presented slow dissociation kinetics with a half-life about 13h after washout when measuring the percentage inhibition of radio labeled glycine (Atkinson et al., 2001). Utilising rat forebrain membrane, Mallorga et al observed that its association with [^{3}H]-ALX5407 presented a $t_{1/2}$ of 13 min and reached equilibrium after 20 min and its dissociation from the membrane had a $t_{1/2}$ of 28min (Mallorga et al., 2003). Administration of ALX5407 reduced glycine uptake 40-50% in rat retina and in oocytes expressing GLYT1b the inhibition was time and dose dependent (Salceda, 2006, Aubrey and Vandenberg, 2001).

It is known that glycine exerts a protective effect in various tissues, such as lung and intestine (Howard and Hirst, 2011). Interestingly, Howard *et al.*, (2010) demonstrated that glycine has antioxidant properties in intestinal and hepatic cells. This was attributed to the increase in GSH levels during oxidative stress, a characteristic dependent on extracellular glycine uptake through GLYT1 (Howard et al., 2010). Tumours frequently face increased levels of reactive oxygen species (ROS) (Hussain et al., 2003, Traverso et al., 2013) and a limited oxygen supply. Thus, exogenous glycine, possibly with uptake dependent on GLYT1, may also be required in order to increase GSH levels to overcome oxidative stress in tumours and tumour-derived cell lines, as observed in intestinal and hepatic cells. GSH contributes to redox equilibrium by its ability to expel and reduce ROS and maintain adequate NADPH/$NADP^+$ levels, required for anabolic metabolism (Traverso et al., 2013). As described earlier, increased GSH is associated with a proliferative response, essential to cell cycle progression and in various tumours related to chemotherapy resistance (Traverso et al., 2013, Estrela et al., 2006, O'Brien and Tew, 1996).

1.4.2 $ATB^{0,+}$

$ATB^{0,+}$, a neutral and cationic amino acid transporter, also belongs to the Na^+ and Cl^- dependent neurotransmitter transporter family, SLC6A14, and is located on chromosome X (Sloan and Mager, 1999). Its primary structure shares 60% similarity

with GLYT1 and GLYT2 (Sloan and Mager, 1999). Similar to these proteins, $ATB^{0,+}$ is predicted to comprise 12 putative transmembrane domains and glycosylation sites for post-translational modifications. Like GLYT1, PKC also seems to be a regulator of $ATB^{0,+}$ activity (Samluk et al., 2010). In contrast to GLYTs, $ATB^{0,+}$ transports all amino acids except glutamate and aspartate, but has a preference for leucine and arginine uptake (Sloan and Mager, 1999, Ganapathy and Ganapathy, 2005, Karunakaran et al., 2008).

$ATB^{0,+}$ mRNA expression is upregulated in some tumour types, having been found at raised levels in colorectal, cervical and breast cancer cells; in normal cells its expression is relatively low, only detected in colon and lung tissues (Karunakaran et al., 2008, Karunakaran et al., 2011, Gupta et al., 2006, Sikder et al., 2017). $ATB^{0,+}$ facilitates uptake of several drugs and its inhibition induces growth arrest, amino acid deprivation, mTOR inhibition and subsequently autophagy (Karunakaran et al., 2008, Karunakaran et al., 2011, Hatanaka et al., 2004). There is therefore significant interest in $ATB^{0,+}$ as a therapeutic target (Karunakaran et al., 2008, Karunakaran et al., 2011, Hatanaka et al., 2004).

1.4.3 PAT

The proton/amino acid transporters (PATs) PAT1 and PAT2 (SLC36A1 and SLC36A2) are H^+ coupled transporters of small neutral amino acids with a preference for L-proline and high affinity for glycine and alanine and, in humans, are located on chromosome 5 (Chen et al., 2003). Both transport small, unbranched amino acids and heterocyclic amino acids containing 4- to 5-membered rings (Thwaites and Anderson, 2011). PAT1 also transports N-methylated amino acids and PAT2 transports dipolar amino and imino acids (Thwaites and Anderson, 2011). Both transport zwitterionic amino acids are coupled with H^+, thus they are able to produce current and are membrane potential sensitive (Thwaites and Anderson, 2011, Boll et al., 2002, Wreden et al., 2003). In rat, PAT2 shares 72% similarity with PAT1 (Chen et al., 2003).

PAT1 is expressed in neurons, small intestine, colon, kidney, lung, liver and spleen (Wreden et al., 2003, Thwaites et al., 1993, Thwaites and Anderson, 2011). PAT2 is present in the lungs, heart, kidney, muscle, testis, spleen, adrenal gland, thymus and sciatic nerve (Boll et al., 2002). PAT2 participates in reuptake of amino acids in the renal proximal tubule (Bröer et al., 2008). PAT1 has been reported as a potential drug transporter (Frølund et al., 2012) and to regulate cell growth in flies and

neonate pigs in which the transporter participated in the amino acid sensing system which interacts with mTORC1 (Heublein et al., 2010, Suryawan et al., 2013). PAT1 knockdown in MCF-7 and HEK-293 cell lines was shown to inhibit cell proliferation and mTORC1 signalling (Goberdhan, 2010, Heublein et al., 2010, Suryawan et al., 2013). PAT1 activity is modulated by pH or membrane potential alterations, and PAT2 activity seems to be regulated through changes in membrane voltage (Foltz et al., 2004).

1.4.4 SNAT

The sodium coupled amino acid transporters (SNATs), belong to the SLC38 gene family of solute carrier proteins and are able to transport small, neutral amino acids such as glycine but have high preference for L-glutamine, L-alanine, L-aspargine and L-histidine (Mackenzie and Erickson, 2004, Jones et al., 2006, Schiöth et al., 2013). SNAT4 is expressed in the brain, retina, liver, kidney and adipose tissues (Schiöth et al., 2013). SNAT2 is distributed ubiquitously in human tissues and is activated in prostate cancer (Okudaira et al., 2011, Schiöth et al., 2013). It was proposed that SNAT2 also functions as a sensor participating in mTORC1 signalling pathway, thus influencing cell growth and differentiation (Pinilla et al., 2011). SNAT2 has also been shown to be highly upregulated during amino acid starvation (Jones et al., 2006, Schiöth et al., 2013).

	Amino acids transported and preference[1]	High amino acid affinity[1]	Kinetics parameters (*km*)	Normal tissue protein expression[8]	Tumour tissue protein expression[8]	Tumour cell lines mRNA expression (TPM)[9]
GLYT1 (SLC6A9)	Na^{+2}, cl^{-2} dependent transporter. Transports glycine and sarcosine. Preference: glycine	Glycine and sarcosine.	[2] Glycine: 72 ± 9 μM	Medium level: Heart muscle, Skeletal muscle, Smooth muscle, Nasopharynx, Bronchus, Pancreas, CNS, Stomach, Duodenum, Small intestine, Colon, Rectum, Kidney, Urinary bladder, Testis, Prostate, Ovary, Endometrium Low level: Cerebral cortex, Gallbladder, Skin, Caudate Bone marrow, Lung, Lymph node, Tonsil	Cases of moderate to strong expression: Colorectal cancers, carcinoids and several cases of melanomas, gliomas, testicular cancers and some cases of renal and lung cancer.	A549: 13 HUVEC: 0.5 HT29: ND Caco-2: 4 A498: ND RT4: 1.7 Normal Tissue colon: 8.3 Lung: 8.5 Kidney: 1.8
PAT1 (SLC36A1)	H^+ couple transporter for small neutral amino acids Preference: proline	Proline and also glycine and alanine	[3]Proline: 2.8 ± 0.1 mM Glycine: 7.0 ± 0.7 mM Alanine: 7.5 ± 0.6 mM	High level: Gallbladder, Cerebral cortex, Ovary, Liver, Cerebellum, Pancreas, Duodenum, Small intestine, Colon, Rectum, Prostate Medium level: Nasopharynx, Bronchus, Caudate, Skin, Hippocampus, Esophagus, Stomach, Tonsil, Endometrium, Heart muscle, Skeletal muscle, Kidney, Urinary bladder, Testis, Cervix uterine, Lung, Seminal vesicle, Oral mucosa	Cases of moderate to strong expression: Breast cancer, Prostate cancer, Carcinoid, Colorectal cancer, Testis cancer, Thyroid cancer, Renal cancer, Endometrial cancer, Liver cancer, Glioma	A549: 8.3 HUVEC: 7.8 HT29: ND Caco-2: 17.4 A498: ND RT4: 6.1 Normal Tissue colon: 14.7 Lung: 6.8 Kidney: 5

SNAT2 (SLC38A2)	Na^+ coupled amino acid transporter. Preference: glutamine, alanine, aspargine and histidine	Alanine, asparagine, cysteine, glutamine, glycine, histidine, methionine, proline, serine	[4]Alanine: 200 ± 18 μM [5]Serine: 800 μM [6]Glycine: ND but > 200μM	High levels: Oral mucosa, Pancreas, Duodenum, Small intestine, Kidney Moderate level: Lymph node, Tonsil, Endometrium, Cervix uterine, Vagina, Breast, Lung, Nasopharynx, Bronchus, Liver, Gallbladder, Cerebral cortex, Fallopian tube, Seminal vesicle, Epididymis, Stomach, Caudate, Cerebellum, Colon, Rectum, Urinary bladder, Testis, Prostate, Skin	Cases of moderate to strong expression: Head and neck cancer, Colorectal cancer, Liver cancer, Urothelial, cancer, Skin cancer, Breast cancer, Pancreatic cancer, Ovarian cancer, Renal cancer, Prostate cancer, Endometrial cancer	A549: 161 HUVEC: 220 HT29: ND A498: ND Caco-2: 17.4 A498: ND RT4: 6.1 Normal Tissue colon: 45.6 Lung: 81.7 Kidney: 69.4
$ATB^{0,+}$ (SLC6A14)	Na^{+2}, cl^{-2} dependent transporter. Transports all amino acids except glutamate and aspartate. Preference: leucine and arginine.	Leucine and arginine.	[7]Non-polar amino acids: 6-100 μM Glycine: 111 ± 30 μM	High levels: Cervix uterine, Breast, Bronchus, Nasopharynx, Lung, Oral mucosa Medium level: Oral mucosa, Bone marrow, Esophagus, Tonsil, Spleen Skin, Placenta, Epididymis, Prostate	Cases of moderate to strong expression: Head and neck cancer, Endometrial cancer, Urothelial cancer, Skin cancer, Cervical cancer, Lymphoma, Lung cancer	A549: 0 HUVEC: 0 HT29: ND A498: ND Caco-2: 17.4 A498: ND RT4: 6.1 Normal tissue colon: 1.4 Lung: 23.9 Kidney: 0

Table 1.1: Glycine transporters amino acid affinities and its normal and tumour tissue and tumour cell lines expression. Where ND= not described and TPM= transcription per million. [1] As described in Section 1.4.1, 1.4.2, 1.4.3 and 1.4.4. [2](Kim et al., 1994). [3](Boll et al., 2002). [4](Zhang and Grewer 2007). [5](Yao et al., 2000). [6](Baird et al., 2006). [7](Sloan and Mager 1999). [8]As described at www.proteinatlas.org (Uhlén et al., 2005, Uhlén et al., 2010, Uhlén et al., 2015, Uhlén et al., 2017). [9]As described at www.proteinatlas.org (Uhlén et al., 2005, Uhlén et al., 2010, Uhlén et al., 2015, Thul et al., 2017).

1.5 Other amino acids transporters related to cancer

The amino acid transporters SLC7A11 (xCT)/SLC3A2 (4F2hc) and SLC7A5 (LAT1) have also been proposed to be involved with transformation of cells.

xCT and 4F2hc together form the X^-c heterodimeric transporter system, a sodium-independent antiporter responsible for cystine uptake coupled with glutamate efflux (Ganapathy et al., 2009, Huang et al., 2005, Sato et al., 2004). Intracellularly, cystine is reduced to cysteine, which participates in GSH synthesis (Huang et al., 2005, Sato et al., 2005). xCT also has 12 putative transmembrane domains and is located on chromosome 4. Inhibition of X-c in A549, HOP-62 and SK-OV-3 cell lines reduced intracellular GSH levels (Huang et al., 2005). Cysteine levels are generally thought to influence GSH production (Wu et al., 2004). X-c is regulated by the oxygen sensitive transcription factor, nuclear factor of the erythroid derived 2 like factor (NRF2) and, similar to GLYT1, by ATF4 in response to amino acid deprivation (Lewerenz et al., 2013, Sato et al., 2004, Sasaki et al., 2002) The xCT gene also contains regulatory binding sites related to transcription factors NF-E2 and AP-1 (Sato et al., 2000). This transport system has been related to chemotherapy resistance in cancer cells and its inhibition reduces tumour replication, invasion and metastasis (Lewerenz et al., 2013, Gout et al., 2001, Huang et al., 2005).

LAT1 is a sodium-independent transporter related to the transport of branched-chain amino acids and neutral amino acids with bulky aromatic side-chains, and is also associated with a 4F2hc subunit (Ganapathy et al., 2009, Oda et al., 2010). This transporter is highly expressed in tongue cancer and associated with metastasis and invasion resulting in a poor prognosis for patients (Toyoda et al., 2014). In fact, LAT1 over expression is observed in a large number of tumours including colon and lung cancers but observed at a lower concentration in normal tissues (Oda et al., 2010, Kanai et al., 1998, Kanai and Endou, 2003).

1.6 Activating Transcription Factors

Cells under stress activate several pathways to restore intracellular homeostasis favouring survival and enabling cell growth. Four protein kinases, namely PERK, GCN2, HRI and PKR, are involved in a stress-response mechanism termed the Integrative Stress Response (Ye et al., 2010). When activated in response to cellular

stress such as accumulation of unfolded proteins in the endoplasmic reticulum (ER-stress) (PERK), oxygen deprivation (PERK), haem deficiency (HRI), viral infection leading to presence of double-stranded RNA (PKR) or accumulation of uncharged tRNAs during amino acid starvation (GCN2), these kinases phosphorylate the α subunit of eukaryotic translation initiation factor 2 (eIF2α) (Harding et al., 2000);(Sood et al., 2000);(Ye et al., 2010).

Phosphorylation of eIF2α leads to a reduction in global protein expression, to conserve energy, and upregulation of activating transcription factor 4 (ATF4) (Harding et al., 2000, Singleton and Harris, 2012). Under normal conditions the two upstream open reading frames (uORF) in the 5'UTR of the ATF4 mRNA, uORF1 and uORF2, are translated by ribosomes leading to an overlap of the uORF2 with the promoter region inhibiting ATF4 translation (Singleton and Harris, 2012, Lu et al., 2004). When phosphorylated, eIF2α induces a delay in ribosome activity that in turn bypasses uORF2 and avoids its overlap with ATF4 promoter region (Singleton and Harris, 2012, Lu et al., 2004). Basal levels of ATF4 mRNA expression are ubiquitous in the organism (Yang and Karsenty, 2004). However, its protein abundance is only expressed in a few organs under normal conditions and upregulated only during specific conditions, e.g. ER stress, in most of the tissues (Yang and Karsenty, 2004). ATF4 translation was observed to be dependent on post-translational mechanisms (Yang and Karsenty, 2004). ATF4 interacts with a portion of ubiquitin ligase, which seems to be dependent on ATF4 Ser219 phosphorylation, then leading to proteasomal degradation (Lassot et al., 2001, Yang and Karsenty, 2004). The interaction of ATF4 protein to the histone acetyltransferase p300 inhibits ubiquitination, stabilising ATF4 protein and enhancing its transcriptional activity (Lassot et al., 2005). ATF4 is able to regulate the transcription of genes related to autophagy, apoptosis, amino acid transport and synthesis, as well as redox balance, in the nucleus (Harding et al., 2003).

Ye *et al.* (2010) demonstrated that during amino acid deprivation in cancer cells the activation of the GNC2–eIF2α–ATF4 pathway has an important role for tumour survival, and that ATF4 is an important regulator of amino acid metabolism (Ye et al., 2010). ATF4 interacts with the amino acid response element (AARE), a consensus binding site present in many genes encoding proteins such as the amino acid transporters, transcription factors and genes involved in amino acid synthesis (Sato et al., 2004, Fernandez et al., 2003, López-Fontanals et al., 2003). ATF4 has been shown to upregulate GLYT1, xCT and SNAT2 (Harding et al., 2003, Sato et al., 2004, López-Fontanals et al., 2003). ATF4 regulates asparagine, serine, glycine, and proline

syntheses inducing ASNS, PSAT1, PHGDH, PSPH, SHMT2, MTHFD2, AND PYCR1 mRNA expression and also amino acid transporters as SLC1a4 (ASCT1), SLC7a1 (CAT-1), SLC7a5 (LAT1) (Adams, 2007). Inhibition of ATF4 reduces about 21% of amino acid levels, decreasing intracellular levels of glycine, serine, proline, among others (Adams, 2007). It was observed that serine starvation activates the GNC2–eIF2α–ATF4 pathway and results in further transcription of PHGDH, PSAT1 and PSPH proteins involved in the serine biosynthesis pathway (Ding et al., 2013, Ye et al., 2012). Additionally, amino acid deprivation activates GCN2/ATF4 pathway that also induce angiogenesis through VEGF expression (Wang et al., 2013b).

ATF4 protein expression can also be upregulated independently of eIF2α kinases by mTORC1, activated by the growth factor insulin (Adams, 2007). This way, there is an increase in mRNA expression of amino acid transporters and synthesising enzymes regulated by ATF4, resulting in higher levels of charged-tRNA that support translation and then cell growth, through enhanced amino acid uptake (Adams, 2007). It was also observed that leucine supplementation in rat muscle cells led to mTOR activation followed by increased ATF4 translation, and consequent enhanced SNAT2 mRNA expression (Luo et al., 2013). Moreover, mutations in ATF4 can cause loss of amino acid homeostasis and consequently a reduction of mTORC1 (Singleton and Harris, 2012, Seo et al., 2009). Thus, when ATF4 upregulates amino acid transporters and metabolism, mTORC1 is activated (Singleton and Harris, 2012).

The PERK–eIF2α–ATF4 pathway is upregulated under hypoxic conditions and is very important in hypoxia resistance and tumour growth (Bi et al., 2005). A potential link between PERK/ATF4 and NRF2 has been established (Miyamoto et al., 2011). NRF2 phosphorylation by PERK is involved in oxidative stress response where it increase ATF4 levels, regulates the synthesis of GSH (Gorrini et al., 2013) and upregulates xCT expression (Gorrini et al., 2013, Sasaki et al., 2002). Recently it was observed that bladder cancer cells require both NRF2 and ATF4 activation (Ye et al., 2014). Moreover, considering the additional importance of GLYT1 in maintaining GSH levels and its regulation by ATF4, it is possible that NRF2 also regulates GLYT1 (Harding et al., 2003, Howard et al., 2010). ATF4 also promotes transcriptional up-regulation of GSH synthesising enzymes in human tumours, thus favouring resistance to oxidative stress and chemotherapeutics (Igarashi et al., 2007).

ATF3 is a transcription factor closely related to ATF4 that appears to play a significant role as an adaptive response protein when cellular homeostasis is disrupted (Hai et al., 2011). In normal cells, ATF3 regulates both apoptosis and cell proliferation

rate (Hackl et al., 2010). ATF3 is also involved in regulation of growth and apoptotic signals in tumours (Thompson et al., 2009). ATF3 is overexpressed in breast, prostate and Hodgkin-lymphoma (Thompson et al., 2009). It was observed that ATF3 promotes metastasis in breast, prostate and colon cancer cell lines and induced colon and Hodgkin-lymphoma tumour cells growth (Thompson et al., 2009, Hai et al., 2011). However, other studies showed that ATF3 might trigger apoptosis, arrest cell cycle progression and reduce metastasis acting as a possible tumour suppressor. Yin et al suggested that ATF3 presents a dichotomous function in normal and cancer cells, promoting apoptosis in untransformed cells, whereas in tumour cells it increases survival and metastasis (Yin et al., 2008). Under stress, PERK/eIF2α/ATF4 and GCN2/eIF2α/ATF4 pathways induce ATF3 expression also ATF4 seems to activate ATF3 translation (Lee et al., 2013, Jiang et al., 2004).

Many tumours express ATF5, and its nuclear localization is higher in these tissues than in non-transformed cells (Nukuda et al., 2016). ATF5 is regulated by ATF4 and CHOP transcription factors (Zhou et al., 2008, Teske et al., 2013). ATF5 promotes tumour cell survival, growth and has been linked to cell invasiveness of lung and breast cancer among others (Nukuda et al., 2016, Deng and Haynes, 2017). Studies have demonstrated that ATF5 activates anti-apoptotic genes in some cancer types and also contributes to chemotherapy and radiotherapy resistance (Deng and Haynes, 2017, Ishihara and Haga, 2015). In lung cancer cells, ATF5 induce the transition of cell cycle from G1 to S phase that can contribute to tumorigenesis (Ishihara and Haga, 2015). However, ATF5 also induces pro-apoptosis genes depending on the cell type and cellular conditions (Teske et al., 2013). During stress and increased levels of unfolded proteins, when the integrated stress response activated by ATF4 is unable to restore cellular homeostasis, there is an increase in CHOP expression and consequently ATF5 expression (Teske et al., 2013). ATF5 and CHOP are involved in the regulation of some genes involved in apoptosis under proteasome inhibition in mouse embryonic fibroblasts (Teske et al., 2013, Wu et al., 2014). Also, in hepatocellular carcinoma, ATF5 possess a tumour-suppressive role being down regulated in this tissue (Wu et al., 2014).

Under ER stress, due to accumulation of unfolded proteins, ATF6, localized in the ER membrane, is activated and translocates to the Golgi compartment where it is cleaved, then the N-terminal cytosolic domain migrates to the nucleus and binds to CRE and ERSE-1 sites activating target genes (Sano and Reed, 2013). Teske and collaborators showed that ATF4 is involved in ATF6 up-regulation, restoring levels of

full length ATF6 mRNA during stress, and in its trafficking to the nucleus (Teske et al., 2011). ATF6 up-regulates CHOP, inducing cell death, but is also involved in adaptation and recovery during prolonged ER stress (Hirsch et al., 2014). ATF6 increases the ER-associated protein degradation system (ERAD) contributing to removal of misfolded proteins as one of the mechanisms to recover ER homeostasis (Notte et al., 2015). However, when there is a prolonged activation of UPR and failure of pro-survival mechanisms to overcome stress, autophagy is activated to promote cancer cell adaptation and survival, assisting in misfolding protein degradation and providing nutrients from degraded cellular organelles (Notte et al., 2015). Interestingly, high proliferation rates of tumours often generate a stress environment as hypoxia and amino acid deprivation where UPR is chronically activated and contribute cell survival (Notte et al., 2015).

1.7 Cell Lines

Considering the relevance of glycine to support rapid tumour cell proliferation the present work utilised well-characterised cell lines as models for rapidly proliferating tumour cells, the non-small cell lung cancer (NSCLC) cell line A549 and the colorectal cancer cell line HT29, slowly proliferating tumour cell, renal cancer cell line A498, and fast growing non-transformed cell line, human umbilical vein endothelial cell line HUVEC, to assess the relevance of GLYT1 in cancer cell proliferation.

The cell lines utilised in this study were selected based on the US National Cancer Institute (NCI) 60 human tumour cell line anticancer drug screen (NCI60) data (Shoemaker, 2006). The NCI60 was created in the 1980s to screen drugs for anticancer activity through *in vitro* experiments utilising cancer cell lines (Shoemaker, 2006). They selected 60 cancer cell lines, representing nine cancer types, based on their adaptability to standard cell culture medium, RPMI-1640, and characterised their growth (De Luca et al., 2012). Then, these cell lines were utilised to test the inhibitory effect of potential chemotherapy drugs as a fast screening to eliminate ineffective compounds, thus avoiding unnecessary preclinical and clinical tests (Shoemaker, 2006, Brodaczewska et al., 2016). The genetic and proliferative profiles of the 60 cell line panel have been extensively studied by the NCI and other research groups around the world (Shoemaker, 2006, Brodaczewska et al., 2016).

A549 cells

A549 is a human epithelial adherent NSCLC cell line isolated in 1973 from a 58 year old Caucasian male (ATCC®). It is known to be a KRAS mutant with gain of function (Heasley et al., 1997) and according to analysis utilising the Genevestigator program it presents high expression of oncogenes JUN, c-MYC, abl and src and medium expression of FOS, ROS and sis (Genevestigator). The suppressor gene p53 does not harbour a codon change and is highly expressed (ATCC®, Genevestigator, O'Connor et al., 1997). According to NCI60 data it represents a rapidly proliferative profile with doubling time of 19.1 hours (NCI).

HT29

The HT29 cell line is a human epithelial adherent colorectal adenocarcinoma derived from a 44 year old adult Caucasian female (ATCC®). This cell line expresses c-myc, K-ras, H-ras, N-ras, Myb, sis and fos oncogenes (Genevestigator). The p53 gene is expressed and harbours a G -> A mutation in codon 273 resulting in an Arg -> His substitution (ATCC®). According to NCI60 panel it represents a rapidly proliferative profile with doubling time of 19.5 hours (NCI).

A498

The A498 cell line is a human epithelial adherent kidney carcinoma isolated from a 52 year old female (ATCC®). According to analysis utilising Genenvestigator program it presents high expression of oncogenes JUN, c-MYC, K-ras, abl, src and sis and medium expression of mTOR and FOS (Genevestigator). According to NCI60 panel, the A498 cell line represents a slow proliferative profile with doubling time of 66.8 hours (NCI).

HUVEC

HUVEC is a human normal adherent primary endothelial cell from the umbilical vein of single donor (Lonza). Age and gender are batch-specific. According to suppliers the doubling time of this cell line can vary between 30-37h depending on the batch.

1.8 Hypothesis

Considering the importance of glycine to cancer cell survival and proliferation, I have investigated the hypothesis that increased glycine transport, which manifests as an increase in the expression and function of one or several glycine transporters, is crucial to the rapid proliferation of some cancer cells and supports their nucleotide and GSH synthesis. Inhibition of glycine uptake may therefore promote cancer cell death and arrest tumour growth. Glycine transporters, specifically GLYT1, are put forward as a potential therapeutic target in highly proliferative cancers, such as those of breast, intestine and skin that are often linked to poor prognosis. As activating transcription factors also play an important role in cellular stress and amino acid deprivation, we propose that ATF4 drives enhanced expression of transporters and enzymes required to meet the enhanced glycine requirement of highly proliferative tumour cells and also contribute to tumour malignancy, increasing expression of ATF3, ATF5 and ATF6.

1.8.1 *Aims and Objectives*

1. Investigate whether down-regulation of glycine transport mRNA expression has an influence on glycine uptake and cell proliferation rate of rapid and slowly proliferating tumour cell lines and also in non-transformed cell, with main focus on the specific glycine transporter GLYT1. Additionally, to evaluate the influence of GLYT1 downregulation on other amino acid transporters able to transport glycine mRNA expression.

2. Evaluate the influence of GLYT1 downregulation on glycine uptake, GSH production and DNA replication and their differences between rapid and slow proliferating tumour cell lines.

3. Evaluate the effect of specific GLYT1 inhibitors on cell proliferation of tumour cells with different proliferating profiles and also in non-transformed cell lines. Additionally, evaluate GLYT1 inhibitor influence on cell proliferation when cells are subject to hypoxia and ER stress conditions.

4. Investigate the role of ATF4 in regulating glycine supply to cancer cells and its effect on cell proliferation rate, glycine transporter expression and function and GSH synthesis. Also investgate possible interactions between ATF4 and ATF3/ATF5/ATF6 and relevance to cancer cell growth and proliferation.

Chapter 2. Materials and Methods

2.1 Materials

2.1.1 *Cell Culture*

The following cell lines were utilised in this work: A549 (non-small cell lung cancer - NSCLC) from ATCC and HUVEC (normal human Umbilical Vein Endothelial cells) from Lonza kindly donated by Dr Mike Gray and Professor Dianne Ford from Newcastle University, respectively; HT29 (colon adenocarcinoma) and A498 (kidney carcinoma), purchased from ATCC (ATCC®, USA). Further details and characterisation of the cell lines is provided in Chapter 3.

Cell culture media, Dulbecco's Modified Eagle's Medium - high glucose (DMEM) and RPMI-1640 (RPMI), and the supplements non-essential amino acids, penicillin/streptomycin (Pen/Strep), glutamine and foetal calf serum (FCS) were obtained from Sigma-Aldrich (UK). The Endothelial Growth Medium BulletKit™ (EGM) was purchased from Lonza, Switzerland.

2.1.2 *Equipment*

All cell culture work was carried out in a sterile environment utilising Safety Cabinets Class II Type Safeflow 1.2 (Bioair, EuroClone, IT) and cells were incubated in Sanyo MCO-20AIC CO_2 incubators with inCu safe, IR sensor and safe cell UV (Sanyo Eletric Co., Ltd., Japan). Cell number was analysed utilising Cellometer AutoT4 Cell Counter (Nexcelom, Bioscience, USA).

Fluorescence and absorbance measurements were performed in TECAN Infinite M200 (Tecan Trading AG, Switzerland) and FLUOstar Omega (BMG Labtech GmbH, Germany) plate readers, respectively. A LightCycler® 480 System (Roche Molecular Systems, Inc.) was utilised to perform qPCR reactions. RNA absorbance was measured on a spectrometer Biomate-3 (Thermo-Scientific, USA). Western Blotting membranes were analysed in Odyssey® Infrared Imaging System (Li-Cor, USA). Radioactivity in samples was determined by liquid scintillation spectrophotometry using a Beckman LS5000 liquid scintillation counter (Beckman-Coulter Ltd, UK).

2.1.3 *Chemicals and substrates*

The inhibitor ALX-5407 as well as all Kreb's buffer reagents were purchased from Sigma-Aldrich (UK). Total RNA extraction kit, CellTiter Blue reagent and GSH-glo assay were obtained from Promega (UK). Click it Edu assay was from ThermoFisher (USA). ATF4 antibody (CREB-2 (C-20): sc-200) was purchased from Santa Cruz Biotechnology (USA) and sense and anti-sense primer pairs were synthesised by IDT (Glasgow). Silencer® Select Negative Control 2, GLYT1 (si2993 and si2991) and ATF4 (si702, si704) siRNAs were purchased from Ambion™ (Invitrogen, ThermoFisher Scientific). Radiolabelled [2-^{3}H]-Glycine was obtained from Perkin Elmer (UK).

2.2 Cell Culture Methods

A549, HT29 and A498 are included in the NCI60 tumour cell line panel and data related to these cell lines are available for public consultation (DTP). According to NCI60 analyses HT29 and A549 cell lines present rapid proliferative phenotype and A498 a slowly proliferating profile (Table 2.1).

Cell Line	HT29	A549	A498
NCI-60 Doubling time (h)	19.5	22.9	66.8

Table 2.1: Cell line doubling times in hours, according to NCI60.

2.2.1 *Cell maintenance*

A549, HT29 and A498 were cultured in high glucose DMEM supplemented with 10% Fetal Calf Serum (FCS), 2mM L-glutamine, 1% non-essential amino acids (NEAAs), 100U /ml penicillin and 100µg/ml streptomycin. Alternatively, all cell lines were cultured in RPMI supplemented with 10% FCS, 2mM L-glutamine, 100U/ml penicillin and 100µg/ml streptomycin prior to treatments. HUVEC cell line was cultured in EBM™ Basal Medium (EGM) supplemented with Bovine Brain Extract, Ascorbic Acid, Hydrocortisone, Epidermal Growth Factor (hEGF), Fetal Bovine Serum (FBS) and Gentamicin/Amphotericin-B. Cells were incubated at 37^{o}C, 5% CO_2 in a sterilised, humidified incubator and grown on 75cm^2 canted neck cell culture flasks (Corning Inc, USA). DMEM and RPMI nutrient concentrations are shown in Table 2.2.

	DMEM + NEAAs	RPMI
Component	**mg/L**	**mg/L**
D-Glucose	**4500**	**2000**
Amino Acids		
L-Alanine	44.5	0
L-Arginine	84	200
L-Aspartic Acid	66.5	20
L-Asparagine	75	50
L-Cysteine	62.6	65.2
L-Glutamic Acid	73.5	20
Glutathione (reduced)	0	1
L-Glutamine	584	300
Glycine	**67.5**	**10**
L- Histidinde	42	15
L-Hydroxy L-Proline	0	20
L-Isoleucine	105	50
L-Leucine	105	50
L-Lysine	146	40
L-Methionine	30	15
L-Phenylalanine	66	15
L- Proline	57.5	20
L-Serine	**94.5**	**30**
L-Threonine	95	20
L-Tryptophan	16	5
L-Tyrosine	103.79	21.84
L-Valine	94	20
Vitamins	0	0
D-Biotin	0	0.2
Choline Chloride	4	3
Folic Acid	4	1
myo-Inositol	7.2	35
Niacinamide	4	1
p-Aminobenzoic Acid	0	1
D-pantothenic Acid	4	0.25
Pyridoxine	4.04	1
Riboflavin	0.4	0.2
Thiamine	4	1
Vitamin B12	0	0.005

Table 2.2: DMEM and RPMI-1640 nutrient composition. Additionally, 10% FCS and 2mM L-glutamine were added to each medium. 1% (5ml) of Non Essential Amino Acids (Sigma Aldridge, M7145) were added to DMEM medium, and reported values are final concentrations. Note, glycine concentration in DMEM is 67.5 mg/L and in RPMI is 10mg/ml; serine concentration in DMEM is 94.5 mg/ml and in RPMI is 30 mg/ml.

Culture medium was changed every 2-3 days. When confluent, monolayers were harvested and passaged to new tissue culture 75cm^3 flasks. For that, cells were washed with phosphate buffered saline (PBS), then 5ml trypsin was added and cells were incubated at 37^{o}C, 5% CO_2 for 3-4 minutes to detach them from the plastic. They were transferred into a sterile universal tube and a minimum of 20ml of medium added. The tubes were centrifuged at 1200rpm for 3 minutes and the pellet resuspended into 10ml of appropriate medium (EGM, DMEM or RPMI) using a syringe to remove clusters. Then, 20µl of suspension was pipetted onto a cell counting chamber and the number of cells counted using a Cellometer *AutoT4* Cell Counter (Nexcelom Bioscience). Suspensions were then diluted and seeded at concentration of 1x10^6 per flask for A549, HUVEC and A498 cell lines and 3x10^6 for HT29 to stock culture. All tissue culture manipulation was undertaken in a class II laminar flow hood.

For experimental purposes, cells were inoculated into multi-well plates. Cells were seeded into 96-well F-bottom culture plates (Greiner Bio One International GmbH) at final concentrations of 1x10^3 cells/well for A549 and A498, and at 3x10^3 cells/well for HT29 and HUVEC cells in a final volume of 100ul of medium. When utilising 24 or 12-well plates all cells were seeded at concentrations of 3.5x10^4 and 7x10^4 cells/well in final volumes of 1 and 2ml of medium, respectively.

2.3 Cell treatments

2.3.1 *Knockdown assays*

Previous to RNA extraction, all cell lines were seeded onto 12-well clear-coated culture plates in RPMI medium and incubated for 24 hours. After this, the medium was replaced with 1ml antibiotic- free RPMI and the cells transfected with small interfering RNAs(siRNAs) for GLYT1 (s12991) or ATF4 (s1704 or s1702) or negative control siRNA (Silencer® Select Negative Control n^{o}2). For transfection reactions, 200µl of a mixture comprising 5pmol of the appropriate siRNA, 4µl Lipofectamine RNAi MAX and 196µl OptiMEM + GlutaMax (Gibco, Life Technologies), previously incubated for 20 min at room temperature, was added to each well. Cell lines treated with Silencer® Select Negative Control n^{o}2 (Life Technologies) were utilised as control; although its siRNA sequence is not provided, the manufacturer confirmed it possesses a similar G/C content as the other siRNAs, about 30% in sense sequence and 43% in antisense

sequence. Cells were incubated at 37ºC for 72 hours before RNA extraction. The experiments were performed in triplicate.

To analyse GLYT1 and ATF4 knockdown influence on cell proliferation, cells were seeded in either 96-well clear-coated culture plates or 96-well dark culture plates. Transfection was performed as described above adjusting transfection mixes of each siRNA to a final volume of 20 µl per well and culturing cells in a final volume of 120µl. Cells were incubated at 37ºC for 72hours before cell viability assays. The experiments were each performed with six replicates.

2.3.2 *ALX-5407*

The specific GLYT1 inhibitor ALX-5407, also known as N [3-(4'-fluorophenyl)-3-(4'-phenylphenoxy) propyl] sarcosine (NFPS), was utilised to inhibit GLYT1 function (figure 2.1). ALX-5407 was first diluted in DMSO to a stock concentration of 10mM. Prior to each experiment a stock aliquot was diluted in RPMI to obtain the required experimental concentrations. A549, HT29 and A498 cells seeded in 24-well plates in RPMI supplemented with 5% FCS and Pen/Strep and HUVEC cells seeded in EGM were incubated for 24h at 37ºC. Then medium was changed and cells were treated with 30, 60,120 or 1000nM ALX-5407 for 72 hours to evaluate its effect on glycine uptake. To evaluate ALX-5407 effect on cell proliferation, cells were seeded in 96-well plates and treated with 120nM ALX-5407 for 6, 24, 48, 72, 96 and 110 hours. Control cells were incubated with normal medium containing the same concentration of DMSO.

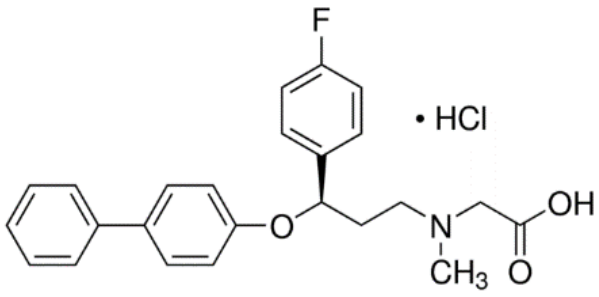

Figure 2.1 ALX-5407 chemical structure.

2.3.3 *Tunicamycin*

Tunicamycin (TM) obtained from Sigma-Aldrich (UK) was first diluted in DMSO to a stock concentration of 1mM (figure 2.2). Prior to each experiment a stock aliquot was diluted in FCS-free RPMI to obtain the required concentrations. Cells were seeded in 96-well plates in RPMI for 72h at 37ºC in an incubator, after this period the medium was changed to a FCS-free medium and cells were treated with 0.1, 0.5, 1, 2 or 4μM TM alone or in association with 120nM ALX-5407 for 12 hours to evaluate its effect on cell proliferation. Control cells were incubated with normal medium containing the same concentration of DMSO.

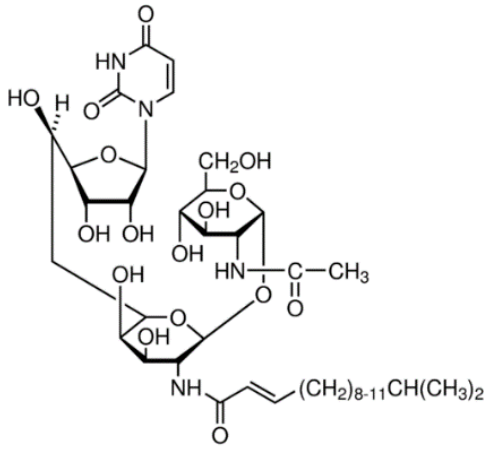

Figure 2.2: Tunicamycin chemical structure.

2.3.4 *Hypoxia*

Cells were seeded in 96-well plates in RPMI for 24h in an incubator at 37ºC before hypoxia treatment. The medium was replaced and cells were treated with 30, 60, 120 or 1000nM ALX-5407 and plates were placed in a hypoxic chamber INVIVO$_2$400 (Baker Ruskinn, USA), with 2% oxygen at 37ºC, for a further 72h. Control cells were treated with the same final concentration of DMSO.

2.4 Molecular Biology

2.4.1 *RNA extraction and Reverse-Transcription*

To analyse the possible influence of medium composition on amino acid transporter expression, total RNA was extracted from confluent monolayer of cells cultured in a 6-well plate in either DMEM or RPMI-1640. In order to verify transfection efficiency and knockout influence on gene expression total RNA was extracted from cells cultured in a 12-well plate following 72h of transfection. The SV Total RNA extraction kit (Promega) was utilised to extract total RNA following the manufacturer's vacuum protocol which includes a DNAse digestion to eliminate possible genomic DNA contamination. RNA yield, concentration and purity was quantified on a spectrometer (Biomate-3) measuring absorbance at $OD_{260/280}$ and $_{240}$.

Total RNA was diluted to obtain 500ng in 12.5µl then 50pmole of random hexamers (GE Bioscience) was added. Samples were incubated at 65^0C for 5 minutes, then immediately placed on ice to melt secondary structures within the template and avoid them reforming. The cDNA was obtained through further incubation of the samples with 12µl M-MLV Reverse Transcriptase (RT) reaction mix, final volume 24.5µl, at 42^{o}C for 2 hours in Px2 Thermo Cycler (Thermo, USA). Each mix contained 0.5mM each dNTP (Promega), 1xRT reaction buffer, 20U ribonuclease inhibitor (RNasin, Promega) and 200U of M-MLV Reverse Transcriptase (RT, Promega). A final step at 70^{o}C for 3 minutes was included to inactivate the RT. In addition to polymerase activity, M-MLVRT has RNase H activity which eliminates the remaining RNA and RNA-DNA double strand. As control some samples were prepared in duplicate and M-MLV RT was omitted (RT-negative control).

2.4.2 *End-point PCR*

For verification of GLYT1, ATF3, ATF4, ATF5, PAT1/2, SNAT2/4, xCT and $ATB^{o,+}$ gene expression in tumour cell lines, cDNAs obtained from A549 and HT29 cells grown in DMEM or RPMI were used as template for end-point PCR reactions. For these, 2µl of RT product was incubated with 1.25U goTaq DNA polymerase (Promega), 0.5µmol of forward and reverse primers (Table 3), 1x goTaq buffer and 0.2mM dNTPs (Promega) in a total volume of 25µl. The amplification used the following incubation conditions in a Px2 Thermo Cycler: 1 cycle at 95^{o}C for 3 min (DNA polymerase

activation); 30 cycles at 92ºC for 20 sec (denaturation), 55-65ºC for 20 sec (annealing), 70ºC for 20 sec (elongation); and 1 cycle at 72ºC for 10 min (final elongation). Samples were resolved on 2% agarose/Tris-borate EDTA (TBE) gels stained with SafeView (NTS Biologicals Ltd.), together with 100bp DNA ladder (Bioline) and the fragment sizes analysed on an AlphaInnotech Gel Document system.

2.4.3 *Quantitative Real-Time PCR (qPCR)*

The transcriptional profile of genes analysed was determined by quantitative real-time qPCR on a Lightcycler 480. Sense and anti-sense primer pairs for target mRNAs were synthesised by IDT (Table 2.3). Primers were designed to obtain amplicons of up to 200bp, have approximately 50% GC content, to avoid secondary structure formation and for the primers in each pair to be located on different exons, thus avoiding amplification of any contaminating genomic DNA. RT-products were diluted 1 in 5 for qPCR reactions. Each qPCR mixture contained 2µl diluted RT product, 1x Lightcycler 480 SYBR Green 1 Master or Lightcycler Probes Master (Roche) and 0.5µM forward and reverse primer. A hot-start cycling protocol (pre-incubation at 95ºC for 5 min) followed by 35-40 cycles of 5" at 95ºC, 10" at 58-62ºC, and 15 sec at 72ºC, was followed by melt curve analysis over a 60-90ºC range to confirm specific product amplification. Each assay included duplicate sample reactions and negative control wells (RT-negative control and blank).

Serial dilutions (1:10) of a positive control, specific for each primer, were included in all qPCR experiments to obtain a standard curve. The positives controls were obtained by cloning the PCR products in the cloning vector pGEM®-T Easy (Promega). Vectors were transfected into E. coli DH5α and the plasmid DNA was extracted and sequenced to confirm primer specificity. Dr. Alison Howard performed these experiments prior to this study. Plasmids were diluted to an optimal concentration and utilised to obtain standard curves, which were included in all experiments permitting the reaction efficiency calculation. The amplification efficiency (E) is calculated according to the slope of the standard curve utilising the equation $E=10^{-1/slope}$, the dilution factor being 10. In an ideal qPCR reaction, the template would double after each amplification cycle, thus implying an amplification efficiency of 2 and, therefore, an optimal slope of the standard curve of -3.32. Thus, it is possible to obtain the slope of the standard curve and the reaction efficiency for every single reaction.

Considering the ideal efficiency for the qPCR reaction (2), the percentage of efficiency is calculated according to the equation %E= (E-1) x 100%. Results with reaction efficiency of 85-105%, or 1.9-2.05, were considered for the study.

Gene name	NCBI id	Primer sequence (with base numbering)	Exon position	Annealing temp. (^{O}C)	Product size (bp)
Glyt1[1]	NM_001024845 (transcript variant 3)	Sense: ^{580}CCATGTTCAAAGGAGTGGGCTA^{601} Antisense[2]: cggc^{651}TGACCACATTGTAGTAGATGCCG^{629}	4:5 5	60	76
xCT	NM_014331	Sense[2]: cggag^{1342}CCTCTCCATGATTCATGTCCG^{1362} Antisense: ^{1437}TCGAGGTCTCCAGAGAAGAGCA^{1416}	9 10	60	96
ATF3 (all)[2]	NM_001674 (transcript variant 1)	Sense: ^{480}TGTCCTCTGCGCTGGAATCAG^{500} Antisense: ^{640}CGTCTTCTCCTTCTTCTTGTTTC^{618}	2 3	60	161
ATF4[3]	NM_001675 (transcript variant 1)	Sense: ^{1011}CTTCAAACCTCATGGGTTCTCCAG^{1034} Antisense: ^{1179}CAGGGCATCCAAGTCGAACTC^{1159}	1 2	60	169
ATF5[4]	NM_012068 (transcript variant 1)	Sense: ^{344} TGTAGCCTCGACCCCTTTGTG^{364} Antisense: ^{284}CAGGCACCAAGGCGAAAGTG^{265}	1 2	60	146
SHMT2[5]	NM_005412 (transcript variant 1)	Sense: ^{1043}CAAGACTCTTGCAGGGGCCAG ^{1063} Antisense: ^{1171}GATGGGAACACGGCAAAGTTG ^{1151}	7 8	60	129
Ki67[6]	NM_002417 (transcript variant 1)	Sense: ^{2375}TACATGTGCCTGCTCGACCC^{2394} Antisense: ^{2499}CTGCGGTTGCTCCTTCACTG^{2480}	12 13	60	125
PAT1	NM_078483	Sense: ^{1180} CATAACCCTCAACCTGCCCAAC^{1201} Antisense: ^{1278} GGGACGTAGAACTGGAGTGC ^{1259}	8 9	58	104
PAT2	NM_181776	Sense: ^{262}GTCAGCAGGCTTGAAGAAGAC^{282} Antisense: ^{369}TTCACAGCGAGGGGTAGTCC^{350}	1 2	58	108
SNAT2	NM_018976	Sense: ^{331}TGCGTGAGAATAGAGACCACC^{351} Antisense: ^{426}GGAATCGGGTGCAGCTAGTA^{407}	1 2	60	96
SNAT4[7]	NM_018018 (transcript variant 1)	Sense: ^{73} CTCGGGACACCCCACTCACAC^{93} Antisense: ^{155}CAAGCCAATCAACACCACCACC^{134}	1 2	60	83
ATB$^{0,+}$	NM_007231	Sense: ^{815}CTTCTTCTGGCTTGGCTCATAG^{836} Antisense: ^{958} TGAAGCACCCTCCAGAGTTGC ^{938}	6 6/7	60	144

Table 2.3: Primers utilised in end-point PCRs and qPCRs. Description includes gene name, NCBI identification number, sequence, exon position, annealing temperature and product size.

[1]This primer pair will detect all GLYT1 transcript variants except the long non-coding variant 6. Primer locations in GLYT1a (variant 3) only are given
[2]This primer pair will detect all ATF3 transcript variants. Primer locations in variant 1 only are given.
[3]This primer pair will detect ATF4 transcript variants 1 and 2; both encode the same protein. Primer locations in variant 1 only are given.
[4]This primer pair will detect ATF5 transcript variants 1 and 2; both encode the same protein. Primer locations in variant 1 only are given. (Note: there are three transcript variants that all encode the same protein; this primer pair will not detect transcript variant 3 (added to Genbank post-design)
[5]This primer pair will detect all SHMT2 transcript variants. Primer locations in variant 1 only are given.
[6]This primer pair will detect Ki67 transcript variants 1 and 2. Variants 1 and 2 both encode the same protein. Primer locations in variant 1 only are given.
[7]This primer pair will detect only SNAT4 transcript variant 1. Variants 1 and 2 both encode the same protein. Primer locations in variant 1 only are given.

The qPCR results for each primer were normalised with housekeeping genes GAPDH, TOP1 and ATP5B (PrimerDesign Southampton, UK). Normalisation factor was generated from geometric averaging of the three reference genes utilising the GeNorm programme(Vandesompele et al., 2002). For each assay a standard curve using five serial dilutions (1:10) of appropriate cloned target PCR products was utilised to infer the arbitrary units of relative mRNA concentration. Since the same sample for each primer was utilised in multiple PCR reactions to generate the qPCR standard curves, the Cp of the standards was utilised to calculate the percentage of the coefficient of variation (CoV) of the qPCR reactions according to the equation: %CoV= (Standard Deviation/Cp mean)*100.

2.4.4 *Protein extraction and measurement*

Following GLYT1 and ATF4 knockdown total protein was extracted utilising RIPA Buffer (Sigma-Aldrich, UK) with 1 x Roche complete mini protease tablet (1%). Bradford Reagent (Sigma-Aldrich) was utilised for protein measurements, this assay utilises Coomassie Brilliant Blue G-250 dye in a solution with phosphoric acid. In acidic conditions the dye is in its protonated cationic form, presenting colour red and maximum absorbance at 470nm. When the dye binds to proteins, it becomes unprotonated presenting colour blue and maximum absorbance at 595nm, which is then measured. Bradford reagent was added to each sample in a proportion 20:100, samples were then incubated for 5 minutes and absorbance measured at 595nm. To obtain a standard curve, serial dilutions of BSA in distilled water were performed to final concentrations of 0.025, 0.125, 0.25, 0.5, 0.75, 1, 1.5, 2µg/ml; then treated with Bradford reagent and absorbance was measured. Protein concentrations were determined utilising the standard curve's equation.

2.4.5 *Western Blotting*

Samples were diluted in sterile distilled water to obtain 1µg/ml of protein. Then 4X NuPAGE LDS sample buffer and 10X Reducing Agent were added to the samples to 1X final concentration. The mixture was heated for 10min at 70ºC and loaded onto the pre-cast NuPAGE gel following the manufacturer's instructions. The mini cell apparatus was set up, the upper chamber was filled with running buffer, checked for

leaks and buffer was added to the lower chamber; 200 V constant voltage was applied for 50 minutes.

For electroblotting, the transfer tank was filled with NuPAGE Transfer buffer containing 10% methanol. Nitrocellulose membranes, blotting pads and filters were soaked in transfer buffer for 10 minutes. The nitrocellulose membrane was placed on the gel, three filter papers and one foam mesh were placed in each side (figure 2.3), and the cassette was clamped shut and placed in the transfer tank. 20 V was applied to the blot overnight with cooling.

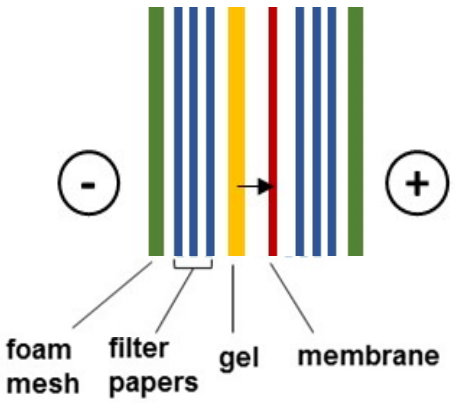

Figure 2.3: Nitrocellulose membrane, gel and filter papers arrangement for electroblotting.

Blocking and antibody incubation

The membrane was wet in 1x PBS for several minutes and blocked in Odyssey Blocking Buffer for 1 hour. Then, the membrane was incubated at 4ºC overnight with primary antibody, rabbit anti-CREB-2 from human origin (anti-ATF4) IgG, diluted 1:250 in Odyssey Blocking buffer with 0.2% Tween-20, to lower the background. The membrane was washed four times for 5 min at room temperature (RT) in PBS:0.1% Tween-20 with gentle shaking then incubated for 60 minutes at RT with secondary antibody, anti-rabbit IgG labelled with AlexaFluor®680 diluted 1:5000 in Odyssey blocking buffer:0.2% Tween-20, with gentle shaking and protected from light. It was then washed four times for 5 min each at RT in PBS:0.1% Tween20 with gentle shaking and protected from light. The membrane was rinsed to remove residual Tween-20 and was then ready to scan. To normalise the results, the process was repeated utilising as primary antibody mouse anti-βactin IgG from human diluted 1:8000 and as

secondary antibody anti-mouse IgG labelled with AlexaFluor®480 diluted 1:10000. The membrane was analysed utilising Odyssey® Infrared Imaging System (Li-Cor,USA).

2.4.6 *Immunocytochemistry*

Cells were seeded on 13mm coverslips placed into 12-well plates and transfected with GLYT1 siRNA or Negative siRNA as described in section 2.3.1. After 72 hours transfection, wells were washed with PBS three times. Cells were then fixed with 4% paraformaldehyde (PFA) in PBS, which was prepared on the day of the experiment, for 30 minutes on ice. Coverslips were washed three times with PBS and permeabilised with 200µl of 0.1% Triton X-100 in PBS for 30 minutes at RT. Coverslips were washed again three times and blocked with 10% donkey serum in PBS for 30 minutes at 4ºC followed by another washing step. Coverslips were incubated with primary antibody, goat anti-rat GLYT1 antibody, diluted 1:150 in PBS, overnight at 4º C. Negative controls were incubated with blocking serum only and washed with PBS. Then cells were incubated with secondary antibody, AlexaFluor® 488-labelled donkey anti-goat IgG diluted 1:8000, for 1h at 4ºC. Coverslips were washed again with PBS and then lowered over slides containing a drop of Vectashield mounting medium with DAPI, to stain cell nuclei. Coverslips were then analysed in an Axio Imager with Apotome microscope (Zeiss, Germany) with fluorescent filters for AlexaFluor®488 and DAPI.

2.5 Cell Proliferation assays

2.5.1 *Cell Titer-blue*

CellTiter Blue (CTB) assay was used to verify cellular viability and proliferation. Viable cells are able to metabolise CTB reagent, rezasurin, in a mitochondrial REDOX reaction to resorufin then fluorescence and/or absorbance can be measured (figure 2.5). Briefly, 20µl of CTB were added to each well and incubated at 37ºC for 3-4 hours, then, for cells growing in transparent plates, absorbance was measured at 570-600nm and for cells growing in dark plates, fluorescence at 560ex/590em and absorbance were measured.

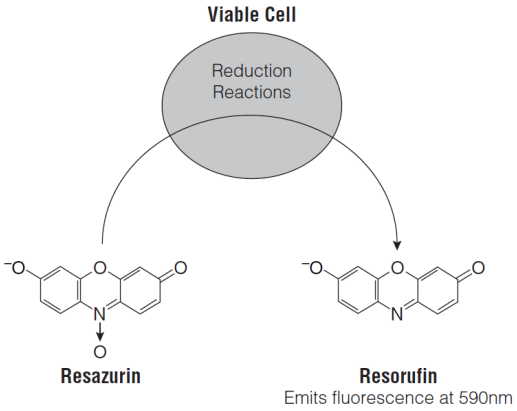

Figure 2.4: Conversion of resazurin to resorufin by viable cells. (From Promega CellTiter-Blue® technical bulletin)

Viable cells are able to reduce resazurin, with absorbance maximum of 605nm, to resorufin, absorbance maximum of 573, so the absorbance at 570nm was measured and normalised to the absorbance at 600nm utilising an equation formulated by Willard et al. (Willard HH et al., 1965) and provided by the AlamarBlue® manufacturer(Invitrogen), (AlamarBlue is another resasurin commercial name) (Figure 2.5). Alternatively, fluorescence can be measured, since resazurin has little intrinsic fluorescence and resorufin is highly fluorescent (560ex/590em).

$$= \frac{(\varepsilon_{OX})\lambda_2 A\lambda_1 - (\varepsilon_{OX})\lambda_1 A\lambda_2}{(\varepsilon_{RED})\lambda_1 A'\lambda_2 - (\varepsilon_{RED})\lambda_2 A'\lambda_1} \times 100$$

Figure 2.5: Equation to calculate the percentage of resazurin reduction to resorufin. Where, C_{RED} = concentration of reduced form Cell-Titer Blue® (RED), C_{OX} = oxidised form of alamarBlue® (BLUE), ε_{OX} = molar extinction coefficient of Cell-Titer Blue oxidised form (BLUE), ε_{RED} = molar extinction coefficient of Cell-Titer Blue reduced form (RED), A = absorbance of test wells, A' = absorbance of negative control well. The negative control well contained only medium and Cell-Titer Blue but no cells, A° = absorbance of positive growth control well; λ_1 = 570nm (540nm may also be used); λ_2 = 600nm (630 may also be used). Considering (εOX)λ2 = 117,216; (εOX)λ1 = 80,586; (εRED)λ1 = 155,677; (εRED)λ2 = 14,652 (Adapted from Alamar Blue guide(Invitrogen))

2.5.2 *Doubling Time*

For proliferation rate experiments, 8,000 cells were seeded in a 96-well plate, incubated at 37ºC, and 20µl of CTB added per well, in six replicates, after 24, 48, 72 and 96h. After each addition the plate was incubated for a further 3h prior to absorbance measurement and calculation of doubling time.

In order to compare and evaluate CTB results for doubling time, cell counting was performed. A549 and HT29 cell lines were seeded in transparent 12-well plates at initial density of $1.48x10^5$ and $1.62x10^5$cells/well with DMEM or RPMI. After 24, 48, 72 and 96h the spent medium was removed, cells washed with PBS and detached from the plates utilising 500µl trypsin per well. Harvested cells were placed into conical universal tubes and 2.5ml of respective medium added and the suspension homogenised with a syringe; finally 20µl cell suspension were placed in a cell chamber and counted in a Cellometer AutoT4 Cell Counter (Nexcelom, Bioscience, USA).

2.5.3 *Click-It EdU assay*

In this assay, a nucleoside analogue of thymidine, EdU (5-ethynyl-2'-deoxyuridine), is utilised during DNA replication and it is incorporated into new DNA strands. Then a fluorescent azide compound, Alexa Fluor® 488, is added to label cells that incorporated EdU during DNA synthesis. First cells were plated on coverslips and follow transfection with GLYT1 or Negative siRNAs as specified in session 2.1.3 for 72h. Then coverslips were transferred into 6-well plate containing 500µl RPMI medium and an equal volume of the 20µM EdU solution, prepared on the day of the experiment from the 10mM in DMSO stock, was added to each well to obtain a 10µM solution and incubated for 50 minutes. In the next step cells were fixed and permeabilised, the medium was removed and 1 mL 3.7% paraformaldehyde (fixative) in PBS was added to each well and the plate was incubated for 15 minutes at RT. The solution was removed and cells washed twice with 1 mL 3% BSA in PBS. Then 1 ml 0.5% Triton® X-100 in PBS (permeabilisation buffer) was added to each well and the plate incubated for 20 minutes. In the last step, Click-iT® reaction cocktail was prepared by adding the following amounts to the Alexa Fluor® amber vial: 100 µL Click-iT® reaction buffer, 800 µL $CuSO_4$ and 100 µL 1X Click-iT® reaction buffer additive that was utilised within 15 minutes after preparation; 0.5 ml Click-iT® reaction cocktail was added to each well and the plate incubated for 30 minutes, protected from light. Click-iT®

reaction cocktail was removed and coverslips were washed twice with 1 mL 3% BSA in PBS, then coverslips were lowered over slides containing a drop of Vectashield mounting medium with DAPI, to stain cell nuclei. Coverslips were then analysed on microscope Axio Imager with Apotome microscope utilising filters appropriate for the Alexa Fluor®488 dye and DAPI.

2.6 Measurement of glycine uptake

Following cell line treatments, knockdown experiments or ALX-5407 treatment, glycine uptake experiments were performed. Kreb's buffer was prepared freshly on the day of the experiments (137mM NaCl, 5.4mM KCl, 1mM $MgSO_4$, 0.3mM KH_2PO_4, 0.3 mM NaH_2PO_4, 10 mM glucose, 10mM HEPES and 2.8mM $CaCl_2$ diluted in water), pH was adjusted to 7.5 and buffer was divided in two vials, one stored at 4ºC and other incubated at 37ºC. Medium was removed from cell culture plates, wells were washed three times with 37ºC Kreb's buffer and cells incubated for 30-60min at 37ºC with Kreb's buffer. For time dependent experiments, 5μM glycine and 0.5μCi/ml [2-^{3}H]-Glycine solutions were prepared and cells were incubated for 0, 5, 10 or 30 minutes at 37ºC. For concentration dependent experiments, 0μM, 1μM, 50μM, 100μM, 200μM, 300μM, 500μM or 1000μM glycine in association with 0.5μCi/ml [2-^{3}H]-Glycine solutions were prepared and incubated for 10 minutes at 37ºC. The reactions were stopped by removing glycine solutions and adding ice-cold Kreb's buffer three times. Then, 250μl of 0.1% SDS was added for at least 30 minutes to lyse the cells. Additionally 100μl of the radiolabelled glycine solutions utilised to incubate the cells were utilised as reaction standards. Cell lysates were transferred to scintillation vials, 2mL of Gold Star Multi-purpose Liquid Scintillation Cocktail (Meridian Biotechnologies Ltd) was added and vials were vortexed.

Calculation of glycine uptake

Radioactivity in the samples was determined by liquid scintillation spectrophotometry using a Beckman LS5000 liquid scintillation counter (Beckman-Coulter Ltd, UK). A vial containing 2ml of scintillation fluid was utilised as blank to subtract background activity from the counts. The amount of substrate was calculated using the following equation:

$$\textbf{Amount of substrate} = \left(\frac{A_{STD}}{DPM_{STD}} \times DPM_{SPL}\right)/X$$

Figure 2.6: Equation to calculate the amount of glycine uptake. Where, A_{STD} = amount of substrate in 100µl of the standard, DPM_{STD}= average disintegration per minute of the radiolabelled substrate from three standards, DPM_{SPL} = represents the disintegration per minute of a sample, **Constant X** = surface area per well, 3.8 and 1.9 for 12 and 24-well plates, respectively, used to express the result in cm^2.

2.7 Quantification of Glutathione Levels

GSH-Glo assay

The GSH-Glo™ Glutathione Assay is a luminescence-based assay for glutathione (GSH) measurement. The assay is based on the conversion of a luciferin derivative into luciferin in the presence of GSH, catalysed by glutathione S-transferase (GST). Luminescence is then generated proportional to the amount of GSH present in the sample (figure 2.7). After GLYT1 siRNA or ALX-5407 treatments in 96 well plates, medium was removed and 100µl of prepared 1X GSH-Glo™ Reagent* was added to each well. Plates were mixed briefly and incubated for 30 minutes. Then 100µl of reconstituted Luciferin Detection Reagent was added to each well. Plates were mixed briefly and incubated for 15 minutes. Luminescence was measured. Standards curves were prepared in all experiments using a GSH standard solution (5mM). First, GSH 5mM stock was diluted in water (1:100), and then serial 1:1 dilutions were performed. Then, 10µl of each diluted standard was transferred to the appropriate wells for the assay. Concentration ranges from 0µM to 5µM were utilised.

* For 96-well plate experiments 10ml of GSH-Glo™ Reagent was prepared immediately prior to use by adding 100µl of Luciferin-NT substrate and 100µl of Glutathione S-Transferase to 10ml of GSH-GloTM Reaction Buffer.

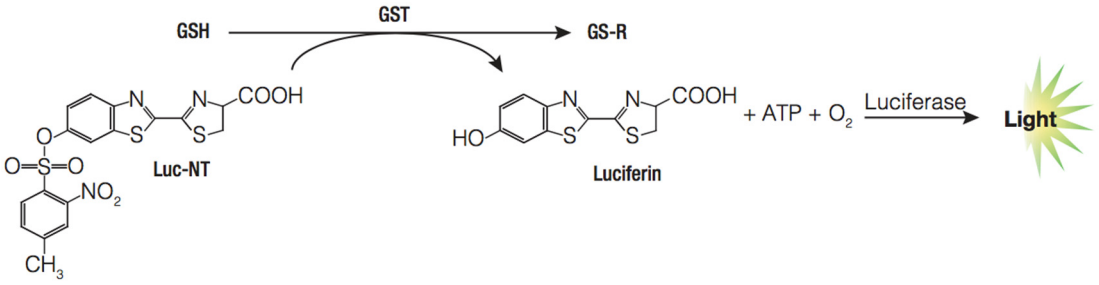

Figure 2.7: GSH-Glo™ Reaction. GSH is converted to GS-R in a reaction catalysed by the enzyme Glutathione S-Transferase (GST) which converts Luciferin-NT substrate to Luciferin that can produce light in a reaction catalysed by the enzyme Luciferase. (From Promega GSH-Glo™ Glutathione Assay manufacturer manual).

2.8 Statistics

All statistical analyses were performed utilising GraphPad Prism 7.0 (GraphPad software Inc, USA). Data are presented as ± standard error of mean (SEM) of the number of replicates, where "N" represents the number of biological replicates, and "n" represents the total number of technical replicates. One-way Analyses of Variance (ANOVA) test was utilised to compare significance of difference between the data of three or more groups. Student *t*-test was utilised to compare significance of difference between two groups, control and treatment. Non-linear regression analyses were performed in glycine uptake experiments.

Chapter 3. Cell Lines Characterisation

3.1 Introduction

This chapter describes the cell lines utilised in this study and their characterisation. According to Jain *et al* (2012) the requirement for glycine was shown to be significantly greater in rapidly proliferating cancer cells than in either slow growing cancer cells or rapidly-proliferating non-cancerous cells (Jain et al., 2012). Therefore, in order to evaluate the influence of glycine transport on cell proliferation, one slowly, A498, and two rapidly, A549 and HT29, proliferating cell lines were selected. Additionally a non-transformed rapidly proliferating normal cell line, HUVEC, was utilised as control. The experimental growth rates of these cell lines were evaluated to confirm the literature data. Then, the competence of these cell lines to transport glycine was assessed by measurement of concentration and time dependent ^{3}H-glycine uptake. RT-PCR and qPCR were performed to assess the gene expression of amino acid transporters able to transport glycine, particularly the specific glycine transporter GLYT1, but also PAT1, SNAT2 and ATB$^{0,+}$. Additionally, the transcriptional profile of an enzyme involved in intracellular production of glycine, SHMT2, the proliferation marker, ki67, and the activating transcription factors (ATFs) ATF3, ATF4, ATF5 and ATF6 were evaluated. Finally, the mRNA expression of enzymes involved in glutathione (GSH) synthesis such as GCLC, GCLM and GSS and also cystine transporter subunit xCT, that also affect GSH synthesis, were analysed.

The number and frequency of cell division vary amongst different cell types (Fox, 2004). Cell proliferation rates are influenced by multiple factors such as genetic and epigenetic characteristics, immune system, and cellular metabolism (Fox, 2004, Morgan, 2007b). As described in chapter 1, when conditions are ideal for cell proliferation, cyclin-Cdk complexes are activated driving progression through the cell cycle at regulatory transition checkpoints (Morgan, 2007b). The levels and activity of these proteins are tightly controlled by multiple mechanisms, such as p53 which blocks the ability of cyclins to stimulate cell division (Fox, 2004, Morgan, 2007b). Nutrient and energy levels, regulated by mTOR, are also amongst the factors that affect cell growth (Mendoza et al., 2011). Some proteins are only expressed in the division phase of the cell cycle, one example is the nuclear protein ki67, which is considered a proliferation marker (Gerdes et al., 1983, Scholzen and Gerdes, 2000). Anti-ki67 antibodies are

being applied in diagnoses for some types of human tumours (Scholzen and Gerdes, 2000). The ki67-labeling index is calculated according to the ki67 positive fraction of the tumour and is utilised as a prognostic value for patient survival and tumour recurrence (Scholzen and Gerdes, 2000).

The rapid proliferation of cancer cells requires metabolic adaptation to sustain new physiological demands, which includes altered nutrient uptake and utilisation (Jain et al., 2012). Recent works are highlighting the relevance of glycine and glycine metabolism to cancer cell proliferation, thus the interest in studying its transporters and their regulators, such as ATF4. The solute carriers (SLCs) of the families SLC6A - SLC6A9 (GLYT1), SLC6A5 (GLYT2), SLC6A14 (ATB0,+), SLC36A - SLC36A1(PAT1), SLC36A2 (PAT2) and SLC38 - SLC38A2 (SNAT2) and SLC38A4 (SNAT4) are amino acid transporters involved in glycine transport. Different from GLYT1 and GLYT2, which are specific glycine transporters, these other amino acid transporters accept multiple amino acids as substrates (Mackenzie and Erickson, 2004, Schiöth et al., 2013, Sloan and Mager, 1999, Ganapathy and Ganapathy, 2005). Since GLYT1 possesses high affinity for glycine and is expressed in multiple organs apart from CNS it was selected as the focus of our study (Howard and Hirst, 2011, Borowsky et al., 1993, Borowsky and Hoffman, 1998). As described in chapter 1, the activation of mTORC1 by PAT1 and SNAT2 influences cell growth and differentiation. Additionally, PAT1, SNAT2 and $ATB^{0,+}$ have all been implicated in cancer progression (Karunakaran et al., 2008, Heublein et al., 2010, Schiöth et al., 2013). Since rapidly proliferative cells require extracellular glycine for purine and GSH production (Jain et al., 2012), these transporters may also play an important role in supporting growth and proliferation. Additionally, glycine is synthesised in the last step of serine synthesis pathway by the mitochondrial enzyme SHMT2, which is linked to poor cancer patient prognosis (Jain et al., 2012). Therefore, the expression of SHMT2 was evaluated.

GLYT1 is regulated by the activating transcription factor ATF4 that was linked to cancer progression (Harding et al., 2003, Singleton and Harris, 2012). Under amino acid starvation the GCN2–eIF2α–ATF4 pathway is activated and upregulates amino acid transporters and metabolism (Ye et al., 2010). For example, serine starvation increases ATF4 mRNA levels resulting in further transcription of the PHGDH, PSAT1 and PSPH proteins involved in the serine synthesis pathway (Ding et al., 2013, Ye et al., 2012). ATF4 contributes to amino acid homeostasis and is known to influence mTOR activation (Wortel et al., 2017). During oxidative stress ATF4 levels are increased and also regulates the synthesis of GSH (Sikalidis et al., 2014, Ehren and

Maher, 2013). ATF4 upregulates xCT, the subunit of the cystine transporter Xc^-, to meet cellular demand for cysteine, which is essential to maintain intracellular levels of GSH during oxidative stress (Sato et al., 2004, Gorrini et al., 2013, Huggins et al., 2015). Other studies also indicate that ATF4 upregulates the catalytic and modifier subunits of the glutamate-cysteine ligase, GCLC and GCLM, respectively, in the first step of GSH synthesis (Sikalidis et al., 2014). Glycine also contributes to GSH formation and is incorporated in the second step of GSH synthesis by the enzyme glutathione synthetase enzyme, GSS (Lu, 2013). The glycine transporter GLYT1 is also important to maintain GSH levels during stress (Howard et al., 2010). Thus, GCL, GSS and xCT mRNA expression were evaluated. ATF3 and ATF5 have been linked to tumour growth, survival and invasiveness (Nukuda et al., 2016, Thompson et al., 2009). ATF6 is activated when there is an accumulation of unfolded protein in the endoplasmic reticulum during stress and it regulates genes involved in autophagy and protein-folding (Sano and Reed, 2013). This way, these ATFs expression were also evaluated in this chapter.

3.2 Results

3.2.1 *Cell-Titer Blue optimisation*

Cell-Titer Blue (CTB) reagent was selected to quantify cell numbers and thus rates of cell proliferation. To verify if CTB assay correlated to cell number and would be a suitable assay for further experiments, cells were incubated in 96-well plates in RPMI in concentrations of $1X10^3$, $2X10^3$, $4X10^3$, $8X10^3$, $1.6X10^4$ and $3.2X10^4$ cells/100µl for 3 hours. Then 20µl/well of CTB was added and cells were incubated for further 4h prior absorbance measurements. All cell lines were able to metabolise the resazurin to resorufin and the percentage reduction was calculated according to the equation presented in chapter 2 Section 2.5.1, according to the absorbance measurements, and correlated to cell numbers. CTB absorbance measurement presented a linear correlation with cell number, from 1,000 up to 20,000 cells (Figure 3.1). This way, the initial seeding density chosen for CTB experiments was 1,000 cells/well for A549 and A498 cell lines and 2,000 cells/well for HT29 cell line, considering their literature doubling times of 22.9, 66.8 and 19.5hours, respectively, and the period of 96 hours required for the planned knockdown experiments. Hence, the cell number in the end of the experiments would not be higher than 20,000 cells/ well and suitable for CTB assay. HT29 cell line require cell to cell contact to grow, therefore the necessity for a higher seeding density, so this cell line could reach the exponential phase at similar rate as the other cell lines. The results are mean of a single experiment with five replicates.

Additionally, a test experiment was performed to analyse if the fold change in cell number following treatment with Negative, GLYT1 and ATF4 siRNAs was equivalent using cell counting and the CTB assay. A549 and A498 cells were seeded into 96-well plates at concentration of $1x10^3$ cells/well and in 12-well plates at concentration $2x10^4$ cells/well and HT29 cell at concentration $2x10^3$ cells/well in 96-well plate and $3x10^4$ cells/well in a 12-well plate in RPMI for 24h. Then, the medium was replaced with fresh antibiotic-free RPMI and cells were transfected with Negative, GLYT1 and ATF4 siRNAs and incubated for 72h. Subsequently cells from the 12-well plates were counted and CTB was added to the 96-well plates and incubated for further 3h prior fluorescence readings. For cell counting after treatments the medium was removed, cells washed with PBS and detached from the plates utilising 500µl trypsin per well. Harvested cells were placed into conical universal tubes and 2.5ml of

respective medium added and the suspension homogenised with a syringe; finally 20µl cell suspension were placed in a cell chamber and counted in a Cellometer AutoT4 Cell Counter.

When the fold change following the treatments were analysed as percentage of controls, both cell counting and CTB experiments presented similar results. For A549 cell lines following GLYT1 and ATF4 siRNA treatments, there was a reduction of 20% ($p<0.01$) and 38% ($p<0.001$) in cell number and 28% ($p<0.05$) and 39% ($p<0.01$) in fluorescence measurements, respectively, when compared to controls (Figure 3.2). For HT29 cell lines following GLYT1 and ATF4 siRNA treatments there was reduction of 35% ($p<0.01$) and 49% ($p<0.001$) in cell number and 30% ($p<0.001$) and 44% ($p<0.0001$) in fluorescence measurements, respectively, when compared to controls (Figure 3.3). For A498 cell lines following GLYT1 and ATF4 siRNA treatments there was reduction of 4% and 56% ($p<0.01$) in cell number and 10% and 57% ($p<0.01$) in fluorescence measurements, respectively, when compared to controls (Figure 3.4). Additionally, when comparing the fold change following each treatment between the two methods no statistical difference was observed. For cell counting experiments the results are mean of a single experiment made in triplicate and for CTB assay the results are mean from a single experiment with five replicates.

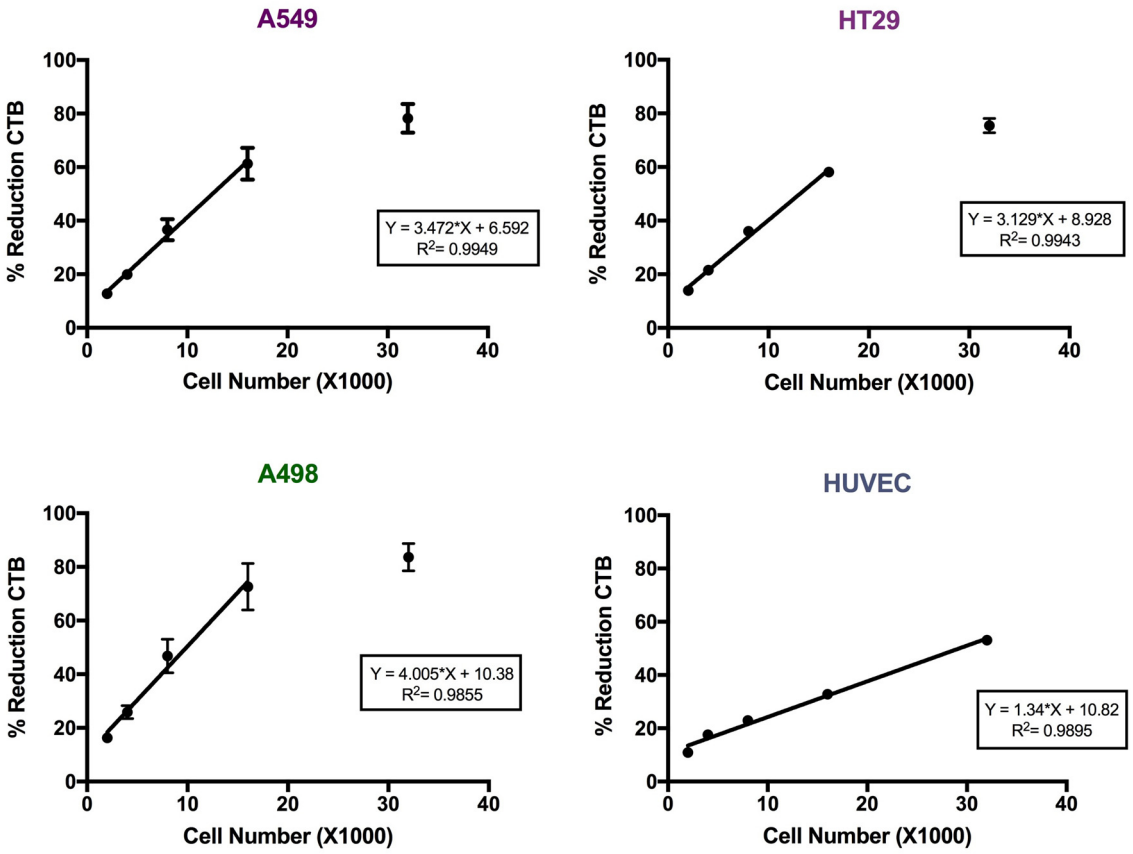

Figure 3.1: Cell-Titer Blue (CTB) assay analysis. Correlation between cell number from serial dilutions (1:1) of each cell line and percentage of resazurin reduction to resorufin, calculated according absorbance measurement at 570 and 600nm. Cells were seeded in RPMI and incubated for 3h prior to 4h incubation with CTB. Data are means ± SD, N=1 and n=5.

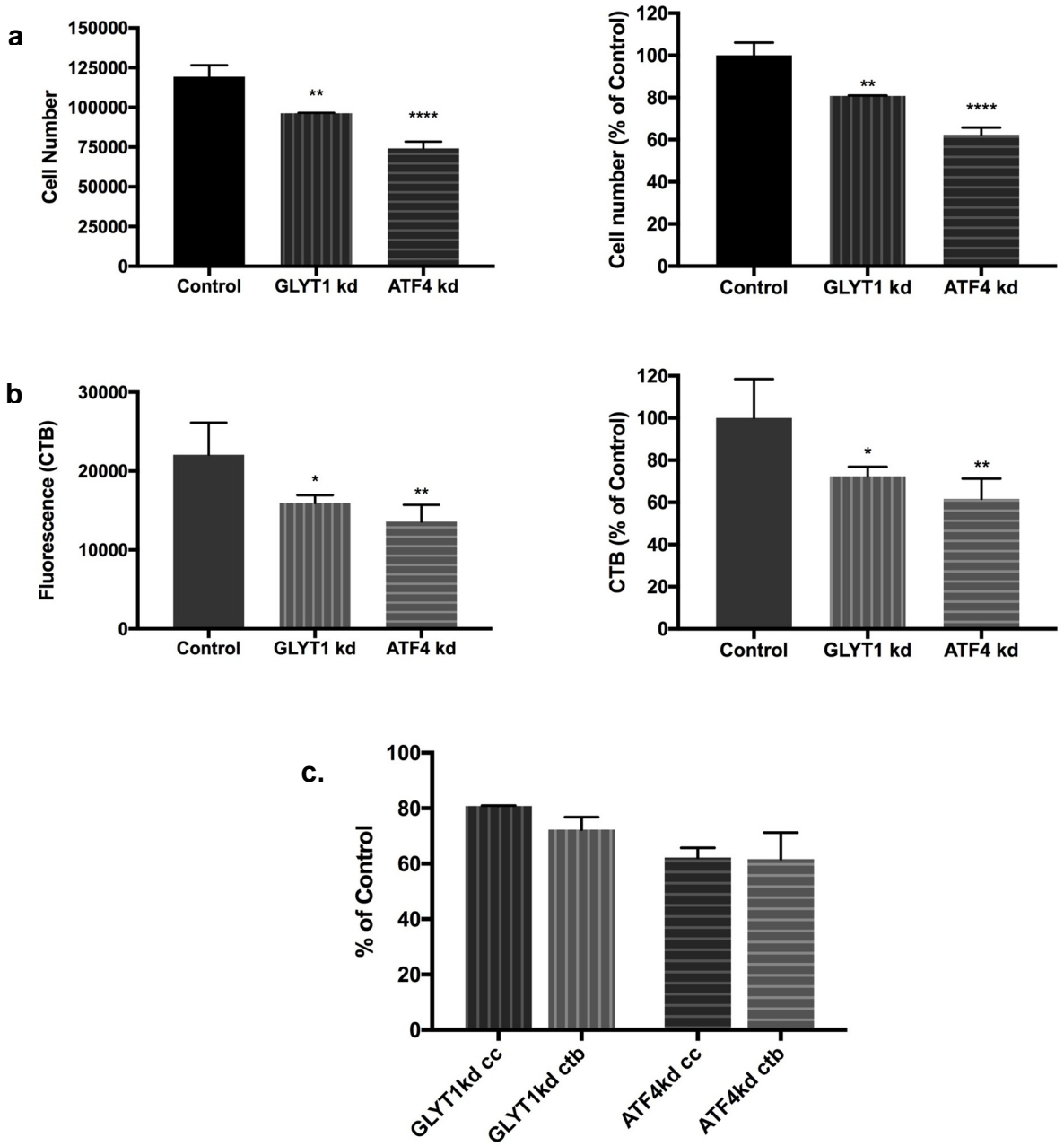

Figure 3.2: A549 CTB specificity. Correlation between cell counting (a) and fluorescence measurements after 4h incubation with CTB (b) following GLYT1 and ATF4 siRNA treatments for 72h. For each treatment the fold change in comparison to control cells (percentage of Control) was calculated to allow comparisons between both methods. No significant difference was observed between cell counting and CTB assay when analysing the effect of each treatment on cell number in comparison to control cells, GLYT1kd cc compared to GLYT1kd ctb and ATF4kd cc compared with ATF4kd ctb (c). For cell counting experiments data are means ± SD, N=1 and n=3. For CTB experiments data are means ± SD, N=1 and n=5.

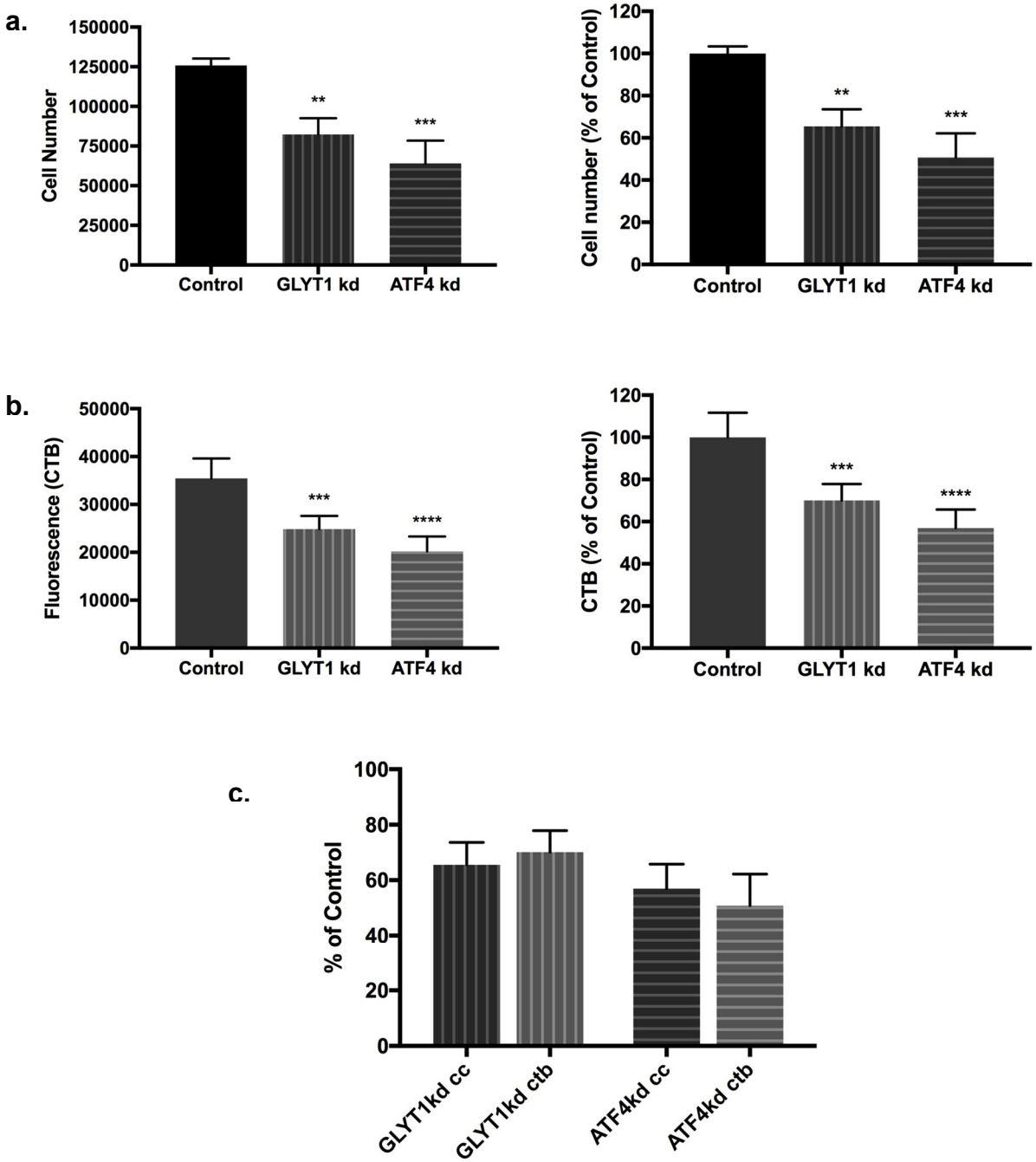

Figure 3.3: HT29 CTB specificity. Correlation between cell counting **(a)** and fluorescence measurements after 4h incubation with CTB **(b)** following GLYT1 and ATF4 siRNA treatments for 72h. For each treatment the fold change in comparison to control cells (percentage of Control) was calculated to allow comparisons between both methods. No significant difference was observed between cell counting (cc) and CTB (ctb) assay when analysing the effect of each treatment on cell number in comparison to control cells, GLYT1kd cc compared to GLYT1kd ctb and ATF4kd cc compared with ATF4kd ctb **(c)**. For cell counting experiments data are means ± SD, N=1 and n=3. For CTB experiments data are means ± SD, N=1 and n=5.

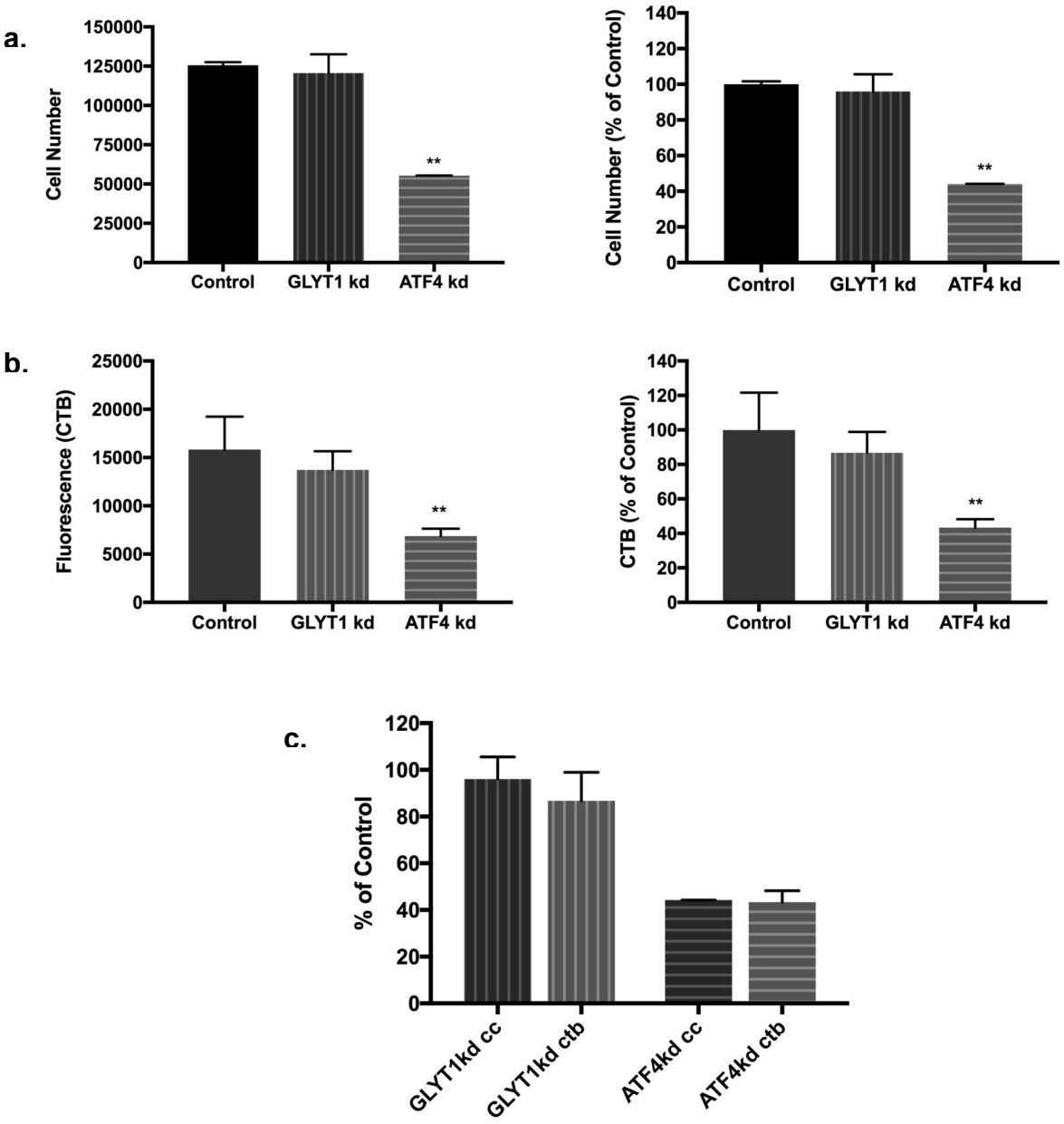

Figure 3.4: A498 CTB specificity. Correlation between cell counting (a) and fluorescence measurements after 4h incubation with CTB (b) following GLYT1 and ATF4 siRNA treatments for 72h. For each treatment the fold change in comparison to control cells (percentage of Control) was calculated to allow comparisons between both methods. No significant difference was observed between cell counting and CTB assay when analysing the effect of each treatment on cell number in comparison to control cells, GLYT1kd cc compared to GLYT1kd ctb and ATF4kd cc compared with ATF4kd ctb (c). For cell counting experiments data are means ± SD, N=1 and n=3. For CTB experiments data are means ± SD, N=1 and n=5.

3.2.2 *Cell line proliferative profiles*

The CTB assay was then utilised to determine cell number after a fixed incubation period and calculate the experimental doubling time for each cell line, in order to confirm the proliferative profiles described in the literature. Cells were cultivated in 96-well plates in 100μl of rich medium, namely DMEM (A549 and HT29), EGM (HUVEC) or EMEM (A498), or minimal medium, RPMI (all cell lines), for 6, 24, 48, 72 or 96 hours. After each point 20μl of CTB was added per well and cells incubated for a further 3 hours prior to absorbance measurement at 570 and 600nm. Additionally, for each time point, the absorbance measurement of three blank wells was performed, where medium was incubated without cells. Then, the percentage of reduction of resazurin to resorufin of each replicate was calculated, according to the equation presented in Chapter 2 Section 2.5.1, to infer the cell number. Doubling times were determined utilising the exponential phase of the growth curve and analysed in GraphPad Prism (Figure 3.5). The results are from a single experiment for each cell line with five replicates for each time point.

As shown in table 3.1, all tumour cell lines grew with similar doubling times to those quoted in the NCI60 database whether they were cultured in DMEM or RPMI, but with a slightly prolonged doubling time in RPMI when compared to growth in DMEM. A549 and HT29 cells presented rapid growth rates, with doubling times in RPMI of 27.5 and 23.6 hours, respectively, whereas A498 presented a slow growth rate, with doubling time of 63 hours.

	A549	**HT29**	**A498**
Rich medium	21.9	21.7	54.8
RPMI	27.5	23.6	63
NCI60 data (RPMI)	19.1	19.5	66.8

Table 3.1: Doubling times of cell lines in hours.

Additionally, gene expression of the proliferation marker ki67 was evaluated and compared among cell lines. Total mRNA was extracted for each cell line from cells incubated at concentrations of $2x10^4$ cells/well for A549 and A498 cells and $3x10^4$ cells/well for HT29 cells in both rich and minimal mediums in 12-well plates for 96 hours. RNA purity was confirmed with absorbance measurements (all RNAs presented a 260/280 ratio of 2), reverse transcribed to cDNA and qPCR was performed utilising primers specific for ki67 mRNA. Only one melt peak was observed and the reaction efficiency was 2.08 or 108%. The results (Figure 3.6) show that the ki67 mRNA level was higher for A549, HT29 and HUVEC cells than for A498 cells. The results are from two experiments for each cell line with two experimental replicates.

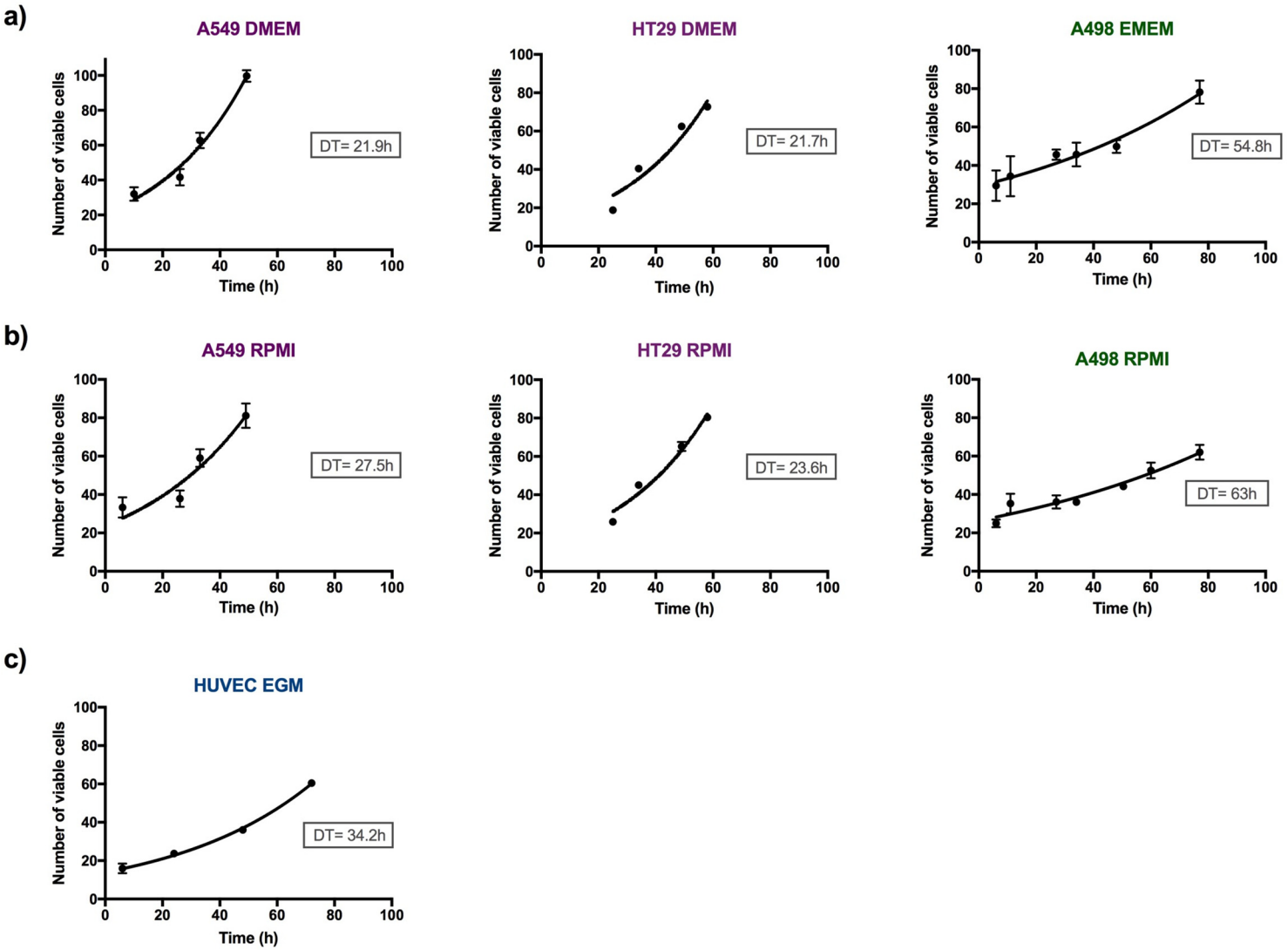

Figure 3.5: Experimental A549, HT29, A498 and HUVEC growth curves. Cell growth was analysed over time in different media with CTB assay and doubling time (DT) calculated for each cell line. Data are means ± SD, N=1 and n=5.

a)

Ki67 (NM_002417 transcript variant 1)	
Primers Forward:^{2375}TACATGTGCCTGCTCGACCC^{2394} Reverse: ^{2499}CTGCGGTTGCTCCTTCACTG^{2480}	Exon Location 12 13
Product length (bp) = 125	Annealing Temperature (°C) = 60

Reference sequence: 2375- **tacatgtgcctgctcgaccc**tacagagtgctcaacaacttcatttccaaccaaaaaatggactttaaggaagat ctttcaggaatagctgaaatgttcaagaccc**cagtgaaggagcaaccgcag** -2499

b)

Ki67 qPCR assay
Standard Curve Efficiency = 2.08 Error =0.0245
Melting Temperature (average) = 80.2°C

c)

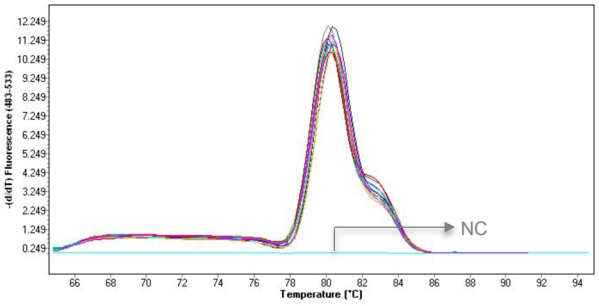

d)

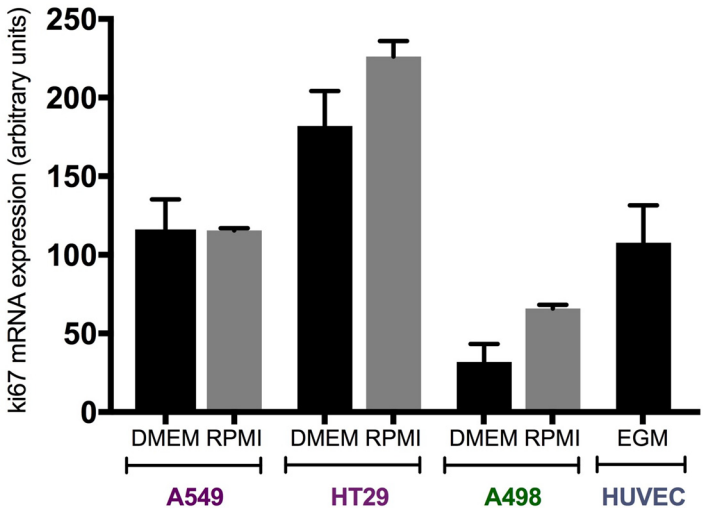

Figure 3.6: ki67 PCR assay. (a) Table showing primer sequences utilised in qPCR, exon location, product length and melting temperature followed by reference sequence with primers highlighted. Numbers in superscript denote the position of the primers within the gene. **(b)** Table showing qPCR standard curve details and product melting temperature. **(c)** Typical melting point plot obtained for ki67 qPCRs. **(d)** Bar charts illustrating the abundance of ki67 mRNA for each cell line in RPMI and DMEM by qPCR analysis. Results showed as arbitrary units normalised to GAPDH, TOP1 and ATP5B mRNA levels and are means ± SD, N=2 and n=4.

3.2.3 *Glycine Uptake*

The ability to uptake glycine was evaluated for A549, HT29 and A498 cell lines. Cells were incubated in HEPES buffer supplemented with glycine concentrations of 0, 5, 50, 100, 200, 300, 500, 1000μM and 0.5μCi/ml [2-^{3}H]-Glycine for 10 minutes or incubated in HEPES buffer supplemented with 5μM glycine and 0.5μCi/ml [2-^{3}H]-Glycine for 0, 5, 10 and 30 minutes followed by intracellular radio-labelled glycine measurement. In all conditions A549, HT29 and A498 cells were able to uptake glycine from the extracellular environment with Vmax of 1250, 635 and 724 pmol.cm^{2}.10^{-1}, respectively (Figure 3.7). Increasing either glycine concentration in HEPES buffer or the period of incubation resulted in a higher glycine uptake in all cell lines. The results are from two experiments for each cell line with three experimental replicates.

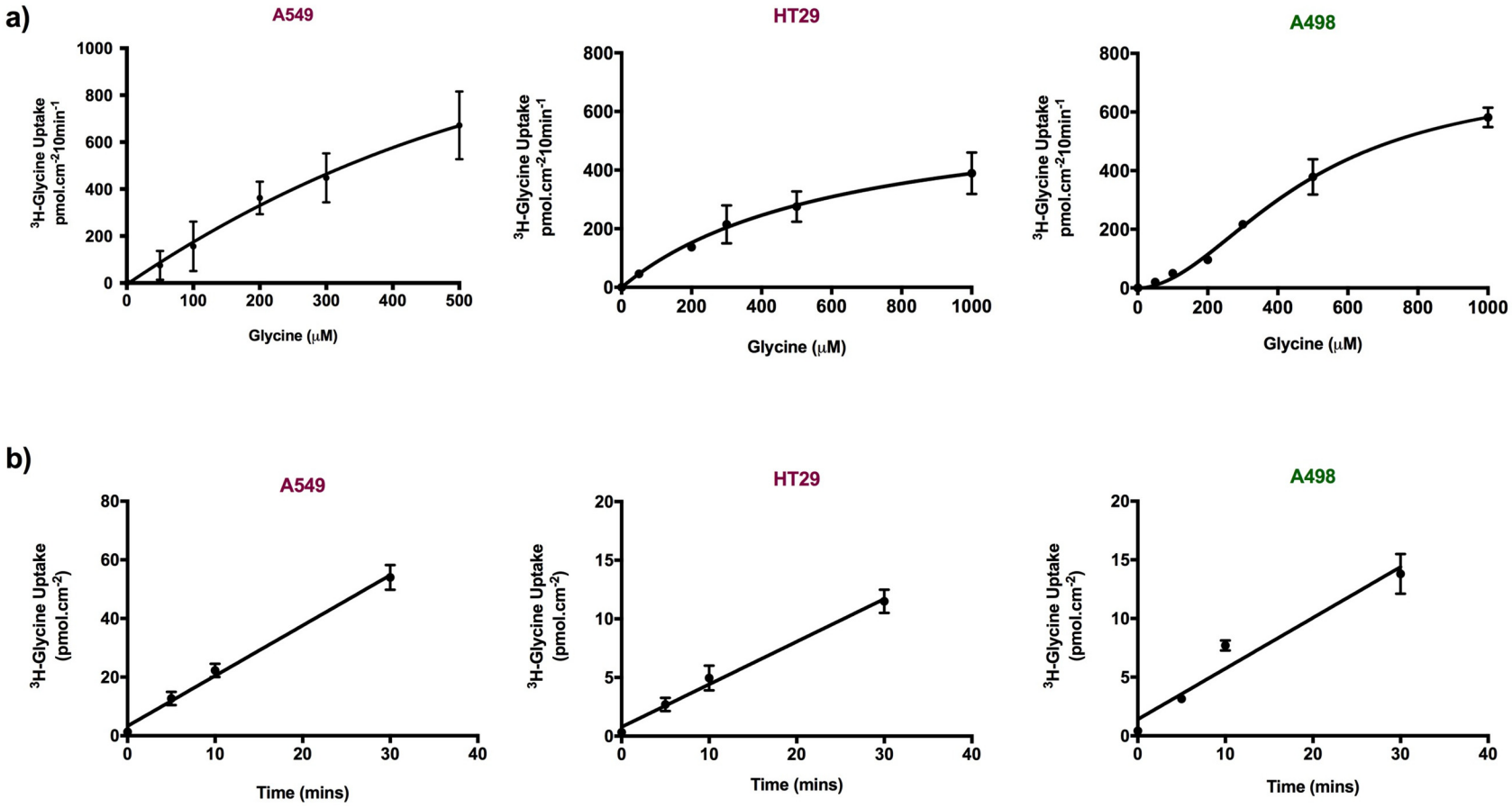

Figure 3.7: Glycine uptake in A549, HT29 and A498 cell lines. (a) Total ^{3}H-glycine uptake was measured in cells incubated in HEPES buffer supplemented with ^{3}H-glycne 0.5μCi/ml and 0, 5, 50, 100, 200, 300, 500 or 1000 μM glycine for 10 minutes. A549 presents a Vmax=1250 pmol.cm^2.10^{-1}, HT29 presents Vmax= 635 pmol.cm^2.10^{-1} and A498 presents Vmax= 724 pmol.cm^2.10^{-1}. **(b)** Total ^{3}H-glycine uptake measurements when cells were incubated with HEPES buffer supplemented with ^{3}H-glycine 0.5μCi/ml and 5μM glycine for 0, 5, 10 and 30 minutes. Data are means ± SD, N=2 and n=6.

3.2.4 *Expression of amino acid transporters and Activating Transcription Factors*

Cells were then screened for mRNA expression of amino acid transporters that accept glycine as a substrate and activating transcription factor (ATFs). A549, HT29 and A498 cell lines were seeded in 12-well plates in DMEM and RPMI at concentrations of $3x10^4$ cells/well and incubated for 95h prior RNA extraction. HUVEC cells were incubated in EGM medium. RNA yield and purity were analysed measuring absorbance at 260 and 280 nm. All RNAs utilised in this study presented a 260/280 ratio between 1.95 and 2.0 indicating an absence of possible contaminants that absorb light at 280nm, as proteins and some organic compounds, therefore suggesting its purity. The correlation between absorbance and RNA concentration was determined according to Beer-Lambert Law, where 1 A_{260} unit of ssRNA is equal to 40 ng/µl. Then, 500ng of total RNA was reverse transcribed to cDNA as described in Chapter 2 Section 2.4.1 and the cDNAs were utilised in qPCR reactions. The qPCR results for each primer were normalised with housekeeping genes GAPDH, TOP1 and ATP5B. For each assay a standard curve using five serial dilutions (1:10) of appropriate cloned target PCR products was utilised to infer the arbitrary units of relative mRNA concentration as described in chapter 2.4.3. As the same cloned PCR product was utilised in different qPCR reactions to generate the standard curve for each gene analysed, the Cp results of the standards were utilised to calculate the coefficient of variation for each primer.

GLYT1, as a specific glycine transporter, and ATF4, as its regulator, were the main focus of this study. This way, A549, HT29 and A498 cell lines were screened for GLYT1 and ATF4 mRNA expression by end-point and qPCR when growing in DMEM and RPMI media. HUVEC cells were also screened when growing in EGM medium.

A combination of end point and qPCR were then used to evaluate mRNA expression of other glycine transporters (PAT1, SNAT2 and $ATB^{0,+}$) and ATFs (ATF3, ATF5 and ATF6). Additionally, mRNAs for the subunit of cystine amino acid transporter xCT and the GSH synthesising enzymes GCLC, GCLM and GSS were evaluated. Only the rapidly proliferating cell lines, A549 and HT29, growing in DMEM and RPMI were utilised in the end-point PCRs and only the tumour cell lines (A549, HT29 and A498) growing in RPMI were utilised in the qPCR experiments. HUVEC cell line was not included in these experiments.

GLYT1

According to end-point PCR results, all tumour cell lines utilised in this study expressed GLYT1 mRNA in both DMEM and RPMI media, as did the HUVEC cell line growing in EGM (Figure 3.8). The GLYT1 primer pair showed one strong amplification band of about 72 base pairs and also weak bands of variable sizes but no amplification in the negative control. However when analysing qPCR results only one melting peak was observed at about 79ºC. The qPCR reaction efficiency was about 2.017n or 101.7% and the CoV between reactions was 3.58% (N=6, n=5). There was a significant reduction in GLYT1 mRNA expression when the A498 cell line was incubated in RPMI than when growing in DMEM and, although not significant, the same tendency was observed for A549 and HT29 cells. The HUVEC cell line had a smaller GLYT1 mRNA abundance than the tumour cell lines. The results are from two experiments for each cell line with two experimental replicates.

ATF4

All tumour cell lines utilised in this study expressed ATF4 mRNA in both DMEM and RPMI media, as did the HUVEC cell line growing in EGM when analysing the end-point PCR results (Figure 3.9). The ATF4 primers generated one amplification band in the agarose gel of approximately 169 base pairs for all the samples analysed except in the negative control and a weak band inferior to 100 base pairs was also observed in all samples and stronger in the negative control, possibly a result of primer-dimer. When analysing qPCR results only one melting temperature was observed at about 86ºC for the samples and some negative controls presented a small melt peak also suggesting primer dimer formation. The ATF4 qPCR reaction efficiency was 2.038, or 103.8% and the CoV between reactions was 2.63% (N=4, n=5). There was no significant difference in ATF4 mRNA expression when comparing growing in DMEM or RPMI. Although not significant, A498 and HUVEC cell lines presented a tendency to increase ATF4 mRNA abundance in comparison to HT29 and A549 cell lines. A549 cell line showed the smallest ATF4 mRNA levels in comparison to the other cell lines. The results are from two experiments for each cell line with two experimental replicates.

PAT1

A549 and HT29 cells expressed PAT1 mRNA in both DMEM and RPMI media, when analysing the end-point PCR results (Figure 3.10). The PAT1 primer set showed

two amplification bands in the agarose gel of approximately 100 and 200 base pairs for all the samples analysed except in the Negative Control (NC) and a weak band inferior to 100 base pairs was also observed in all samples, this was stronger in the negative control thus possibly a result of primer dimer. When analysing qPCR results only one melting temperature peak was detected at 82ºC, but an attempt to a second melting peak formation was also observed in some samples. PAT1 qPCR efficiency was 1.955 or 95.5% and the CoV between reactions was 3.0% (N=7, n=4). There was no significant difference in PAT1 mRNA expression between A549, HT29 and A498 cell lines. The results are from two experiments for each cell line with three experimental replicates.

$ATB^{0,+}$

A549 and HT29 cells expressed $ATB^{0,+}$ mRNA in both DMEM and RPMI media, when analysing the end-point PCR results (Figure 3.11). The $ATB^{0,+}$ primers resulted in two amplification bands in the agarose gel of approximately 144 base pairs for all the samples analysed except in the Negative Control (NC) and a weak band inferior to 100 base pairs was also observed in all samples and in the negative control and is possibly a result of primer dimer formation. When analysing qPCR results only one melting temperature was observed at about 81ºC. $ATB^{0,+}$ qPCR efficiency was 1.931 or 93.1% and the CoV between reactions was 3.59% (N=5, n=4). There was no significant difference in $ATB^{0,+}$ mRNA expression between A549, HT29 cell lines whereas A498 cell line did not expressed this amino acid transporter. The results are from two experiments for each cell line with three experimental replicates.

SNAT2

End-point PCR results showed that A549 and HT29 cells expressed SNAT2 mRNA in both DMEM and RPMI media (Figure 3.12). The SNAT2 reaction showed one amplification band on the agarose gel of approximately 96 base pairs for all the samples analysed except in the Negative Control (NC) and a very weak band inferior to 100 base pairs was also observed in all samples and in the negative control, as with other amplifications this is possibly a result of primer dimers. However, when analysing qPCR results only one melting temperature was observed at about 88ºC. SNAT2 qPCR efficiency was 1.911 or 91.1% and the CoV between reactions was 0.51% (N=2, n=5). There was no significant difference in SNAT2 mRNA expression between A549, HT29 and A498 cell lines, but A549 cell presented the smallest SNAT2 mRNA abundance and A498 cell line presented the highest among the cell lines analysed.

The results are from two experiments for each cell line with three experimental replicates.

SHMT2

A549 and HT29 cells expressed SHMT2 mRNA in both DMEM and RPMI media, when analysing the end-point PCR results (Figure 3.13). The SHMT2 primer set showed two amplification bands in the agarose gel of approximately 129 base pair and also weak bands of variable sizes for all the samples analysed except in the Negative Control (NC) and a weak band inferior to 100 base pairs was also observed in all samples and stronger in the negative control, again possibly a result of primer dimers. When analysing qPCR results only one melting temperature was detected at about 85ºC. SHMT2 qPCR efficiency was 1.962 or 96.2% and the CoV between reactions was 2.78% (N=3, n=4). All cell lines analysed expressed SHMT2 mRNA and there was no significant difference in SHMT2 mRNA abundance between A549, HT29 and A498 cell lines. The results are from two experiments for each cell line with three experimental replicates.

ATF3

A549 and HT29 cells expressed ATF3 mRNA in both DMEM and RPMI media, when analysing the end-point PCR results (Figure 3.14). The ATF3 primer pair showed two amplification bands in the agarose gel of approximately 161 base pairs except in the Negative Control (NC) and a weak band inferior to 100 base pairs was also observed in all samples and stronger in the negative control, possibly a result of primer dimers. When analysing qPCR data only one melting temperature was observed at about 84ºC. ATF3 qPCR efficiency was 1.948, or 94.8% and the CoV between reactions was 1.27% (N=2, n=3). All cell lines analysed expressed ATF3 mRNA and its abundance was less in the A549 cell line than in HT29 and A498 lines. The results are from two experiments for each cell line with three experimental replicates.

ATF5

A549 and HT29 cells expressed ATF5 mRNA in both DMEM and RPMI media, when analysing the end-point PCR results (Figure 3.15). The ATF5 primer pair showed one amplification band in the agarose gel of approximately 146 base pairs except in the Negative Control (NC) and a weak band inferior to 100 base pairs was also observed in all samples and stronger in the negative control, possibly a result of primer dimers. When analysing qPCR data only one melting temperature was observed at about 90ºC. ATF5 qPCR efficiency was 1.966 or 96.6% and the CoV between

reactions was 0.4% (N=2, n=3). All cell lines analysed expressed ATF5 mRNA with no significant difference among them. The results are from two experiments for each cell line with three experimental replicates.

ATF6

A549 and HT29 cells expressed ATF6 mRNA in both DMEM and RPMI media, when analysing the end-point PCR results (Figure 3.16). The ATF6 primers showed one amplification band in the agarose gel of approximately 151 base pair except in the Negative Control (NC) and a weak band inferior to 100 base pairs was also observed in all samples and stronger in the negative control, possibly a result of primer dimers. When analysing qPCR data only one melting temperature was detected at about 80ºC. ATF6 qPCR efficiency was 1.852 or 85.2% and the CoV between reactions was 3.88% (N=2, n=4). All cell lines analysed expressed ATF6 mRNA and its abundance was smaller in A549 cell line than in HT29 and A498 lines. The results are from two experiments for each cell line with three experimental replicates.

xCT

End-point PCR results showed that A549 and HT29 cells expressed xCT mRNA in both DMEM and RPMI media (Figure 3.17). When analysing qPCR results only one melting temperature was observed at about 80ºC. xCT qPCR efficiency was 2.077, or 107.7%, and the CoV between reactions was 1.36% (N=2, n=3). There was no significant difference in xCT mRNA expression among A549, HT29 and A498 cell lines, but A549 cell presented the smallest xCT mRNA abundance among the cell lines analysed. The results are from two experiments for each cell line with three experimental replicates.

GCLC

According to GCLC qPCR results only one melting temperature was observed at about 80ºC. GCLC qPCR efficiency was 1.972 or 97.2% and the CoV between reactions was 2.70% (N=3, n=3) (Figure 3.18). A498 cells presented the highest GCLC mRNA abundance among the cell lines analysed. The results are from two experiments for each cell line with three experimental replicates.

GCLM

According to GCLC qPCR results only one melting temperature was observed at about 81ºC. GCLC qPCR efficiency was 1.949 or 94.9% and the CoV between reactions was 2.82% (N=3, n=4) (Figure 3.19). A498 cells presented the highest GCLM

mRNA abundance among the cell lines analysed. The results are from two experiments for each cell line with three experimental replicates.

GSS

According to GCLC qPCR results only one melting temperature was observed at about 82ºC. GCLC qPCR efficiency was 1.937 or 93.7% and the CoV between reactions was 1.33% (N=3, n=4) (Figure 3.20). There was no significant difference in GSS mRNA expression among A549, HT29 and A498 cell lines. The results are from two experiments for each cell line with three experimental replicates.

a)

GLYT1 (NM_001024845)	
Primers	Exon Location
Forward: ^{580}CCATGTTCAAAGGAGTGGGCTA^{601} Reverse: cggc^{651}TGACCACATTGTAGTAGATGCCG^{629}	4:5 5
Product length (bp) = 72	Annealing Temperature (ºC) = 60

Reference sequence (5'-3'): 580-**ccatgttcaaaggagtgggcta**tggtatgatggtggtgtccacctacat**cggcatctactac aatgtggtca**-651

b)

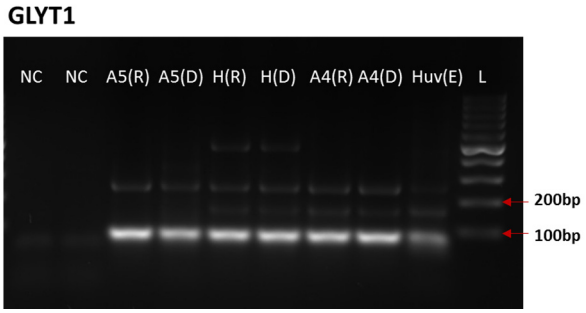

c)

GLYT1 qPCR assay
Standard Curve Efficiency = 2.017 Error =0.0346
Melting Temperature (average) = 79.5ºC

d)

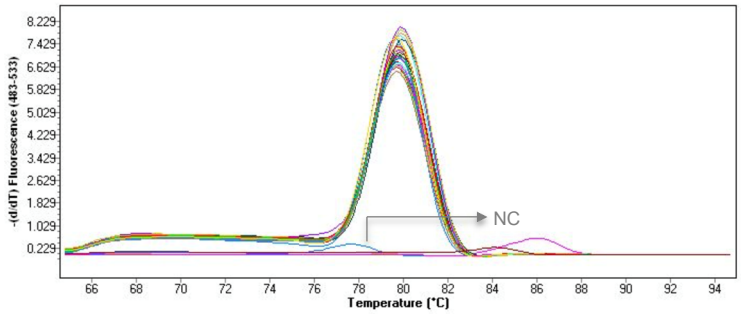

e)

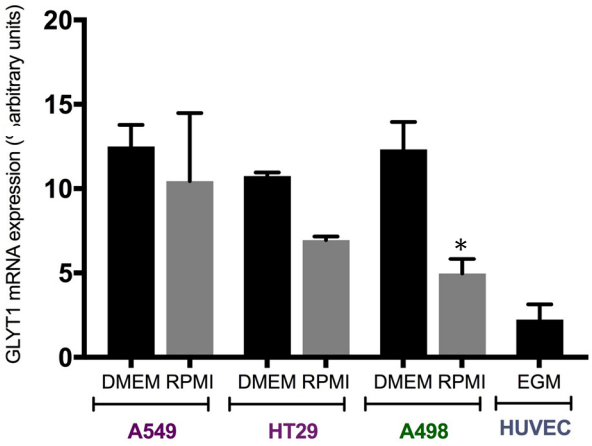

Figure 3.8: GLYT1 PCR assay. (a) Primer sequences utilised in end-point PCR and qPCR, exon location, product length and melting temperature followed by reference sequence with primer positions highlighted. Numbers in superscript denote the position of the primers within the cDNA. **(b)** Products of end-point PCR visualised on 2% agarose gel under UV light of A549 (A5), HT29 (H), A498 (A4) or HUVEC (Huv) cells cultured in DEMEM (D), RPMI (R) or EGM (E). The 100 base pair (bp) ladder (L) was utilised to evaluate band sizes and reaction negative controls (NC) were included. **(c)** qPCR standard curve details and product melting temperature. **(d)** Typical melting point plot obtained for GLYT1 qPCRs. **(e)** Abundance of GLYT1 mRNA for each cell line in different medium by qPCR analysis. Results showed as arbitrary units normalised to GAPDH, TOP1 and ATP5B mRNA levels. Data are means ± SD, N=2 and n=4.

a)

ATF4 (NM_001675)	
Primers Forward: ^{1016}CTTCAAACCTCATGGGTTCTCCAG^{1039} Reverse: ^{1184}CAGGGCATCCAAGTCGAACTC^{1164}	Exon Location 1 2
Product length (bp) = 169	Annealing Temperature (°C) = 60

Reference sequence (5'-3'): 1011-**cttcaaacctcatgggttctccag**cgacaaggctaaggcgggctcctccgaatggct ggctgtggatgggttggtcagtccctccaacaacagcaaggaggatgccttctccgggacagattggatgttggagaaaatggatttgaag**ga gttcgacttggatgccctg**-1179

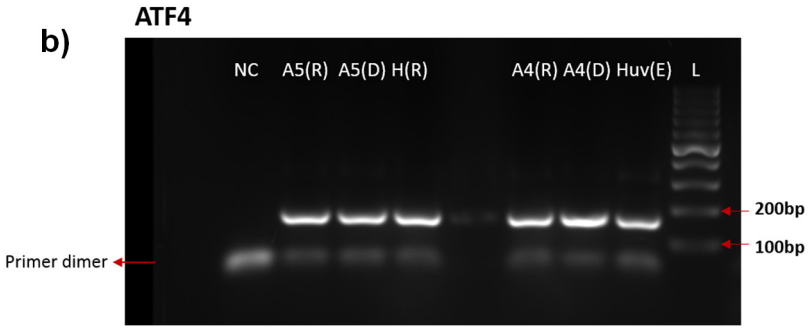

c)

ATF4 qPCR assay
Standard Curve Efficiency = 2.038 Error =0.0428
Melting Temperature (average) = 86°C

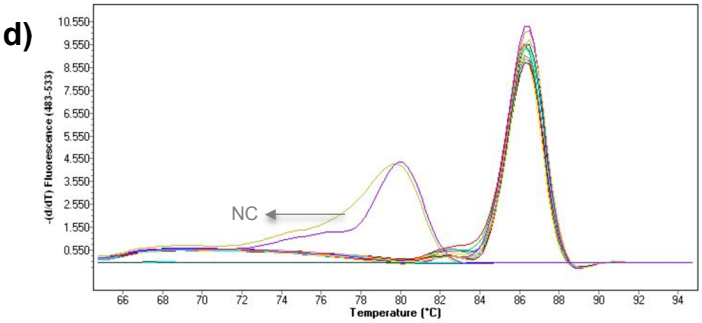

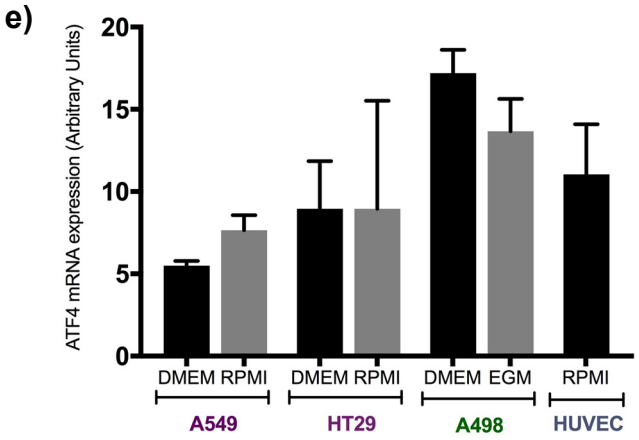

Figure 3.9: ATF4 PCR assay. (a) Primer sequences utilised in end-point PCR and qPCR, exon location, product length and melting temperature followed by reference sequence with primers highlighted. Numbers in superscript denote the position of the primers within the gene. **(b)** Products of end-point PCR visualised on 2% agarose gel under UV light of A549 (A5), HT29 (H), A498 (A4) or HUVEC (Huv) cells cultured in DEMEM (D), RPMI (R) or EGM (E). The 1000 base pair (bp) ladder (L1) and 1000 base pair (bp) ladder (L2) were utilised to evaluate band sizes and reaction negative controls (NC) were included. **(c)** qPCRs standard curve details and product melting temperature. **(d)** Typical melting point plot obtained for ATF4 qPCRs. **(e)** Abundance of ATF4 mRNA for each cell line in different medium by qPCR analysis. Results showed as arbitrary units and are means ± SD, N=2 and n=4.

a)

PAT1 (NM_078483)	
Primers Forward: ^{1180} CATAACCCTCAACCTGCCCAAC^{1201} Reverse: ^{1278} GGGACGTAGAACTGGAGTGC ^{1259}	Exon Location 8 9
Product length (bp) = 104	Annealing Temperature (ºC) = 58

Reference sequence (5'-3'): 1141-**cataaccctcaacctgcccaac**tgctggttgtaccagtcagttaagctg ctgtactccatcgggatcttttcacctac**gcactccagttctacgtccc**-1278

b)

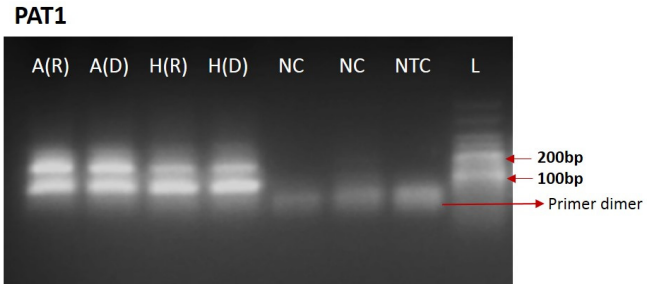

c)

PAT1 qPCR assay
Standard Curve Efficiency = 1.955 Error =0.271
Melting Temperature (average) = 82ºC

d)

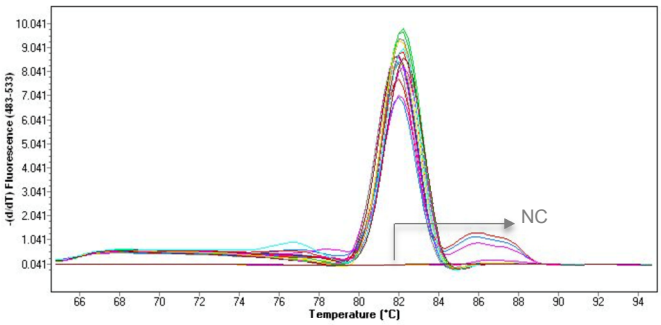

e)

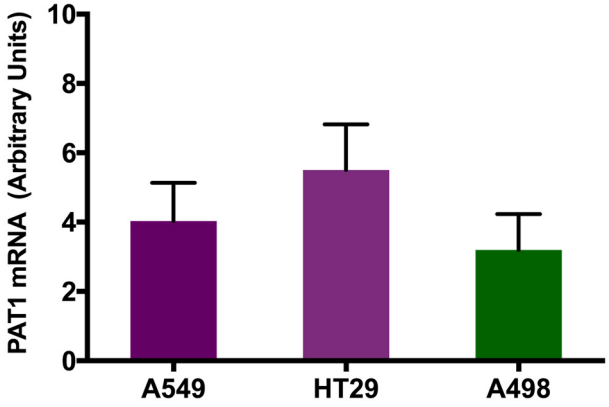

Figure 3.10: PAT1 PCR assay. (a) Primer sequences utilised in end-point PCR and qPCR, exon location, product length and melting temperature followed by reference sequence with primers highlighted. Numbers in superscript denote the position of the primers within the gene. **(b)** Products of end-point PCR visualised on 2% agarose gel under UV light of A549 (A) and HT29 (H) cells cultured in DEMEM (D) or RPMI (R). The 100 base pair (bp) ladder (L) was utilised to evaluate band sizes and reaction negative controls (NC) and no template control (NTC) were included. **(c)** qPCRs standard curve details and product melting temperature. **(d)** Typical melting point plot obtained for PAT1 qPCRs. **(e)** Abundance of PAT1 mRNA for each cell line in RPMI by qPCR analysis. Results showed as arbitrary units and are means ± SD, N=2 and n=6.

a)

$ATB^{0,+}$ (NM_007231)	
Primers	Exon Location
Forward: ^{858}CTTCTTCTGGCTTGGCTCATAG^{879} Reverse: ^{1001} TGAAGCACCCTCCAGAGTTGC ^{981}	6 6/7
Product length (bp) = 144	Annealing Temperature (°C) = 58

Reference sequence (5'-3'): 781-**cttcttctggcttggctcatag**ttggagcagcactatttaaaggaatcaaatcg tctggcaaggtggtatattttacagctcttttcccctatgtggtcctactcatcctgttagtacgaggt**gcaactctggagggtgctt caaaaggcatttca**-1001

b)

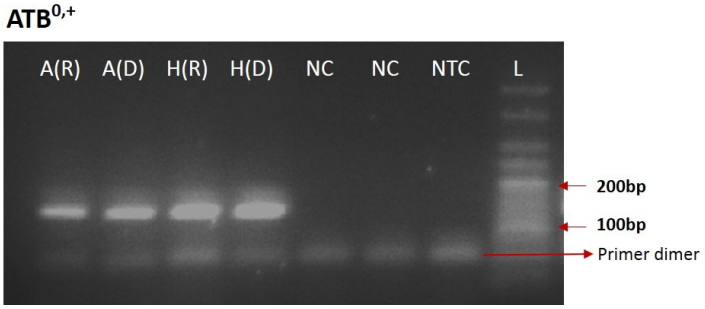

c)

$ATB^{0,+}$ qPCR assay
Standard Curve Efficiency = 1.931 Error =0.103
Melting Temperature (average) = 81.5°C

d)

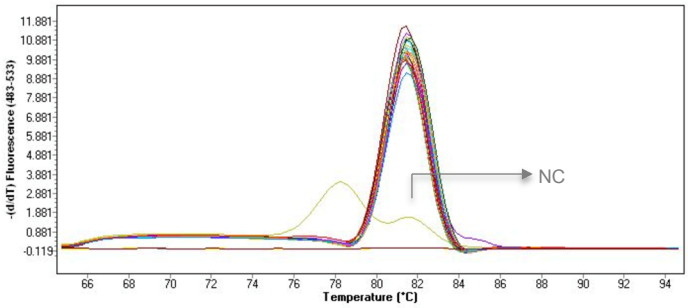

e)

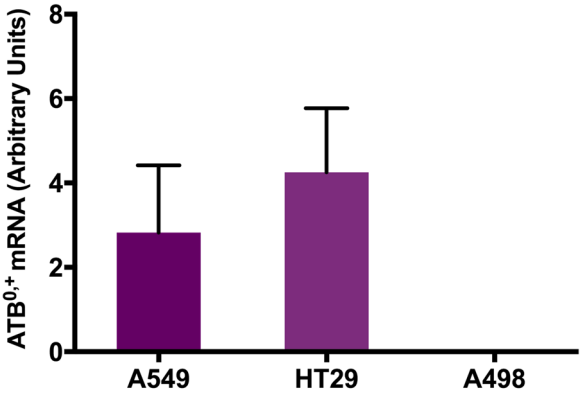

Figure 3.11: $ATB^{0,+}$ PCR assay. (a) Primer sequences utilised in end-point PCR and qPCR, exon location, product length and melting temperature followed by reference sequence with primers highlighted. Numbers in superscript denote the position of the primers within the gene. **(b)** Products of end-point PCR visualised on 2% agarose gel under UV light of A549 (A) and HT29 (H) cells cultured in DEMEM (D) or RPMI (R). The 100 base pair (bp) ladder (L) was utilised to evaluate band sizes and reaction negative controls (NC) and no template control (NTC) were included. **(c)** qPCRs standard curve details and product melting temperature. **(d)** Typical melting point plot obtained for $ATB^{0,+}$ qPCRs. **(e)** Abundance of $ATB^{0,+}$ mRNA for each cell line in RPMI by qPCR analysis. Results showed as arbitrary units and are means ± SD, N=2 and n=6.

a)

SNAT2 (NM_018976)	
Primers Forward: ^{331}TGCGTGAGAATAGAGACCACC^{351} Reverse: ^{426}GGAATCGGGTGCAGCTAGTA^{407}	Exon Location 1 2
Product length (bp) = 96	Annealing Temperature (°C) = 60

Reference sequence (5'-3'): 331-**tgcgtgagaatagagaccacc**gaggccgactcgcgggccgctgcacccac cgccaaggacaaaaggagcccagcgc**tactagctgcacccgattcc**-426

b)

c)

SNAT2 qPCR assay
Standard Curve Efficiency = 1.911 Error =0.0189
Melting Temperature (average) = 88°C

d)

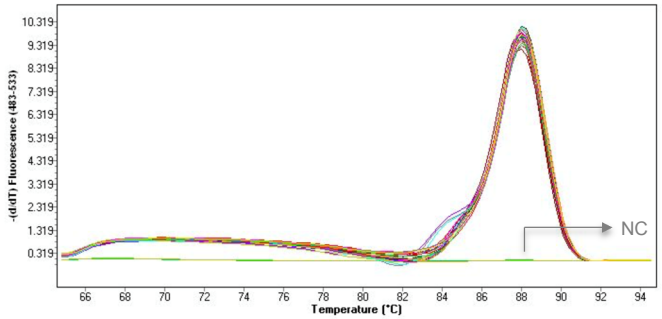

e)

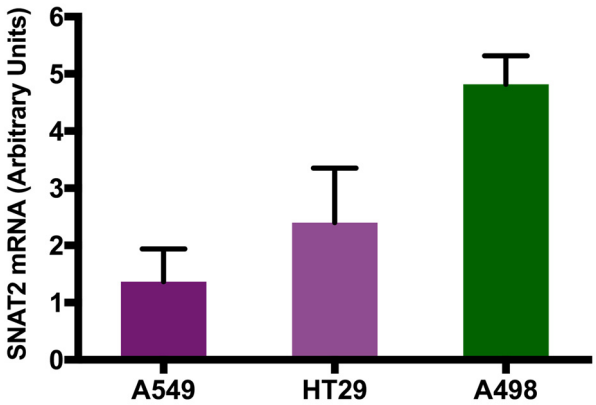

Figure 3.12: SNAT2 PCR assay. (a) Primer sequences utilised in end-point PCR and qPCR, exon location, product length and melting temperature followed by reference sequence with primers highlighted. Numbers in superscript denote the position of the primers within the gene. **(b)** Products of end-point PCR visualised on 2% agarose gel under UV light of A549 (A) and HT29 (H) cells cultured in DEMEM (D) or RPMI (R). The 100 base pair (bp) ladder (L) was utilised to evaluate band sizes and reaction negative controls (NC) and no template control (NTC) were included. **(c)** qPCRs standard curve details and product melting temperature. **(d)** Typical melting point plot obtained for SNAT2 qPCRs. **(e)** Abundance of SNAT2 mRNA for each cell line in RPMI by qPCR analysis. Results showed as arbitrary units and are means ± SD, N=2 and n=6.

a)

SHMT2 (NM_005412)	
Primers	Exon Location
Forward: ^{1043}CAAGACTCTTGCAGGGGCCAG ^{1063} Reverse: ^{1171}GATGGGAACACGGCAAAGTTG ^{1151}	7 8
Product length (bp) = 129	Annealing Temperature (ºC) = 60

Reference sequence (5'-3'): 1043-**caagactcttcgaggggccag**gtcagggctcatcttctaccggaaaggg gtgaaggctgtggaccccaagactggccgggagatcccttacacatttgaggaccgaat**caactttgccgtgttcccatc**-1171

b)

SHMT2 qPCR assay
Standard Curve Efficiency = 1.962 Error = 0.0488
Melting Temperature (average) = 85.2 ºC

c)

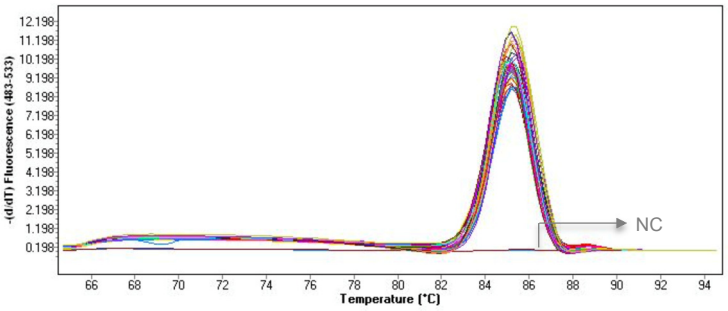

d)

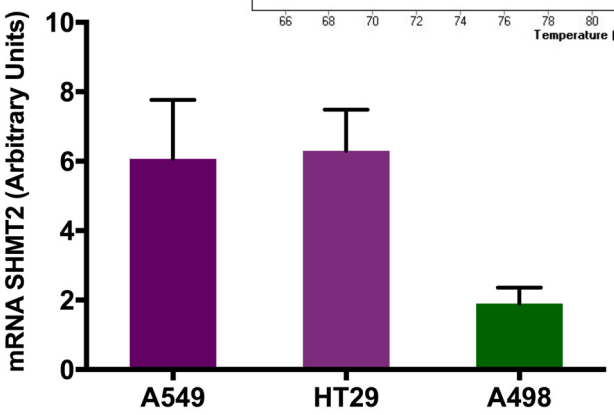

Figure 3.13: SHMT2 PCR assay. (a) Primer sequences utilised in qPCR, exon location, product length and melting temperature followed by reference sequence with primers highlighted. Numbers in superscript denote the position of the primers within the gene. **(b)** qPCR standard curve details and product melting temperature. **(c)** Typical melting point plot obtained for SHMT2 qPCRs. **(d)** Abundance of SHMT2 mRNA for each cell line in RPMI by qPCR analysis. Results showed as arbitrary units and are means ± SD, N=2 and n=6.

a)

ATF3(NM_001674)	
Primers	Exon Location
Forward: ^{480}TGTCCTCTGCGCTGGAATCAG^{500} Reverse: ^{640}CGTCTTCTCCTTCTTCTTGTTTC^{618}	2 3
Product length (bp) = 161	Annealing Temperature (^{o}C) = 60

Reference sequence (5'-3'): 480-**tgtcctctgcgctggaatcag**tcactgtcagcgacagacccctcggggtg tccatcacaaaagccgaggtagcccctgaagaagatgaaaggaaaaagaggcgacgagaaagaaataagattgca gctgcaaagtgcc**gaaacaagaagaaggagaagacg**-640

b)

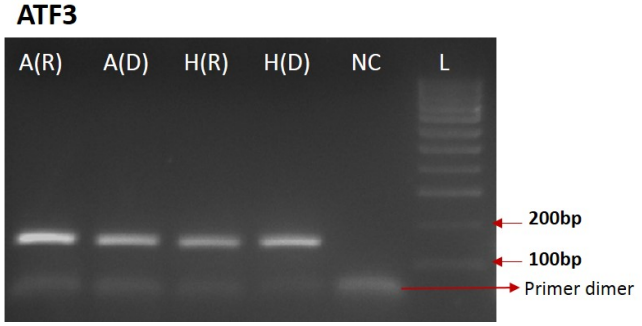

c)

ATF3 qPCR assay
Standard Curve Efficiency = 1.948 Error =0.0239
Melting Temperature (average) = 84.2^{o}C

d)

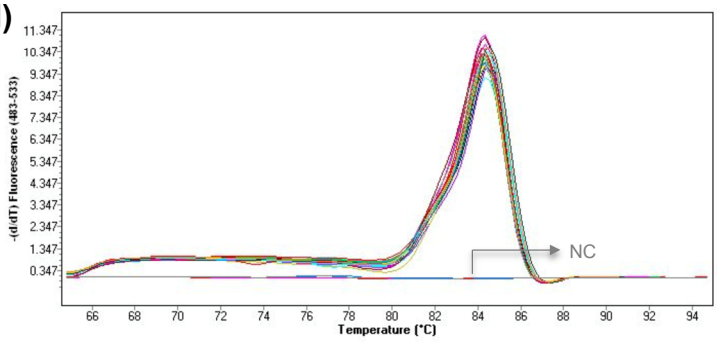

e)

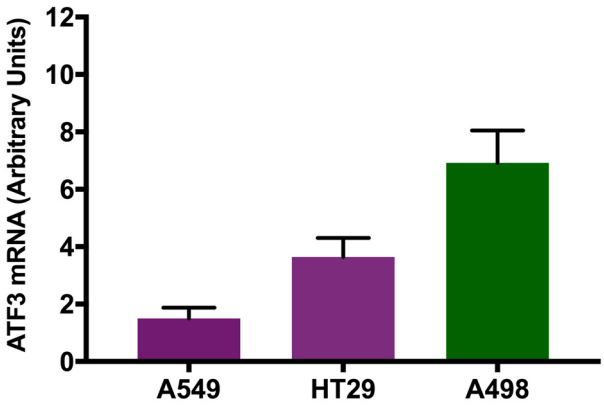

Figure 3.14: ATF3 PCR assay. (a) Primer sequences utilised in end-point PCR and qPCR, exon location, product length and melting temperature followed by reference sequence with primers highlighted. Numbers in superscript denote the position of the primers within the gene. **(b)** Products of end-point PCR visualised on 2% agarose gel under UV light of A549 (A) and HT29 (H) cells cultured in DEMEM (D) or RPMI (R). The 100 base pair (bp) ladder (L) was utilised to evaluate band sizes and reaction negative controls (NC) were included. **(c)** qPCR standard curve details and product melting temperature. **(d)** Typical melting point plot obtained for ATF3 qPCRs. **(e)** Abundance of ATF3 mRNA for each cell line in RPMI by qPCR analysis. Results showed as arbitrary units and are means ± SD, N=2 and n=6.

a)

ATF5 (NM_012068)	
Primers Forward: ^{344} TGTAGCCTCGACCCCTTTGTG^{364} Reverse: ^{489}CAGGCACCAAGGCGAAAGTG^{470}	Exon Location 1 2
Product length (bp) = 146	Annealing Temperature (°C) = 60

Reference sequence (5'-3'): 301-**tgtagcctcgacccctttgtgc**ccccggcccgtctccgcgctcaccacgcctgcgc tctccgctcccaccttctttcttcagccgaggccgccgccgcctctccttgctgcagccatggagtc ttc**cactttcgccttggtgcctg**-489

b)

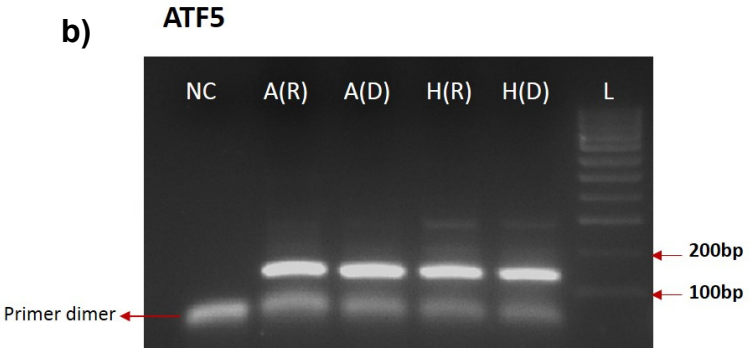

c)

ATF5 qPCR assay
Standard Curve Efficiency = 1.966 Error =0.0331
Melting Temperature (average) = 90.3°C

d)

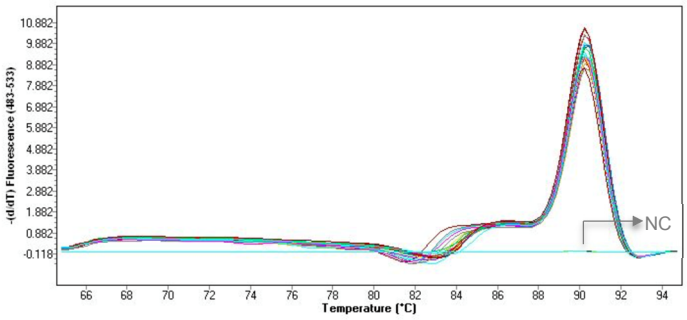

e)

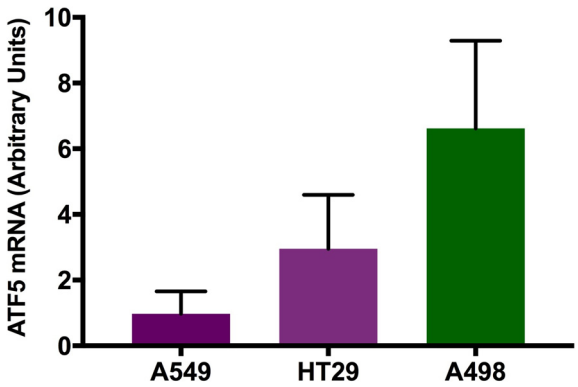

Figure 3.15: ATF5 PCR assay. (a) Primer sequences utilised in end-point PCR and qPCR, exon location, product length and melting temperature followed by reference sequence with primers highlighted. Numbers in superscript denote the position of the primers within the gene. **(b)** Products of end-point PCR visualised on 2% agarose gel under UV light of A549 (A) and HT29 (H) cells cultured in DEMEM (D) or RPMI (R). The 100 base pair (bp) ladder (L) was utilised to evaluate band sizes and reaction negative controls (NC) were included. **(c)** qPCR standard curve details and product melting temperature. **(d)** Typical melting point plot obtained for ATF5 qPCRs. **(e)** Abundance of ATF5 mRNA for each cell line in RPMI by qPCR analysis. Results showed as arbitrary units and are means ± SD, N=2 and n=6.

a)

ATF6 (NM_007348.3)	
Primers	Exon Location
Forward: ^{422}TCTCGTCTCCTCGGTCAGTG^{441} Reverse: ^{572}TTATCTTCCTTCAGTGGCTCC^{552}	4 5
Product length (bp) = 151	Annealing Temperature (°C) = 60

Reference sequence (5'-3'): 422 - **tctcgtctcctcggtcagtg**gactcttattcttcaactcagcatgttcctgaggagttggatttgtcttctag ttctcagatgtctccccttttccttatatggtgaaaactctaatagtctctcttcagc**ggagccactgaaggaagataa** -572

b)

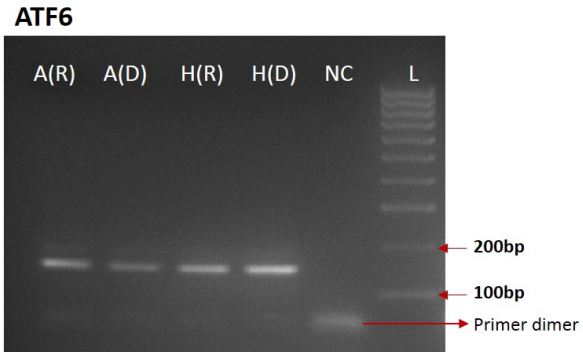

c)

ATF6 qPCR assay
Standard Curve Efficiency = 1.842 Error =0.0274
Melting Temperature (average) = 80.3°C

d)

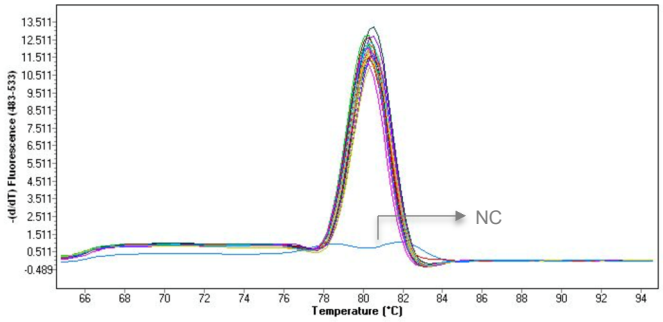

e)

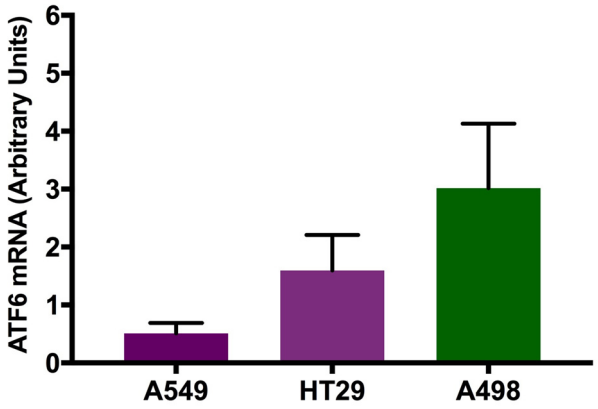

Figure 3.16: ATF6 PCR assay. (a) Primer sequences utilised in end-point PCR and qPCR, exon location, product length and melting temperature followed by reference sequence with primers highlighted. Numbers in superscript denote the position of the primers within the gene. **(b)** Products of end-point PCR visualised on 2% agarose gel under UV light of A549 (A) and HT29 (H) cells cultured in DEMEM (D) or RPMI (R). The 100 base pair (bp) ladder (L) was utilised to evaluate band sizes and reaction negative controls (NC) were included. **(c)** qPCR standard curve details and product melting temperature. **(d)** Typical melting point plot obtained for ATF6 qPCRs. **(e)** Abundance of ATF6 mRNA for each cell line in RPMI by qPCR analysis. Results showed as arbitrary units and are means ± SD, N=2 and n=6.

a)

xCT (NM_014331)	
Primers	Exon Location
Forward: cggag^{1342}CCTCTCCATGATTCATGTCCG^{1362}	9
Reverse: ^{1437}TCGAGGTCTCCAGAGAAGAGCA^{1416}	10
Product length (bp) = 96	Annealing Temperature (ºC) = 60

Reference sequence (5'-3'): 1321-**cctctccatgattcatgtccg**caagcacactcctctaccagctgttattgttttgcacccttt gacaatgataa**tgctcttctctggagacctcga**-1437

b)

xCT qPCR assay
Standard Curve Efficiency = 2.077 Error =0.0771
Melting Temperature (average) = 80.6ºC

c)

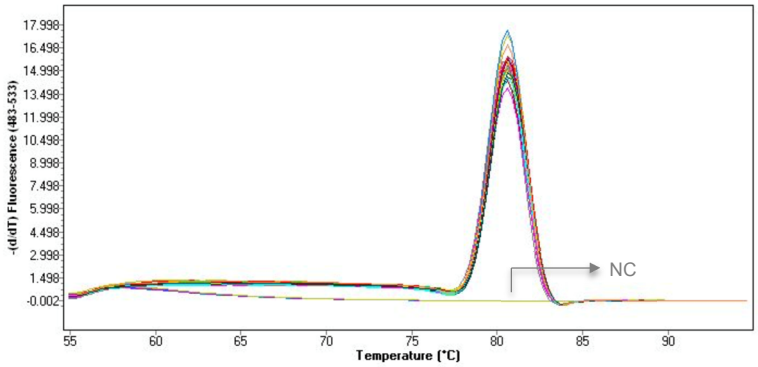

d)

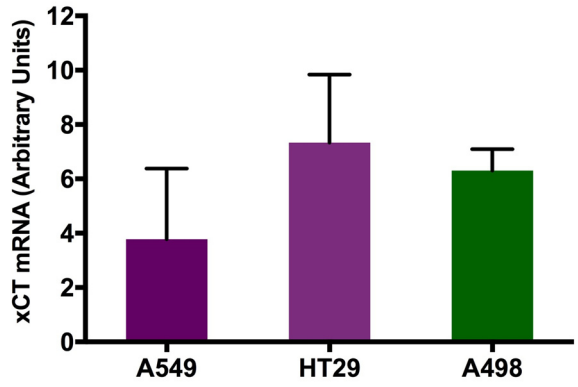

Figure 3.17: xCT PCR assay. (a) Primer sequences utilised in qPCR, exon location, product length and melting temperature followed by reference sequence with primers highlighted. Numbers in superscript denote the position of the primers within the gene. **(b)** qPCR standard curve details and product melting temperature. **(c)** Typical melting point plot obtained for xCT qPCRs. **(d)** Abundance of xCT mRNA for each cell line in RPMI by qPCR analysis. Results showed as arbitrary units and are means ± SD, N=2 and n=6.

a)

GCLC (NM_001498 variant 1)	
Primers	Exon Location
Forward: ^{2077}TCCTGGACTGATCCCAATTCTG^{2098} Reverse: ^{2248}CTTGTAGTCAGGATGGTTTGCG^{2227}	15 16
Product length (bp) = 172	Annealing Temperature (ºC) = 60ºC

Reference sequence (5'-3'): 2077- **tcctggactgatcccaattctg**aactcttaccttgaaaacatggaagtggatgtggac accagatgtagtattctgaactacctaaagctaattaagaagagagcatctggagaactaatgacagttgccagatggatgagggagtttat**c gcaaaccatcctgactacaag**-2248

b)

GCLC qPCR assay
Standard Curve Efficiency = 1.972 Error =0.0171
Melting Temperature (average) = 80.6ºC

c)

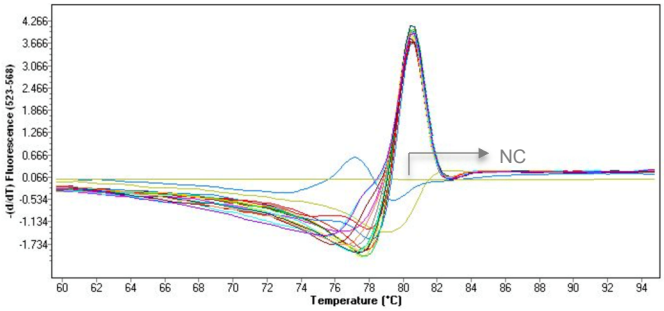

d)

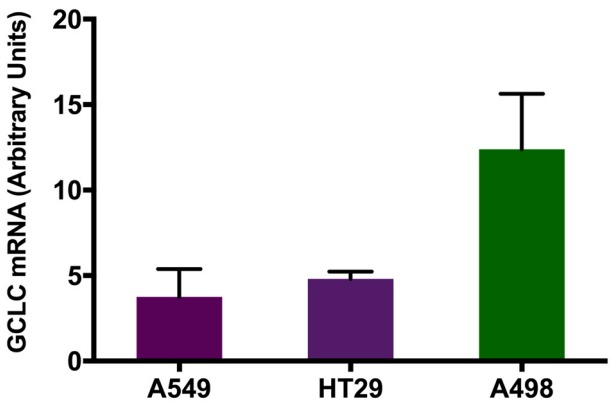

Figure 3.18: GCLC PCR assay. (a) Primer sequences utilised in qPCR, exon location, product length and melting temperature followed by reference sequence with primers highlighted. Numbers in superscript denote the position of the primers within the gene. **(b)** qPCR standard curve details and product melting temperature. **(c)** Typical melting point plot obtained for GCLC qPCRs. **(d)** Abundance of GCLC mRNA for each cell line in RPMI by qPCR analysis. Results showed as arbitrary units and are means ± SD, N=2 and n=6.

a)

GCLM (NM_002061)	
Primers	Exon Location
Forward: ^{849}TTCCTTGGAGCATTTACAGCCTTAC^{873}	5
Reverse: ^{1046}GCAAATGCAGTCAAATCTGGTG^{1025}	6
Product length (bp) = 198	Annealing Temperature (ºC) = 60

Reference sequence (5'-3'): 841- **ttccttggagcatttacagccttac**tgggaggaattagaaaacttagttcagagcaaaa agattgttgccataggtacctctgatctagacaaaacacagttggaacagctgtatcagtgggcacaggtaaaaccaaatagtaaccaagtta atcttgcctcctgctgtgtgatgc**caccagatttgactgcatttgc** -1046

b)

GCLM qPCR assay
Standard Curve
Efficiency = 1.949
Error =0.0583
Melting Temperature (average) = 81.6ºC

c)

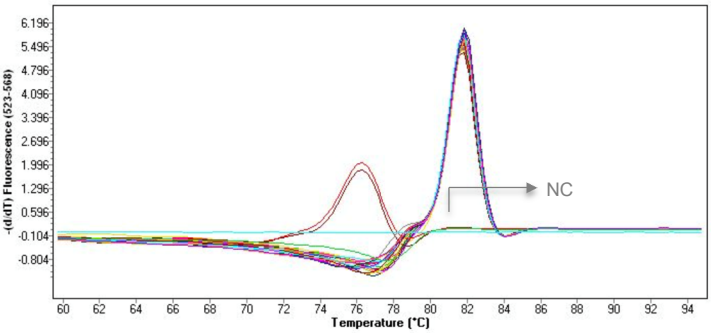

d)

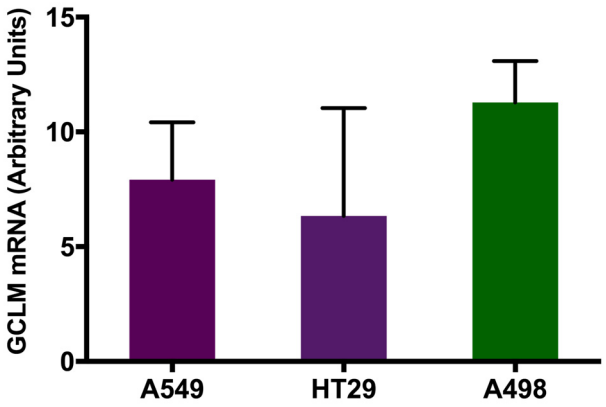

Figure 3.19: GCLM PCR assay. (a) Primer sequences utilised in qPCR, exon location, product length and melting temperature followed by reference sequence with primers highlighted. Numbers in superscript denote the position of the primers within the gene. **(b)** qPCR standard curve details and product melting temperature. **(c)** Typical melting point plot obtained for GCLM qPCRs. **(d)** Abundance of GCLM mRNA for each cell line in RPMI by qPCR analysis. Results showed as arbitrary units and are means ± SD, N=2 and n=6.

a)

GSS (NM_000178)	
Primers	Exon Location
Forward: ^{878}AAATTGCTGTGGTTTACTTCCG^{899} Reverse: ^{978}CTTGGCAGCATGTGACCTCTC^{958}	9 10
Product length (bp) = 101	Annealing Temperature (^{o}C) = 62

Reference sequence (5'-3'): 878- **aaattgctgtggtttacttccg**ggatggctacatgcctcgtcagtacagtctacagaattgggaag cacgtctactgctg**gagaggtcacatgctgccaag-**978

b)

GSS qPCR assay
Standard Curve
Efficiency = 1.937 Error =0.145
Melting Temperature (average) = 82.1^{o}C

c)

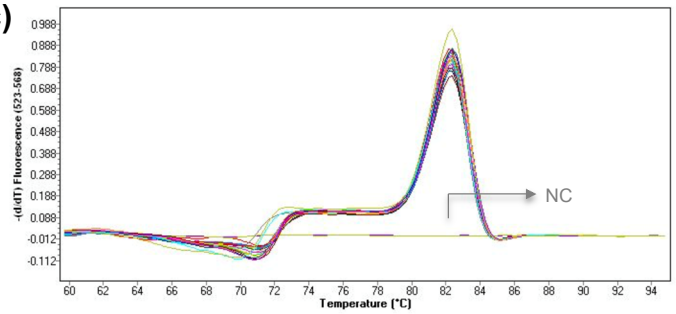

d)

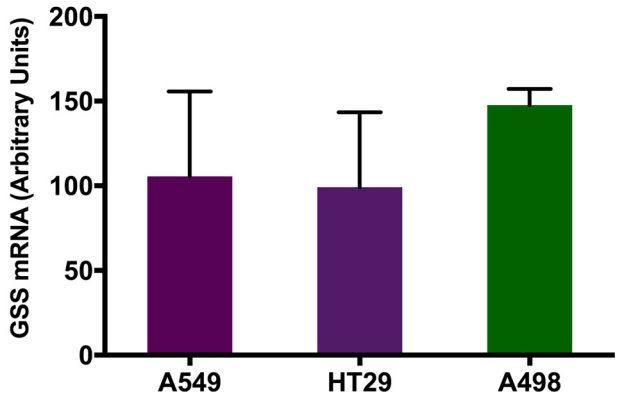

Figure 3.20: GSS PCR assay. (a) Primer sequences utilised in qPCR, exon location, product length and melting temperature followed by reference sequence with primers highlighted. Numbers in superscript denote the position of the primers within the gene. **(b)** qPCR standard curve details and product melting temperature. **(c)** Typical melting point plot obtained for GSS qPCRs. **(d)** Abundance of GSS mRNA for each cell line in RPMI by qPCR analysis. Results showed as arbitrary units and are means ± SD, N=2 and n=6.

3.3 Summary of results and discussion

The data presented in this chapter show that CTB is a non-toxic and fast method to assess the number of viable cells present in a culture. Due its high sensitivity it can be utilised to perform experiments in 96-well plates, this way the amount of reagents required is less than utilised in 12-well plates and allows a higher number of replicates per experiment. CTB has proven to be a reliable assay with a good linear correlation with the number of viable cells, for concentrations up to 200,000 cells/ml, and suitable to evaluate cell growth over time in further experiments. For cells seeded in concentrations of $1X10^3$, $2X10^3$, $4X10^3$, $8X10^3$ and $1.6X10^4$ cells/100µl and subsequently incubated with CTB, the percentage of resazurin reduction by viable cells showed a linear correlation with cell number. Additionally when analysing the fold change in cell number, determined by counting, following GLYT1 and ATF4 siRNA treatment when compared to control, it presented the same result as the fold change in CTB fluorescence readings for the same treatment in the same conditions. Moreover, the similarity of data from the NCI60 database and that obtained in this study, when cell growth curves and doubling times were evaluated, also suggest that the CTB assay, normally used to measure cell viability following toxic challenge, is appropriate for these studies where changes in cell viability are used as an indicator of differences in cell proliferation. Therefore, this cell viability assay has been demonstrated to be interchangeable with cell counting for A549, HT29, A498 and HUVEC cell lines and was utilised in further experiments to assess the number of viable cells following treatments to demonstrate variations in cell proliferation.

As predicted, HUVEC, A549 and HT29 cell lines presented rapid proliferative profiles and A498 was characterised as a slow growing cell line. Analysing their doubling times, the cells presented minor reduction in proliferation when seeded in RPMI in comparison to their growth in DMEM. Additionally, the fast growing cells presented higher mRNA levels of the proliferation marker ki67 than A498 cells. Thus, different growth rates of A549 and HT29 cells in comparison to A498 cell make these cell lines suitable for further investigation of their requirement for extracellular glycine and its impact on cells with different proliferation rates. The rapidly proliferating profile of HUVEC cell line make it a good control to evaluate if extracellular glycine would affect a normal, non-transformed, cell line or if it would have an isolated effect on tumour cells. Additionally other studies observed that endothelial cells express GLYT1

(Guo et al., 2017). Additionally, A549, HT29 and A498 cells were able to accumulate glycine from the extracellular environment suggesting that manipulations that affect glycine uptake could have an effect in these cell lines.

All primer sets presented a good efficiency in qPCRs. A549, HT29, A498 and HUVEC cells amplified GLYT1 and ATF4 in all media tested when utilising total mRNA as observed in end point PCRs. Moreover, end point PCRs for A549 and HT29 cell lines growing in DMEM and RPMI media utilising SNAT2, $ATB^{0,+}$, SHMT2, ATF3, ATF5 and ATF6 mRNA primers amplified a single PCR product, as one strong band appears in the agarose gels with the correct length. Two amplification products were observed when utilising primer for PAT1 in end point PCR. In all experiments, except for GLYT1 end point PCR, a weak band below 100 base pairs was observed for all samples, including negative controls, in the agarose gel; this was proposed as primer dimer, a PCR by-product. However, when qPCRs were performed with each primer pair only one melting point was observed, suggesting that a single product was amplified. In PAT1 qPCR, there is an attempt of forming a second melting point higher than 82^0C, but the shorter annealing and elongation times, 10 and 15 seconds, respectively, in comparison to the 20 seconds utilised in the end point PCR, probably interrupted the amplification of a second PCR product, as only one melting temperature was detected. Additionally, end point PCR and qPCRs utilise different buffers with different $MgCl_2$ concentrations and both PCRs present different hot start period, 5 min in qPCR and 3 min in end point PCR, which can avoid the formation of primer-dimers and improve specificity when amplifying low copy number of cDNA. All qPCR experiments were performed with a standard curve and in all reactions considered in this work the efficiency were close to 2 (100%).

All cell lines presented positive gene expression for GLYT1, a specific glycine transporter, and of its regulator ATF4. GLYT1 mRNA expression presented a tendency to be downregulated in RPMI when compared to DMEM incubation although the only significant reduction in mRNA levels was observed for A498 cell line. HUVEC cell line presented a low GLYT1 mRNA expression when compared to the other cell lines. The HUVEC is an endothelial cell and the other cell lines are epithelial cells; possibly different cell types present different levels of GLYT1 mRNA. Additionally, high glycine concentrations were observed to reduce endothelial cell line proliferation, this way a reduction in glycine uptake will contribute to tumour survival (Rose et al., 1999, Bruns et al., 2016, Bruns et al., 2014). However, ATF4 mRNA expression was greater in A498 cells growing in RPMI and HUVEC cells when compared to the other cell lines, the

same cells that presented low GLYT1 mRNA levels. Hence, low levels of GLYT1 may reduce glycine uptake that could influence cell proliferation leading to an increased doubling time when cells were seeded in RPMI. Thus, A549, HT29, A498 and HUVEC proved to be appropriate *in vitro* models for this study, which is focused to evaluate the effect of GLYT1 and ATF4 downregulation on cell proliferation.

A549 and HT29 expressed other amino acid transporters involved in glycine uptake, namely PAT1, SNAT2 and $ATB^{0,+}$. PAT1 when localised in the lysosome senses the amino acid availability in the lysosomal lumen and interacts with mTORC1, having an impact on cell replication, survival and metabolism (Zheng et al., 2016, Goberdhan, 2010). SNAT2 is upregulated under amino acid starvation and also has been described to interact with mTORC1 and is upregulated by the eIF2α (Zheng et al., 2016, Gjymishka et al., 2008). This way, PAT1 and SNAT2 participate in the amino acid sensing system, but the mechanisms that the amino acid transporters sense amino acid starvation or if they can interact with each other is not yet fully understood. The A498 cell line expressed PAT1 and SNAT2 but not $ATB^{0,+}$. As discussed previously, normal cells other than colorectal and lung cells do not express $ATB^{0,+}$, and even in these there is low expression of this gene product (Sikder et al., 2017). Its expression is, though, increased in a few cancer cell types such as colorectal, breast, pancreatic and stomach (Sikder et al., 2017). Therefore, in the following chapters PAT1, SNAT2 and $ATB^{0,+}$ were further investigated following GLYT1 and ATF4 knockdown, as a possible compensatory upregulation of one or several of these genes could have an impact on glycine uptake and then on cell proliferation.

All cells were able to express other activating transcription factors, ATF3, ATF5 and ATF6. Studies have demonstrated that under amino acid starvation there is an accumulation of unfolded protein in the ER leading to ER stress and to the unfolded protein response (UPR) triggering the PERK/eIF2α~P/ATF4 pathway, which activates the translation of ATF3, ATF5 and ATF6 (Lee et al., 2013, Jiang et al., 2004, Zhou et al., 2008, Teske et al., 2011). This way, ATF4 may influence the translation of other ATFs. In fact, when ATFs mRNA levels were analysed, A549 cell line presented reduced levels of ATF4 mRNA and also reduced ATF3 and ATF6 mRNA abundance when compared to the other cancer cell lines in this study, suggesting a link among these transcription factors. Additionally, studies have shown that ATF4 also activates the transcription of xCT, the subunit of the cystine transporter, (Gorrini et al., 2013, Sasaki et al., 2002) and as expected xCT mRNA levels were also lower in A549 cell line than the other cells analysed. Cystine is rapidly converted to cysteine in cells,

which is essential for GSH synthesis, the major cellular antioxidant (Huang et al., 2005, Sato et al., 2005). Thus, the possible effect of ATF4 knockdown on ATF3, ATF5, ATF6 and xCT mRNA expression was also evaluated in further experiments.

Chapter 4. GLYT1 knockdown

4.1 Introduction

This chapter discusses the influence of the specific glycine transport GLYT1 on tumour cell proliferation. The rapidly proliferating cell lines, A549 and HT29, the slow proliferating cell line, A498, and the normal cell line, HUVEC, were transfected with GLYT1 siRNA. The efficiency of GLYT1 knockdown was confirmed by qPCR analysis of GLYT1mRNA expression and the effect on function was assessed by evaluating the influence on total glycine uptake. Then, the number of viable cells, the number of proliferating cells and the mRNA expression of the proliferation marker ki67 were evaluated following GLYT1 knockdown and compared to control cells. Additionally, the effect of GLYT1 downregulation on mRNA levels of other amino acid transporters able to transport glycine, such as PAT1, SNAT2 and $ATB0^{,+}$, and on intracellular enzymes involved in glycine synthesis, such as SHMT2, was analysed by qPCR. Finally, the effect of GLYT1 knockdown on glutathione levels and on mRNA expression of glutathione synthesising enzymes was evaluated.

As described in previous chapters, recent studies have highlighted the relevance of glycine and glycine metabolism to cancer cell proliferation. Clinical studies correlated high glycine levels in tumour tissue to poor patient prognosis (Cao et al., 2012, Redalen et al., 2016). A recent study utilising mouse models for lymphoma and for intestinal cancer observed that glycine and serine starvation improved animal survival (Maddocks et al., 2017). Jain and collaborators showed that the requirement for glycine was significantly greater in rapidly proliferating cancer cells than in either slow growing cancer cells or rapidly-proliferating non-cancerous cells (Jain et al., 2012). Although the authors showed that part of the increased demand for glycine in rapidly proliferating tumour cells was met by upregulation of mitochondrial glycine synthesis via SHMT2 they also demonstrated a need for extracellular glycine in maintenance of cell proliferation (Jain et al., 2012). Extracellular glycine is utilised in purine and glutathione (GSH) synthesis (Jain et al., 2012). GSH is a tripeptide composed of glutamine, cysteine and glycine and its synthesis is catalysed by the enzymes GCL (GCLC and GCLM) and GSS (Lu, 2013). GSH synthesis is dependent

on L-cysteine transported by Xc- cystine transporter, that subunit xCT is also regulated by ATF4 (Huang et al., 2005, Wu et al., 2004, Sasaki et al., 2002, Gorrini et al., 2013, Sato et al., 2004). Additionally, previous work from our group demonstrated that an increase in glycine uptake dependent on GLYT1 transporter results in higher GSH levels during oxidative stress (Howard et al., 2010). Therefore, these data suggest that manipulation of glycine availability targeting GLYT1 may allow a novel therapeutic approach to treatment of highly progressive cancers.

Glycine can be transported into the cell by the specific glycine transporter GLYT1 (SLC6A9) (Howard and Hirst, 2011). The majority of studies involving GLYT1 are in neuronal cells. Glycine acts as a neurotransmitter and this transporter is involved in glycine reuptake at the synaptic cleft, interrupting the glycine effects (Howard and Hirst, 2011, Harsing and Matyus, 2013, Eulenburg et al., 2005). A large number of GLYT1 inhibitors are being tested due their potential use as treatments for schizophrenia, pain and alcohol dependence (Harvey and Yee, 2013).

GLYT1 protein levels are upregulated in certain tumour types, according to the Human Protein Atlas - an open access database that contains 216 different cancer samples analysed for protein expression levels using immunohistochemistry (Uhlén et al., 2005, Uhlén et al., 2010, Uhlén et al., 2015, Uhlén et al., 2017). The antibody utilised in this study was HPA013977 from Sigma Aldrich specific for GLYT1 (Uhlén et al., 2005, Uhlén et al., 2010, Uhlén et al., 2015, Uhlén et al., 2017). Although the accuracy of this antibody in immunohistochemistry was stated as uncertain, being only partly correlated with gene/protein data from literature and mainly not consistent with RNA expression, they were able to detect variable levels of protein expression in different tumour types (Uhlén et al., 2017). The majority of cancer tissues analysed were weakly stained with GLYT1 antibody or negative, but some patient tissue samples of carcinoid, colorectal, melanoma, glioma, lung and renal cancer showed moderate to strong cytoplasmic staining not verified in normal tissues (Figure 4a) (Uhlén et al., 2017). However, it is important to take into consideration that the poor staining observed in some cancer tissues analysed could be due to a lack of efficient antibody for GLYT1 protein commercially available. Moreover, GLYT1 is regulated by the activating transcription factor ATF4 itself linked to cancer proliferation (Harding et al., 2003, Singleton and Harris, 2012). Despite this information little is known about GLYT1 influence in cancer.

Glycine can be transported also by other amino acid transporters including, as described previously, PAT1, SNAT2 and $ATB^{0,+}$ (Schiöth et al., 2013, Sloan and Mager, 1999). PAT1 and SNAT2 participate in the amino acid sensing system and function as sensors regulating mTORC1 influencing cell growth (Zheng et al., 2016). The complex regulation in the amino acid sensing system and interaction between amino acid transporters and activation of mTORC1 is not yet fully understood. Thus our interest in evaluating if GLYT1 downregulation and consequently glycine depletion would affect other amino acid transporters such as PAT1, SNAT2 and $ATB^{0,+}$, possibly upregulating them as an attempt to maintain intracellular levels of glycine and then maintain cell proliferation.

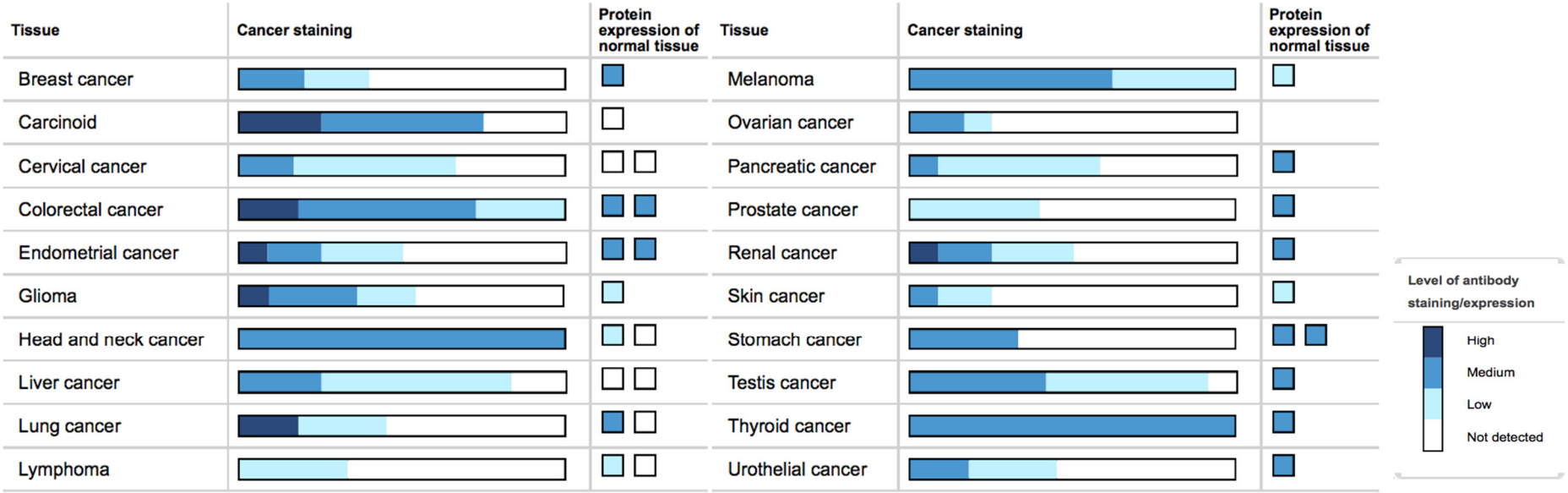

Figure 4a: Levels of GLYT1 protein expression from 216 patient tumour tissues analysed by immunohistochemistry. The protein expression is then compared to normal tissue from samples of three individuals. The levels of staining/expression of GLYT1 protein was classified as high, medium, low or not detected. In breast cancer tissues 2 out of 10 patients showed medium expression the same level observed in normal tissue. For carcinoid, 3 of 4 patients showed high/medium expression whereas in normal tissue the protein was not detected. In cervical cancer 2 patients showed medium and 6 patients showed low expression whereas in normal tissue the protein was not detected. In colorectal cancer 2 of 11 patients analysed showed high expression whereas normal tissue present moderate expression. In endometrial cancer tissue 1 of 12 patients presented high expression of GLYT1, in normal tissue the expression was moderate. In glioma tissues 4 of 11 patients presented high expression whereas in normal tissue the expression level is low. In head and neck cancer 3 of 3 patients presented moderate expression whereas in normal tissues the expression low/not detected. In liver cancer 10 of 12 patient showed medium/low expression and normal tissue levels was not detected. In lung cancer tissues 2 of 11 patients presented high expression and normal tissue presented moderate/not detected expression. In melanoma tissues 5 of 8 patient presented moderate expression and normal tissue showed low expression. In ovarian cancer tissues 3 of 12 patient presented moderate/ low expression. In skin cancer, 1 of 12 presented high expression of GLYT1 in comparison to moderate expression in normal tissue. In skin cancer 1 of 12 patients showed moderate expression whereas normal tissue presents low expression. For the other cancer types analysed no increase in GLYT1 expression was observed in the patients analysed in comparison to a normal sample. (Figure from www.proteinatlas.org) (Uhlén et al., 2005, Uhlén et al., 2010, Uhlén et al., 2015, Uhlén et al., 2017).

4.2 Results

4.2.1 *GLYT1 knockdown efficiency*

Primarily the efficiency of GLYT1 knockdown experiments was assessed analysing GLYT1 mRNA expression and total glycine uptake following transfection with GLYT1 siRNA. Briefly, A549, HT29, A498 and HUVEC cell lines were seeded in 12 and 24-well plates in RPMI, transfected with Negative or GLYT1 siRNA and incubated for further 72 hours in RPMI. Then, total RNA was extracted and ^{3}H-glycine uptake experiments were performed as described in Chapter 2.

In order to evaluate if transfection with GLYT1 siRNA was efficient, qPCR analyses were performed to verify its effect on GLYT1 mRNA abundance. Following RNA extraction, RNA yield and purity were analysed by measuring absorbance at 260 and 280 nm. All RNAs utilised in this study presented a 260/280 ratio between 1.95 and 2.0 suggesting its purity, indicating an absence of possible contaminants that absorb light at 280nm, such as proteins and some organic compounds. The correlation between absorbance and RNA concentration was determined according to Beer-Lambert Law, where 1 A_{260} unit of ssRNA is equal to 40 ng/µl, this way absorbance measurements at 260 nm were multiplied by 40. Then 500ng of total RNA extracted following transfection with Negative or GLYT1 siRNA was reverse transcribed to cDNA as described in Section 2.4.1 and qPCR was performed utilising a specific primer pair for GLYT1 mRNA. As shown in Figure 4.1, GLYT1 mRNA expression was significantly reduced following transfection with GLYT1 siRNA when compared to the control, when cells where transfected with a Negative siRNA. When compared to controls, GLYT1 mRNA expression was reduced 86.2% ($p<0.0001$) in A549, 79.02% ($p<0.0001$) in HT29, 92.8% ($p<0.0001$) in A498 and 55.6% in HUVEC cell lines. Therefore, a significant reduction in GLYT1 mRNA abundance was observed for all cell lines confirming GLYT1 knockdown and the efficiency of the method utilised.

Following GLYT1 knockdown total glycine uptake was evaluated in order to assess a possible reduction in functional activity. This method was chosen as previous attempts to estimate GLYT1 protein abundance using commercially available antibodies in Western blotting and related techniques have proven unsuccessful as have attempts by this group to generate antibodies. As described in Section 2.6, the transfection medium was removed, cells were washed three times and then incubated

for 30 minutes in Kreb's buffer at 37^0C. Then, the Kreb's buffer was replaced with fresh buffer containing 0μM, 1μM, 50μM, 100μM, 200μM, 500μM or 1000μM of glycine in association with 0.5μCi/ml [2-^{3}H]-Glycine and incubated for 10 minutes. The amount of glycine uptake was then calculated and normalised with the number of viable cells at the end of GLYT1 knockdown experiments. GLYT1 knockdown reduced the amount of glycine uptake when compared to control cells at all concentrations and for all cell lines tested (Figure 4.2, left panel graphs). GLYT1 knockdown in A549 and HT29 reduced glycine uptake by 34.8% ±13.1 ($p<0.0001$) and 31.4% ±9.0 ($p<0.0001$), respectively, and in A498 reduced it to 40.9% ± 7.9 ($p<0.0001$) of total glycine uptake when compared to control cells (Figure 4.2, left panel graphs). These data are consistent with the reductions in GLTY1 mRNA leading to a reduction of glycine transport, suggesting mediation, at least in part, by a reduction in GLYT1 protein levels.

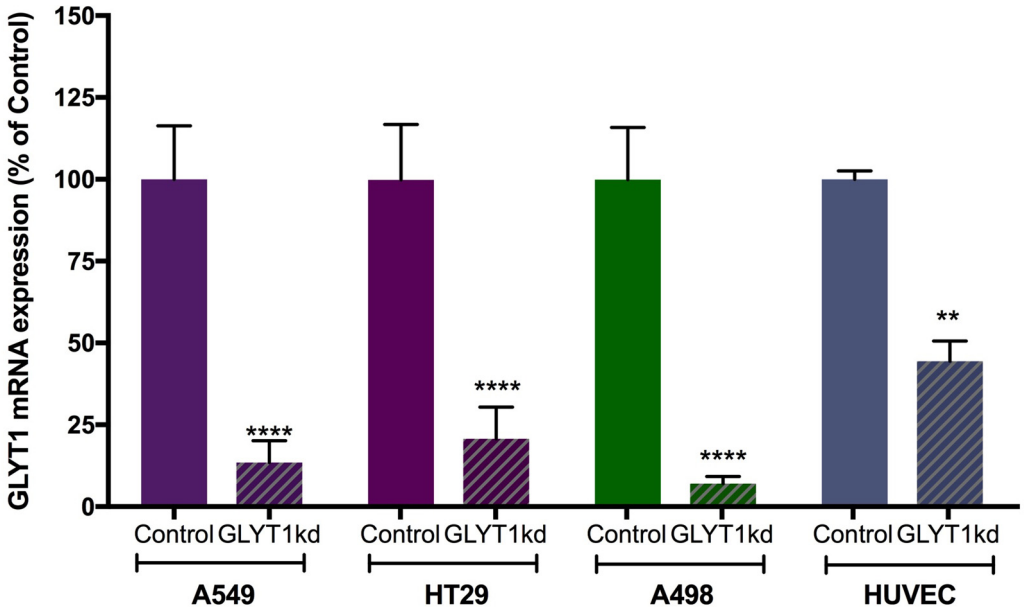

Figure 4.1: GLYT1 knockdown efficiency. Relative abundance of GLYT1 mRNAs in the cell samples. Data bars for cells transfected with GLYT1 siRNA are marked GLYT1 kd and cells transfected with Negative siRNA are referred to as Control. Data are means ± SEM, N=3 and n=9 for A549, HT29 and A498 and N=2, n=4 for HUVEC cell line. Statistical analysis comparing the treatments (knockdowns) and controls were performed by one-way-ANOVA with Tukey's post hoc analysis. Values significantly different from controls are marked: $p<0.01$ (**) and $p<0.0001$ (****).

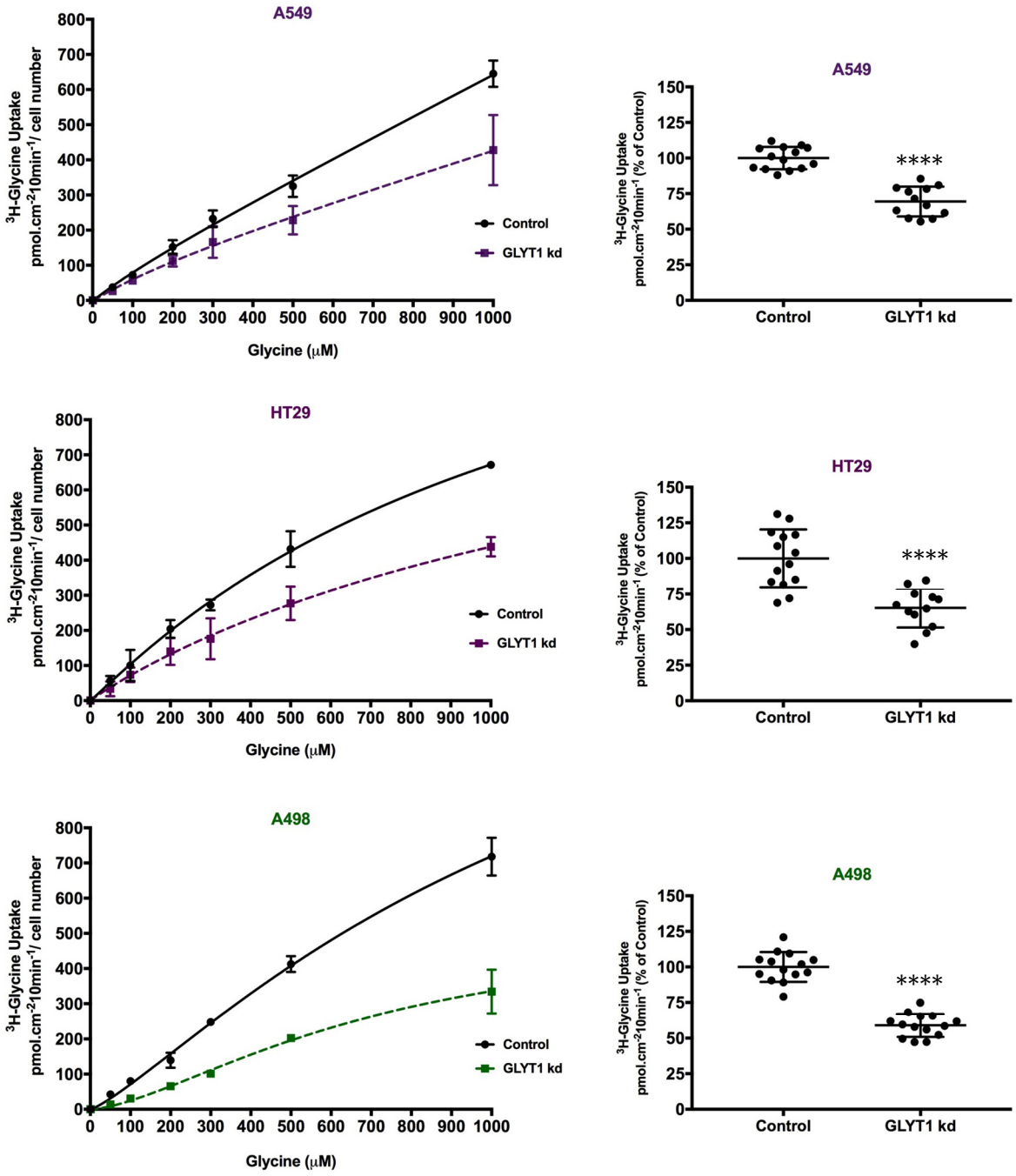

Figure 4.2: ^{3}H-Glycine Uptake measurements for A549, HT29 and A498 cell lines. Amount of total glycine uptake measured after 72h transfection with GLYT1 or Negative siRNAs referred to as GLYT1 kd and Control, respectively, for each cell line. The amount of glycine uptake was calculated and normalised with the number of viable cells post transfection. Data are means ± SEM, N=2 and n=6. Statistical analysis comparing GLYT1 kd treatment and control was performed by unpaired t-test considering $p<0.0001$ (****).

4.2.2 GLYT1 knockdown effect on cell proliferation

Once the efficiency of knockdown experiments was verified, the effect of glycine uptake limitation through GLYT1 downregulation on cancer cell proliferation was evaluated. The number of viable cells was assessed following GLYT knockdown (GLYT1kd) as well as the number of replicating cells.

Cell viability assay

A549, HT29, A498 and HUVEC cells were plated in a 96-well plate and the number of viable cells was measured 72h post-transfection with GLYT1 or Negative (Control) siRNAs by adding 20µl CTB to each well and incubating for a further 3 hours prior to fluorescence measurement. GLYT1kd reduced the number of viable A549 and HT29 cells, compared with Control siRNA treatment, but had no significant effect on A498 and HUVEC cell lines. Microcopy images showed a visual reduction in cell number of A549 (Figure 4.3a) and HT29 (Figure 4.4a) cell lines following GLYT1kd and the following CTB analysis confirmed a reduction of 35.2%, $p<0.0001$ (Figure 4.3b) and 30.9%, $p<0.0001$ (Figure 4.4b) in the number of viable cells when compared to respective controls. In contrast, GLYT1 downregulation had only a minimal effect in A498 cells according to microscopy images and presenting only 8.9%, $p<0.05$, reduction in the number of viable cells (Figure 4.5). Additionally GLYT1kd had no significant effect on the normal rapidly proliferating HUVEC cell line in this experiment (Figure 4.6). When compared between the cell lines GLYT1 knockdown influence on reducing cell viability was significantly greater in the rapidly proliferative cancer cell lines, A549 and HT29, than in the slowly proliferative one, A498, and the rapidly proliferating normal cell line, HUVEC (Figure 4.7).

Cell proliferation assay

In order to investigate if a decrease in cell proliferation resulted in the observed reduction in cell number following GLYT1kd, a cell proliferation assay was performed. The tumour cell lines A549, HT29 and A498 were plated in 12 well-plates containing 13mm coverslips and the number of proliferating nuclei was evaluated 72h post-transfection with GLYT1 or Negative (Control) siRNAs using the Click-it EdU assay followed by fluorescent microscopy. The number of replicating cells where evaluated by analysing the levels of fluorescent EdU incorporation, and the results are presented as percentage of proliferating index (number of replicating nuclei/ number of total

nuclei). For A549 cell line 47% of the control cells and 20% of GLYTkd cells were proliferating (Figure 4.8). For HT29 cell line 68% of the control cells and 37% of GLYT kd cells were proliferating (Figure 4.9). For A498 cell line only 25% of the control cells and 21% of GLYT kd cells were proliferating (Figure 4.). Therefore, a significant reduction in cell proliferation of 58% ($p<0.001$) and 45% ($p<0.01$) was observed for the fast growing cell lines, A549 and HT29, respectively, when compared to control cells, whereas no significant difference was observed for the slow growing cell line, A498 (Figure 4.10). Moreover, comparing the proliferation index of the control cells between the different cell lines is possible to confirm their proliferative profile, as A549 and HT29 presented higher proliferation rates, 47% and 68%, respectively, then A498 cells, 25% (Figure 4.11).

Ki67

The mRNA expression of the proliferation marker ki67 was analysed following GLYT1kd. When compared to the controls, there was a reduction in ki67 mRNA abundance of 45.5% ($p< 0.05$) for A549 cells and 52.2% ($p<0.001$) for HT29 cells, respectively, following GLYT1 kd, but no significant difference was observed in ki67 mRNA levels for the A498 cell line (Figure 4.12). These results are in agreement with the previous experiments, suggesting that downregulation of GLYT1 affects proliferation only in the rapidly proliferating cancer cell lines.

A)

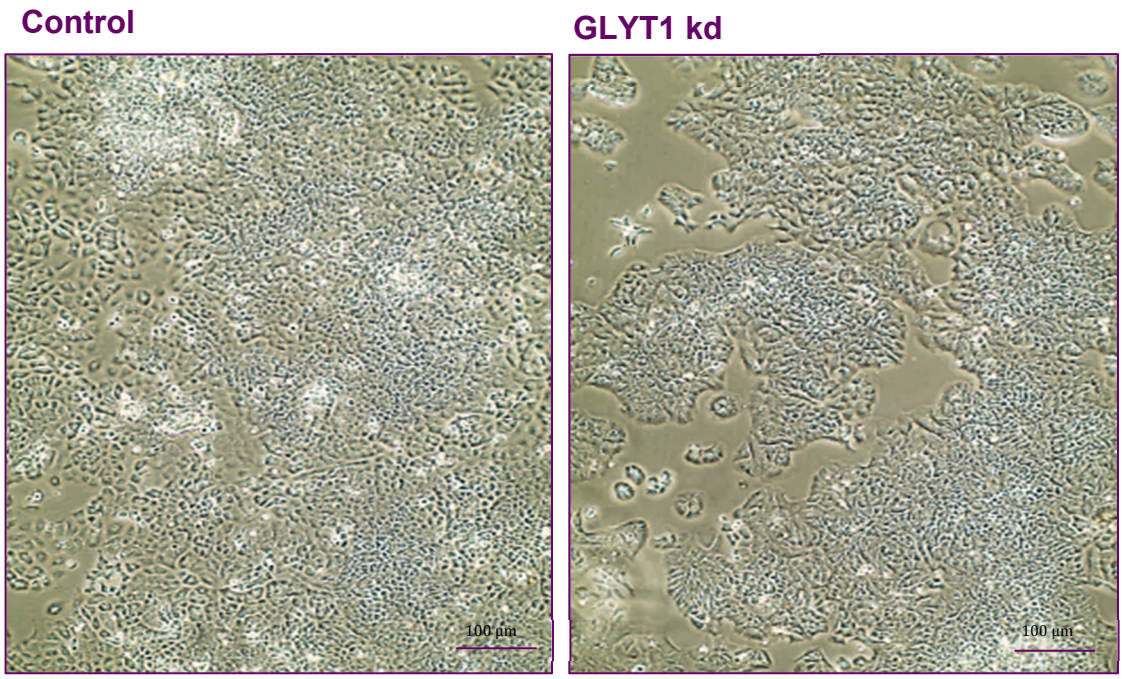

B)

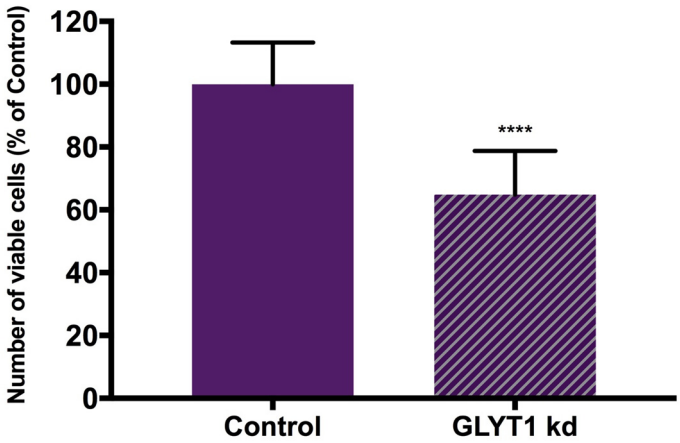

Figure 4.3: A549 cell number following GLYT1 Knockdown experiments. 20X microscopy representative images (A) and CTB assay analysis (B) of A549 cell line after 72 hours transfection with Negative siRNA (Control) or GLYT1 siRNA (GLYT1 kd). Number of viable cells presented as percentage of control according to fluorescence measurement of 96-well plate wells after 3h incubation with CTB reagent. Data are presented as mean ± SEM, N=3 and n=15 per group. Statistical analysis comparing GLYT1 kd treatment and control was performed by unpaired t-test considering $p<0.0001$ (****).

A)

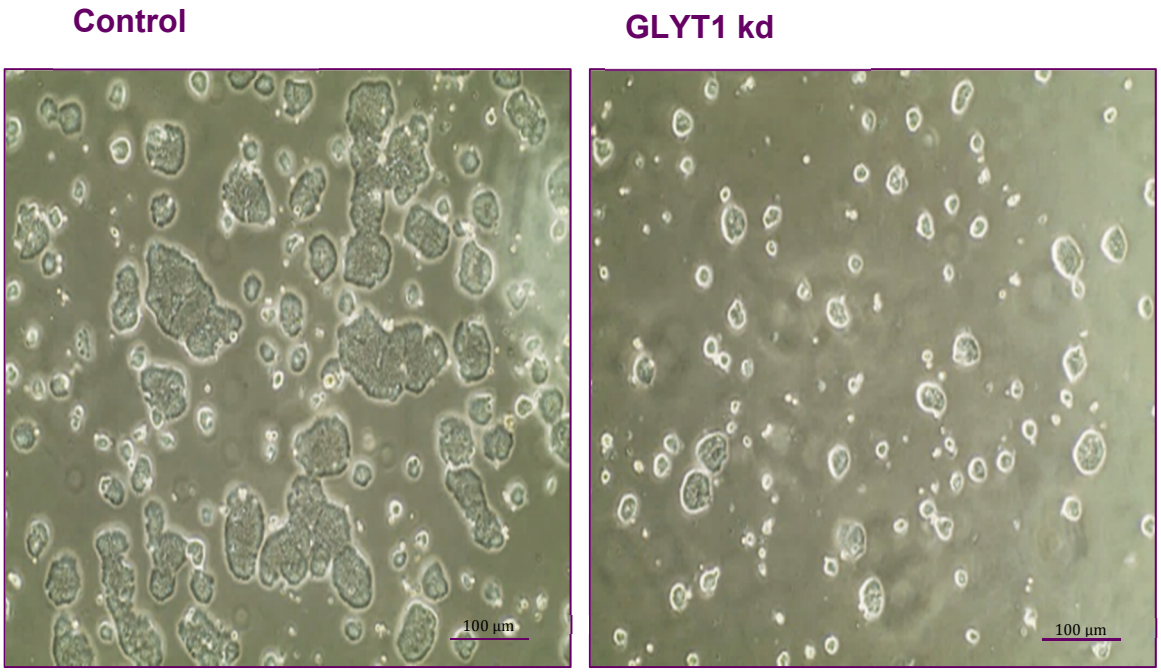

B)

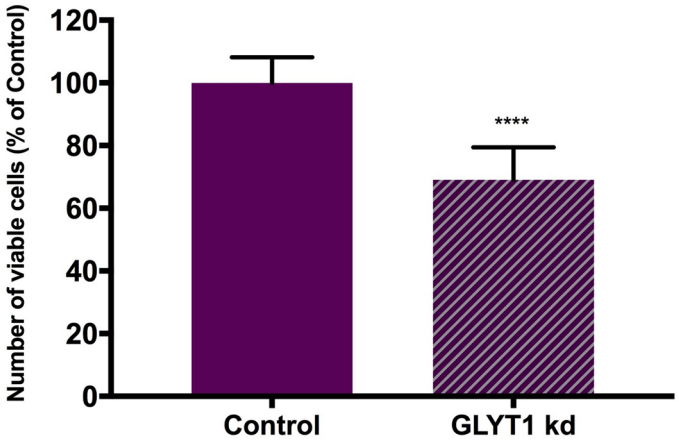

Figure 4.4: HT29 cell number following GLYT1 Knockdown experiments. (A) 20X microscopy representative images and (B) CTB assay analysis of HT29 cell line after 72 hours transfection with Negative siRNA (Control) or GLYT1 siRNA (GLYT1 kd). (B) Number of viable cells presented as percentage of control according to fluorescence measurement of 96-well plate wells after 3h incubation with CTB reagent. Data are presented as mean ± SEM, N=3 and n=15 per group. Statistical analysis comparing GLYT1 kd treatment and control was performed by unpaired t-test considering $p<0.0001$ (****).

A)

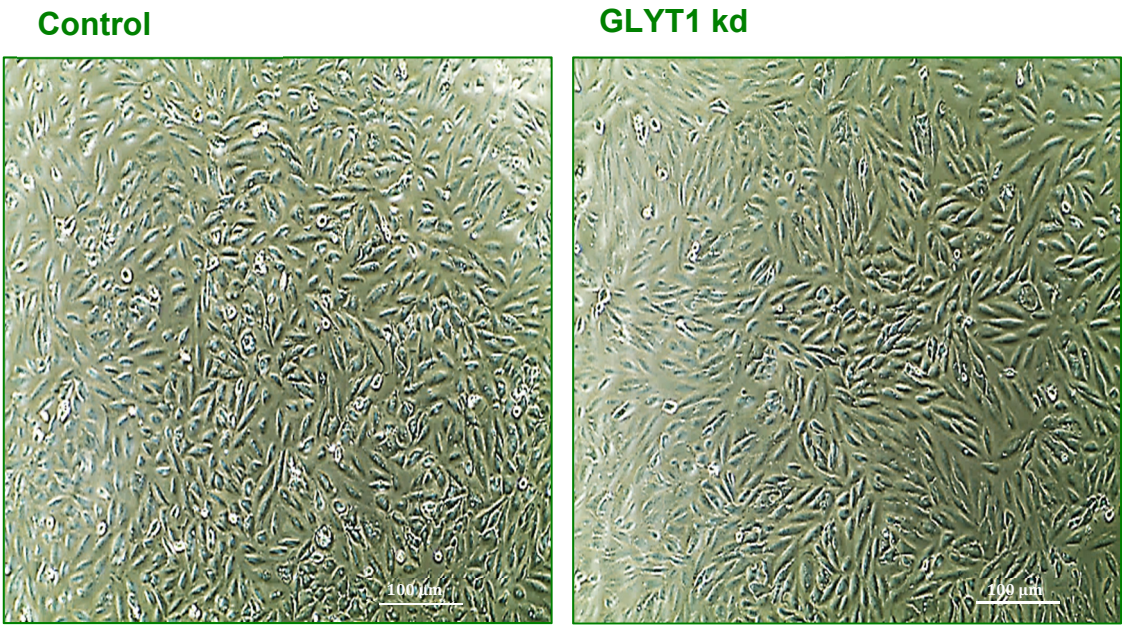

B)

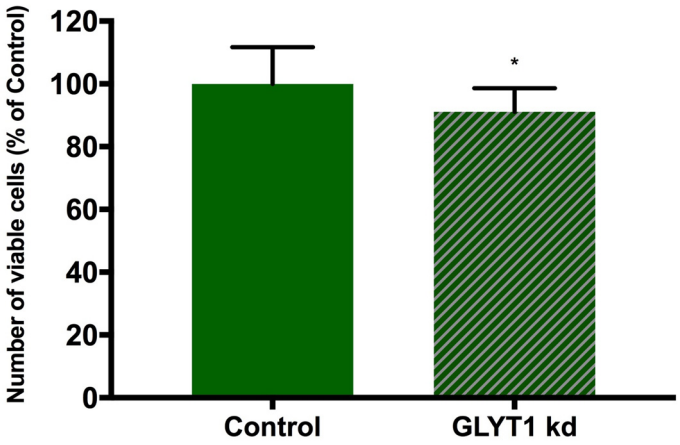

Figure 4.5: A498 cell number following GLYT1 Knockdown experiments. (A) 20X microscopy representative images and (B) CTB assay analysis of A498 cell line after 72 hours transfection with Negative siRNA (Control) or GLYT1 siRNA (GLYT1 kd). Number of viable cells presented as percentage of control according to fluorescence measurement of 96-well plate wells after 3h incubation with CTB reagent. Data are presented as mean ± SEM, N=3 and n=15 per group. Statistical analysis comparing GLYT1 kd treatment and control was performed by unpaired t-test considering $p<0.05$ (*).

A)

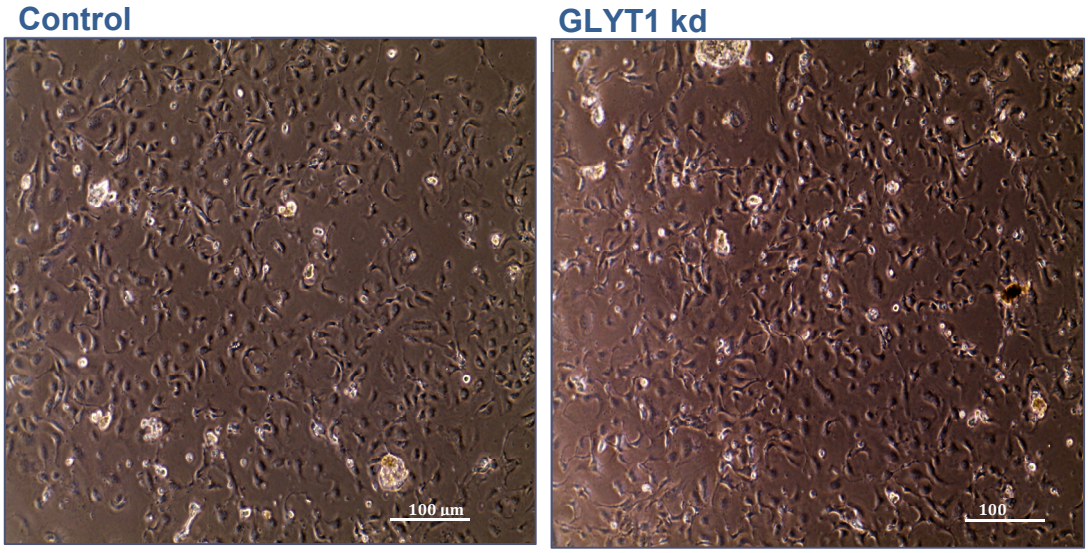

B)

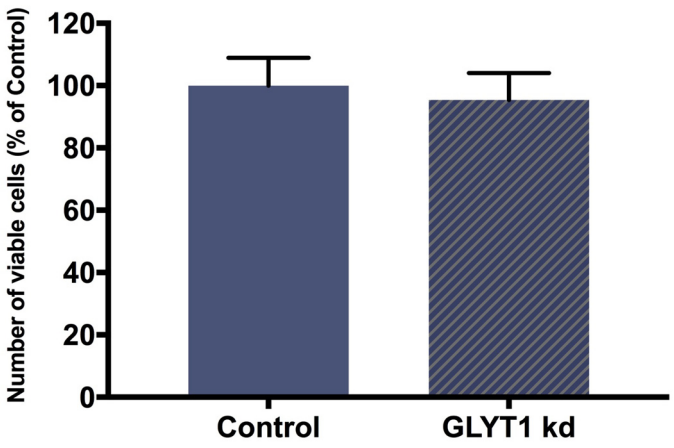

Figure 4.6: HUVEC cell number following GLYT1 Knockdown experiments. (A) 20X microscopy representative images and (B) CTB assay analysis of HUVEC cell line after 72 hours transfection with Negative siRNA (Control) or GLYT1 siRNA (GLYT1 kd). Number of viable cells presented as percentage of control according to fluorescence measurement of 96-well plate wells after 3h incubation with CTB reagent. Data are presented as mean ± SEM, N=2 and n=10 per group. Statistical analysis comparing GLYT1 kd treatment and control was performed by unpaired t-test.

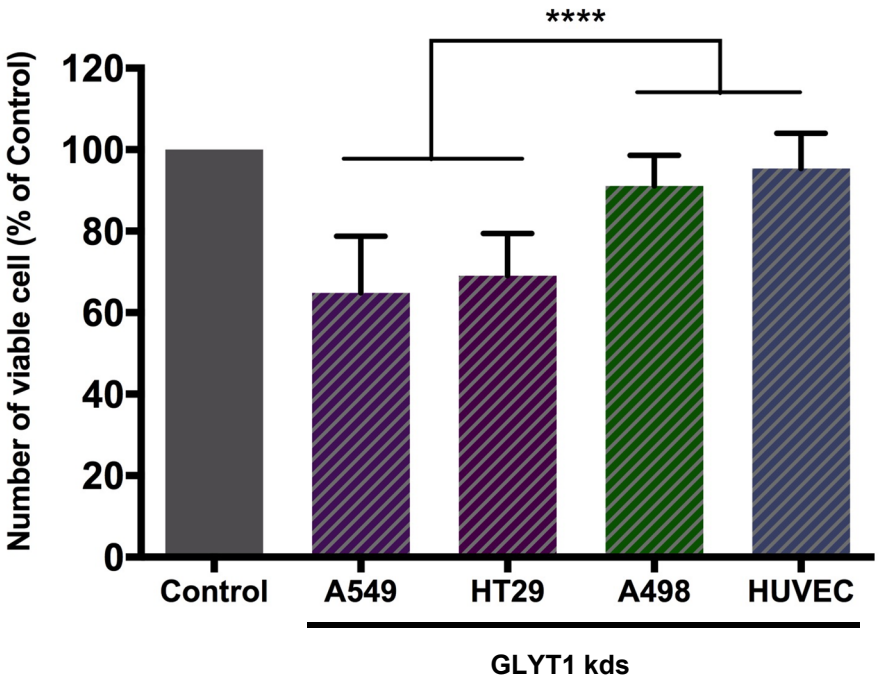

Figure 4.7: GLYT1 knockdown (kd) different effects on cell growth between cell lines. The effect of GLYT1 kd, compared with control siRNA treatment, on the number of viable cells was significantly different and smaller in slowly proliferative cell, A498, and normal cell line, HUVEC, than in the rapidly proliferative cell lines, A549 and HT29 following GLYT1 kd. Data are presented as mean ± SEM, with N=3, n=15 for A549, HT29 and A498 and N=2, n=10 for HUVEC cell line. Statistical analysis comparing GLYT1 kd effect between cell lines were performed by one-way-ANOVA with Tukey's post hoc analysis considering $p<0.0001$ (****).

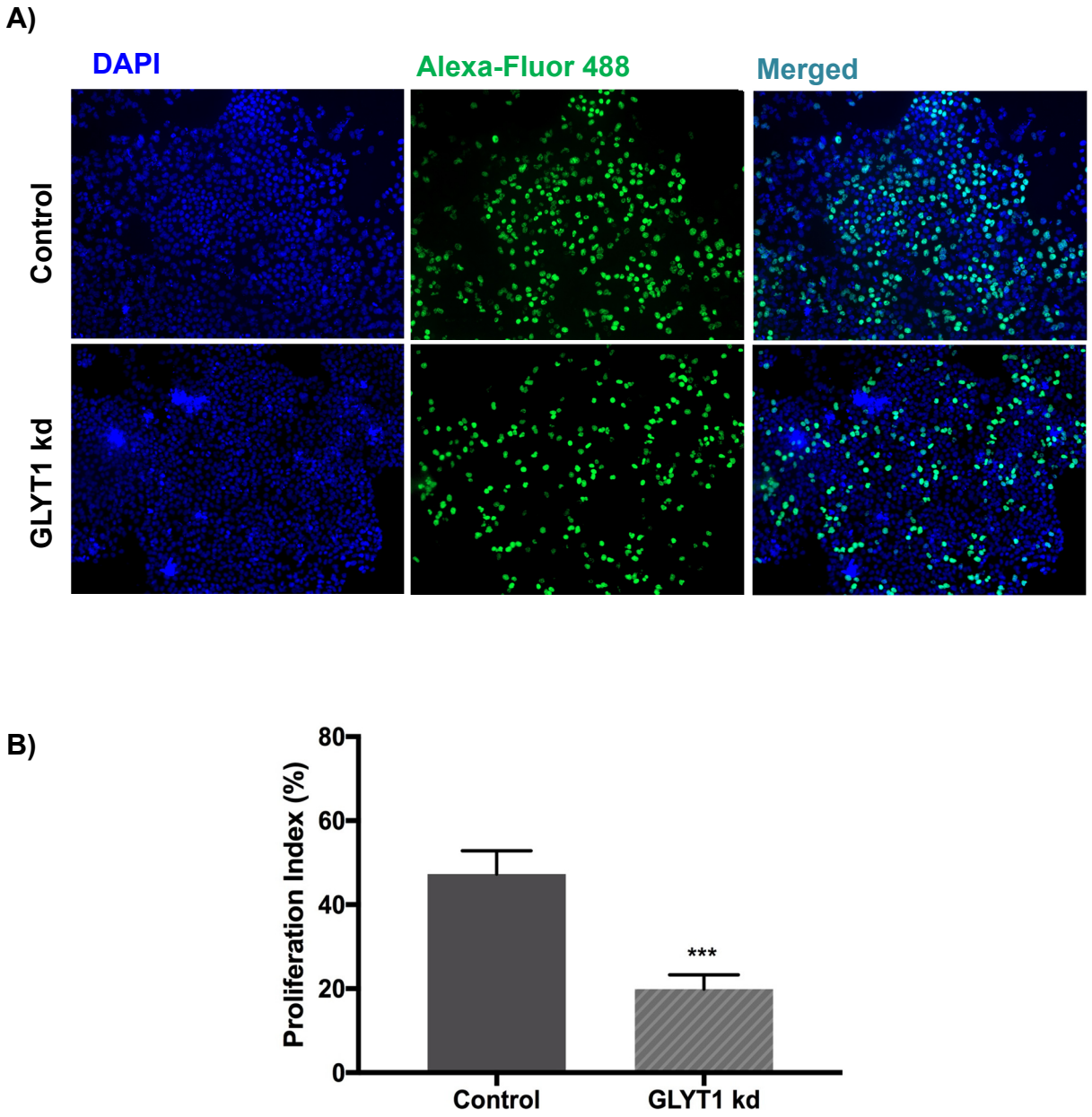

Figure 4.8: GLYT1 knockdown reduced A549 cell proliferation. Click-it EdU cell proliferation assay was performed following GLYT1 knockdown experiments. (A) Fluorescent microscopy images of total nuclei stained with DAPI (blue) and proliferating nuclei stained with EdU labelled with AlexaFluor®488 (green). (B) Four photographs were randomly selected for each group, Control and GLYT1 kd, and number of EdU positive and total nuclei were counted utilising ImageJ program. Percentage proliferation index was calculated dividing the number of proliferating nuclei by the total number of nuclei. Data represent mean ± SEM, n=4. Statistical analysis comparing the treatment (GLYT1 kd) and control of each cell line were performed by unpaired t-test considering $p<0.001$ (***).

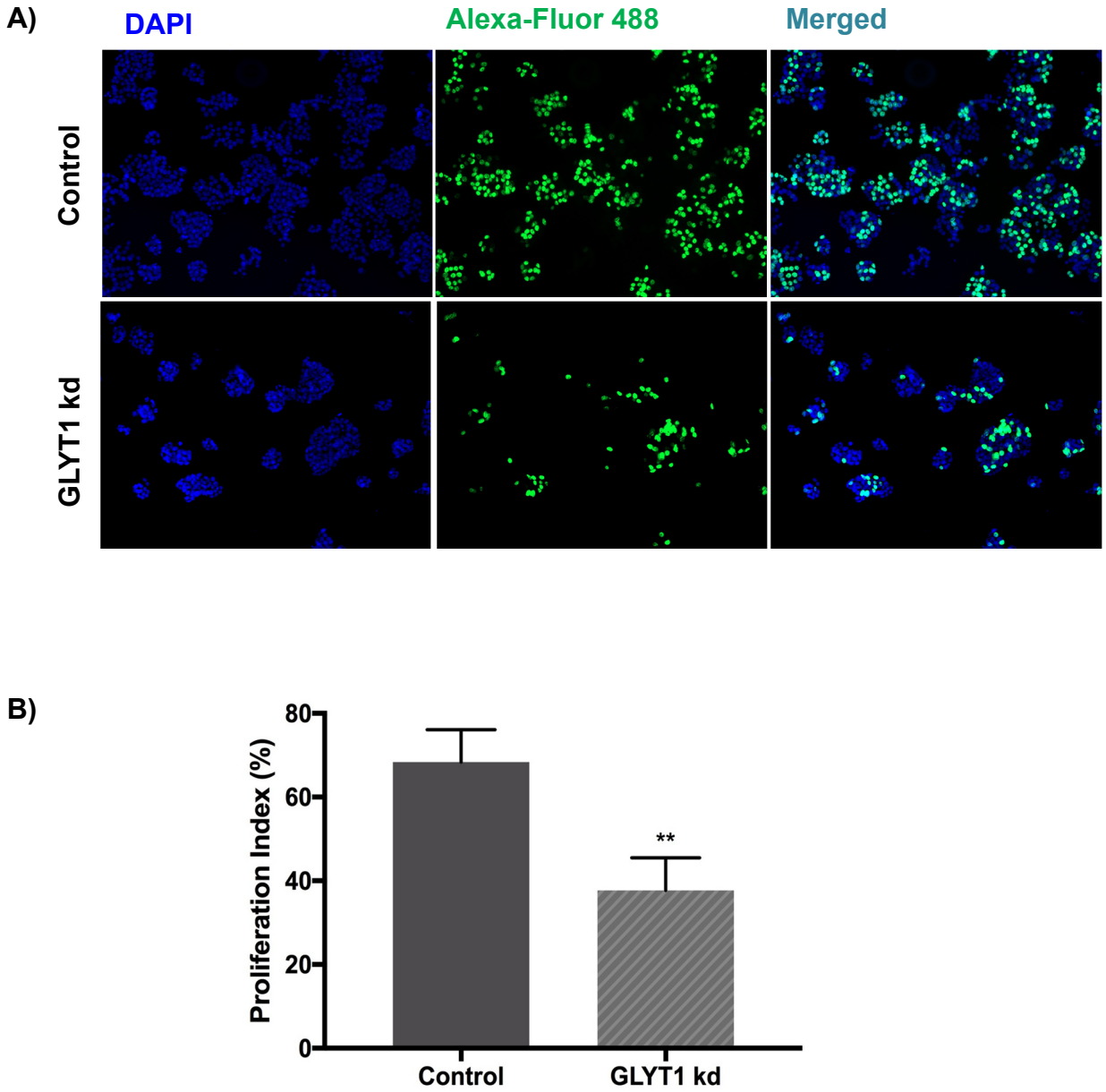

Figure 4.9: GLYT1 knockdown reduced HT29 cell proliferation. Click-it EdU cell proliferation assay was performed following GLYT1 knockdown experiments. (A) Fluorescent microscopy images of total nuclei stained with DAPI (blue) and proliferating nuclei stained with EdU labelled with AlexaFluor®488 (green). (B) Four photographs were randomly selected for each group, Control and GLYT1 kd, and number of EdU positive and total nuclei were counted utilising ImageJ program. Percentage proliferation index was calculated dividing the number of proliferating nuclei by the total number of nuclei. Data represent mean ± SEM, n=4. Statistical analysis comparing the treatment (GLYT1 kd) and control of each cell line were performed by unpaired t-test considering $p<0.01$ (**).

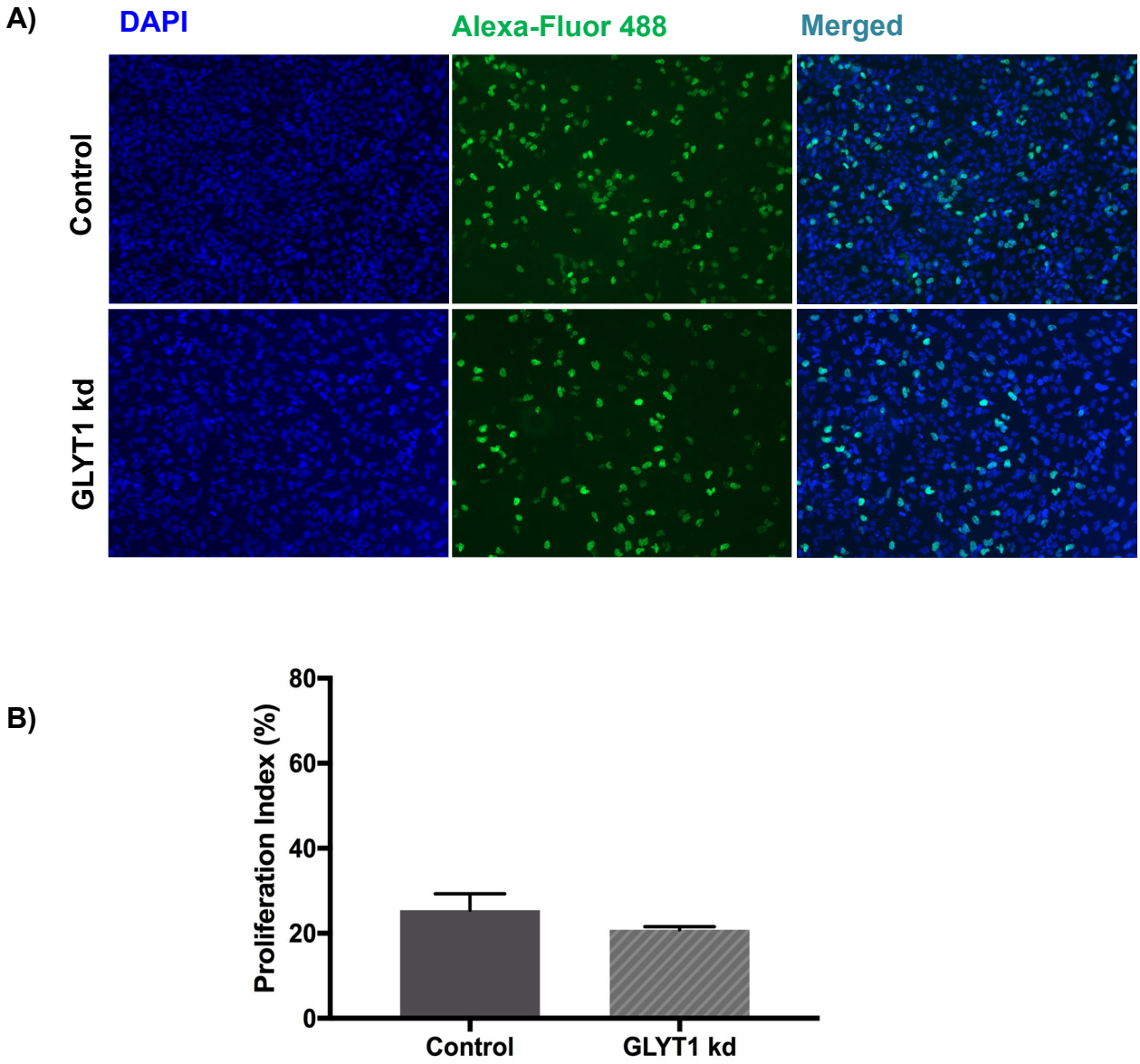

Figure 4.10: GLYT1 knockdown had no effect on A498 cell proliferation. Click-it EdU cell proliferation assay was performed following GLYT1 knockdown experiments. (A) Fluorescent microscopy images of total nuclei stained with DAPI (blue) and proliferating nuclei stained with EdU labelled with AlexaFluor®488 (green). (B) Four photographs were randomly selected for each group, Control and GLYT1 kd, and number of EdU positive and total nuclei were counted utilising ImageJ program. Percentage proliferation index was calculated dividing the number of proliferating nuclei by the total number of nuclei. Data represent mean ± SEM, n=4.

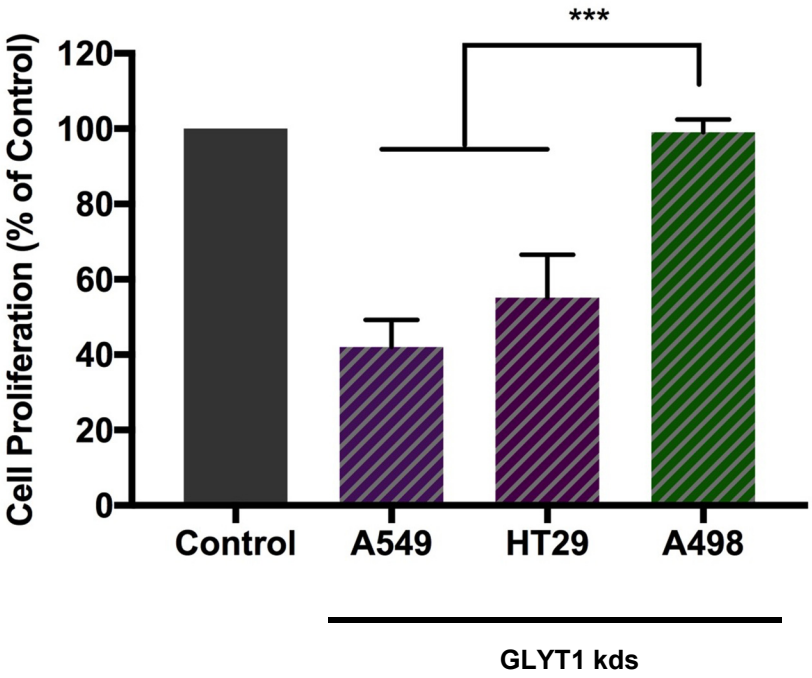

Figure 4.11: GLYT1 knockdown different effects on cell proliferation between cell lines. Bar charts illustrate the cell proliferation as percentage of respective control following GLYT1 kd for each cell line. The effect of GLYT1 kd on cell proliferation was smaller for A498 when compared to A549 and HT29 cell lines. Data are presented as mean ± SEM, n=4. Statistical analysis were performed by one-way-ANOVA with Tukey's post hoc analysis considering $p<0.001$ (***).

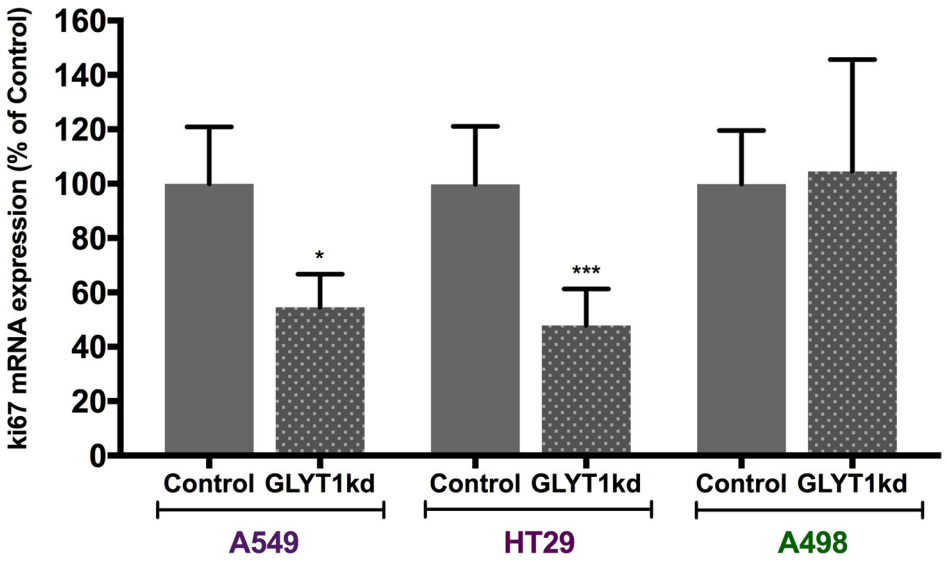

Figure 4.12: GLYT1 knockdown reduced ki67 mRNA expression of A549 and HT29 cells, but had no effect on A498 cell line. Real time qPCR analysis of the influence of GLYT1 kd on the proliferation marker ki67 mRNA expression as percentage of control. Data are presented as mean ± SEM, N=3 and n=9 per group. Statistical analysis comparing the treatment (GLYT1 kd) and control of each cell line were performed by unpaired t-test considering $p<0.05$ (*) and $p<0.001$ (***).

4.2.3 *Influence of GLYT1 knockdown on gene expression of other glycine transporters and glycine synthesising enzyme*

The reduction in GLTY1 following knockdown might be compensated by upregulating other amino acid transporters able to transport glycine, such as PAT1, SNAT2 and $ATB^{0,+}$, or enzymes involved in its intracellular synthesis, such as SHMT2. To investigate these possibilities, qPCR analysis of these transporter or enzyme mRNAs were performed. Cells were transfected with GLYT1 and Negative siRNA and incubated for 72h prior to RNA extraction as described before.

PAT1

GLYT1 knockdown downregulated PAT1 mRNA expression in all cell lines analysed (Figure 4.13). For A549 cells, a reduction of 53% ($p<0.0001$) was observed following GLYT1kd when compared to control. For HT29 cells, PAT1 mRNA abundance was reduced 38% ($p<0.0001$) when compared to control. For A498 GLYT1kd cells, there was a decrease of 69% ($p<0.0001$) when compared to controls.

SNAT2

GLYT1 knockdown also reduced SNAT2 mRNA levels in all cell lines analysed (Figure 4.14). After GLYT1kd, for A549 cells, there was a reduction of 41% ($p<0.0001$) when compared to control cells. For HT29 cells, SNAT2 mRNA levels were reduced 53.8% ($p<0.0001$) when compared to control cells. For A498 cells, SNAT2 mRNA levels reduced 52% ($p<0.0001$) following GLYT1kd when compared to control cells.

$ATB^{0,+}$

In HT29 cells only, the knockdown of GLYT1 resulted in a 55% ($p<0.001$) up-regulation of an alternative glycine transporter, $ATB^{0,+}$, when compared to control (Figure 4.15). However GLYT1kd had no effect on $ATB^{0,+}$ mRNA levels in the other rapidly proliferative cancer cell line, A549. A498 control cells did not express $ATB^{0,+}$ mRNA and no changes were observed following GLYT1kd.

SHMT2

Following GLYT1kd, the rapidly proliferative cancer cell lines, A549 and HT29, up-regulated SHMT2 mRNA expression (Figure 4.16). In A549 cells there was an increase of 72% ($p<0.0001$) when compared to control cells. In HT29 cells treated with GLYT1 siRNA, an upregulation of 90% ($p<0.0001$) was observed when compared to

control cells. However, for A498 cells no significant change in SHMT2 mRNA abundance was observed after GLYT1kd when compared to control cells.

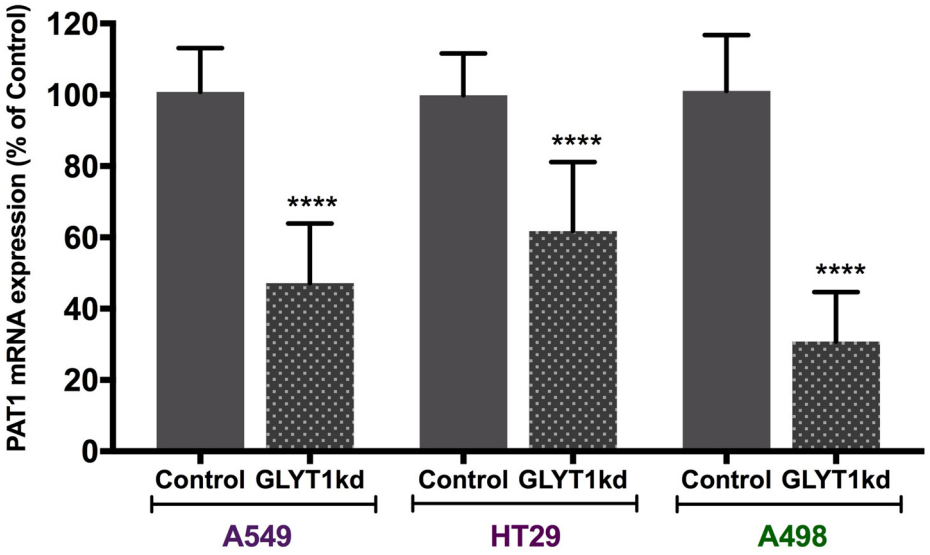

Figure 4.13: GLYT1 knockdown reduced PAT1 mRNA expression in A549, HT29 and A498 cell lines. Real time qPCR analysis of the influence of GLYT1 kd on the amino acid transporter PAT1 mRNA expression as percentage of control (Negative siRNA). Data are presented as mean ± SEM, N=3 and n=9 per group. Statistical analysis comparing the treatment (GLYT1 kd) and control of each cell line were performed by unpaired t-test considering $p<0.0001$ (****).

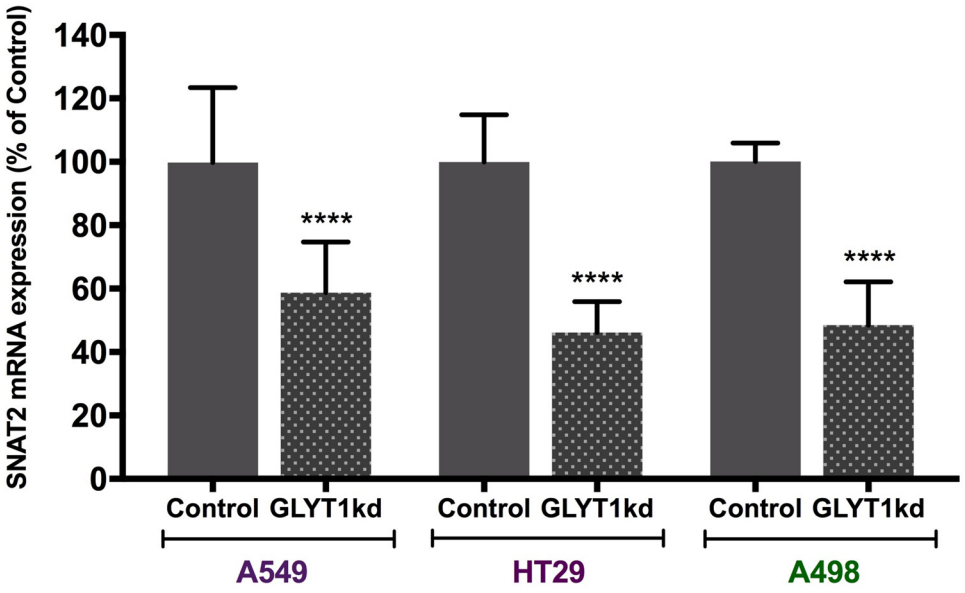

Figure 4.14: GLYT1 knockdown reduced SNAT2 mRNA expression of A549, HT29 and A498 cell lines. Real time qPCR analysis of the influence of GLYT1 kd on the amino acid transporter SNAT2 mRNA expression as percentage of control (Negative siRNA). Data are presented as mean ± SEM, N=3 and n=9 per group. Statistical analysis comparing the treatment (GLYT1 kd) and control of each cell line were performed by unpaired t-test considering $p<0.001$ (****).

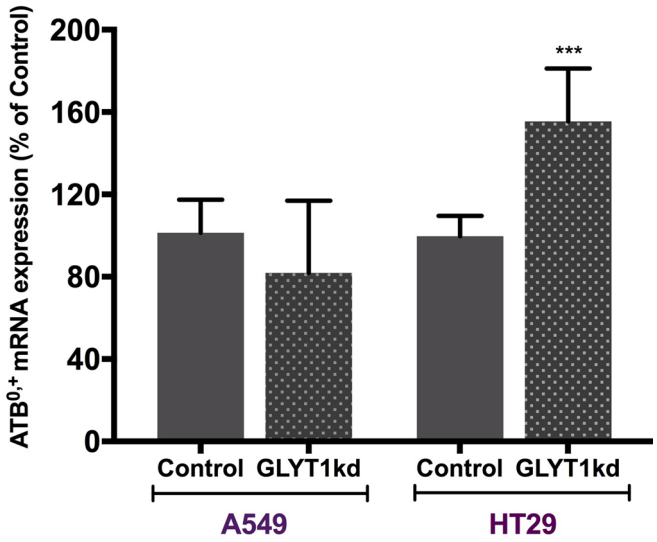

Figure 4.15: GLYT1 knockdown upregulated $ATB^{0,+}$ mRNA expression of HT29, but had no effect on A549 cell line. Real time qPCR analysis of the influence of GLYT1 kd on the amino acid transporter $ATB^{0,+}$ mRNA expression as percentage of control (Negative siRNA). Data are presented as mean ± SEM, N=3 and n=9 per group. Statistical analysis comparing the treatment (GLYT1 kd) and control of each cell line were performed by unpaired t-test considering $p<0.001$ (***).

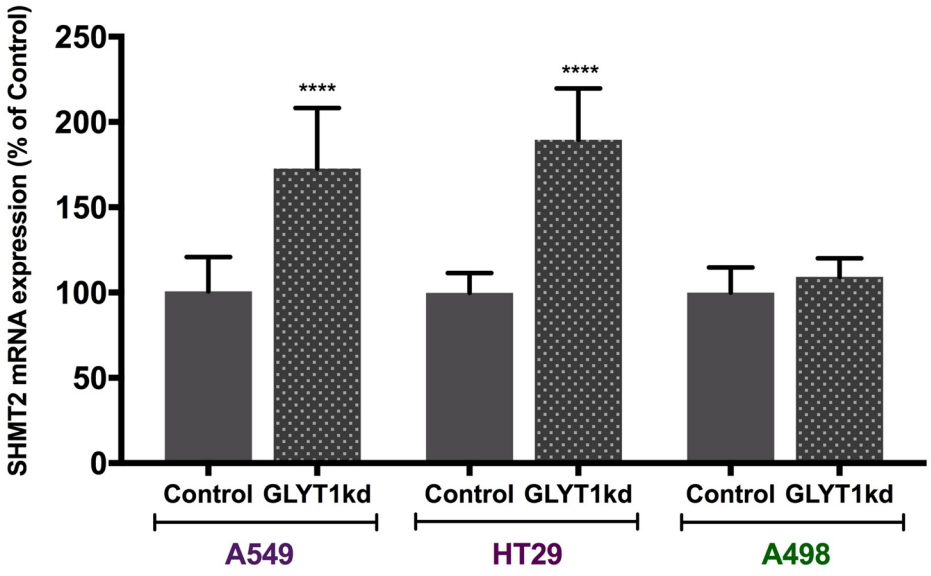

Figure 4.16: GLYT1 knockdown upregulated SHMT2 mRNA expression in A549 and HT29, but had no effect in A498 cell line. Real time qPCR analysis of the influence of GLYT1 kd on the glycine synthesising enzyme SHMT2 mRNA expression as percentage of control (Negative siRNA). Data are presented as mean ± SEM, N=3 and n=9 per group. Statistical analysis comparing the treatment (GLYT1 kd) and control of each cell line were performed by unpaired t-test considering $p<0.0001$ (****).

4.2.4 *Influence of GLYT1 knockdown on gene expression of glutathione synthesising enzymes and cystine transporter*

GSH synthesis occurs in a two steps reaction catalysed by the enzymes GCL and GSS and is dependent on the amino acids glycine, cysteine and glutamine. Thus, the effect of glycine limitation following GLYT1 knockdown on GSH levels, GSH synthesising enzymes and on cysteine transporter subunit xCT was evaluated for A549, HT29 and A498 cell lines. Cells were transfected with GLYT1 or Negative siRNA and incubated for 72h as described before.

GSH levels

GLYT1 downregulation reduced GSH levels of A549, HT29 and A498 cell lines (Figure 4.17). Following GLYT1kd GSH levels were reduced 34% ($p<0.001$) in A549, 19% ($p<0.001$) in HT29 and 15% ($p<0.0001$) in A498 cell lines. As expected the reduction in glycine uptake following GLYT1kd limited the synthesis of GSH.

xCT

As described before, xCT expression is essential in providing cystine that is converted to cysteine inside the cells, being essential for GSH synthesis. Therefore, the effect of GLYTkd on xCT mRNA levels was evaluated. xCT mRNA expression was downregulated in all cell lines following GLYT1kd when compared to controls (Figure 4.18), a similar finding to that was observed for the other amino acid transporters, PAT1 and SNAT2. A reduction of 42% ($p<0.0001$), 66% ($p<0.0001$) and 43% ($p<0.01$) in xCT mRNA levels was observed following GLYT1kd in A549, HT29 and A498 cell lines, respectively (Fig. 4.18).

GCL

GLYT1 downregulation had different effects on mRNA expression of GCL subunits GCLC and GCLM depending on the cell type (Figure 4.19). GCLC mRNA expression was reduced 48% ($p<0.001$) and 33% ($p<0.01$) in A498 and A549 cell lines following GLYT1kd when compared to control cells, respectively. However, GLYT1kd enhanced GCLC mRNA abundance by 24% ($p<0.0001$) in HT29 cells (Fig. 4.19). GCLM mRNA expression was upregulated following GLYT1 knockdown in rapidly proliferative cell lines, 33% ($p<0.0001$) in A549 and 77% ($p<0.001$) in HT29, when compared to the controls, whereas GLYT1 kd had only a small influence on A498 cell line, a reduction of 8% ($p<0.0001$) in GCLM mRNA abundance (Figure 4.19).

GSS

Following GLYT1kd GSS mRNA expression was upregulated in the rapidly proliferating cells, A549 and HT29, but downregulated in the slow growing cell line, A498 (Figure 4.20). GLYT1kd reduced by 19% ($p<0.01$) GSS mRNA levels in A498 cells when compared to control. However, GLYT1kd increased 10% ($p<0.01$) and 50% ($p<0.05$) GSS mRNA abundance in A549 and HT29 cells, respectively, when compared to Control cells.

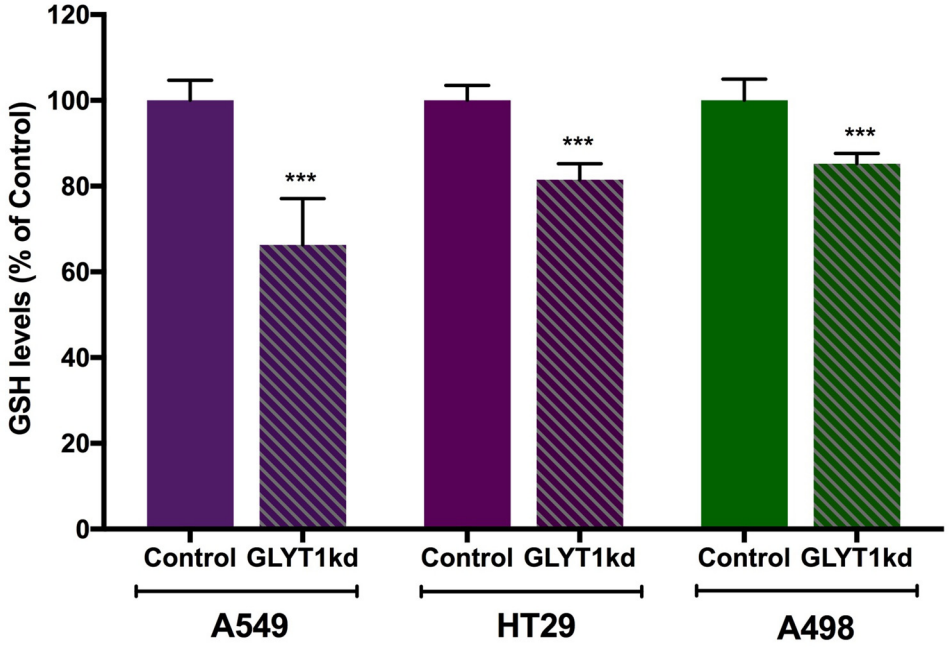

Figure 4.17: GLYT1 knockdown reduced GSH levels in A549, HT29 and A498 cell lines. GSH-Glo assay analysis after 72 hours transfection with Negative siRNA, Control, or GLYT1 siRNA, GLYT1 kd, in 96-well plate. GSH levels presented as percentage of control according to luminescence measurement. Data are presented as mean ± SEM, N=2 and n=6 per group. Statistical analysis comparing GLYT1 kd and control of each cell line were performed by unpaired t-test considering $p<0.001$ (***).

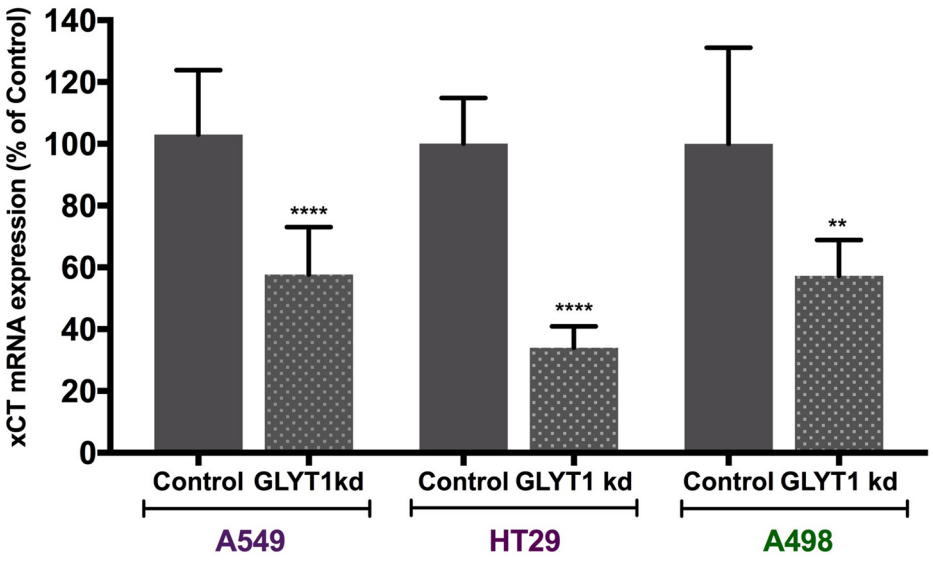

Figure 4.18: GLYT1 knockdown reduced xCT mRNA expression in A549, HT29 and A498 cell lines. Real time qPCR analysis of the influence of GLYT1 kd on the cystine amino acid transporter subunit xCT mRNA expression as percentage of control (Negative siRNA). Data are presented as mean ± SEM, N=3 and n=9 per group. Statistical analysis comparing the treatment (GLYT1 kd) and control of each cell line were performed by unpaired t-test considering $p<0.01$(**) and $p<0.001$ (****).

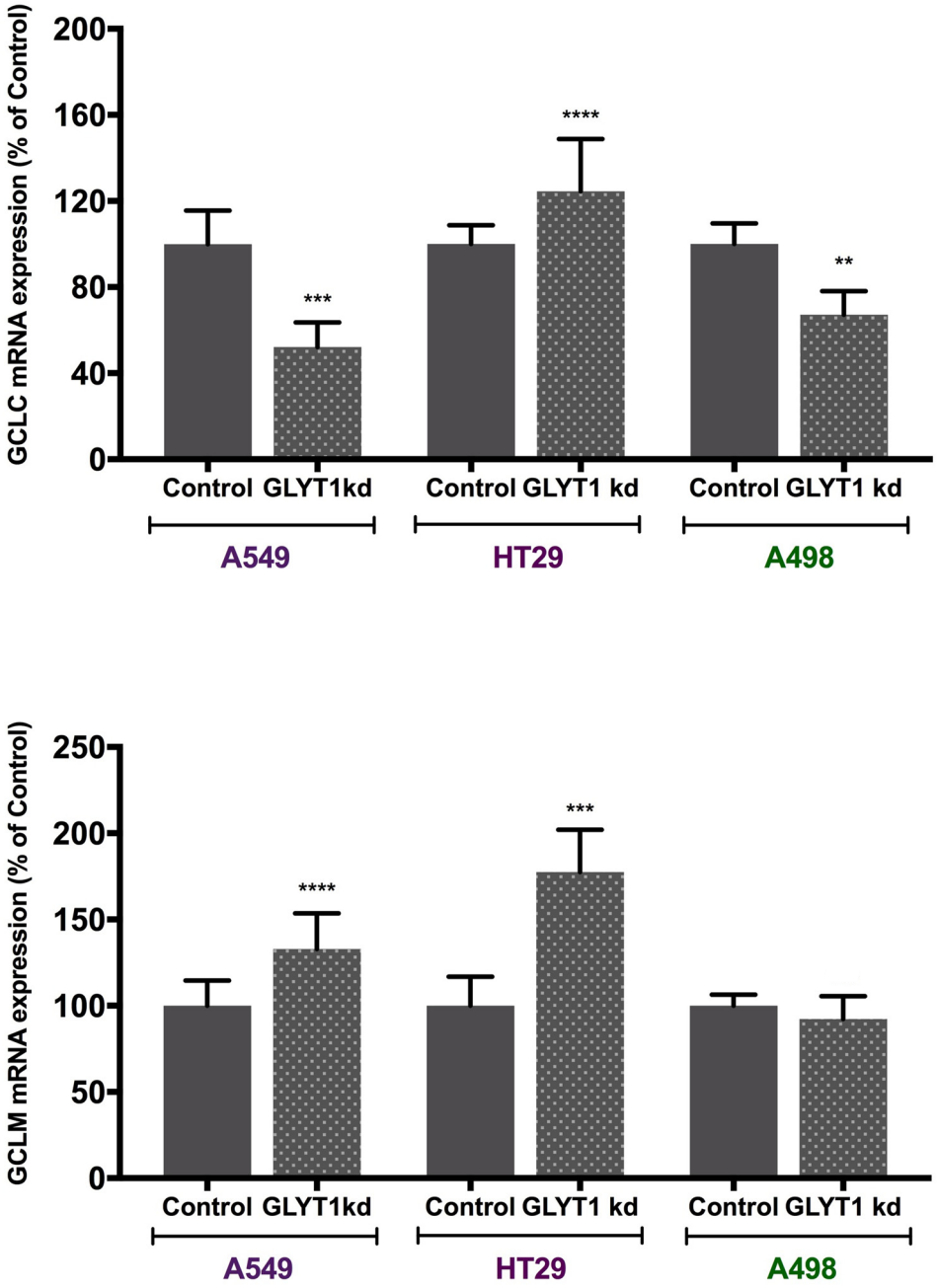

Figure 4.19: GLYT1 knockdown effect on GCL subunits, GCLC and GCLM, mRNA expression in A549, HT29 and A498 cell lines. Bar charts illustrate real time qPCR analysis of the influence of GLYT1 kd on GCL catalytic subunit, GCLC, and modifier subunit, GCLM, mRNA expression as percentage of control (Negative siRNA). Data are presented as mean ± SEM, N=3 and n=9 per group. Statistical analysis comparing the treatment (GLYT1 kd) and control of each cell line were performed by unpaired t-test considering $p<0.01$(**), $p<0.001$(***) and $p<0.001$ (****).

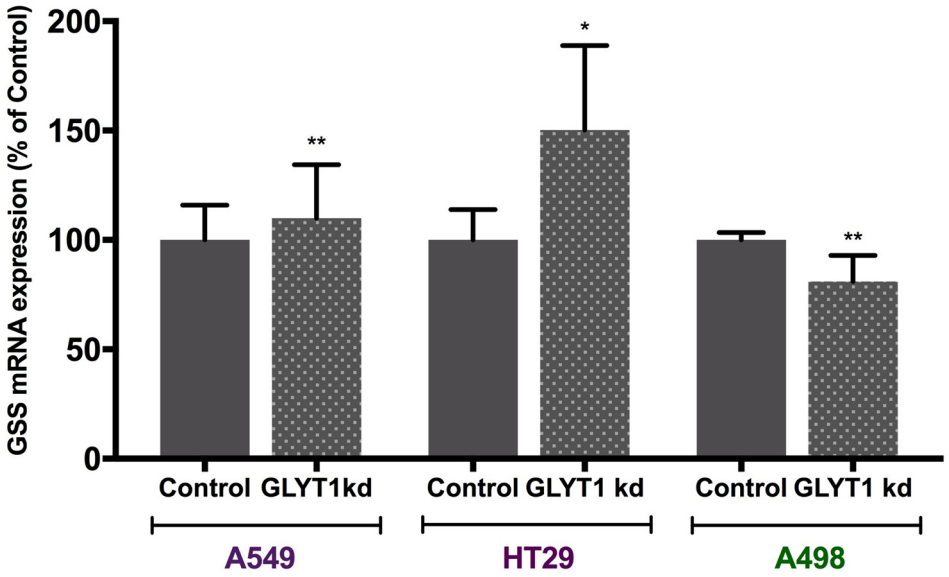

Figure 4.20: GLYT1 knockdown upregulated GSS mRNA expression in A549 and HT29, but downregulated its expression in A498 cell line. Real time qPCR analysis of the influence of GLYT1 kd on GSS mRNA expression as percentage of control (Negative siRNA). Data are presented as mean ± SEM, N=3 and n=9 per group. Statistical analysis comparing the treatment (GLYT1 kd) and control of each cell line were performed by unpaired t-test considering $p<0.05$ (*) and $p<0.01$ (**).

4.3 Summary of results and Discussion

Recent studies have highlighted the relevance of extracellular glycine in maintaining the high proliferation profiles of some cancer types and correlated high glycine concentrations with poor prognosis of patients with aggressive tumours (Jain et al., 2012, Redalen et al., 2016). The experimental data presented in this chapter aimed to elucidate a possible influence of the specific glycine transporter GLYT1 on glycine uptake and cell proliferation. The transfection with a specific GLYT1 siRNA was effective to knockdown GLYT1 mRNA expression (GLYT1kd) and consequently reduce total glycine uptake in A549, HT29 and A498 tumour cell lines. Consistent with the studies of Jain et al. (2012), where extracellular glycine was limited, GLYT1kd led to a significant reduction in cell proliferation of the rapidly proliferative cell lines A549 and HT29, but had no effect on the slowly proliferative cell line A498. Additionally, GLYT1kd had no significant effect on HUVEC cell line growth.

Interestingly, when analysing the effect of GLYT1kd on other amino acid transporters able to transport glycine, a downregulation of PAT1 and SNAT2 transporters was observed instead of a compensatory upregulation that might have been predicted. PAT1, as described earlier, participates in amino acid sensing; its knockdown in MCF-7, a breast cancer cell lines, inhibited cell proliferation and mTORC1 signalling (Goberdhan, 2010, Heublein et al., 2010). It has been proposed that SNAT2 also functions as a sensor participating in the mTORC1 signaling pathway, thus influencing cell growth and differentiation (Pinilla et al., 2011). Therefore, PAT1 and SNAT2 downregulation may also have contributed to the inhibition in cell proliferation. A significant reduction in PAT1 and SNAT2 mRNA levels following GLYT1kd may suggest a link between these transporters in the amino acid sensing system and/or some form of regulation following a reduction in glycine uptake. However, the specific mechanism through which GLYT1 influences PAT1 and SNAT2 mRNA abundance is unknown and needs to be elucidated. Another hypothesis is that GLYT1 and glycine levels do not affect directly PAT1 and SNAT2 expression. Considering the reduced proliferation following GLYT1kd, these cells will consume less nutrients than control cells. Thus without a depletion in amino acid levels, PAT1 and SNAT2 would not be upregulated, whereas a possible relative amino acid starvation in control cells, due a higher rate of proliferation, might result in a relative overexpression of these transporters.

The upregulation of $ATB^{0,+}$ in HT29 and SHMT2 in A549 and HT29 cell lines following GLYT1kd may indicate that these cells are trying to compensate their requirement for glycine by upregulating alternative genes involved in glycine uptake and synthesis. $ATB^{0,+}$ mRNA expression is upregulated in some tumour types, having been found at raised levels in colorectal and breast cancer cells, but in normal cells its expression is relatively low and generally absent (Gupta et al., 2006, Karunakaran et al., 2011). $ATB^{0,+}$ upregulation in HT29 may be a possible explanation for the slightly smaller effect of GLYT1kd in this cell line in comparison to A549 cells, although no significant difference was observed between them. Moreover, SHMT2 upregulation was not able to meet the cellular demands for glycine and maintain the proliferation levels in the rapidly proliferating cell lines as also observed by Jain and collaborators (Jain et al., 2012). In this study they observed that, although SHMT2 silencing associated with glycine starvation had a major impact impairing proliferation of a rapid melanoma cell line LOX IMVI, excluding only glycine from the medium was able to reduce its proliferation rate but had no effect on cell proliferation of the slow growing cell line A498, the same as used in this current study (Jain et al., 2012). They also observed that the proliferation of an shSHMT2 cell line was rescued with glycine supplementation but not with formate, which can be utilised as a source of one-carbon units, indicating that glycine itself, and not one-carbon units generated in GCS, was essential to maintain the proliferation levels (Jain et al., 2012).

The relevance of glycine in supporting cell proliferation is not reproducible with all rapidly proliferating cancer cell lines as demonstrated by Labuschagne et al (Labuschagne et al., 2014). In this study analysing a colon cancer cell line HCT116 they did not notice any difference in proliferation levels when glycine was excluded from the medium but they demonstrated that in this cell line serine had a major impact on proliferation (Labuschagne et al., 2014). Additionally, high levels of glycine in HCT116 and HEK293T cell lines (higher than 10 times the normal concentration in humans) decreased cell proliferation when cells were starved of serine (Labuschagne et al., 2014). In this situation all glycine consumed was utilised in the reverse reaction catalysed by SHMT2 to produce serine and then depleting meTHF levels, which in turn halts synthesis of purines and consequently proliferation (Labuschagne et al., 2014). The requirement for extracellular glycine in supporting cancer growth therefore appears in some cases to be dependent on availability of other amino acids. Different medium composition in these experiments could influence the proliferative response to glycine deprivation. In the Jain *et al*. paper the basal medium utilised was a minimum

medium RPMI whereas in Labuschagne *et al*. and Fan *et al*. studies the basal medium was the rich DMEM (Labuschagne et al., 2014, Jain et al., 2012, Fan et al., 2014). The excess of nutrients in the medium could make cells less dependent on glycine uptake. Glycine can be synthesised from serine but also from threonine, choline and sarcosine, which are all in higher concentrations in DMEM than RPMI medium. Additionally GLT1kd appears to have a great impact on DNA replication in the fast growing cells A549 and HT29. Possibly in these cell lines reduction in glycine levels could be affecting purine synthesis through its direct incorporation. This way, glycine contribution to cell proliferation seems to be cell type and concentration dependent as glycine starvation and high levels of glycine reduced cancer cell growth *in vitro* in different cell lines (Jain et al., 2012, Labuschagne et al., 2014).

Glycine consumed by rapidly proliferative cancer cells is also incorporated either directly into GSH or via one-carbon metabolism (Nelson and Cox, 2005, Thelwall et al., 2012, Labuschagne et al., 2014). As observed in a rat model for breast cancer, extracellular glycine supports serine synthesis that can be utilised in the transsulphuration pathway and produce cysteine, which is then utilised in GSH synthesis in tumour tissue (Thelwall et al., 2012). Glycine, through GCS and further oxidation reactions, also contributes to NADPH as described in Chapter 1 (Fan et al., 2014). Additionally, studies by our group demonstrated glycine uptake through GLYT1 supports GSH levels during oxidative stress (Howard et al., 2010). This indicates that glycine is a major contributor to overcome oxidative stress. This way, as predicted, reduction in glycine uptake following GLYT1kd reduced GSH levels in all cell lines analysed. Therefore, glycine uptake through GLYT1 can contribute to cell survival during oxidative stress and could contribute to chemotherapy resistance through supporting high levels of GSH.

As GLYT1kd and consequent reduction in glycine uptake was shown to affect GSH levels, its influence on gene expression of proteins involved in GSH synthesis was evaluated. The expression of xCT, a subunit of the cystine transporter, is essential for GSH synthesis and its inhibition has been shown to reduce tumour replication, invasion and metastasis (Lewerenz et al., 2013, Huang et al., 2005). Additionally, xCT mRNA expression is also regulated by ATF4 (Sato et al., 2004). Therefore, the influence of GLYT1kd on xCT mRNA expression was evaluated. GLYT1kd significantly reduced xCT mRNA abundance in all tumour cell lines analysed, indicating a possible link between these transporters. Moreover, a reduction in xCT mRNA expression may also contribute to a reduction in proliferative profile. GSH synthesis requires both

cysteine and glycine, thus the lack of one amino acid might have influenced the requirements for the other, but the exact mechanisms by which GLYT1 influenced xCT mRNA expression remains to be elucidated.

GLYT1kd also affected GSH synthesising enzymes. GLYT1kd reduced GCLC mRNA expression in A549 and A498 cell lines. GCLC is the rate limiting enzyme in the GSH synthesis pathway and is known to be regulated by cysteine levels (Lu, 2013); once GLYT1kd downregulated xCT expression, possibly reducing the intracellular levels of cysteine, the abundance of GCLC mRNA may be reduced by feedback. Alternatively, low levels of glycine possibly lead to a low concentration of GSH due to the limited substrate of GSS. It is known that high levels of GSH have a negative feedback on GCLC. Without this inhibition, an over-stimulation of ɣ-glutamylcysteine synthesis occurs, and ɣ-glutamylcysteine in high concentrations is then converted to 5-oxoproline (Larsson and Mattsson, 1976, Shi et al., 1996), thus possibly generating a negative feedback downregulating GCLC mRNA expression. Another possibility is the influence of glycine levels on GCLC mRNA expression regulation, although these assumptions remain yet to be tested. However, HT29 cell upregulation of GCLC following GLYT1 knockdown indicates that GCLC in this cell line is less susceptible to negative feedback and its overexpression might have been an attempt to increase intracellular levels of GSH.

GCLM upregulation in the rapidly proliferating cell lines, A549 and HT29, might have been an attempt to improve the GCL activity and maintain GSH production, since it reduces the K_m of GCL for glutamate and increases the K_i for GSH, another known regulator of GCLC (Lu, 2013). Additionally A549 and HT29 cells overexpressed GSS mRNA following GLYT1kd and consequent reduction in glycine levels, possibly this enzyme is less susceptible to feedback regulation when substrate concentrations are low in rapidly proliferative tumour cells.

In summary, data presented in this chapter suggest that GLYT1 might be essential to maintain adequate glycine levels in fast growing colorectal and lung cancer cell lines, HT29 and A549, respectively, and sustain their growth. As the results demonstrated, the extracellular glycine transported by GLYT1 probably supports purine and GSH synthesis. Therefore, GLYT1 is a possible specific therapeutic target for highly proliferative tumours and encourages further investigations of GLYT1 inhibitors as promising new treatment for aggressive tumours.

Chapter 5. GLYT1 Pharmacological Approach

5.1 Introduction

This chapter will discuss investigations of a pharmacological approach to down-regulating GLYT1 and its effect on cell proliferation. Cells were treated with a specific GLYT1 inhibitor, N-[3-(4′-Fluorophenyl)-3-(4′-phenylphenoxy)propyl]sarcosine hydrochloride, also known as ALX-5407 hydrochloride or NFPS hydrochloride for 120h. Then, total glycine uptake was measured and cell proliferation analysed. Moreover, ALX-5407 was also tested when cells were incubated under hypoxia condition, to generate oxidative stress, and in association with tunicamycin that triggers ER stress.

GLYT1 and GLYT2, in neuronal cells, participate in glycine reuptake at the synaptic cleft, thus interrupting the glycine inhibitory and excitatory effects in glycinergic and glutamatergic synapses, respectively (Howard and Hirst, 2011, Harsing and Matyus, 2013, Eulenburg et al., 2005). Additionally, a large number of GLYT1 inhibitors are being tested due to their potential use as treatments for schizophrenia, pain and alcohol dependence (Harvey and Yee, 2013).

GLYT2 is mainly present in neuronal tissues and also in macrophages, whereas the protein isoform GLYT1 is also present in peripheral tissues including intestine, kidney and lung (Borowsky et al., 1993, Howard and Hirst, 2011). According to tissue distribution the main focus of this work was to evaluate GLYT1 role in supporting tumour cell proliferation and if could be considered a possible new target in cancer therapy. As described in details in Chapter 1, Section1.4.1, ALX-5407 is a potent GLYT1 inhibitor presenting IC_{50} of 30nM and a dissociation $t_{1/2}$ of about 13h after wash-out in QT6-1C cells transfected with GLYT1 and treated with 60nM ALX-5407 (Atkinson et al., 2001). This compound has been extensively used in *in vitro* and *in vivo* experiments as an effective GLYT1 inhibitor (Salceda, 2006, Aubrey and Vandenberg, 2001, Barthel et al., 2014, Komatsu et al., 2015, Huang et al., 2016). Therefore ALX-5407 was utilised in this study to evaluate a pharmacological approach to reduce glycine uptake in the NSCLC, colon and renal cancer cell lines and evaluate its effect on cell proliferation.

5.2 Results

5.2.1 *ALX-5407 effect on total glycine uptake*

In order to evaluate if the specific GLYT1 inhibitor, ALX-5407, would be effective in reducing total glycine uptake of A549, HT29 and A498 tumour cells as shown with the GLYT1 siRNA approach, radiolabelled glycine uptake experiments were performed. As described in detail in Chapter 2, cells were seeded in 24-well plates in RPMI medium for 24 hours, then medium was replaced and cells were treated with 0, 30, 60, 120 or 1000 nM ALX-5407 for a further 72 hours prior to glycine uptake experiments. Medium was then discarded and the cells incubated with Kreb's buffer containing 0, 30, 60, 120 or 1000 nM ALX-5407 for 30 minutes. Cells were then incubated in Kreb's buffer with the same concentrations of ALX-5407 in association with 5μM glycine and 0.5 μCi/ml [2-^{3}H]-glycine for 10 min. For each cell line nine experimental replicates were performed on each of three independent occasions.

Treatment with the specific GLYT1 inhibitor reduced total glycine uptake in all cell lines. For A549 cells treated with 30, 60, 120 and 1000nM ALX-5407 there was a reduction of 36.6% ($p<0.01$), 41.1% ($p<0.01$), 49% ($p<0.0001$) and 44.7% ($p<0.01$), respectively, when compared to untreated cells (figure 5.1). For HT29 cells, there was a reduction of 33.4% ($p<0.01$), 49.3% ($p<0.0001$) and 51.6% ($p<0.0001$) when cells were treated with 60, 120 and 1000nM ALX-5407, respectively, but no significant difference when cells were treated with 30nM of the GLYT1 inhibitor, when compared to control cells (figure 5.2). Finally, the A498 cell line treated with 120 and 1000nM ALX-5407 presented a decrease in glycine uptake of 40.5% (p<) and 47.9% (p<), respectively, whereas no significant difference was observed when cells were treated with 60nM ALX-5407, in comparison to control cells (figure 5.3). Therefore, 120nM of ALX-5407 was selected for the next experiments, as it was the smallest concentration that presented a significant effect in reducing total glycine uptake.

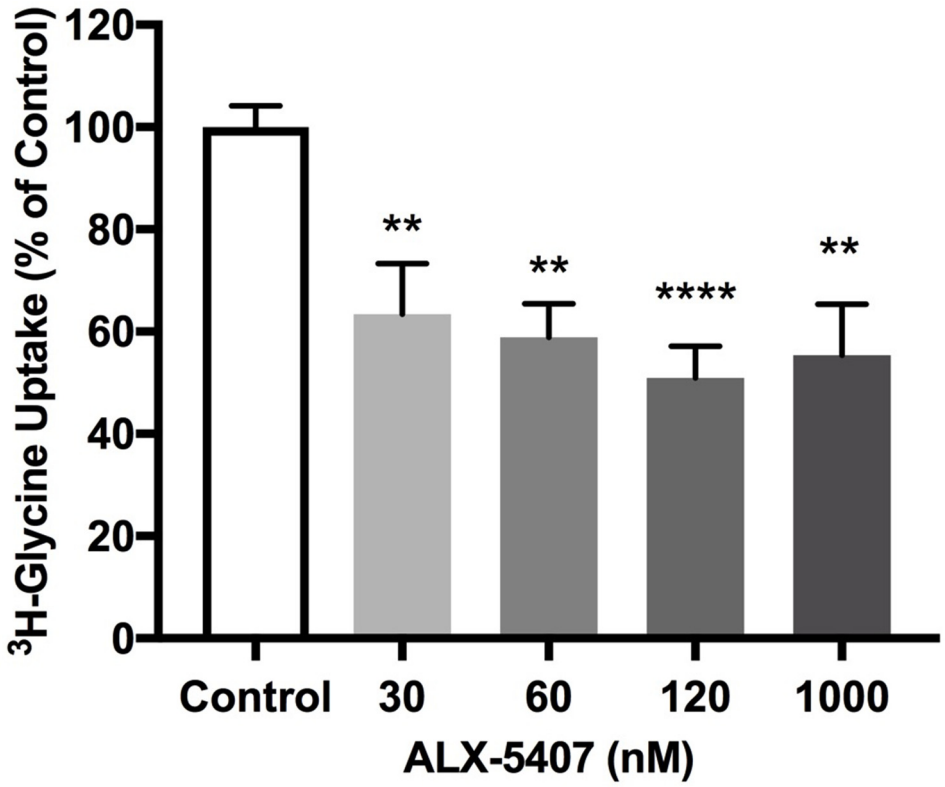

Figure 5.1: Effect of ALX-5407 treatment on total glycine uptake of the A549 cell line. Effect on total glycine uptake by A549 cells growing with 0 (Control), 30, 60, 120 and 1000nM ALX-5407 for 72h in RPMI as percentage of control (untreated cells). Cells were incubated with 5μM glycine in association with ^{3}H-Gly 0.5 μCi/ml in Kreb's buffer with or without ALX-5407 for further 10 min prior to DPM readings. Data are presented as mean ± SEM, N=3 and n=9 per group. Statistical analysis comparing control and ALX-5407 treatments were performed by one-way-ANOVA with Dunnets post hoc analysis considering $p<0.01$ (**) and $p<0.0001$ (****).

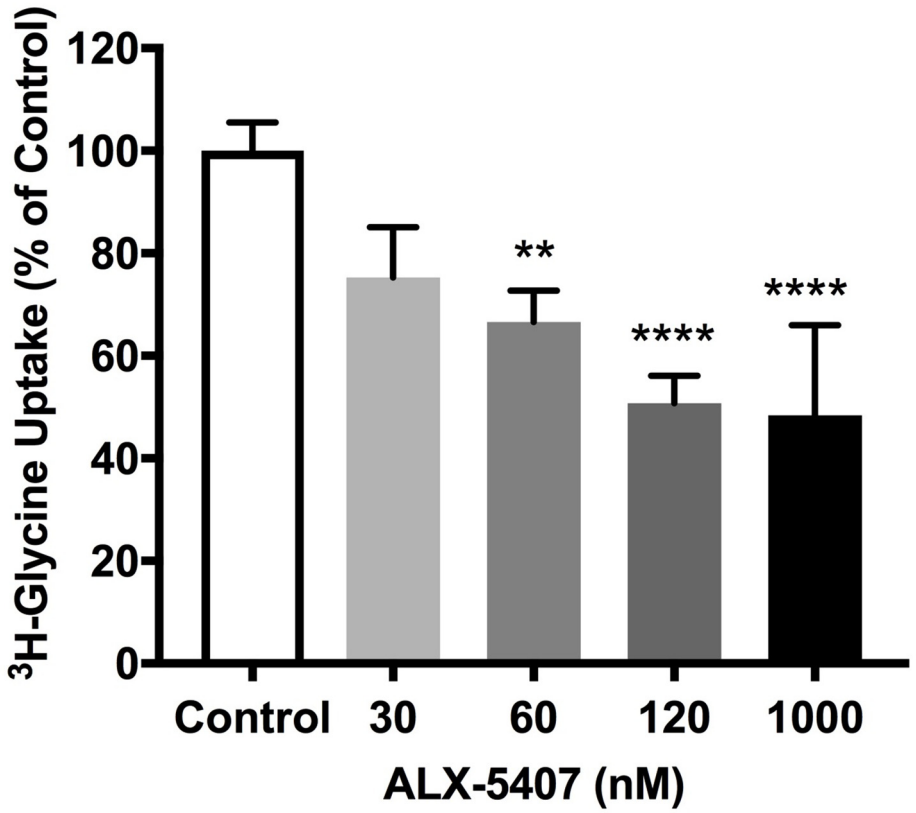

Figure 5.2: Effect of ALX-5407 treatment on total glycine uptake of HT29 cell line. Effect on total glycine uptake by HT29 cells growing with 0 (Control), 30, 60, 120 and 1000nM ALX-5407 for 72h in RPMI as percentage of control (untreated cells). Cells were incubated with 5μM glycine in association with ^{3}H-Gly 0.5μCi/ml in Kreb's buffer with or without ALX-5407 for further 10 min prior to DPM readings. Data are presented as mean ± SEM, N=3 and n=9 per group. Statistical analysis comparing Control and ALX-5407 treatments were performed by one-way-ANOVA with Dunnets post hoc analysis considering $p<0.01$ (**) and $p<0.0001$ (****).

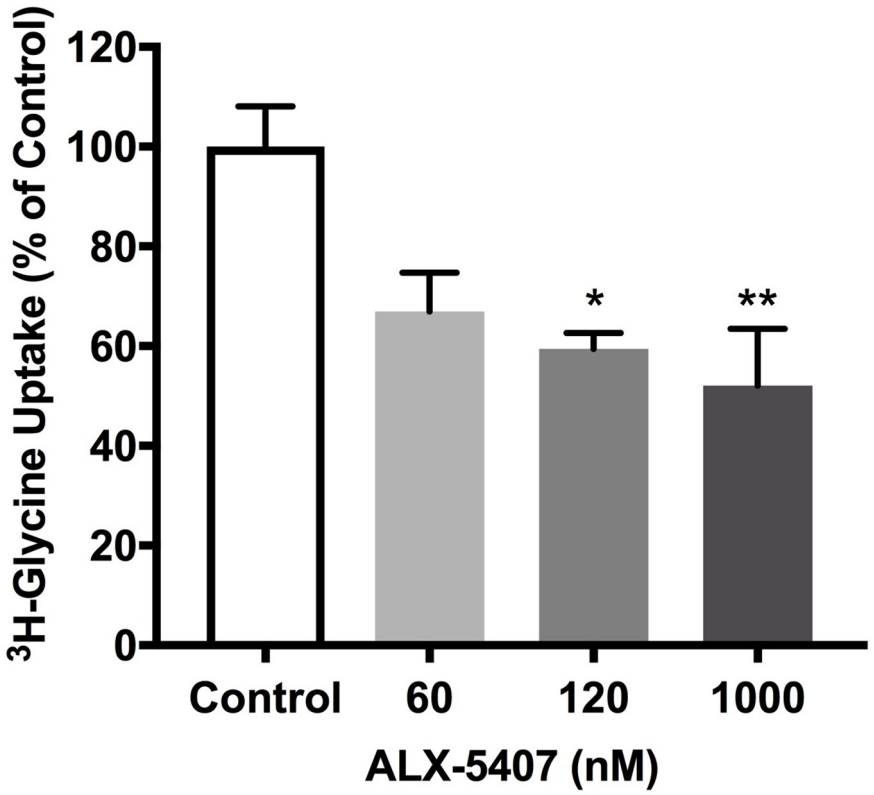

Figure 5.3: Effect of ALX-5407 treatment on total glycine uptake of the A498 cell line. Effect on total glycine uptake of A498 cells growing with 0 (Control), 60, 120 and 1000nM ALX-5407 for 72h in RPMI as percentage of Control (untreated cells). Cells were incubated with 5μM glycine in association with ^{3}H-Gly 0.5μCi/ml in Kreb's buffer with or without ALX-5407 for further 10 min prior to DPM readings. Data are presented as mean ± SEM, N=2 and n=6 per group. Statistical analysis comparing Control and ALX-5407 treatments were performed by one-way-ANOVA with Dunnets post hoc analysis considering $p<0.05$ (*) and $p<0.01$ (**).

5.2.2 *ALX-5407 influence on cell proliferation*

Tumour cell lines, A549, HT29 and A498, were treated with ALX-5407 and its effect on cell proliferation was analysed. For this experiment, cells were seeded in 96-well plates in RPMI with (ALX-5407) or without (Control) 120nM ALX-5407 and the number of viable cells was observed at 6, 24, 48, 72, 96 and 110h. CTB was added to the wells to be analysed and cells were incubated for a further 3h prior to absorbance measurement at each time point. Results were calculated as percentage of the last time point measurement (110 hours) for Control cells and represent experiments performed on three different occasions.

The growth of the rapid proliferating tumour cell lines, A549 and HT29, treated with GLYT1 inhibitor was reduced, whereas the ALX-5407 treatment had no effect on proliferation of the slow proliferating cell line, A498. For A549 cells, when analysing the exponential growth curve of the ALX-5407 treated cells the doubling time was increased by 8.4h and the last two time points, 96 and 110h, presented a significant reduction in the number of viable cells, 29.2% ($p<0.05$) and 18% ($p<0.01$), respectively, when compared to control cells (figure 5.4). For HT29 cells, when analysing the exponential growth curve of the ALX-5407 treated cells the doubling time was increased by 8.1h and the time point, 110h, presented a significant reduction in the number of viable cells, 23% ($p<0.05$) when compared to control cells (figure 5.5). However, the proliferation rate of A498 (figure 5.6) and HUVEC (figure 5.7) cells treated with ALX-5407 had no significant difference compared with control cells. These results indicate that inhibiting GLYT1 with a specific GLYT1 inhibitor reduces proliferation of NSCLC (A549) and colon cancer cell lines (HT29) with a rapid proliferative profile.

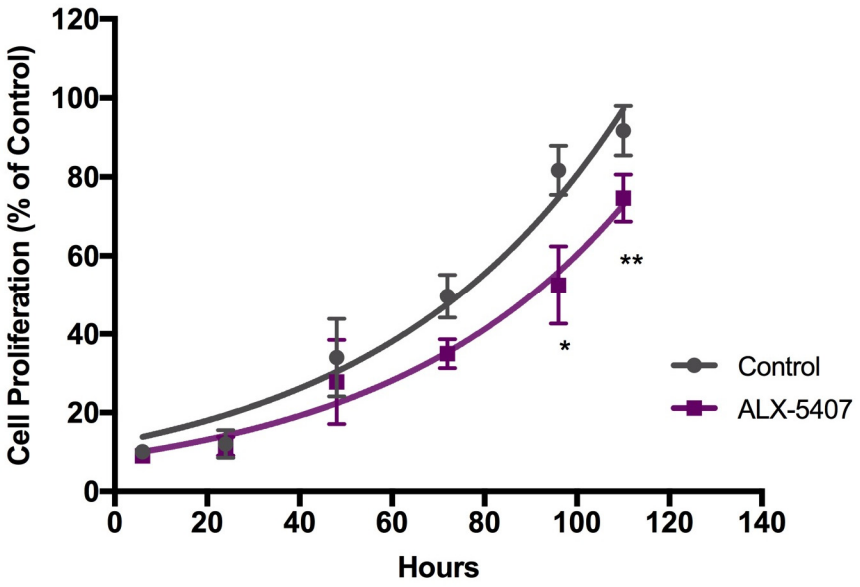

Figure 5.4: Effect of ALX-5407 treatment on A549 cell proliferation. Effect on proliferation of A549 cells treated with 120nM ALX-5407 over 6, 24, 48, 72, 96 and 110 hours as percentage of last point of control (untreated cells). The grey curve represents the growth curve of control cells and the purple line represents the growth curve of cells treated with ALX-5407. Data are presented as mean ± SEM, N=3 and n=9. Statistical analysis comparing control and ALX-5407 treatment for each time point was performed by unpaired t-test considering $p<0.05$ (*) and $p<0.01$(**).

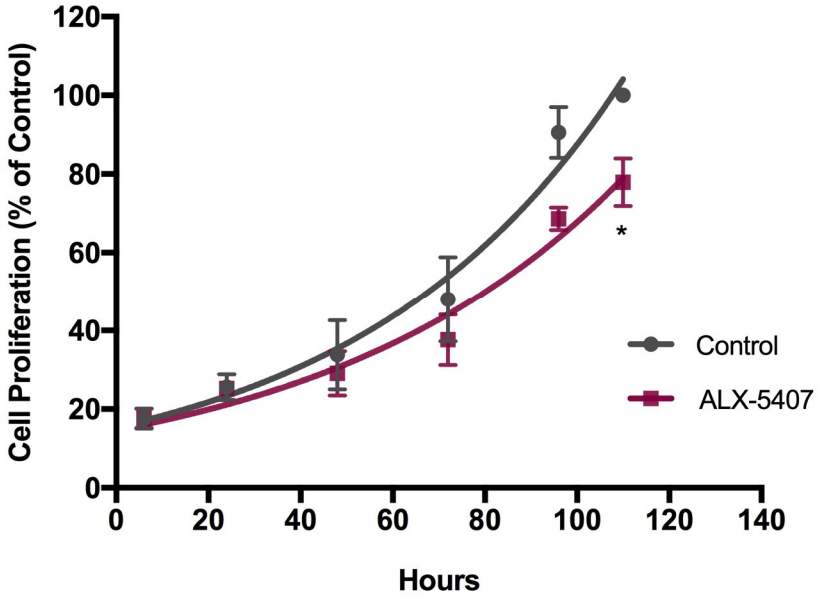

Figure 5.5: Effect of ALX-5407 treatment on HT29 cell proliferation. Effect on proliferation of HT29 cells treated with 120nM ALX-5407 over 6, 24, 48, 72, 96 and 110 hours as percentage of last point of control (untreated cells). The grey curve represents the growth curve of control cells and the purple line represents the growth curve of cells treated with ALX-5407. Data are presented as mean ± SEM, N=3 and n=9. Statistical analysis comparing control and ALX-5407 treatment for each time point was performed by unpaired t-test considering $p<0.05$(*).

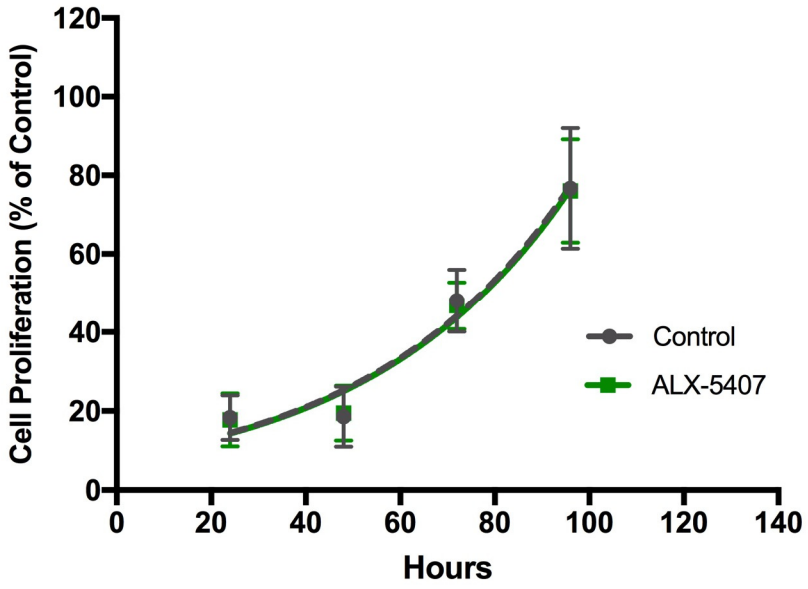

Figure 5.6: Effect of ALX-5407 treatment on A498 cell proliferation. Effect on proliferation of A498 cells treated with 120nM ALX-5407 over 6, 24, 48, 72, 96 and 110 hours as percentage of last point of control (untreated cells). The grey curve represents the growth curve of control cells and the green line represent the growth curve of cells treated with ALX-5407. Data are presented as mean ± SEM, N=3 and n=9. Statistical analysis comparing control and ALX-5407 treatment for each time point was performed by unpaired t-test.

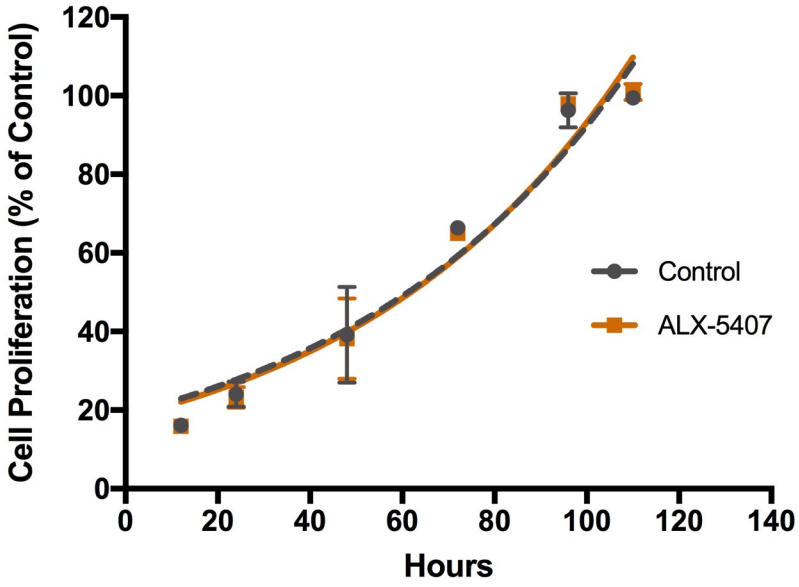

Figure 5.7: Effect of ALX-5407 treatment on HUVEC cell proliferation. Effect on proliferation of HUVEC cells treated with 120nM ALX-5407 over 6, 24, 48, 72, 96 and 110 hours as percentage of last point of control (untreated cells). The grey curve represents the growth curve of control cells and the orange line represents the growth curve of cells treated with ALX-5407. Data are presented as mean ± SEM, N=3 and n=9. Statistical analysis comparing control and ALX-5407 treatment for each time point was performed by unpaired t-test.

5.2.3 *ALX-5407 in association with hypoxia condition*

The growth of tumour cells treated with GLYT1 inhibitor was evaluated under hypoxia in comparison to normal levels of oxygen. A549, HT29 and A498 cell lines were seeded in two 96-well plates containing RPMI medium and incubated under normal conditions for 24h. Then, medium was replaced with RPMI with (ALX-5407) or without (Control) 120nM ALX-5407 and one plate was incubated under normal oxygen levels and other plate was placed in a hypoxic chamber containing 2% oxygen for further 72h. Following this period CTB was added to both plates and incubated for a further 3h prior to fluorescence measurement. Results are presented as percentage of respective controls (untreated cells under hypoxia or normoxia conditions) and are mean of six replicates of experiments performed on two separate occasions.

Only A549 cell proliferation was affected by ALX-5407 treatment under hypoxic conditions when compared to control. Following treatment with GLYT1 inhibitor for 72h under hypoxia, A549 cell proliferation was reduced by 21.5% when compared to untreated cells, whereas no significant difference on cell growth was observed between control and treated cells under normal conditions (figure 5.8). For HT29 cells under normal conditions after 72h, treatment with ALX-5407 had no effect on cell proliferation when compared to control; when cells were under hypoxic stress although no significant difference was observed between cells treated with GLYT1 inhibitor and in control cells there was a tendency to reducing the number of viable cells when glycine uptake was reduced (figure 5.9). For A498 cells, treatment with ALX-5407 had no effect on cell proliferation under hypoxia or normal conditions (figure 5.10). Therefore, extracellular glycine supplied by GLYT1 transporter may affect NSCLC ability to maintain normal proliferation rates and overcome hypoxic stress.

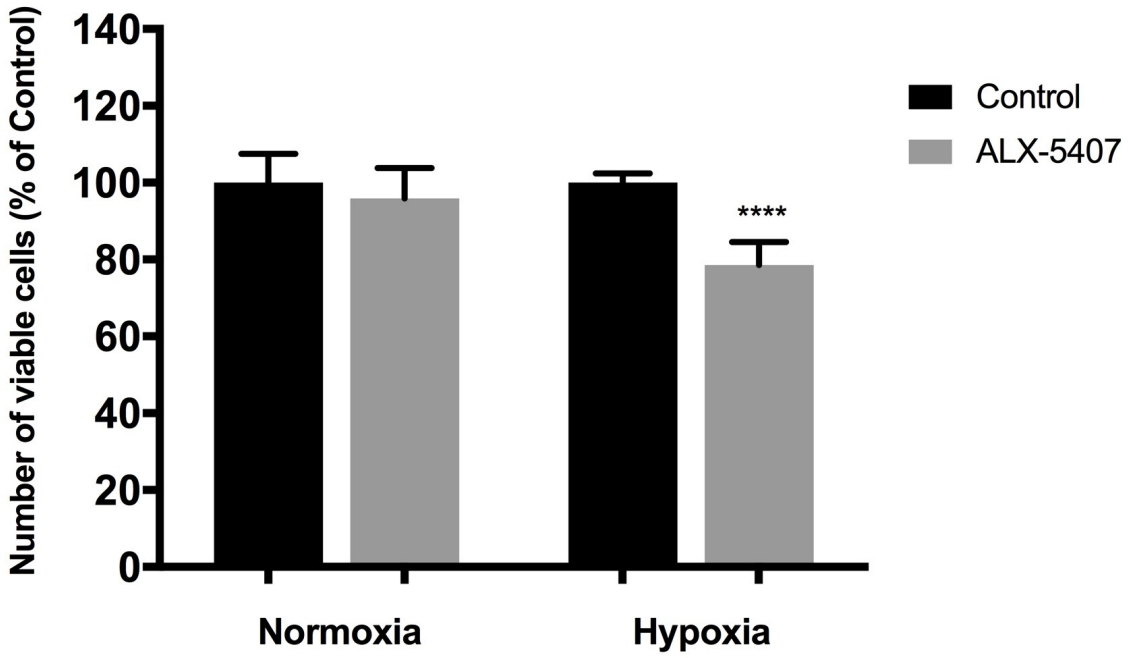

Figure 5.8: Effect of ALX-5407 treatment on A549 cell growth under normoxia and hypoxia. Effect of treatment with 120nM ALX-5407 on A549 cell proliferation as percentage of control (untreated cells) when cells were growing in RPMI under normoxia or hypoxia conditions for 72h. Black bars represent control cells and grey bars represent cells treated with ALX-5407. Data are presented as mean ± SEM, N=2 and n=6 per group. Statistical analysis comparing Control and ALX-5407 treatment was performed by unpaired t-test considering $p<0.0001$ (****).

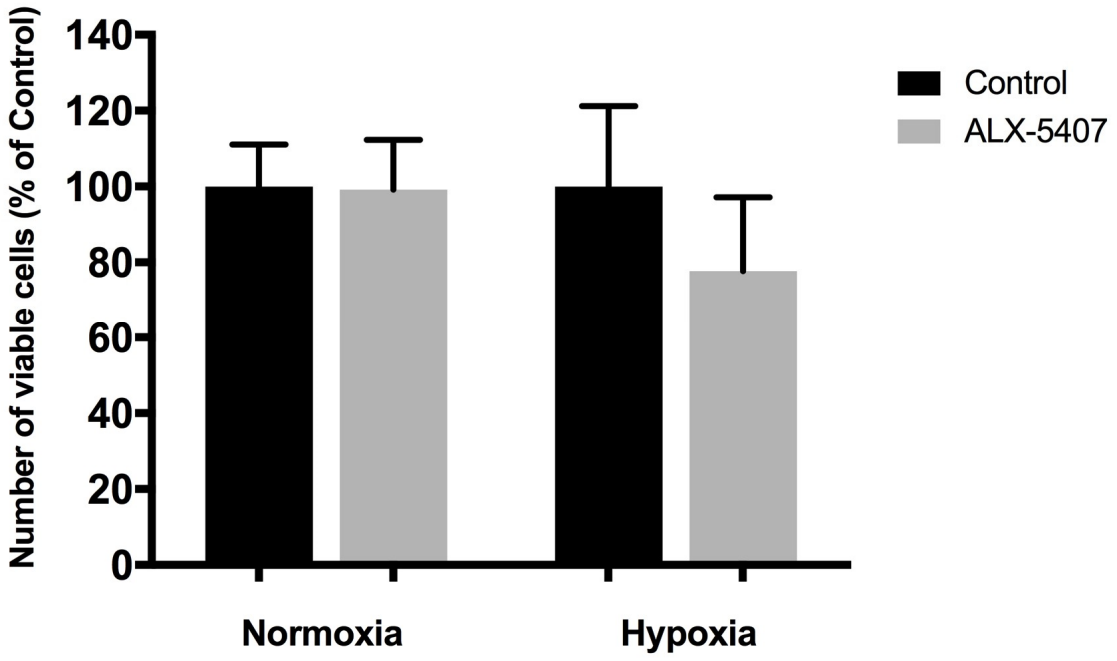

Figure 5.9: Effect of ALX-5407 treatment on HT29 cell growth under normoxia and hypoxia. Effect of treatment with 120nM ALX-5407 on HT29 cell proliferation as percentage of Control (untreated cells) when cells were growing in RPMI under normoxia or hypoxia conditions for 72h. Black bars represent Control cells and grey bars represent cells treated with ALX-5407. Data are presented as mean ± SEM, N=2 and n=6 per group. Statistical analysis comparing Control and ALX-5407 treatment was performed by unpaired t-test.

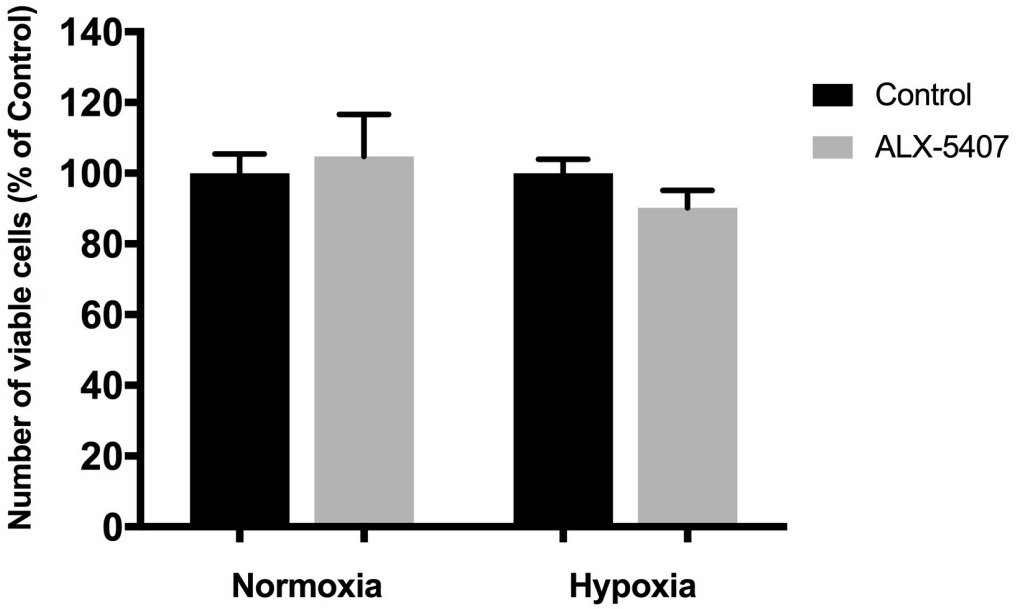

Figure 5.10: Effect of ALX-5407 treatment on A549 cell growth under normoxia and hypoxia. Effect of treatment with 120nM ALX-5407 on A549 cell growth as percentage of Control (untreated cells) when cells were growing in RPMI under normoxia or hypoxia conditions for 72h. Black bars represent Control cells and grey bars represent cells treated with ALX-5407. Data are presented as mean ± SEM, N=2 and n=6 per group. Statistical analysis comparing Control and ALX-5407 treatment was performed by unpaired t-test.

5.2.4 *ALX-5407 in association with induction of ER stress*

The growth of tumour cells treated with GLYT1 inhibitor was evaluated under induced ER stress. A549, HT29 and A498 cell lines were seeded in two 96-well plates containing RPMI medium and incubated for 24h. Then, medium was replaced with RPMI with (ALX-5407) or without (Control) 120nM ALX-5407 and cells were incubated for a further 72h. Then cells were treated with 0.1, 0.2, 0.5, 1.0, 2.0 and 4.0μM tunicamycin (TM) for 12h. Following this period CTB was added and plates were incubated for a further 3h prior to fluorescence measurement. Results are presented as percentage of respective controls (TM untreated cells with or without ALX-5407) and are mean of 12 replicates of experiments performed on three separate occasions.

Tunicamycin, an antibiotic produced by *Streptomyces* sp., inhibits N-glycosylation being cytotoxic to cells and generating an accumulation of mis-folded glycoprotein in the ER resulting in ER-stress (Guha et al., 2017, Banerjee et al., 2011). GLYT1 inhibition increased the effect of TM on cell proliferation only for the HT29 cell line. For A549 cells, increasing TM concentrations enhanced the reduction of proliferation when compared to untreated cells regardless of the presence or absence of ALX5407 (figure 5.11). For the HT29 cell line, increasing the concentration of TM augmented the reduction of the number of viable cells when compared to controls and treatment with ALX-5407 in association with the higher concentrations of TM, 2.0 and 4.0μM, significantly increased the effect of TM in reducing cell growth about 18% ($p<0.05$) and 22% ($p<0.01$), respectively (figure 5.12). For the A498 cell line, different concentrations of TM treatment resulted in the same effect on reducing cell proliferation, and no difference was observed between cells treated with ALX-5407 and untreated cells (figure 5.13).

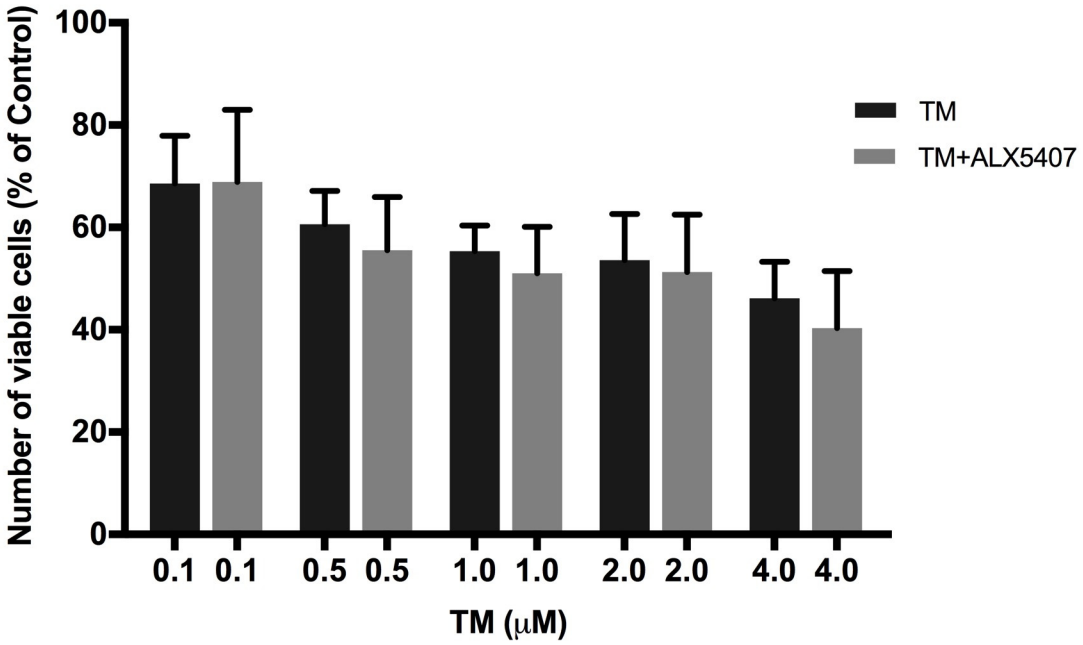

Figure 5.11: Effect of ALX-5407 treatment on A459 cell growth under ER stress conditions. Effect of treatment with 0.1, 0.2, 0.5, 1.0, 2.0 and 4.0μM tunicamycin (TM) for 4h alone (black bars) or in association with 120nM ALX-5407 (grey bars) on A549 cell growth as percentage of control (untreated cells). Data are presented as mean ± SEM, N=3 and n=12 per group. Statistical analysis comparing TM and TM + ALX-5407 treatments for each concentration were performed by one-way-ANOVA with Tukey's post hoc analysis.

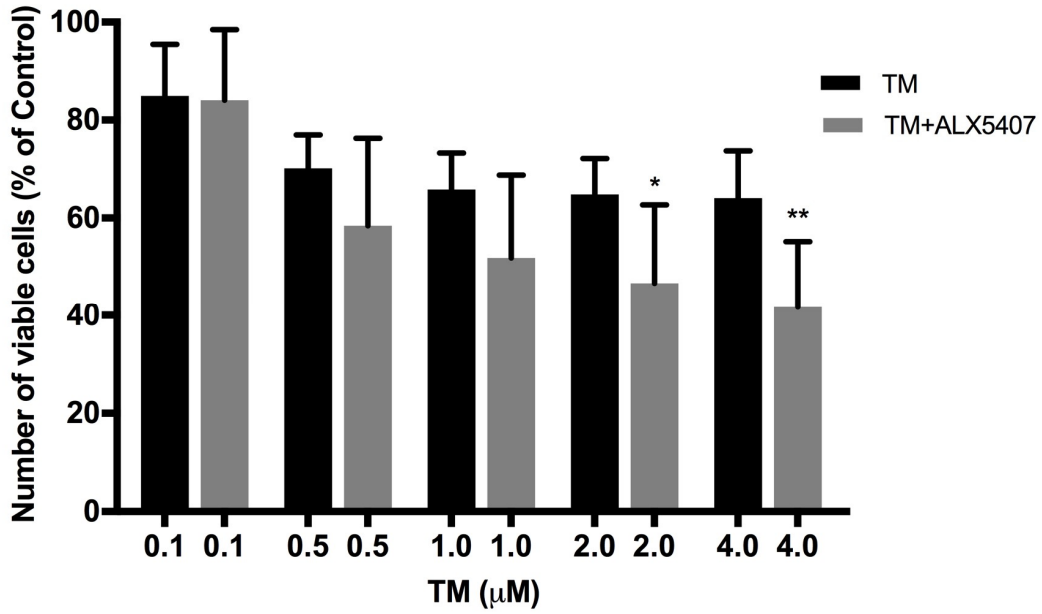

Figure 5.12: Effect of ALX-5407 treatment on HT29 cell growth under ER stress conditions. Effect of treatment with 0.1, 0.2, 0.5, 1.0, 2.0 and 4.0μM tunicamycin (TM) for 4h alone (black bars) or in association with 120nM ALX-5407 (grey bars) on HT29 cell growth as percentage of control (untreated cells). Data are presented as mean ± SEM, N=3 and n=12 per group. Statistical analysis comparing TM and TM + ALX-5407 treatments for each concentration were performed by one-way-ANOVA with Tukey's post hoc analysis considering $p<0.05$ (*) and $p<0.01$ (**).

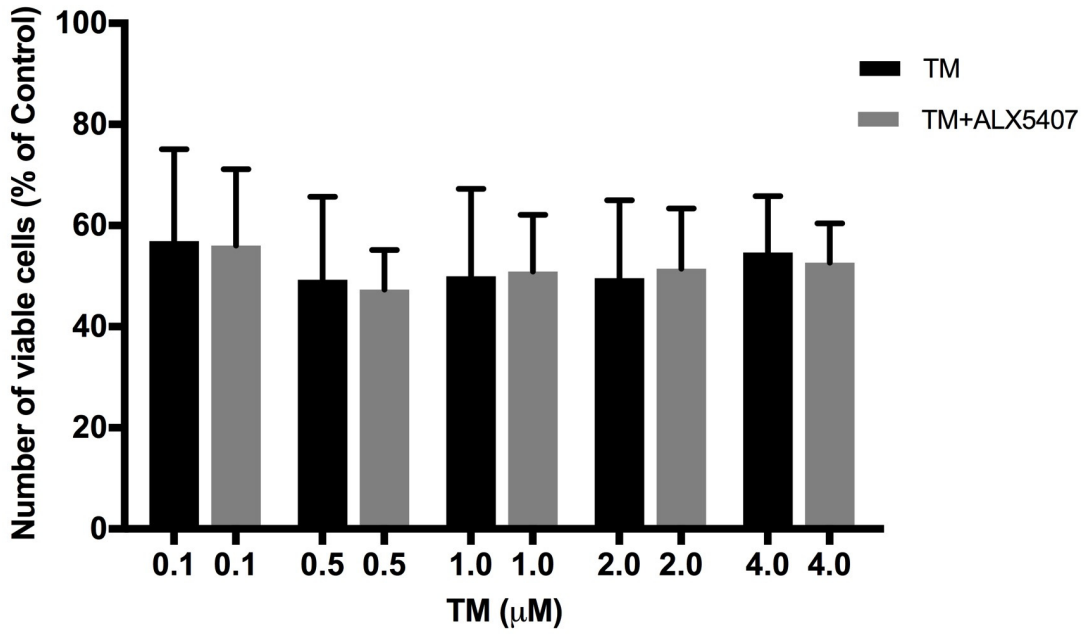

Figure 5.13: Effect of ALX-5407 treatment on A498 cell growth under ER stress conditions. Effect of treatment with 0.1, 0.2, 0.5, 1.0, 2.0 and 4.0μM tunicamycin (TM) for 4h alone (black bars) or in association with 120nM ALX-5407 (grey bars) on A498 cell growth as percentage of Control (untreated cells). Data are presented as mean ± SEM, N=3 and n=12 per group. Statistical analysis comparing TM and TM + ALX-5407 treatments for each concentration were performed by one-way-ANOVA with Tukey's post hoc analysis.

5.3 Summary of results and discussion

Extracellular glycine uptake dependent on GLYT1 transporter was observed to contribute to GSH synthesis and cellular protection against injuries (Howard et al., 2010). As demonstrated in Chapter 4, GLYT1 knockdown contributed to reduced glycine uptake leading to a decrease in GSH levels for all tumour cell lines analysed in this study and a reduction in DNA replication of the rapidly proliferative cells, A549 and HT29. GLYT1 inhibitors have been studied for more than a decade with the focus on treatment of disorders involving the CNS, such as schizophrenia, for which some drugs are in phase I or II clinical trials (Harvey and Yee, 2013). Therefore, in this chapter, the effect of a pharmacological approach to downregulate GLYT1 function utilising a specific GLYT1 inhibitor ALX-5407 on tumour cell proliferation was evaluated in normal conditions.

The influence of ALX-5407 on total glycine uptake was evaluated. Different concentrations of ALX5407 were tested and for the tumour cells analysed the lowest concentration of the inhibitor that presented a significant effect on inhibiting glycine uptake was 120nM and therefore this concentrations was utilised in further experiments. This dose is four times the stated IC_{50} for ALX5407, 30nM, and two-fold higher than the concentration utilised in other studies, 60nM (Atkinson et al., 2001). For NSCLC and colon cancer cell lines, A549 and HT29, respectively, treatment with 120nM ALX5407 reduced total glycine uptake by about 49% and for the renal cancer cell line, A498, a reduction of 40% was observed when compared to untreated cells. These data indicate that the GLYT1 inhibitor has a great impact on glycine uptake in these cells. Moreover, this result was similar to another *in vivo* study evaluating the effect of ALX5407 on glycine uptake in rat retina, in which they observed a reduction of 50% in total glycine uptake when compared to control (Salceda, 2006).

Treatment with 120nM ALX5407 reduced cell proliferation of the rapidly proliferating cells A549 and HT29, whereas the proliferation rate of the slowly proliferating tumour cell line A498 and the fast growing normal endothelial cell line HUVEC remained unchanged. The doubling time of A549 and HT29 was increased by about 8h, and a major and significant influence on cell growth following ALX5407 treatment occurred only after long period incubations, 96-110h time points, where there was a reduction in cell proliferation of about 20%. Following a long period of incubation there is a high cell concentration, especially for the rapidly proliferating cells, thus the

nutrient availability is reduced and/or metabolic waste products might accumulate in the medium, considering that medium was changed every 48hours. This may lead to stress and therefore increase in cellular demand for extracellular glycine to assist in GSH synthesis, to replenish meTHF or NADPH levels, or to participate in purine synthesis to maintain the rapid rates of DNA replication and cellular proliferation.

To address the question whether extracellular glycine supplied by GLYT1 becomes essential in maintaining cell proliferation of highly proliferating tumour cells during stress, ALX-5407 treatment was evaluated when cells were incubated under stress conditions. GLYT1 is regulated by ATF4, which is involved in the response to cellular stresses, such as nutrient starvation, hypoxia and ER stress (Harding et al., 2003). It is known that hypoxia and ER stress, generated by tunicamycin, reduce cell proliferation in tumour cells (Yadav et al., 2017, Guha et al., 2017). Additionally, GLYT1 mRNA expression was elevated in mice embryonic fibroblast cells treated with tunicamycin and an increase in glycine synthesis was observed in regions of incomplete hypoxia in glioma tumour (Harding et al., 2003, Maudsley et al., 2014). Thus, it was investigated whether ALX-5407 treatment in association with hypoxia condition or ER stress (tunicamycin treatment) increased the detrimental effect of this stress conditions on tumour cell proliferation. After cellular exposure to stress conditions such as oxidative stress during hypoxia, for A549 cell line, and ER stress induction, for HT29, the cell growth was further reduced by about 20% when cells were treated with ALX5407 for 72h, when compared to cells growing under stress only.

Therefore, these data suggest that under normal conditions fast growing cancer cells may not require extracellular glycine to maintain their cellular proliferation, only utilising their intracellular reserves, whereas under conditions of stress, such as nutrient limitation, ER stress or hypoxia, extracellular glycine supplied by GLYT1 becomes necessary to maintain a rapidly proliferative profile.

Chapter 6: ATF4 knockdown

6.1 Introduction

This chapter discusses the effect of ATF4 knockdown on A549, HT29, A498 and HUVEC cell proliferation, its influence on expression of other related genes, on total glycine uptake and on glutathione levels. Following transfection with ATF4 siRNA, the knockdown was confirmed through qPCR and Western blotting. ATF4 knockdown influence on cell proliferation was then assessed for all cell lines. Additionally, its influence on glycine uptake and on expression of the mRNAs encoding the specific glycine transporter GLYT1 and other amino acid transporters able to transport glycine, $ATB0^{,+}$, PAT1 and SNAT2 mRNA was also analysed. Moreover the influence of ATF4 knockdown on other activating transcription factors, ATF3, ATF5 and ATF6, was also analysed. Finally, the influence of ATF4 knockdown on glutathione levels, glutathione synthesising enzymes, GCL and GSS, and the xCT subunit of the cystine transporter was also investigated.

ATF4 is one of the key regulators of cellular stress and is highly activated in many tumour types (Wortel et al., 2017). Several ATF4 targets are involved in pro-survival mechanisms to overcome stress conditions and create an adaptive response (Wortel et al., 2017). However, ATF4 also activates expression of some genes involved in apoptosis, cell cycle arrest and is involved in regulation of autophagy genes (Wortel et al., 2017). ATF4 interacts with the amino acid response element (AARE) or, probably as heterodimer with members of the C/EBP family, in the C/EBP-ATF response elements (CARE), consensus-binding sites being present in many genes (Sato et al., 2004, Kilberg et al., 2009, Bröer and Bröer, 2017). Recent studies suggest that ATF4 is subjected to specific enzymatic modulation and post-translational modifications or histone modifications that possibly influence which target genes will be activated and then influence the cells pro-survival mechanisms or induction of apoptosis (Wortel et al., 2017). Moreover, some studies have demonstrated that ATF4 is more likely to promote cell survival in highly proliferative cells that have a balance between catabolism and anabolism, due to the elevated rates of protein synthesis which counterbalances the loss of essential material, therefore being also relevant to tumour development (Wortel et al., 2017). Additionally, it is well established that overexpression of ATF4 in tumours supports cell proliferation, adaptation to stress,

drug resistance and metastasis and is also involved in angiogenesis (Wortel et al., 2017). Therefore, ATF4 effect on cell proliferation was analysed.

As discussed in Chapter 1, during ER stress and hypoxia PERK-eIFα-ATF4 pathway is activated and under amino acid limitation cells trigger GNC2–eIF2α–ATF4 pathway. ATF4 up-regulates genes encoding proteins for amino acid transporters, including GLYT1 and synthesis, such as serine synthesis enzymes PHGDH, PSPH and SHMT2, and also genes involved in glutathione (GSH) synthesis, such as the cysteine transporter subunit xCT and is involved in GCL up-regulation, in an attempt to restore homeostasis (Sikalidis et al., 2014, Sato et al., 2004, Harding et al., 2003, Adams, 2007, Gorrini et al., 2013). Additionally, ATF4 is indirectly involved in protein synthesis, activating GADD34 transcription, which in turn dephosphorylates eIF2α, thus restoring protein translation, and also up-regulates some autophagy genes, which in a catabolic pathway can restore some nutrient levels in the cell and activate mTOR (Wortel et al., 2017). Some tumour cells are known to utilise autophagy as a survival mechanism (Wortel et al., 2017). As described in previous chapters, ATF4 also up-regulates other transcription factors such as ATF3, ATF5 and ATF6 (Lee et al., 2013, Zhou et al., 2008, Teske et al., 2011), which have been related to some tumour types survival, progression and invasiveness, as described in Chapter 1. While there is some evidence suggesting that these transcription factors interact with each other to regulate expression of target genes, there is so far little information regarding the role they play in the regulation of nutrient transport in cancer cells. This way, the influence of ATF4 on glycine amino acid transporters, GSH synthesis enzymes and on other ATFs transcription in rapidly and slowly proliferating cells lines was evaluated.

6.2 Results

6.2.1 *ATF4 knockdown efficiency*

The efficiency of ATF4 knockdown experiments was assessed analysing ATF4 mRNA and protein expression following transfection with ATF4 siRNA. Briefly, A549, HT29, A498 and HUVEC cell lines were seeded in two 12-well plates in RPMI, transfected with Negative or ATF4 siRNA and incubated for a further 72 hours in RPMI. Then, total RNA was extracted (see Chapter 2 Section 2.2) or protein extracted utilising RIPA buffer (Chapter 1, Session 2.4.4). Prior to protein extraction and following ATF4 siRNA transfection, cells were treated with thapsigargin 300nM for 8hours to increase ATF4 expression and facilitate detection in Western blotting assay.

The efficiency of the transfection with ATF4 siRNA was first evaluated with qPCR experiments to verify its effect on ATF4 mRNA abundance in comparison to control cells treated with Negative siRNA for A549, HT29, A498 and HUVEC cell lines. Following RNA extraction, RNA yield and purity were analysed measuring absorbance at 260 and 280 nm. All RNAs utilised in this study presented a 260/280 ratio between 1.95 and 2.0 suggesting its purity. Then, 500ng of total RNA extracted following transfection with Negative or ATF4 siRNA was reverse transcribed to cDNA as described in Section 2.4.1. Finally, qPCR was performed utilising a specific primer pair for ATF4 mRNA. As shown in figure 6.1a, ATF4 mRNA expression was significantly reduced following transfection with ATF4 siRNA when compared to the control, where cells where transfected with a Negative control siRNA. When compared to controls, ATF4 mRNA expression was reduced 86.9% ($p<0.0001$) in A549, 85.8% ($p<0.0001$) in HT29, 80.9% ($p<0.001$) in A498 and 55% ($p<0.0001$) in HUVEC cell lines. Therefore, a significant reduction of ATF4 mRNA abundance was observed for all cell lines confirming ATF4 knockdown.

Additionally, following transfection with ATF4 and Negative siRNAs and thapsigargin (Tg) treatment, protein was extracted with RIPA buffer for the tumour cell lines A549, HT29 and A498. Protein levels were quantified utilising Bradford Reagent, following incubation, the absorbance was measured at 595nm and the sample concentration was determined according to the linear equation of the standard curve performed in the same experiment. Samples were then diluted to 1µg/ml and Western blotting assay was performed with a specific anti-ATF4 antibody as described in Chapter 2 Section 2.4.5 and utilising anti-β-actin antibody as loading control. Although

weakly stained, Figure 6.1b shows that the ATF4 protein levels were reduced following ATF4 knockdown in comparison to the control cells, whereas β-actin protein expression presented similar expression pattern between ATF4 knockdown and Controls. Hence, these data suggest the efficiency of the method utilised to downregulate ATF4 expression.

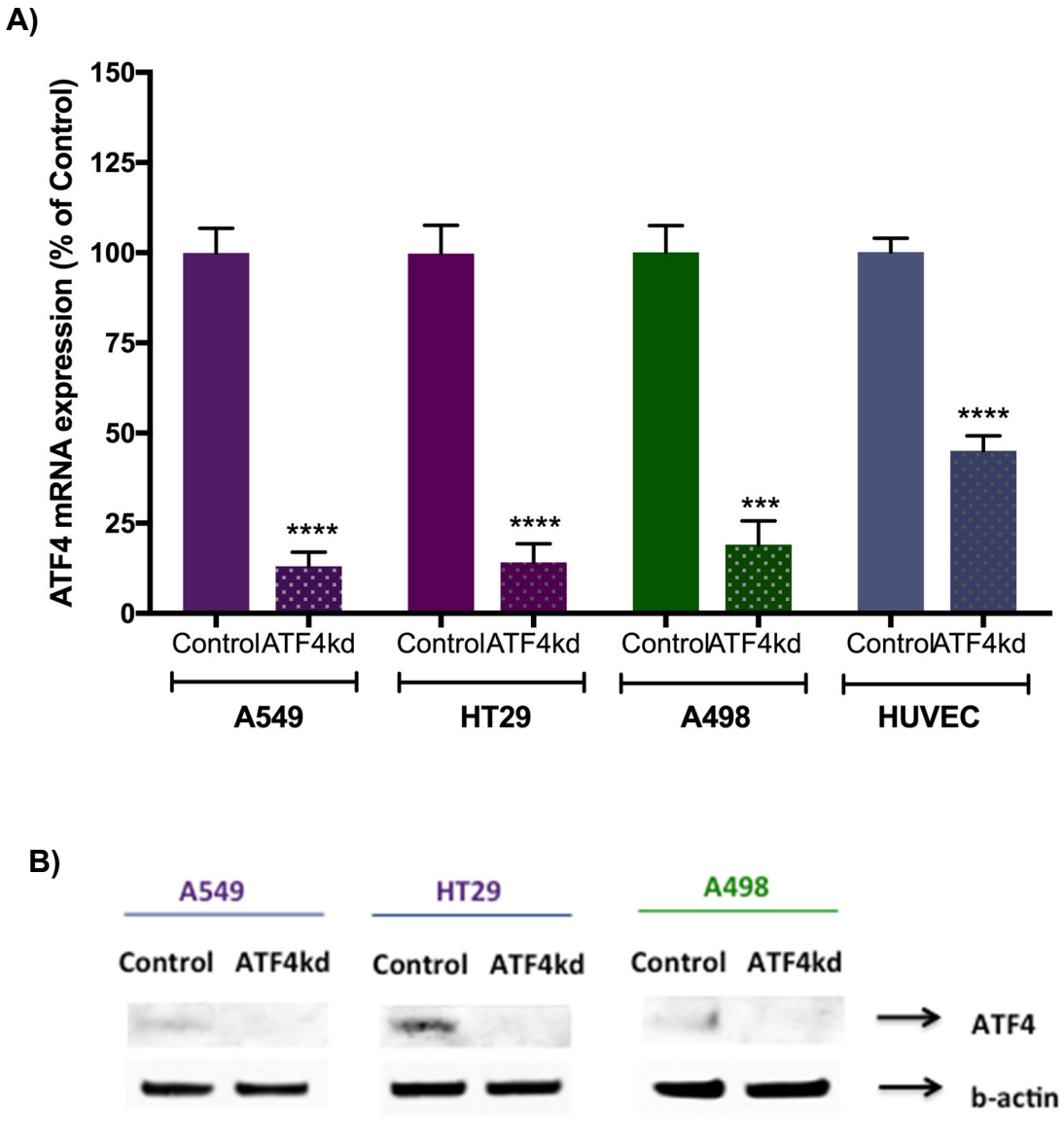

Figure 6.1: ATF4 knockdown efficiency. (A) Relative abundance of ATF4 mRNA in the A549, HT29, A498 and HUVEC cell lines. Data bars for cells transfected with ATF4 siRNA are marked ATF4kd and cells transfected with Negative siRNA are referred to as Control. Data are means ± SEM, N=3 and n=9 for A549, HT29 and A498 and N=2, n=4 for HUVEC cell line. Statistical analysis comparing the treatments (knockdowns) and controls were performed by one-way-ANOVA with Tukey's post hoc analysis. Values significantly different from controls are marked: $p<0.001$ (***) and $p<0.0001$ (****). **(B)** ATF4kd and Control samples of A549, HT29 and A498 cells utilised in Western blotting analysis with anti-ATF4 antibody referred to as ATF4 and anti-β-actin antibody as loading control marked as β-acting.

6.2.2 *ATF4 knockdown effect on cell proliferation*

Once the efficiency of knockdown experiments was verified, the effect of ATF4 downregulation on A549, HT29, A498 and HUVEC cell proliferation was evaluated. The number of viable cells and the proliferation marker ki67 mRNA expression were assessed following ATF4 knockdown (ATF4kd) and compared to Control.

CTB assay

A549, HT29, A498 and HUVEC cells were seeded in a 96-well plate, transfected with ATF4 or Negative (Control) siRNA and the number of viable cells was measured 72h post-transfection by adding 20µl CTB to each well and incubating for a further 3 hours prior to fluorescence measurement. ATF4kd reduced the number of viable epithelial tumour cells for the A549, HT29 and A498 lines, but increased proliferation of the normal endothelial HUVEC cell line. Microscopy images showed a visual reduction in cell number for the A549 (Figure 6.2a), HT29 (Figure 6.3a) and A498 (Figure 6.4a) cell lines following ATF4kd and the following CTB analysis confirmed a reduction of 39%, $p<0.0001$ (Figure 6.2b), 41%, $p<0.0001$ (figure 6.3b) and 37%, $p<0.0001$ (Figure 6.4b) in the number of viable cells when compared to respective Controls. However, ATF4kd increased cell proliferation of the normal rapidly proliferating HUVEC cell line by 11% ($p<0.05$) when compared to Control (Figure 6.5). ATF4kd influence on cell proliferation was similar among all the tumour cell lines analysed, but significantly different in the normal cell line, HUVEC, which presented the opposite effect (Figure 6.6).

Ki67

The mRNA expression of the proliferation marker ki67 was then analysed following ATF4kd by qPCR. When compared to the Controls, there was a reduction in ki67 mRNA abundance of 42.5% ($p< 0.5$) for A549 cells, 56.9% ($p<0.001$) for HT29 cells and 35.1% ($p<0.001$) for A498 cell line, following ATF4kd, but no significant difference was observed in ki67 mRNA levels for HUVEC cell line (Figure 6.7). These results are in agreement with the previous experiments, suggesting that down-regulation of ATF4 affects only the tumour epithelial cell lines analysed, but had a minor effect on normal endothelial cell line HUVEC.

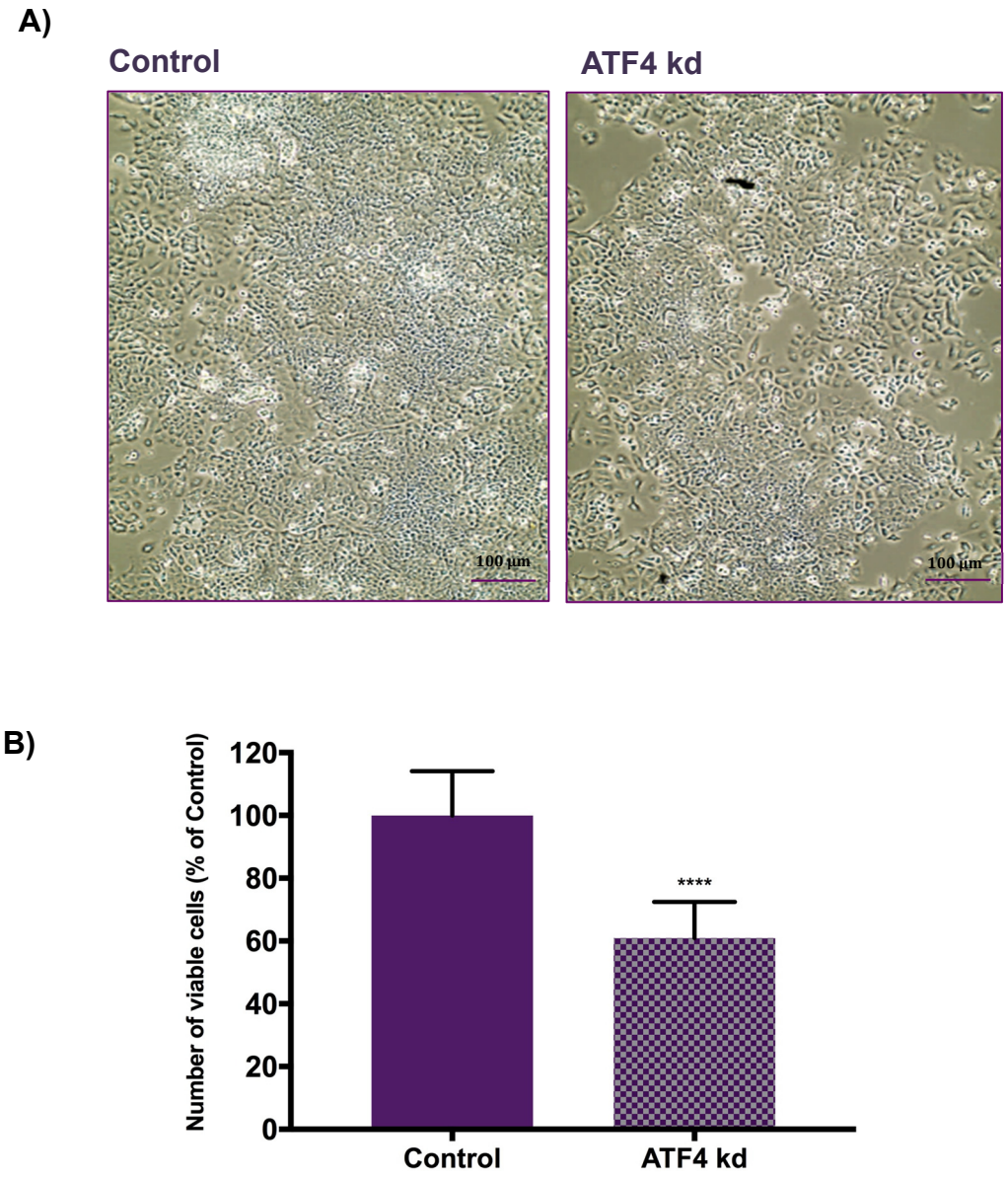

Figure 6.2: A549 cell number following ATF4 Knockdown experiments. (A) 20X microscopy images **(B)** and CTB assay analysis of A549 cell line after 72 hours transfection with Negative siRNA (Control) or ATF4 siRNA (ATF4 kd). Number of viable cells presented as percentage of control according to fluorescence measurement after 3h incubation with CTB reagent. Data are presented as mean ± SEM, N=3 and n=12. Statistical analysis comparing ATF4 kd treatment and Control was performed by unpaired t-test considering $p<0.0001$ (****).

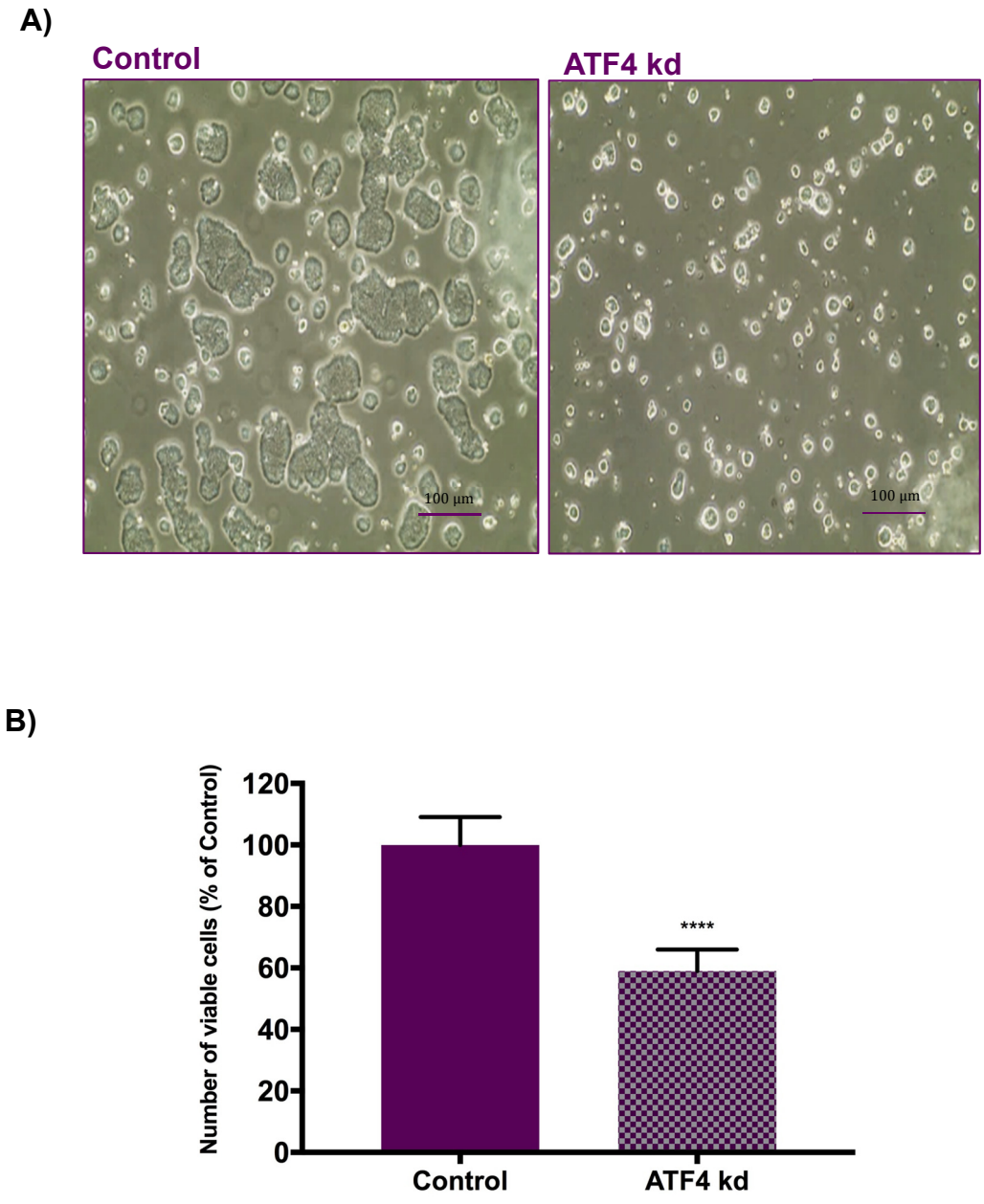

Figure 6.3: HT29 cell number following ATF4 Knockdown experiments. (A) 20X microscopy images **(B)** and CTB assay analysis of HT29 cell line after 72 hours transfection with Negative siRNA (Control) or ATF4 siRNA (ATF4 kd). Number of viable cells presented as percentage of control according to fluorescence measurement after 3h incubation with CTB reagent. Data are presented as mean ± SEM, N=3 and n=15. Statistical analysis comparing ATF4 kd treatment and Control was performed by unpaired t-test considering $p<0.0001$ (****).

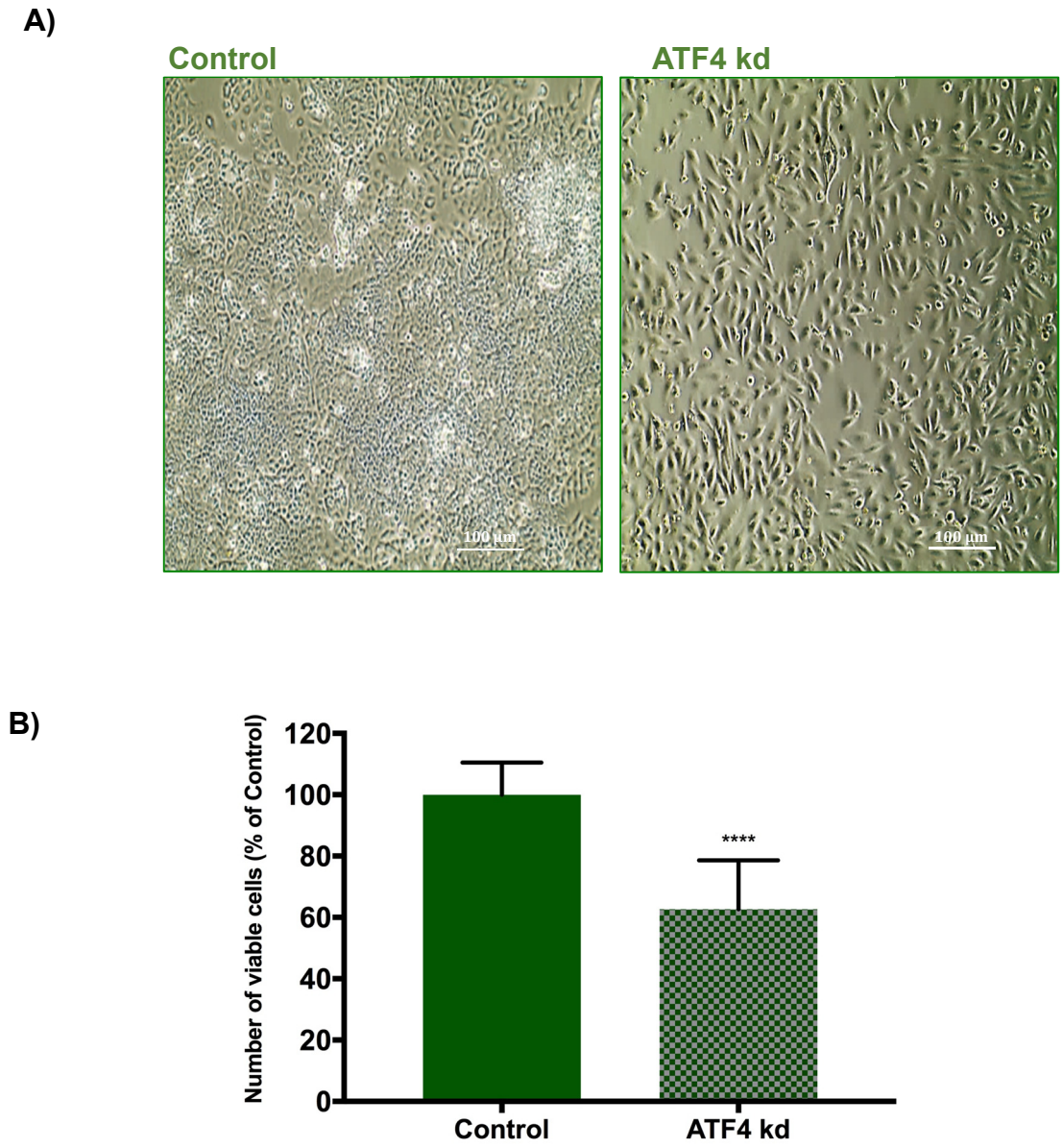

Figure 6.4: A498 cell number following ATF4 Knockdown experiments. (A) 20X microscopy images **(B)** and CTB assay analysis of A498 cell line after 72 hours transfection with Negative siRNA (Control) or ATF4 siRNA (ATF4 kd). Number of viable cells presented as percentage of control according to fluorescence measurement after 3h incubation with CTB reagent. Data are presented as mean ± SEM, N=3 and n=12. Statistical analysis comparing ATF4 kd treatment and Control was performed by unpaired t-test considering $p<0.0001$ (****).

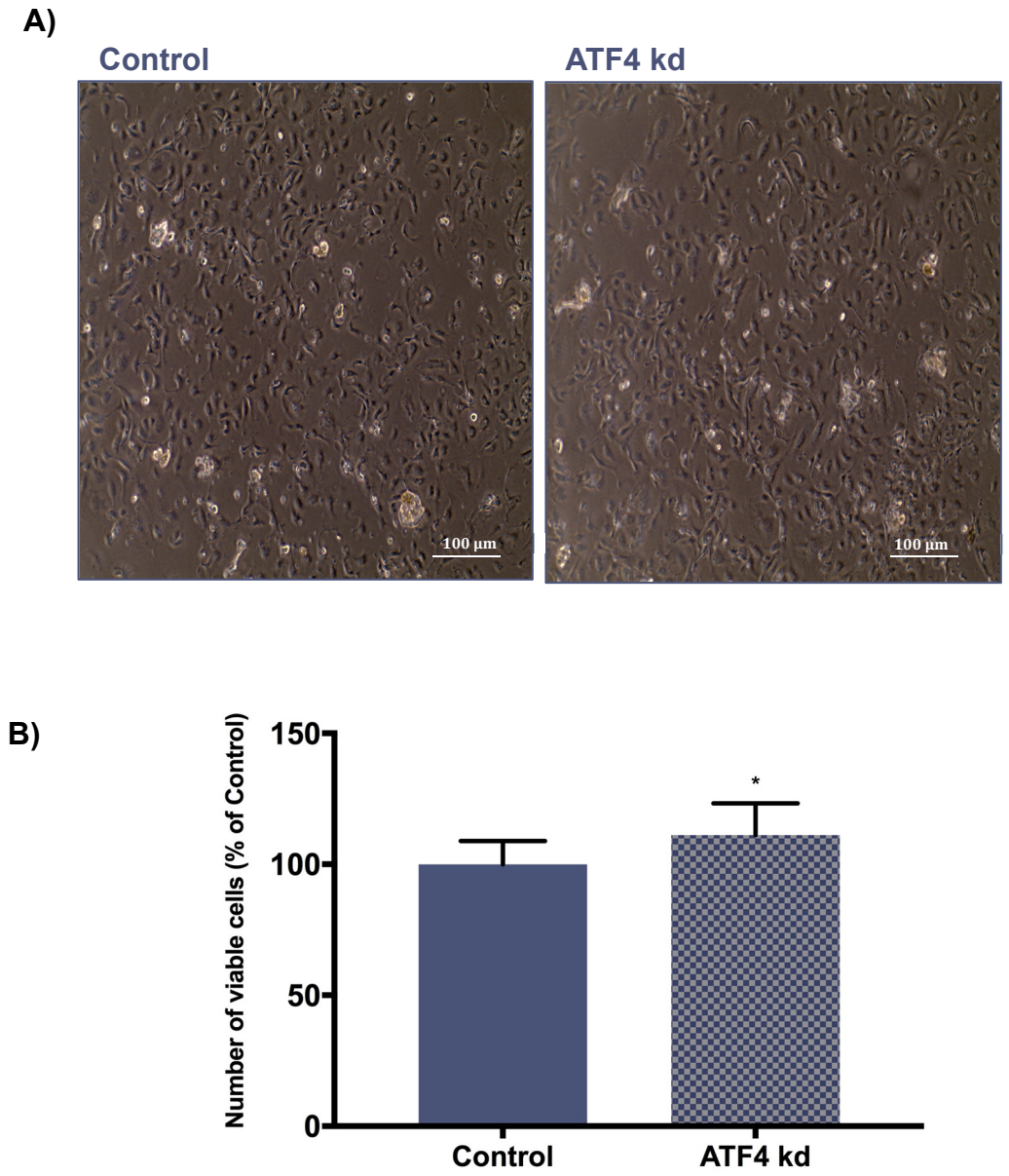

Figure 6.5: HUVEC cell number following ATF4 Knockdown experiments. (A) 20X microscopy images **(B)** and CTB assay analysis of HUVEC cell line after 72 hours transfection with Negative siRNA (Control) or ATF4 siRNA (ATF4 kd). Number of viable cells presented as percentage of control according to fluorescence measurement after 3h incubation with CTB reagent. Data are presented as mean ± SEM, N=3 and n=15. Statistical analysis comparing ATF4 kd treatment and Control was performed by unpaired t-test considering $p<0.05$ (*).

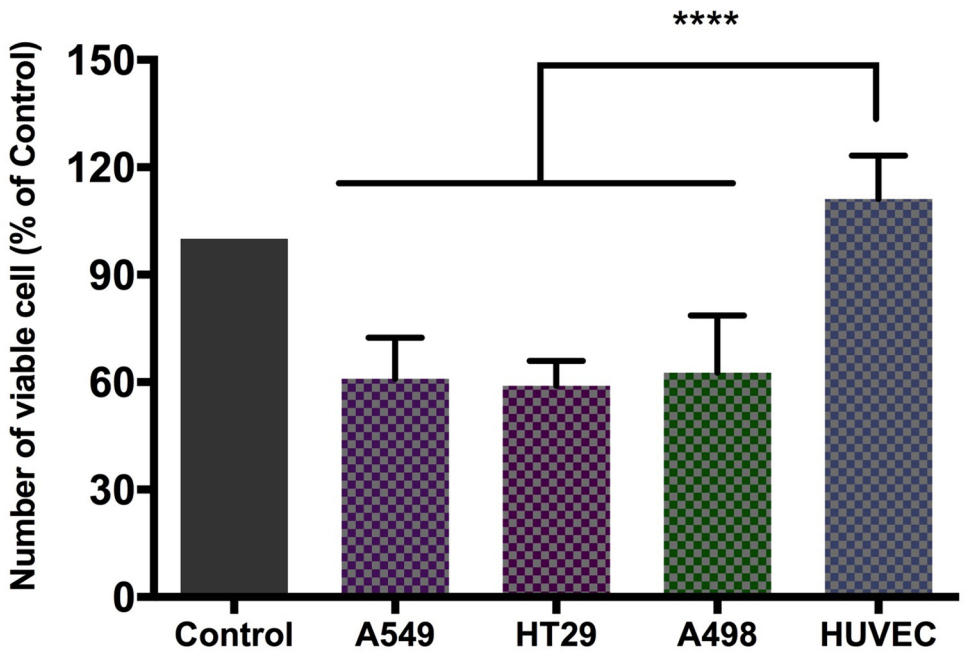

Figure 6.6: ATF4 knockdown different effects on cell growth between cell lines. The effect of ATF4kd, compared with Control, Negative siRNA, on the number of viable cells was significantly different between the tumour cell lines, decrease in cell proliferation, and the normal cell line, HUVEC, increase in cell proliferation. Data are presented as mean ± SEM, with N=3, n=15 for A549, HT29 and A498 and N=2, n=10 for HUVEC cell line. Statistical analysis comparing GLYT1 kd effect between cell lines were performed by one-way-ANOVA with Tukey's post hoc analysis considering $p<0.0001$ (****).

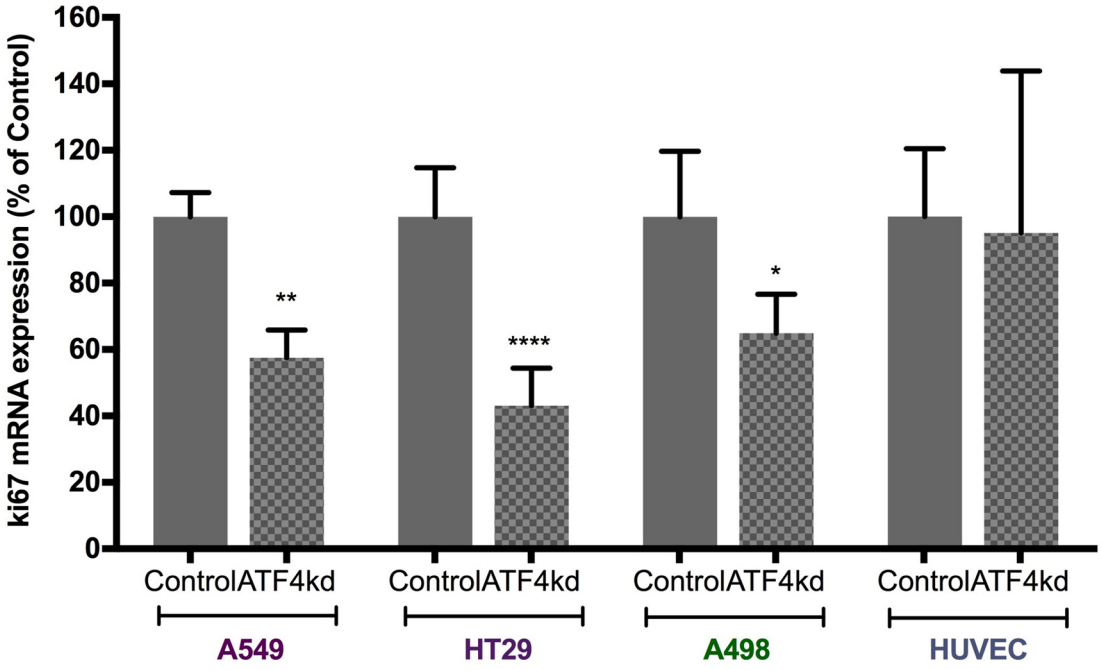

Figure 6.7: ATF4 knockdown reduced ki67 mRNA expression in A549, HT29 and A498 cells, but had no effect on HUVEC cell line. Real time qPCR analysis of the influence of ATF4 kd on the proliferation marker ki67 mRNA expression as percentage of Control (Negative siRNA). Data are presented as mean ± SEM, N=3 and n=9. Statistical analysis comparing the treatment (ATF4kd) and control of each cell line were performed by unpaired t-test considering $p<0.05$ (*), $p<0.01$ (**) and $p<0.0001$ (****).

6.2.3 *Influence of ATF4 knockdown on gene expression of other glycine transporters and glycine synthesising enzyme*

In order to evaluate if ATF4 downregulation in the tumour cell lines would affect the mRNA expression of amino acid transporters able to transport glycine, GLYT1, PAT1, SNAT2 and $ATB^{0,+}$, or enzymes involved in its intracellular synthesis, SHMT2, qPCR analyses were performed. Cells were transfected with ATF4 and Negative (Control) siRNA and incubated for 72h prior to RNA extraction as described before. The HUVEC cell line was not utilised in these experiments.

GLYT1

ATF4kd had a great effect on GLYT1 mRNA expression. Following ATF4kd, GLYT1 mRNA expression was significantly reduced in all cell lines analysed (Figure 6.8). For A549 cells, when ATF4 was downregulated, a reduction of 51.7% ($p<0.0001$) in comparison to Control was observed. For HT29 cells, GLYT1 mRNA abundance was reduced 88.3% ($p<0.0001$) when compared to Control. For A498 ATF4kd cells, there was a decrease of 85.6% ($p<0.0001$) when compared to controls.

PAT1

ATF4 knockdown downregulated PAT1 mRNA expression in HT29 cell line, but had no effect on A549 and A498 cells (Figure 6.9). For HT29 cells, a minor reduction of 24.1% ($p<0.05$) was observed following ATF4kd when compared to Control. For A549 and A498 cells, PAT1 mRNA abundance was not affect by ATF4kd when compared to Control.

SNAT2

ATF4 downregulation reduced SNAT2 mRNA levels in A498 cells only (figure 6.10). After ATF4kd, for A498 cell line, there was a reduction of 41.6% ($p<0.0001$) when compared to Control cells. For the rapidly proliferating tumour cells A549 and HT29, although there was a tendency in downregulating SNAT2 mRNA expression following ATF4kd, no significant difference was observed.

$ATB^{0,+}$

In HT29 cells only the knockdown of ATF4 resulted in downregulation of $ATB^{0,+}$ (figure 6.11). When compared to Control, $ATB^{0,+}$ was reduced 50.3% ($p<0.0001$) following ATFkd for HT29 cell line. However, ATF4kd had no significant effect on $ATB^{0,+}$ mRNA levels in the other rapidly proliferative cancer cell line, A549, although

there was a tendency in downregulating $ATB^{0,+}$ gene expression. A498 Control cells did not express $ATB^{0,+}$ mRNA and no changes were observed following ATF4kd.

SHMT2

Following ATF4kd, SHMT2 mRNA expression was downregulated in all cell lines (figure 6.12). In A549 cells there was decrease of 29.4% ($p<0.01$) when compared to Control cells. In HT29 cells treated with ATF4 siRNA, a downregulation of 44.1% ($p<0.001$) was observed when compared to Control cells. For A498 ATF4kd cells, SHMT2 mRNA abundance was reduced 33.9% ($p<0.05$) when compared to Control cells.

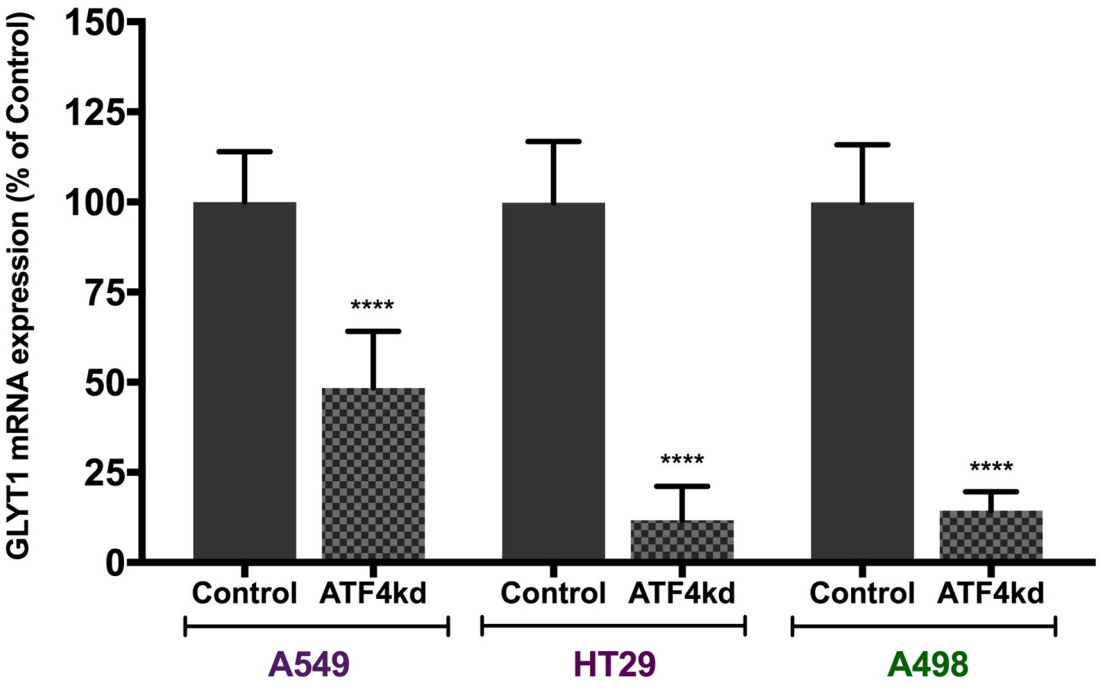

Figure 6.8: ATF4 knockdown reduced GLYT1 mRNA expression of A549, HT29 and A498 cell lines. Real time qPCR analysis of the influence of ATF4kd on the specific glycine transporter GLYT1 mRNA expression as percentage of control (Negative siRNA). Data are presented as mean ± SEM, N=3 and n=9 per group. Statistical analysis comparing the treatment (ATF4 kd) and control of each cell line were performed by unpaired t-test considering $p<0.0001$ (****).

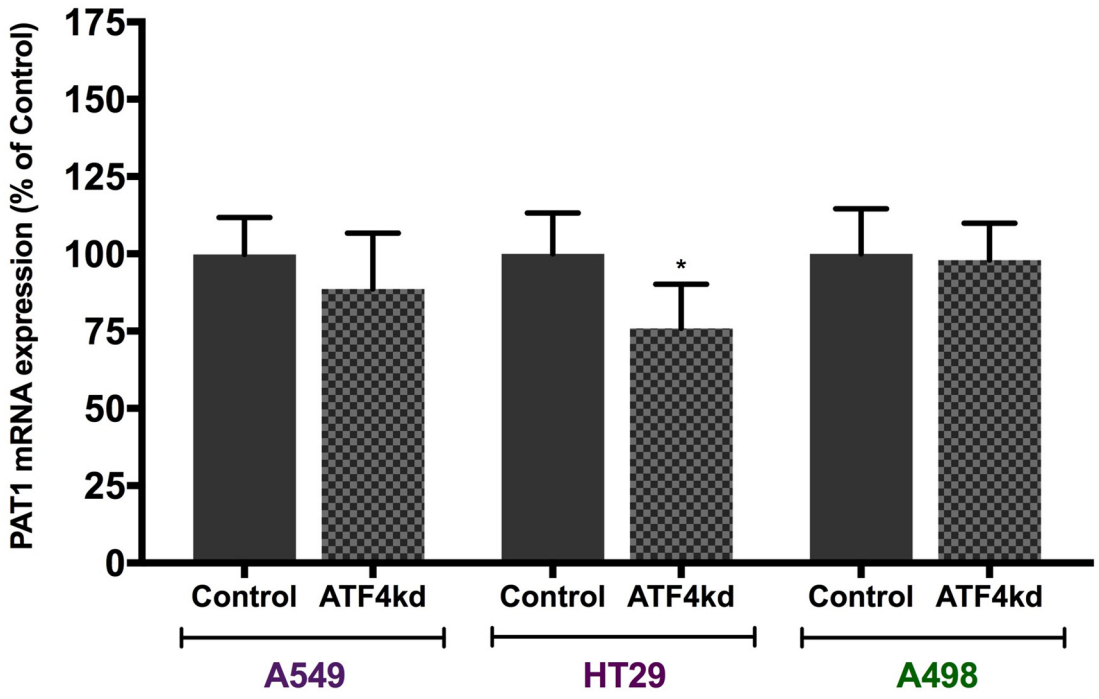

Figure 6.9: ATF4 knockdown reduced PAT1 mRNA expression of HT29 cells and had no effect in A549 and A498 cell lines. Real time qPCR analysis of the influence of ATF4 kd on the amino acid transporter PAT1 mRNA expression as percentage of control (Negative siRNA). Data are presented as mean ± SEM, N=3 and n=9 per group. Statistical analysis comparing the treatment (ATF4 kd) and control of each cell line were performed by unpaired t-test considering $p<0.05$ (*).

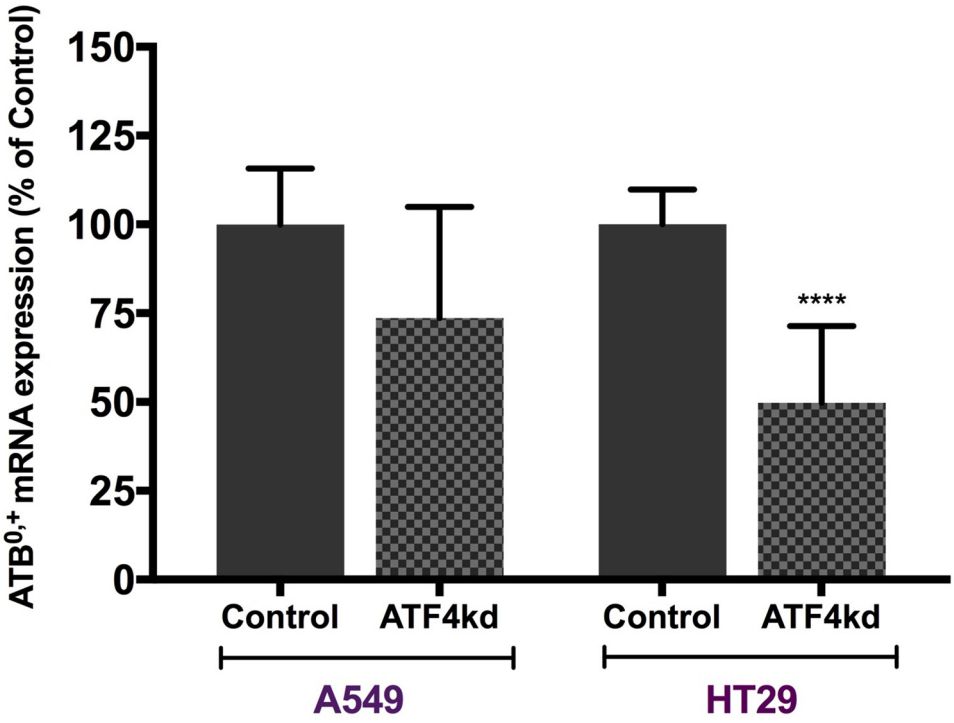

Figure 6.10: ATF4 knockdown reduced $ATB^{0,+}$ mRNA expression of HT29 cells and had no effect on A549 cells. Real time qPCR analysis of the influence of ATF4 kd on the amino acid transporter $ATB^{0,+}$ mRNA expression as percentage of control (Negative siRNA). Data are presented as mean ± SEM, N=3 and n=9 per group. Statistical analysis comparing the treatment (ATF4 kd) and control of each cell line were performed by unpaired t-test considering $p<0.0001$ (****).

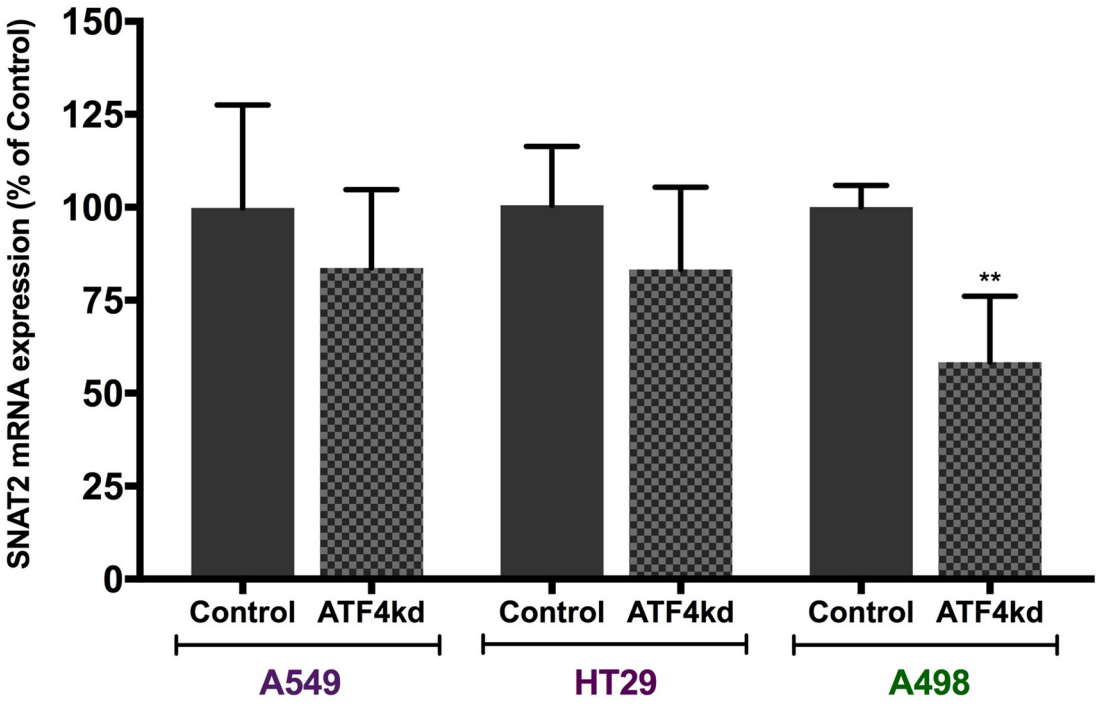

Figure 6.11: ATF4 knockdown reduced SNAT2 mRNA expression of HT29 cells and had no effect on A549 cell lines. Real time qPCR analysis of the influence of ATF4 kd on the amino acid transporter SNAT2 mRNA expression as percentage of control (Negative siRNA). Data are presented as mean ± SEM, N=3 and n=9 per group. Statistical analysis comparing the treatment (ATF4 kd) and control of each cell line were performed by unpaired t-test considering $p<0.01$ (**).

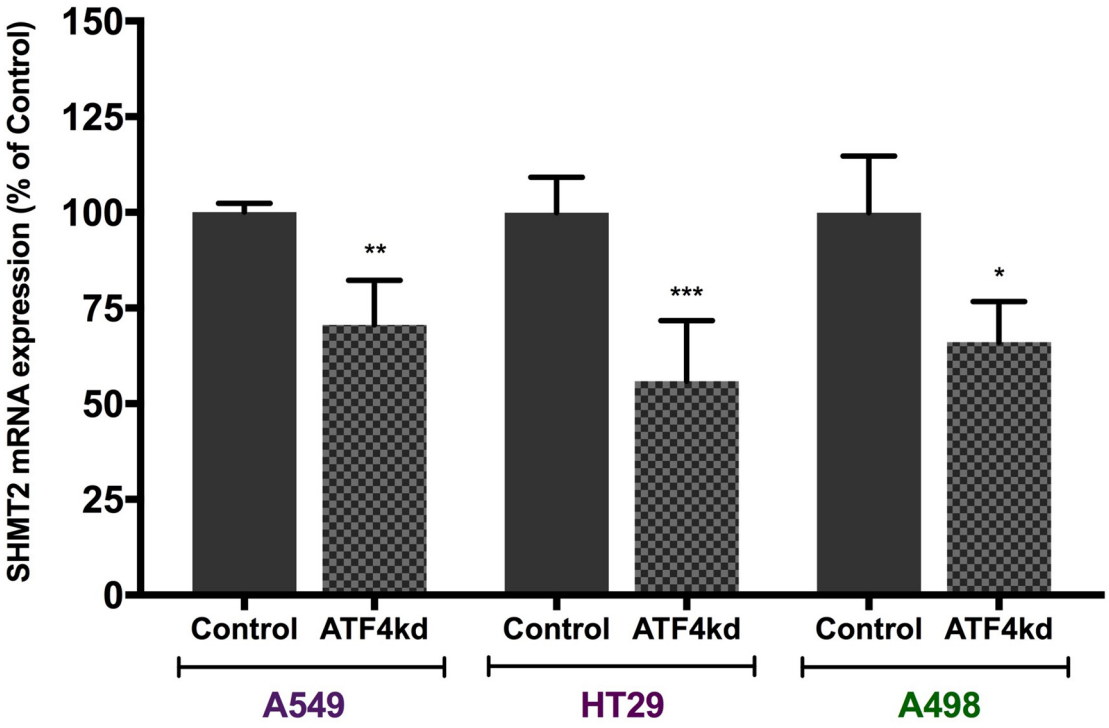

Figure 6.12: ATF4 knockdown reduced SHMT2 mRNA expression of A549, HT29 and A498 cell lines. Real time qPCR analysis of the influence of ATF4 kd on the enzyme involved in intracellular synthesis of glycine in the serine biosynthesis pathway SHMT2 mRNA expression as percentage of control (Negative siRNA). Data are presented as mean ± SEM, N=3 and n=9 per group. Statistical analysis comparing the treatment (ATF4 kd) and control of each cell line were performed by unpaired t-test considering $p<0.05$ (*), $p<0.01$ (**) and $p<0.001$ (***).

6.2.4 *Influence of ATF4 downregulation on total glycine uptake*

As ATF4kd had a major effect reducing GLYT1 mRNA abundance in all tumour cell lines tested, its effect on total glycine uptake was evaluated and compared to Control, Negative siRNA, cells. As described in Chapters 2 and 4, the transfection medium was removed, cells were washed three times and then incubated for 30 minutes in Kreb's buffer at 37^0C. Then, the Kreb's buffer was replaced with fresh buffer containing 0μM, 1μM, 50μM, 100μM, 200μM, 500μM or 100μM of glycine in association with 0.5μCi/ml [2-^{3}H]-Glycine and incubated for 10 minutes. The amount of glycine uptake was then calculated and normalised with the number of viable cells at the end of ATF4 knockdown experiments. In the A549 and A498 cell lines ATF4 knockdown had only a small effect, reducing the amount of glycine uptake when compared to control cells for some glycine concentrations but had no significant effect in the HT29 cell line incubated in different glycine concentrations (Figure 6.13, left panel graphs). ATF4 knockdown, on average, reduced by 21.3% ($p<0.05$) and 14.2% ($p<0.0001$) total glycine uptake for A549 and A498 cells, respectively, when compared to control, Negative siRNA, cells, but had no significant effect on HT29 total glycine uptake (Figure 6.13, right panel graphs).

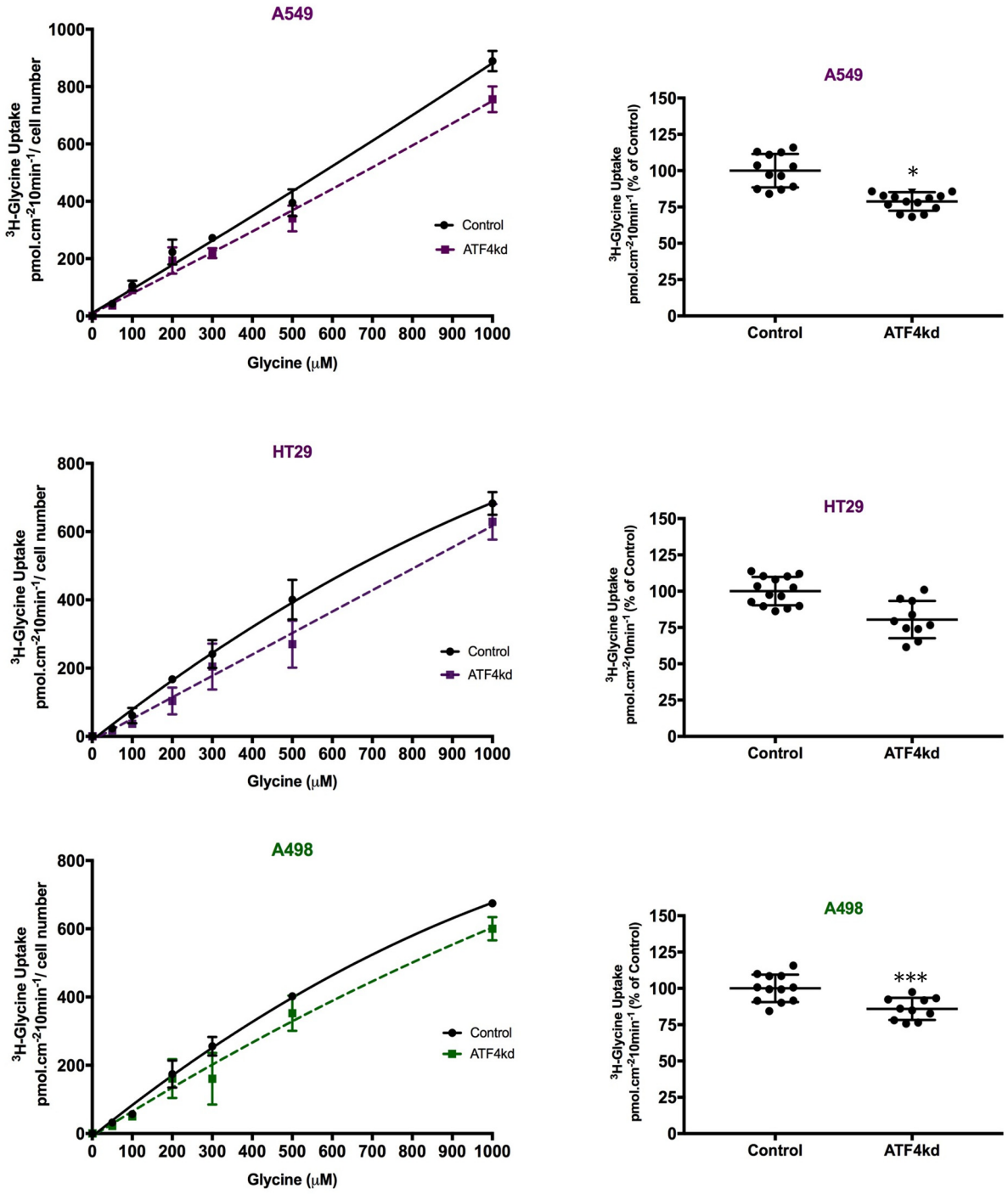

Figure 6.13: ^{3}H-Glycine Uptake measurements for A549, HT29 and A498 cell lines. (Left panel graphs) Amount of total glycine uptake measured after 72h transfection with ATF4 or Negative siRNAs referred to as ATF4kd and Control, respectively, for each cell line incubated with 1, 50, 100, 200, 300, 500 and 10000μM glycine in Kreb's buffer for 10 minutes. The amount of glycine uptake was calculated and normalised with the number of viable cells post transfection. **(Right panel graphs)** Data from left panel presented as average of percentage of Control of the different concentrations. Data are means ± SEM, N=2 and n=6. Statistical analysis comparing the treatment (ATF4 kd) and control of each cell line were performed by unpaired t-test considering $p<0.05$ (*) and $p<0.001$ (***).

6.2.5 *Influence of ATF4 knockdown on gene expression of other activating transcription factors*

Since other ATFs such as ATF3, ATF5 and ATF6 influence cell survival and proliferation under stress conditions and their transcription is upregulated in some cell lines by ATF4, the effect of ATF4kd on their mRNA expression in the tumour cell lines A549, HT29 and A498 was evaluated.

ATF3

ATF4 knockdown downregulated ATF3 mRNA expression in rapidly proliferative tumour cell lines A549 and HT29 (Figure 6.14). For ATF4kd, in A549 cells ATF3 mRNA abundance was reduced 40.5% ($p<0.0001$) when compared to Control, Negative siRNA. For HT29 cells following ATF4kd, ATF3 mRNA level was downregulated 44.6% ($p<0.001$), when compared to Control. For the slow proliferating cell line A498 ATF4kd had no significant influence on ATF3 mRNA expression.

ATF5

Following ATFkd, the mRNA levels of ATF5 were also downregulated in the rapidly proliferating cell lines (Figure 6.15). For A549, when ATF4 was downregulated there was a reduction of 57.8% ($p<0.001$) in ATF5 mRNA abundance. For ATF4kd HT29 cells, ATF5 mRNA expression was downregulated 46.9% ($p<0.05$) when compared to Control, Negative siRNA, cells. Although there was a tendency in reducing ATF5 mRNA levels in A498 following ATF4kd, no significant difference was observed when compared to Control.

ATF6

ATF4 downregulation reduced ATF6 mRNA levels in all tumour cell lines analysed in this study (figure 6.16). For ATF4kd in the A549 cell line, there was a reduction of 32.7% ($p<0.01$) in ATF6 mRNA abundance, when compared to Control, Negative siRNA. For ATF4kd in HT29 cells, ATF6 mRNA expression was downregulated 44.7% ($p<0.001$) when compared to Control. For ATF4kd in A498 cells, there was a reduction of 25% ($p<0.05$) in ATF6 mRNA levels, when compared to respective Control.

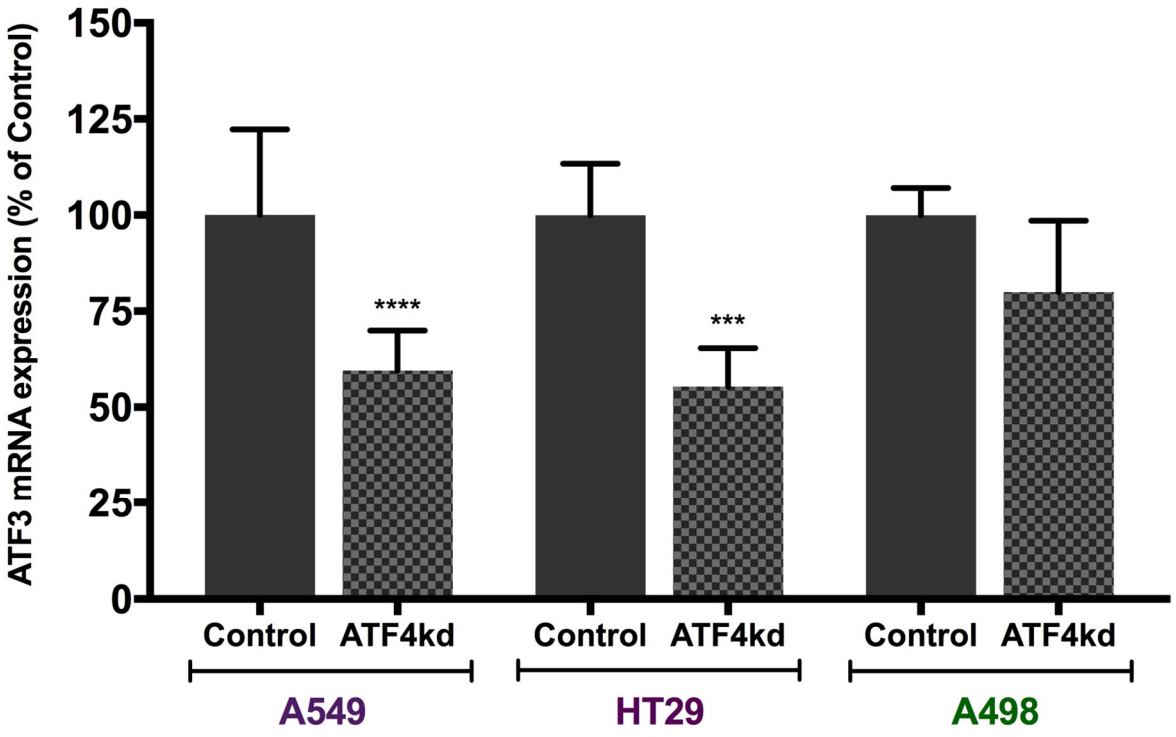

Figure 6.14: ATF4 knockdown reduced ATF3 mRNA expression of A549 and HT29 cells and had no effect on A498 cell line. Real time qPCR analysis of the influence of ATF4 kd on ATF3 mRNA expression as percentage of control (Negative siRNA). Data are presented as mean ± SEM, N=3 and n=9 per group. Statistical analysis comparing the treatment (ATF4kd) and control of each cell line were performed by unpaired t-test considering $p<0.001$ (***) and $p<0.0001$ (****).

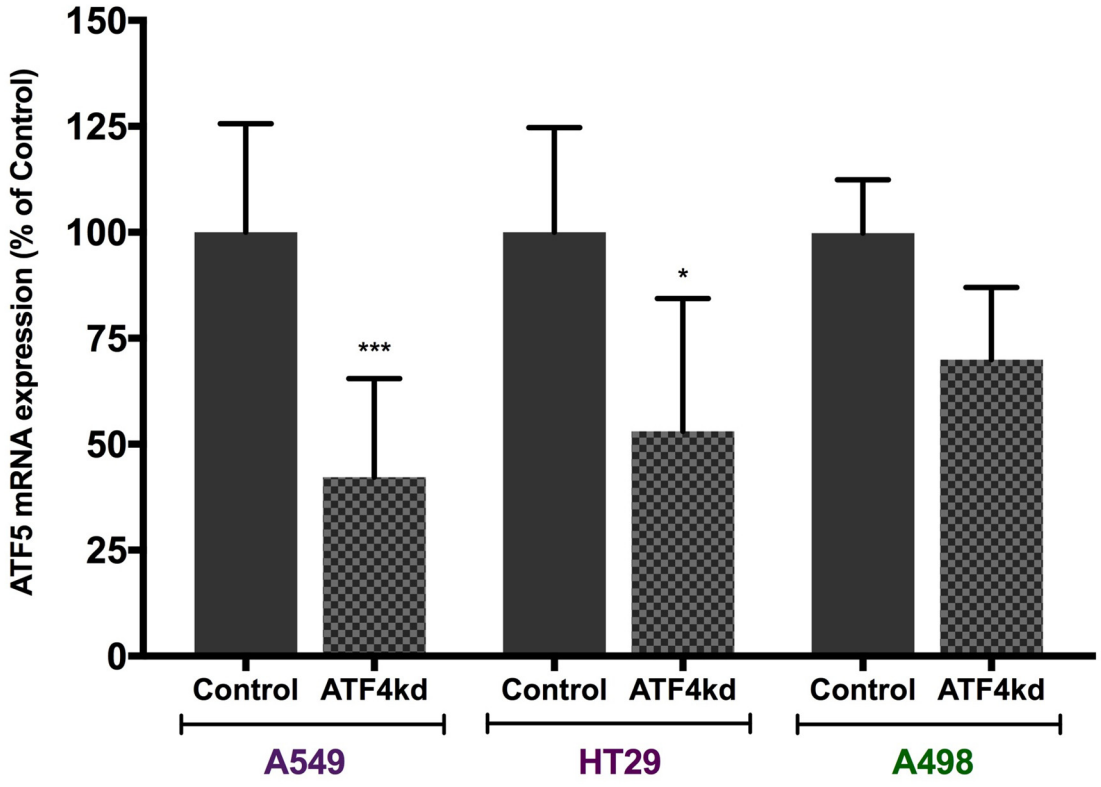

Figure 6.15: ATF4 knockdown reduced ATF5 mRNA expression of A549 and HT29 cells and had no effect on A498 cells. Real time qPCR analysis of the influence of ATF4 kd on ATF5 mRNA expression as percentage of control (Negative siRNA). Data are presented as mean ± SEM, N=3 and n=9 per group. Statistical analysis comparing the treatment (ATF4kd) and control of each cell line were performed by unpaired t-test considering $p<0.05$ (*) and $p<0.01$ (**).

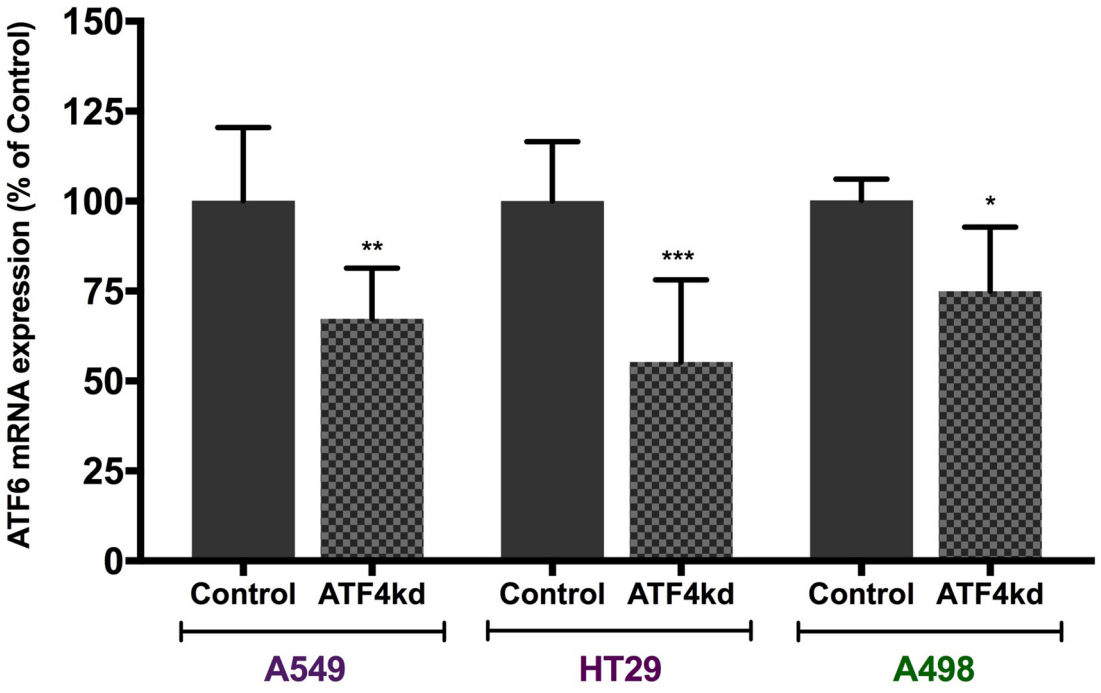

Figure 6.16: ATF4 knockdown reduced ATF6 mRNA expression in A549 and HT29 cells and had no effect on A498 cells. Real time qPCR analysis of the influence of ATF4 kd on ATF6 mRNA expression as percentage of control (Negative siRNA). Data are presented as mean ± SEM, N=3 and n=9 per group. Statistical analysis comparing the treatment (ATF4kd) and control of each cell line were performed by unpaired t-test considering $p<0.05$ (*), $p<0.01$ (**) and $p<0.001$ (***).

6.2.6 *Influence of GLYT1 knockdown on gene expression of glutathione synthesising enzymes and cystine transporter*

As described in the introduction ATF4 also influences GSH synthesis in some tumour cells. ATF4 regulates the expression of some GSH enzyme synthesising genes such as the GCLC subunit of the GCL enzyme. Also, ATF4 activates the transcription of the xCT subunit of the cystine transporter, crucial to maintain intracellular levels of cysteine which is a limiting substrate in GSH synthesis. Thus, the effect of ATF4 knockdown on GSH levels, GSH synthesising enzymes and on xCT was evaluated for A549, HT29 and A498 cell lines. Cells were transfected with GLYT1 and Negative siRNA and incubated for 72h prior to GSH measurement experiments as described before.

GSH levels

ATF4 downregulation reduced GSH content of A549, HT29 and A498 cell lines under normal experiment conditions. Following ATF4kd GSH content was reduced by 20% ($p<0.001$) in A549, 21.2% ($p<0.001$) in HT29 and 12.4% ($p<0.001$) in A498 cell lines, when compared to respective Controls (figure 6.17).

xCT

ATF4 downregulation had a major effect reducing xCT mRNA expression as also observed for the specific glycine transporter, GLYT1. Decreases of 66.7% ($p<0.0001$), 74% ($p<0.0001$) and 56.8% ($p<0.001$) in xCT mRNA levels was observed following ATF4kd in A549, HT29 and A498 cell lines, respectively, when compared to Control (figure 6.18).

GCL

ATF4kd downregulated mRNA expression of GCL subunits GCLC and GCLM in all cell lines analysed. GCLC mRNA expression was reduced by 46.4% ($p<0.0001$), 29.3% ($p<0.001$) in HT29 and 60% ($p<0.0001$) in A498 cell line following ATF4kd when compared to respective Control cells (figure 6.19a). Moreover, GCLM mRNA abundance was reduced 47.6% ($p<0.0001$) in A549 cells, 33.5% ($p<0.01$) in HT29 cells and 37.3% ($p<0.001$) in A498 cells following ATFkd, when compared to Control cells (figure 6.19b).

GSS

Following ATFkd, GSS mRNA expression was downregulated in A549 and A498 cells (figure 6.20). ATF4kd reduced by 27% ($p<0.01$) GSS mRNA levels in the A549 cell line when compared to Control. For ATF4kd in A498 cells, there was a reduction of 23.6% ($p<0.5$) in GSS mRNA abundance, when compared to Control. Although ATF4 downregulation showed a tendency in reducing GSS mRNA expression in HT29 cells, no significant difference was observed in comparison to Control.

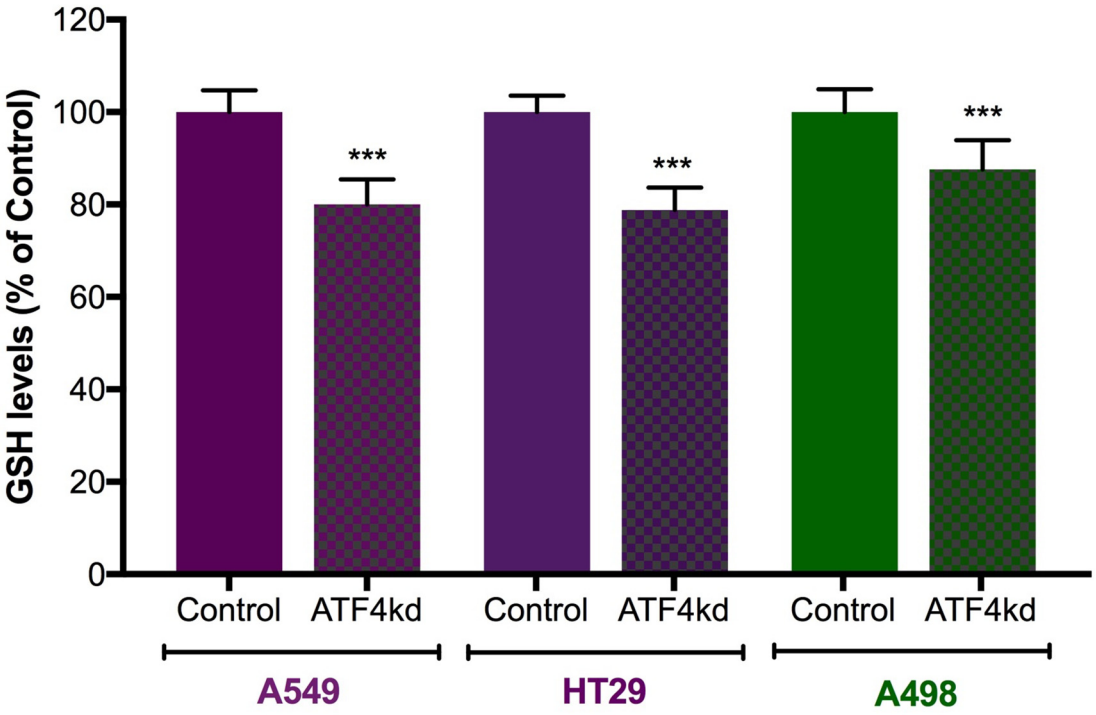

Figure 6.17: ATF4 knockdown reduced GSH levels in A549, HT29 and A498 cell lines. GSH-Glo assay analysis 72 hours post transfection with Negative siRNA (Control) or ATF4 siRNA (ATF4kd) in 96-well plates. GSH levels are presented as percentage of control according to luminescence measurement. Data are presented as mean ± SEM, N=2 and n=6 per group. Statistical analysis comparing ATF4kd and Control of each cell line were performed by unpaired t-test considering $p<0.001$ (***).

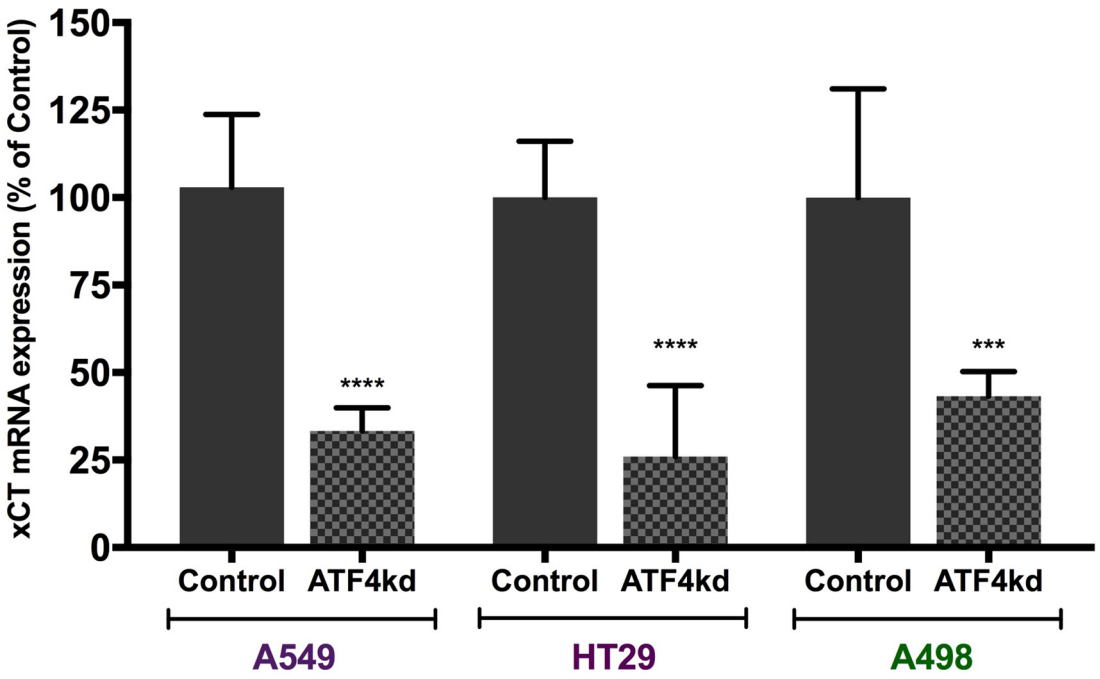

Figure 6.18: ATF4 knockdown downregulated xCT mRNA expression in A549, HT29 and A498 cell lines. Real time qPCR analysis of the influence of ATF4kd on the cystine transporter subunit xCT mRNA expression as percentage of Control. Data are presented as mean ± SEM, N=3 and n=9 per group. Statistical analysis comparing the treatment (ATF4kd) and control (Negative siRNA), of each cell line were performed by unpaired t-test considering $p<0.001$ (***) and $p<0.0001$ (****).

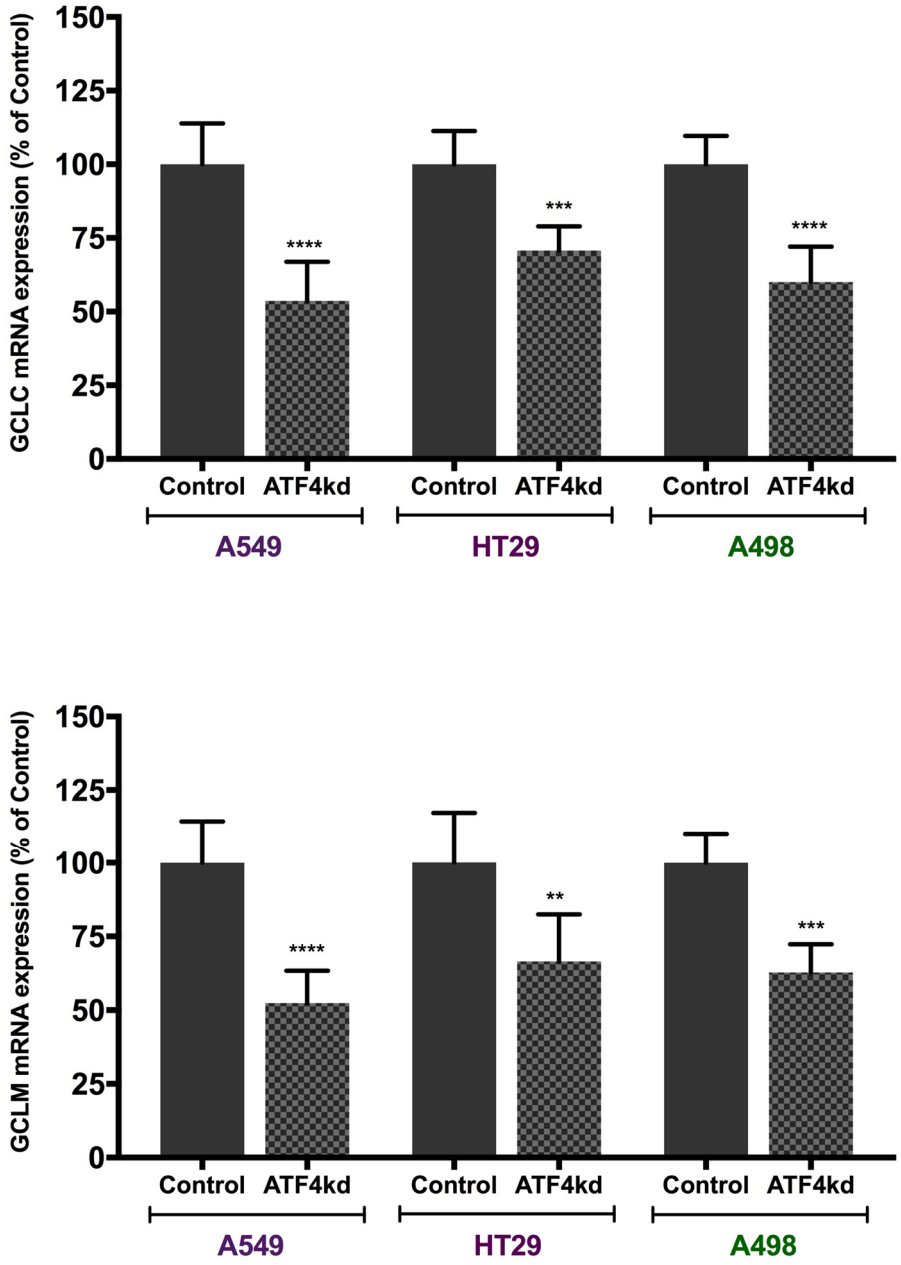

Figure 6.19: ATF4 knockdown downregulated mRNA expression of both subunits of GCL enzyme, GCLC and GCLM, in A549, HT29 and A498 cell lines. Real time qPCR analysis of the influence of ATF4 kd on GCL catalytic subunit, GCLC, and modifier subunit, GCLM, mRNA expression as percentage of control (Negative siRNA). Data are presented as mean ± SEM, N=3 and n=9 per group. Statistical analysis comparing the treatment (ATF4kd) and control of each cell line were performed by unpaired t-test considering $p<0.01$ (**), $p<0.001$(***) and $p<0.001$ (****).

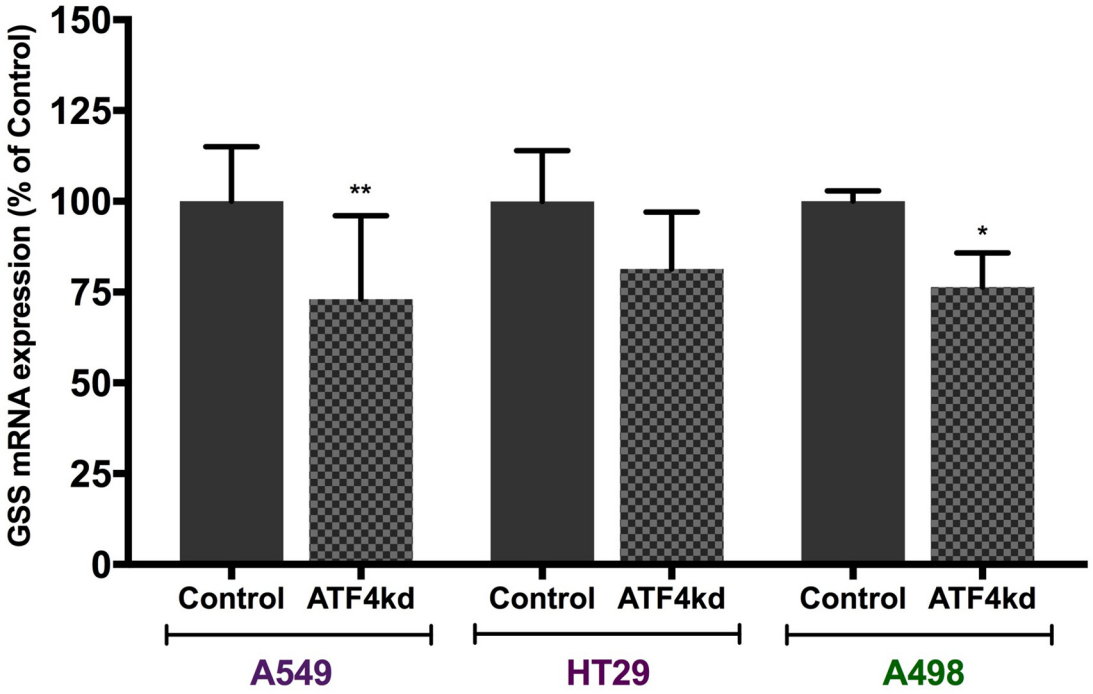

Figure 6.20: ATF4 knockdown downregulated GSS mRNA expression in A549 and A498 cells, but had no effect in the HT29 cell line. Real time qPCR analysis of the influence of ATF4kd on GSS mRNA expression as percentage of Control (Negative siRNA). Data are presented as mean ± SEM, N=3 and n=9 per group. Statistical analysis comparing the treatment (ATF4kd) and control of each cell line were performed by unpaired t-test considering $p<0.05$ (*) and $p<0.01$ (**).

6.3 Summary of results and discussion

Cell transfection with ATF4 siRNA was effective in reducing ATF4 mRNA expression. When cells were treated with thapsigargin, a sarcoplasmic/ER Ca^{2+} ATPase inhibitor and known ER stress inducer, to increase ATF4 protein levels and facilitate detection in Western blotting assay, it was possible to observe a reduction in protein abundance in ATF4kd cells when compared to Control cells. Therefore, a reduction in both mRNA and protein levels confirmed the knockdown of ATF4 following transfection treatment and was utilised in further experiments to evaluate ATF4 influence on cell proliferation, expression of other genes and glycine uptake.

ATF4 knockdown reduced cell proliferation in all tumour cell lines analysed, A549, HT29 and A498 cells, whereas it increased proliferation of normal endothelial cell line, HUVEC. Additionally, following ATF4 downregulation, the proliferation marker ki67 mRNA expression was reduced in all tumour cells, but not in the normal cell line HUVEC. As discussed previously, ATF4 activates transcription of genes involved in pro-survival and pro-apoptosis mechanisms depending on the cell type and environmental conditions (Wortel et al., 2017). ATF4 has been linked to upregulation of genes involved in autophagy, an important mechanism to provide nutrients and maintain cell survival in some cancers (Wortel et al., 2017). Tumour cells, due to the high cell proliferation and high protein expression rates, are able to maintain a balance between anabolism and catabolism and therefore ATF4 generally supports pro-survival mechanisms in these cells (Wortel et al., 2017), whereas normal cell lines, such as HUVEC, might be unable to restore the essential material lost during autophagy and then ATF4 induces transcription of genes whose encoded proteins are involved in apoptosis. An alternative hypothesis is that tumour cells are more resistant to apoptosis than normal cell lines due to mutations in apoptotic genes. This way, ATF4 apparently supports tumour cell proliferation of NSCLC, colon and renal cancer cells, A549, HT29 and A498, respectively, whereas it may induce cell death of the normal umbilical vein/cord endothelial cell line HUVEC.

ATF4 knockdown drastically reduced GLYT1 expression in all cell lines. This result agrees with previous work from our group that showed that, in Caco2 cells, GLYT1 expression is dependent on ATF4 and with studies by Harding and collaborators study (Harding et al., 2003)(Howard et al.). ATF4 knockdown slightly reduced PAT1 mRNA expression in HT29 cells, whereas it had no influence on PAT1 mRNA level in the other cell lines. A minor downregulation of PAT1 possibly is a

consequence of the impact of ATF4 on other amino acid transporters and non-essential amino acid synthesis. Therefore, a possible reduction of amino acid availability in HT29 cells, might have an impact on PAT1 mRNA expression since this transporter is also involved in the amino acid sensing system, working as a sensor and interacting with mTORC1 (Zheng et al., 2016, Goberdhan, 2010). Interestingly, ATF4 knockdown reduced $ATB^{0,+}$ mRNA abundance in HT29 cell when compared to the control. As described previously, $ATB^{0,+}$ is not expressed in the majority of normal cells presenting low levels of expression only in some cells, for example in colon tissue, however in some tumours, such as breast and especially colorectal cancers, it is highly expressed (Sikder et al., 2017). A possible regulation of $ATB^{0,+}$ mRNA expression by ATF4 is so far unrecognised and requires further investigation.

ATF4 knockdown presented no significant impact on SNAT2 mRNA expression of highly proliferative cells, although a tendency in downregulation was observed, whereas it significantly reduced SNAT2 mRNA abundance in the A498 cell line. SNAT2 expression in normal conditions is low, however under amino acid starvation its expression is highly increased, possibly mediated by the GCN2-eIFα-ATF4 pathway (Bröer and Bröer, 2017, Gaccioli et al., 2006). Amino acid transport via SNAT2 is increased during mild hyperosmotic stress by GADD34 that consequently reduces eIF2α phosphorylation (Krokowski et al., 2015). The study observed that GADD34 is upregulated independently of the eIF2α-P/ATF4 pathway and that high levels of eIF2α-P inhibit SNAT2 in a posttranslational manner (Krokowski et al., 2015). Moreover, SNAT2 transcription was not affected by UPR even with ATF4 and CHOP interacting with the CARE site, only the amino acid response pathway was able to increase its activity (Gjymishka et al., 2008, Wortel et al., 2017). Interestingly, when both UPR and AAR pathways are activated, the UPR inhibits SNAT2 transcription, suggesting its upregulation by AAR only (Gjymishka et al., 2008, Wortel et al., 2017, Krokowski et al., 2015). This way, although SNAT2 gene includes a CARE site, its transcriptional regulation dependent on ATF4 is only observed in specific conditions such as amino acid deprivation and further activation of the AAR pathway. The experiments in this study were performed in minimal medium RPMI, but not in amino acid deprivation, thus possibly the AAR pathway is not activated and ATF4 presents no influence on SNAT2 mRNA expression.

Following ATF4 knockdown, glycine uptake was reduced in the A549 and A498 cell lines, but not in the HT29 cell line. Although ATF4 knockdown reduced GLYT1 mRNA abundance, the reduction of total glycine uptake was smaller than for GLYT1

knockdown. Possibly the period of incubation was not sufficient to translate mRNA abundance to GLYT1 protein levels, however this couldn't be assessed due a lack of antibody which works in protein blotting protocols. Additionally ATF4 knockdown had only a small influence on transcription of other amino acid transporters able to transport glycine. However, ATF4 downregulation reduced SHMT2 mRNA abundance possibly decreasing intracellular glycine synthesis. Downregulation of SHMT2 also affects the generation of one-carbon units and consequently meTHF formation, which is used in purine synthesis, one carbon units from serine can also be utilised in the methionine cycle affecting methylation in epigenetic regulation, and the transsulphuration pathway influencing cysteine and GSH synthesis (Locasale, 2013).

As described previously, some studies have demonstrated that ATF4 also activates the transcription of other transcription factors including ATF3, ATF5 and ATF6. In agreement with the literature, ATF4 knockdown reduced ATF3 and ATF5 transcription in the rapidly proliferating cells A549 and HT29, but not in the slowly proliferating cell line A498. ATF4 binds to CARE and ATF/CRE sites upstream of the ATF3 gene and up-regulates ATF3 transcription (Fu and Kilberg, 2013). ATF5 transcription is activated by eIFα and ATF4 also contributes to its basal expression (Zhou et al., 2008). Several studies have demonstrated that both transcription factors, ATF3 and ATF5, are involved in some tumour cell growth and survival under stress conditions, as described in Chapter 1. This way downregulating expression of these genes possibly contributes to the reduced proliferative profile following ATF4 knockdown. The A498 cell line possibly is under less stress due its reduced proliferation rate leading to the reduced cell number at the end of the experiment, when compared to the rapidly proliferating cells. Therefore, A498 cells possibly have more nutrients available and possibly lower protein expression, so presenting a reduced activation of the stress response pathways, which in turn activates the ATFs. ATF6 mRNA expression was downregulated following ATF4 knockdown. This result is in agreement with previous work that observed that in liver cells the PERK/eIFa/ATF4 pathway enhances ATF6 mRNA expression and activation under stress (Teske et al., 2011). Teske and collaborators also showed that ATF4 increases expression of proteins involved in protein trafficking from ER to Golgi, therefore affecting ATF6 translocation and further activation (Teske et al., 2011). This way, a reduction of ATF6 abundance following ATF4 knockdown may influence NSCLC, colon and renal cancer cell survival, and contribute to the reduction in proliferation observed in previous experiments.

GSH content of cells was then evaluated following ATF4 knockdown. ATF4 down-regulation reduced GSH content of all cell lines analysed. This result is in agreement with other studies that have shown a possible regulation of GSH levels by ATF4 (Sikalidis et al., 2014). Additionally, it has been observed that ATF4 promotes transcriptional up-regulation of GSH synthesising enzymes and xCT, a subunit of the Xc^- transporter involved in cystine uptake, in human tumours (Sato et al., 2004, Ye et al., 2014, Gorrini et al., 2013). As expected, ATF4 knockdown downregulated xCT mRNA expression and expression of both GCL subunits in all cell lines analysed. These results agree with previous work that observed that xCT expression is dependent on ATF4 and that ATF4 plays an important role regulating the GSH synthesizing enzymes (Sato et al., 2004, Ye et al., 2014). Moreover a study showed that mRNA levels of GCL subunits are increased under starvation of some amino acids, such as cysteine, and that this upregulation is activated by GCN2/ATF4 pathway (Sikalidis et al., 2014). Interestingly, GCLC and GCLM genes do not contain upstream CARE or AARE sites indicating that ATF4 might activate expression of genes coding for proteins, downstream transcription factors, involved in the GCL subunits regulation (Sikalidis et al., 2014). ATF4 regulates proteins responsible for GCLC mRNA expression activation and proteins involved in stabilisation of GCLM mRNA, avoiding its degradation, consequently only GCLM protein levels are increased by ATF4 activity, but not GCLC protein abundance (Sikalidis et al., 2014). Thus, ATF4 influences GSH synthesis by regulating expression of amino acid transporters involved in glycine and cystine uptake and also affecting GCL subunit expression.

Chapter 7. Final Discussion

Glycine is a small, versatile, conditionally essential amino acid (Wang et al., 2013a). It is produced in the last step of the serine biosynthesis pathway, in a reaction catalysed by the enzyme SHMT (Wang et al., 2013a). The mitochondrial SHMT (SHMT2) is thought to be ubiquitous and responsible for glycine production in most cell types and the less active cytosolic enzyme (SHMT1) is present in liver and kidneys (Wang et al., 2013a). Glycine is also produced in the last step of choline oxidative degradation, which generates methyl groups, where sarcosine is converted to glycine by the enzyme sarcosine oxidase and in the threonine dehydrogenase pathway, a two-step reaction that generates glycine (Wang et al., 2013a). Moreover, some studies have suggested that glycine can be obtained by transamination of glyoxylate, itself generated from 4-hydroxyproline in a reaction dependent on alanine (Wang et al., 2013a). Glycine is degraded through the glycine cleavage system (GCS), which is highly active in liver (Baggott et al., 2007, Kikuchi et al., 2008). Additionally, excess glycine can be conjugated with benzoic acid in the mitochondria, generating hippuric acid that is excreted in urine in the glycine deportation system and contributes to glycine homeostasis in concert with GCS (Wang et al., 2013a, Beyoğlu and Idle, 2012).

Glycine and its metabolism present important functions for humans and animals. In adult humans, glycine abundance in proteins is generally 11% and its plasma concentration in adult is about 250 μM (Wang et al., 2013a, Beyoğlu and Idle, 2012). In young mammals, about 80% of total glycine is utilised in protein synthesis, being required for growth and necessary for metabolic functions (Wang et al., 2013a, Razak et al., 2017). Glycine is necessary for purine synthesis contributing to DNA replication in proliferating cells (Nelson and Cox, 2005). Glycine is also required for glutathione (GSH) formation, the major cellular antioxidant, and is also utilised in porphyrin synthesis (Wang et al., 2013a, Razak et al., 2017). Glycine modulates intracellular Ca^{2+} levels in leukocytes and macrophages influencing the synthesis of cytokines (Wang et al., 2013a, Razak et al., 2017). It is also conjugated with bile acids in the liver, enhancing their solubility, that are ultimately secreted in the intestine, following a fat diet (Wang et al., 2013a, Di Ciaula et al., 2017). Extracellular glycine presented cytoprotective activity in liver, kidney, lung, intestine and skeletal muscle following ischemia-reperfusion injuries experiments and reduced apoptosis in

endothelial cells (Wang et al., 2013a). Glycine supplied through the specific glycine transporter GLYT1 was observed to protect human intestinal cells in vitro from oxidative stress maintaining intracellular levels of GSH (Howard et al., 2010). Some fast growing tumour cells also require extracellular glycine to support a high demand for purine and GSH synthesis and maintain their proliferative rates (Jain et al., 2012).

Additionally, glycine participates in the one-carbon metabolism, as discussed in the introduction chapter. Conversion of serine into glycine by SHMT and glycine decarboxylation via GCS generates one-carbon units that are associated to THF in the folate cycle (Locasale, 2013). One carbon units can then be utilised in serine, cysteine, purine, GSH and are involved in methylation of histones, DNA and RNA (Locasale, 2013). When cells are not proliferating, one carbon metabolism contributes to anabolic reactions mainly in liver and kidney assisting in creatinine and choline synthesis (Ducker and Rabinowitz, 2017). In other tissues one-carbon metabolism is involved in nucleotide and amino acid homeostasis and also in ATP and NADPH production (Ducker and Rabinowitz, 2017).

In vivo studies observed that high glycine levels reduced tumour growth of melanoma and colon cancer in mouse models and of a mammary cancer cell model (Rose et al., 1999, Bruns et al., 2016, Amin et al., 2003). Glycine significantly reduced angiogenesis and tumour vascularisation of these tumours (Rose et al., 1999, Bruns et al., 2016). In endothelial cells, when the extracellular levels of glycine are elevated, glycine binds to GlyR increasing its activity, which in turn inhibits cell proliferation induced by VEGF (Bruns et al., 2016, Bruns et al., 2014). However, under normal levels of glycine in the medium, VEGF induced GLYT1 activation leading to an enhanced glycine uptake into endothelial cells which in turn participates in a signalling pathway that increased mitochondria function and promoted angiogenesis (Guo et al., 2017).

Recent studies have observed that glycine levels and glycine metabolism are altered in rapidly proliferative tumours. An *in vitro* study demonstrated that fast growing cancer cell lines are dependent on extracellular glycine to maintain their rapidly proliferative profile (Jain et al., 2012). Wang and collaborators also observed that incubation of an osteosarcoma cell line MG63 with glycine increased cell proliferation by about 50% when compared to control cells (Wang et al., 2017). Moreover, clinical studies have shown a correlation of high glycine concentration in tumour tissue with poor patient prognosis (Cao et al., 2012, Redalen et al., 2016). It has also been observed that glycine levels are reduced in plasma and increased in lung tumour tissue

when compared to normal individuals (Zhao et al., 2014). A further link between glycine and cancer is that GLYT1 expression is regulated by ATF4 (Harding et al., 2003), which is linked to cancer progression and proliferation (Igarashi et al., 2007).

Thus, the requirement for extracellular glycine may be increased during stress to protect cells from damage or to support rapid cell proliferation where the rate of synthesis may be insufficient to meet cellular demand. Glycine can be transported into cells via GLYT1, as described before, and also by other amino acid transporters able to transport glycine such as PAT1, SNAT2 and $ATB^{0,+}$, however these transporters have a much lower affinity for glycine than GLYT1 (Schiöth et al., 2013, Sloan and Mager, 1999). Therefore, the influence of GLYT1, a specific glycine transporter, in supporting the uptake of glycine and thus proliferation of rapid and slow proliferating tumour cell lines has been investigated in the novel work presented in this thesis.

GLYT1 influence on tumour cell proliferation

Data from this study confirmed the preliminary hypothesis - that GLYT1 supports cellular demand for intracellular glycine, so contributing to maintenance of proliferation rates of fast growing tumour cell lines. GLYT1 downregulation, utilising a specific siRNA for GLYT1, was accompanied by a reduction of about 30-50% on total glycine uptake in the NSCLC (A549), colon (HT29) and renal (A498) cancer cell lines studied. In the rapidly proliferating cell lines, A549 and HT29, the reduction in glycine mRNA expression and glycine uptake was concomitant with a reduction in cell proliferation rate of about 30%, whereas a similar reduction in glycine uptake following GLYT1 knockdown in A498 cells resulted in only a 9% reduction in cell proliferation. Additionally, the growth of a rapid proliferative non-transformed cell line, HUVEC, remained unchanged following GLYT1 knockdown. When analysing the proliferation marker ki67 expression, the same pattern was observed, being downregulated in the rapid proliferative cell lines and presenting no change in the slow growing renal cancer cell line following GLYT1 mRNA depletion. Putting together these results indicates that rapidly proliferating tumour cells are dependent on glycine uptake to maintain their proliferative profile, in agreement with the previous work of Jain and collaborators (Jain et al., 2012), and that GLYT1 is essential for glycine transport into these cells.

However, some studies have proposed that rapidly proliferating tumours are dependent on serine levels, rather than glycine, to support their proliferation and survival and that glycine starvation only affected proliferation under serine depletion

(Maddocks et al., 2013, Labuschagne et al., 2014). Labuschagne and collaborators showed that in the first 16 hours of incubation in DMEM medium HCT116, RKO, SW480, A549 and MCF7 cell lines release glycine and avidly consumed serine (Labuschagne et al., 2014). They also observed that during 5 days of incubation, glycine starvation did not affect cell proliferation and that glycine wasn't able to rescue proliferation during serine starvation (Labuschagne et al., 2014). Moreover, it was observed that with serine starvation, an increase in glycine concentration, about ten times plasma levels, reduced purine synthesis and cell proliferation (Labuschagne et al., 2014). Studies suggest that under serine starvation excess of glycine is utilised in serine synthesis by SHMT, therefore depleting meTHF levels, which in turn reduces purine synthesis (Labuschagne et al., 2014, Fan et al., 2014). These studies all utilised DMEM medium compared with RPMI utilised in this work and in Jain et al experiments. It might be possible that a higher concentration of other amino acids, such as serine and threonine, about 3-4 times higher in DMEM medium, make rapidly proliferating tumours less reliant on extracellular glycine to maintain cell proliferation, as these amino acids may be converted into glycine. However, with limited nutrient and oxygen levels, as occurs in in many tumours due to low vascularisation, cells might become dependent on glycine uptake for purine and GSH synthesis to maintain cell proliferation and overcome stress.

An *in vivo* study utilising mouse models of intestinal cancer (defective Apc) and lymphoma (Myc activation) showed that a serine/glycine (SG) starvation diet resulted in a reduction in tumour growth and increased survival when compared to mice fed a normal diet (Maddocks et al., 2017). However, SG starvation did not improve survival in a model of pancreatic cancer (activated Kras) (Maddocks et al., 2017). Activated Kras increases transcription of serine synthesis pathway (SSP) enzymes, which were upregulated with a SG-free diet, making this cancer type less dependent on extracellular SG levels (Maddocks et al., 2017). Following SG starvation serine levels were decreased in tumour tissues of lymphoma and pancreatic cancer model mice, whereas the levels of glycine were decreased only in the lymphoma models, intestinal cancer mice were not evaluated (Maddocks et al., 2017). Consistently, after SG starvation the levels of GSH were decreased in lymphoma, but remained unchanged in the pancreatic cancer tissues when compared to the control group (Maddocks et al., 2017). Therefore, the results from Maddocks and collaborators study supports the idea that when cells are unable to upregulate SSP enzymes in association with reduced glycine uptake, a consequent decrease of GSH levels may be detrimental to tumour

cell survival and proliferation. Moreover, a recent study observed that pancreatic tumour cells are able to obtain nutrients from catabolism of extracellular proteins, such as albumin, through macropinocytosis. In pancreatic, but not liver, tumour tissue, there was an increase of glycine levels, but not in serine levels, supplied by albumin macropinocytosis, which was higher than in normal pancreatic tissue (Davidson et al., 2017). Even though protein scavenging by macropinocytosis remained unchanged when pancreatic cells were under SG starvation in comparison to normal diet (Maddocks et al., 2017), the supply of extracellular glycine by this process might contribute to the survival rates in the pancreatic tumour mice.

GLYT1 is reversible, being able to release glycine to the extracellular environment when physiological changes to the electrochemical gradient occur, such as modification to the membrane potential and to Na^+ levels (Roux and Supplisson, 2000, Betz et al., 2006). Some studies suggest that excess of glycine is released from tumour cells and that inhibition of GCS with increase in SHMT2 expression lead to accumulation of glycine that is metabolised to toxic products, such as amino acetone and methyl-glyoxal, halting tumour growth (Labuschagne et al., 2014, Kim et al., 2015). Hence, an alternative hypothesis is that GLYT1 knockdown could lead to toxic accumulation of glycine in cells reducing tumour growth or causing cells to die. Since no signs of toxic effects were observed following 72 hours transfection with GLYT1 siRNA, as cells increased in number over time but with a reduction in DNA replication, as will be discussed further, apoptosis assays or live/dead assays were not performed. However, further investigations on a possible toxic intracellular accumulation of glycine following GLYT1 downregulation might be useful. Labuschagne et al. showed that under serine limitation, increased glycine levels reduce cancer cell proliferation, due to an attempt to restore serine levels from glycine in the reaction catalysed by SHMT2 and consequently reducing meTHF levels, halting purine synthesis and leading to an increased glycinamide ribonucleotide (GAR) concentration (Labuschagne et al., 2014). So, if an accumulation of glycine occurs in association with serine depletion the deviation of meTHF for serine synthesis could also explain the phenotype observed in this study, with a reduction in DNA replication that would affect fast growing tumour cells. However, as GLYT1 knockdown reduced glycine uptake, suggesting that in these experimental conditions this transporter is involved in glycine uptake and not export, investigations on glycine release were not performed.

GLYT1 influence on DNA replication and glutathione synthesis

Extracellular glycine supports *de novo* purine synthesis, being incorporated directly and via one-carbon units, as described in Chapter 1. Thus, a reduction in DNA replication could be a possible explanation for the decrease in cell proliferation following GLYT1 downregulation. In the second step of purine synthesis, C_2N of glycine is condensed to 5-phosphoribosylamine forming GAR, this reaction is catalysed by GAR synthetase (Nelson and Cox, 2005). In the third step of purine synthesis, the glycine amino group is formylated by N^{10}-Formyl-THF (Nelson and Cox, 2005). Glycine also contributes with one-carbon units to form methylene-THF, in some cell types with active mitochondrial GCS, which is further converted to 10-formyl-THF by mthfd2 enzyme (Figure 7.1) (Baggott et al., 2007). Therefore, glycine can contribute in two steps of purine synthesis. Hence, and as expected from the data on cell proliferation, GLYT1 knockdown and subsequent reduction in glycine uptake presented a greater impact on reducing DNA replication, possibly due to a reduction in purine synthesis, of A549 and HT29 cell lines, when compared to the small effect seen in the slow growing A498 cells, that presents a reduced rate of DNA replication being less dependent on high levels of purine synthesis. These data suggest that the decrease in glycine uptake led to a reduction in purine synthesis having a major effect on cells with rapid proliferative profiles. However, further analyses investigating radiolabelled glycine incorporation into purine ring by mass spectrometry, for example, are required to confirm if the reduced glycine uptake in GLYT1kd cells led to a reduction in purine levels, which therefore contribute to reduced DNA replication.

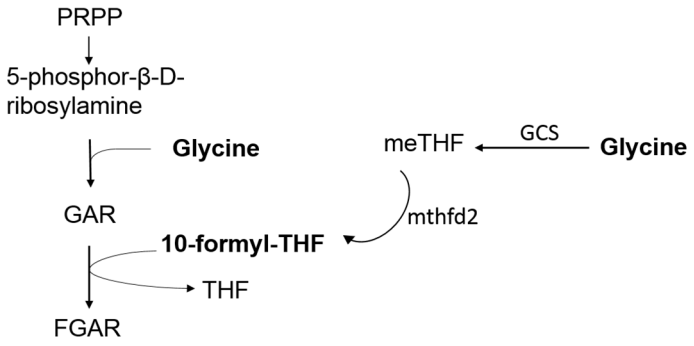

Figure 7.1: Glycine contribution to *de novo* purine synthesis. On the left side, schematic representation of the first three steps of de novo purine synthesis highlighting glycine contribution, being incorporated directly and via one-carbon units through formyl-THF. On the right side, glycine cleavage system representing the flow of glycine one-carbon units incorporated into THF, forming meTHF and subsequently formyl-THF by the enzyme mthfd2.

As discussed in Chapter 1, extracellular glycine can also be incorporated into GSH (figure 7.2). In the last step of GSH synthesis glycine is joined to γ–glutamylcysteine, a reaction catalysed by the enzyme GSS (Lu, 2013). GLYT1 knockdown decreased GSH abundance in all tumour cell lines analysed in this study. This result is in agreement with previous work from Howard and collaborators, as described earlier, indicating that extracellular glycine supplied through GLYT1 is essential to maintain adequate intracellular levels of GSH. Additionally extracellular glycine was observed to be involved in serine synthesis, which is then utilised in transsulphuration pathways increasing cysteine levels in a breast cancer animal model (Thelwall et al., 2012). Therefore a possible reduction in intracellular cysteine synthesis following GLYT1 knockdown could also contribute to the reduction in GSH levels observed in this study. However, further investigations evaluating incorporation of radiolabelled glycine into ɣ-glutamylcyteine is necessary to test this speculation.

It is known that GSH supports cell proliferation being crucial for cell cycle progression. One of the mechanisms is that GSH maintains reduced glutaredoxin a source of reducing equivalents for ribonucleotide reductase, a rate-limiting enzyme in DNA synthesis, responsible for reduction of ribonucleotides to deoxyribonucleotides (Nelson and Cox, 2005, Traverso et al., 2013, Lu, 2013). In melanoma cells, GSH abundance contributes to cell proliferation and metastasis (Traverso et al., 2013). In this thesis, analysis of GLYT1 knockdown on GSH synthesising enzymes showed an upregulation of GCLM, the modulatory subunit of GCL, and GSS mRNA expression in the fast growing tumour cell lines, but not in the slow growing cell line. It is suggested that an increase in GCLM augments k_{cat} of GCL and facilitates GSH synthesis (Lee et al., 2006). Therefore, the increase in these GSH synthesising enzymes mRNA levels might lead, in the rapidly proliferative cells, to maintenance of GSH levels, essential to support high rates of proliferation. In the A498 cell line, GSS downregulation following GLYT1 knockdown may occur as a negative feedback due a reduction in the enzyme substrate, glycine.

GLYT1 downregulation resulted in a significant reduction in mRNA abundance of the catalytic subunit of the X_c^- cystine transporter, xCT. The potential mechanisms by which GLYT1 influences xCT expression remain to be elucidated. No data in the literature was identified informing of possible influences between GLYT1 and xCT transporters, suggesting that this is a new finding and requires further investigation. It is known that X_c^- activity is induced by electrophilic agents, oxygen and by cysteine

starvation, which also induce xCT expression (Lewerenz et al., 2013). Possibly, the reduction in GSH synthesis, due the limited glycine availability in GLYT1kd, led to an accumulation of intracellular cysteine and therefore a reduction in xCT expression in comparison to control cells (Lewerenz et al., 2013, Sato et al., 2004). However, experiments measuring intracellular levels of cysteine in control and GLYT1kd utilising LC-MS are required to test this assumption. Additionally, although the GLYT1 siRNA (si2991 or si2993) utilised in these experiments is thought to be specific for GLYT1 mRNA, it might have some nonspecific effect on xCT transcription as well. It is also known that X_c^- transporter supports replication, invasion and metastasis of some tumours (Lewerenz et al., 2013, Gout et al., 2001, Huang et al., 2005). Therefore, xCT downregulation could contribute to the reduction in cell proliferation of fast growing tumour cells following GLYT1 knockdown.

Figure 7.2: GSH synthesis pathway. Schematic figure of GSH synthesis pathway and contribution of X_c^- and GLYT1 transporters in providing precursors, cysteine and glycine, respectively, to GSH synthesis.

GLYT1 influence on other amino acid transporters able to transport glycine

GLYT1 knockdown also affected other amino acid transporters able to transport glycine: PAT1, SNAT2 and $ATB^{0,+}$. Interestingly, GLYT1 knockdown lead to a decrease in PAT1 and SNAT2 abundance in all tumour cell lines analysed, instead of an upregulation, especially in SNAT2, to maintain glycine uptake as a compensatory mechanism. These transporters have been related to cancer cell proliferation or survival, as descried in chapter 1, consequently their downregulation may also be affecting tumour cell proliferation. However, the mechanism that these amino acid transporters may influence each other remains to be elucidated. It may be possible that a decrease in glycine levels affect other amino acid transporters through signalling

pathway (discussed in details below) or, as describe previously for xCT, it is possible that GLYT1 siRNA might have some off-target effect on PAT1 and SNAT2 transcription as well.

PAT1 is localised in late endosomes and lysosomes (LELs) and in plasma membrane of multiple tissues as described in chapter 1. It was observed that PAT1 glycosylation is involved in its cell membrane localisation and that under nutrient starvation it is translocated to the lysosome (Wu et al., 2016, Luo et al., 2017). PAT1 in the lysosome exports amino acids out of the lumen (Zoncu et al., 2011a). PAT1kd in tumour cell lines reduced cell growth mediated by mTORC1 (Zheng et al., 2016). It was proposed that PAT1 senses amino acid levels in the lumen of LEL and form a complex with Rag/Ragulator/v-ATPase leading to activation of mTORC1 and cell growth (Zheng et al., 2016). However, an upregulation of PAT1 prevented accumulation of amino acid in the lysosome and impaired activation of mTORC1 (Zoncu et al., 2011a). SNAT2 is present in plasma membrane and its distribution is ubiquitous in the organism, but its mRNA expression is low under normal conditions, whereas under amino acid amino acid starvation SNAT2 mRNA expression is upregulated by ATF4 (Zheng et al., 2016). There is evidence that SNAT2 also functions as a sensor in the amino acid sensing system activating mTORC1 (Zheng et al., 2016).

As discussed in details in Chapter 1, glycine has been linked to mTOR activation. Glycine transport via GLYT1 is activated by VEGF in endothelial cells and is involved in angiogenesis signalling through GLYT1-glycine-mTOR signalling pathway (Guo et al., 2017). Glycine supplementation in myoblasts activated mTORC1 via Akt, increasing protein synthesis (Sun et al., 2016). Glycine sensitises mTORC1 for further activation, mainly promoted by leucine (Dyachok et al., 2016). Thus, glycine seems to induce mTORC1 activity and might influence the amino acid sensing system. Since PAT1 and SNAT2 are also involved in mTORC1 activation, depletion in intracellular levels of glycine may indirectly downregulate them, leading to suppression of mTORC1 signalling and reduced cell growth under glycine deficiency. Further investigation of PAT1 and SNAT2 mRNA expression with cells grow under glycine-free medium could elucidate if the influence relies on amino acid levels. Also, investigations of GLYT1 influence on mTORC1 activity in tumour cell lines might be relevant.

Only in HT29 cells was $ATB^{0,+}$ expression upregulated following GLYT1 knockdown. $ATB^{0,+}$ transports a wide range of amino acids, 18 of the 20 common amino acids, leading to the ability to concentrate them inside cells (McCracken and Edinger, 2015). This transporter is expressed at low levels in normal tissues being

detected only in lung and ileum/colon; but is upregulated in colorectal, pancreatic, stomach, cervical and estrogen receptor-positive breast cancers, whereas is downregulated lung cancer (Sikder et al., 2017). In patients with pancreatic and colorectal cancer, overexpression of $ATB^{0,+}$ was related to poor patient prognostic (Sikder et al., 2017). Thus, an upregulation of $ATB^{0,+}$ may be the result of an attempt to increase glycine uptake and meet cellular demands for glycine in the colorectal cell line, although no significant difference on effect in cell proliferation from A549 cell line was observed; this may reflect the tissue source, A549 being derived from the lung. Furthermore, GLYT1 mRNA depletion leads to an increased SHMT2 mRNA expression in the rapidly proliferating cell lines, A549 and HT29, but not in the slow growing tumour cell, A498. The rapidly proliferative tumour cells upregulated SHMT2 possibly as effort response to increase intracellular production of glycine, therefore supporting the idea that glycine levels are necessary to maintain their proliferation rate. However, considering the reduction in cell proliferation of the fast growing tumour cells following GLYT1kd, this increase in SHMT2 probably was insufficient to meet cellular demands, as also observed by Jain and collaborators (Jain et al., 2012).

GLYT1 pharmacological approach

The GLYT1 specific inhibitor ALX-5407 was tested to evaluate its effects on proliferation of the different cell lines. GLYT1 inhibition reduced proliferation of the A549 and HT29 cell lines, increasing their doubling times but had no effect on A498 and HUVEC cell proliferation. The effect of ALX-5407 in reducing glycine uptake was similar or even better than GLYT1 knockdown experiments, however, its influence in reducing cell proliferation was slightly smaller and required a longer period of time. Possibly GLYT1 inhibition did not induce the downregulation of other amino acid transporter transcription brought about by GLYT1 knockdown that, as discussed above, could also have contributed to reduced cell proliferation. This way, a possible nonspecific effect of GLYT1 siRNA on PAT1 and SNAT2 mRNA expression should be considered. Analysis on these transporters expression following ALX-5407 treatment is also required and were not performed in this study. Additionally, during longer periods of incubation cell numbers increase which may lead to nutrient limitation and/or accumulation of toxic products, suggesting that glycine provided by GLYT1 may be required under stress conditions to support rapidly proliferative profiles. Since GLYT1 is regulated by ATF4, which is activated under stress conditions, the proliferation of

tumour cells growing under hypoxia and ER stress in the presence of ALX-5407 was evaluated. Data from chapter 5 show that treatment with GLYT1 inhibitor increased the deleterious effect of ER stress and hypoxia in the colorectal cancer cell line and NSCLC cell line, respectively. Thus, extracellular glycine provided by GLYT1 seems to become crucial in maintaining rapid proliferating rates of tumour cells mainly under stress conditions, such as amino acid starvation, hypoxia and ER stress. Since these stress conditions are all observed in tumour tissues (Koumenis, 2006), suggest that the current glycine inhibitors, already being used in clinical trials for other conditions, might also be effective in treating some types of fast proliferating, aggressive tumours, or to assist in the current treatment of chemotherapy resistant tumours involving glutathione.

Glycine acts as a neurotransmitter in the CNS and GLYT1 is responsible for its reuptake from the synaptic cleft, therefore modulating its effects (Harvey and Yee, 2013). Many *in vivo* studies have suggested that GLYT1 inhibitors, and consequent increase of glycine action in the CNS, have positive effects in schizophrenia treatment and some of these drugs are currently in clinical phase II trials (Harvey and Yee, 2013). A meta-analysis of cohort studies observed that patients with schizophrenia present a small but significant reduction in colorectal and prostate cancer incidence in male patients (Li et al., 2017). Data from previous research analysed in this study suggested that antipsychotic drugs may reduce prostate cancer development (Li et al., 2017). If glycine inhibitor drugs were approved in major clinical trials, it would be interesting to perform a study evaluating cancer incidence in these patients. GLYT1 inhibitors also have been proven to provide analgesic effect in some animal models of pain, including a bone cancer mice model (Harvey and Yee, 2013, Motoyama et al., 2014). GLYT1 controls glycinergic and glutamatergic neurotransmission in the region of the brain involved in pain signalling (Harvey and Yee, 2013). Studies have demonstrated that augmenting the glycinergic inhibitory neurotransmission suppresses the transmission of these signals resulting in pain relief (Harvey and Yee, 2013). Thus, GLYT1 inhibitors might be utilised as an analgesic in association with cancer treatment.

There is evidence that some tumour cells consume more glycine than normal cells, depleting its levels in the extracellular environment. Glycine levels were significantly reduced in the culture medium of rapidly proliferating cancer cells when compared to slow growing cancer cells and non-tumorous cells (Jain et al., 2012). As described in previous chapters, glycine levels in lung cancer patients are reduced in the plasma and increased in the tumour tissue (Zhao et al., 2014). Zhao and

collaborators measured tissue free amino acids in lung tumour tissues and paracarcinomous tissues of 27 patients and observed a significant increase in glycine levels in tumour tissues, 2891±166 μmol/kg wet wt, when compared to paracarcinomous tissue, 2387±177 μmol/kg wet wt (Zhao et al., 2014). They also measured plasma free amino acids in these lung cancer patients and in 22 healthy individuals and observed a significant reduction in glycine concentrations in plasma from patients, 298±29 μmol/L, compared with healthy individuals, 454±29 μmol/L (Zhao et al., 2014). As described earlier, increased extracellular levels of glycine facilitate interaction with GlyR resulting in angiogenesis inhibition (Guo et al., 2017). Therefore, it is possible to speculate that GLYT1 inhibition may increase glycine concentration in the extracellular environment, possibly reducing its concentration in tumour tissue and uptake by endothelial cells, which may contribute to a decrease in angiogenesis.

The reduction in cell proliferation following ALX-5407 of fast growing cancer cells encourages further investigations utilising *in vivo* models of tumours treated with GLYT1 inhibitors. The effect of GLYT1 inhibitors on tumour growth, angiogenesis, survival rate and pain might then be evaluated.

ATF4 influence on proliferation, glycine uptake and glutathione synthesis

ATF4 is a key component in stress responses and is essential for many cancer cell types survival and proliferation (Igarashi et al., 2007). ATF4 downregulation reduced fibrosarcoma and endometrial cancer growth in mice models (Liu et al., 2017, Ye et al., 2010). ATF4 promoted cell growth, migration, induced angiogenesis and conferred a multidrug resistance phenotype in glioma cells (Chen et al., 2017). ATF4 was also involved with poor prognosis in esophageal squamous cell carcinoma and related to invasiveness and metastasis (Zhu et al., 2014). Moreover, under stress VEGF expression is upregulated through ATF4, consequently, increasing angiogenesis in tumours (Wang et al., 2013b, Terashima et al., 2013, Wang et al., 2012). ATF4 transcriptional regulation affects genes that restore cellular homeostasis following ER stress and amino acid starvation, this way influencing mTORC1 activity and cellular growth (Wortel et al., 2017). In the current work, when ATF4 was downregulated in NSCLC, colorectal and renal cancer cell lines a decrease in cell proliferation was observed, whereas growth of the endothelial non-transformed cell line

was increased. These results are in agreement with the literature suggesting that ATF4 is involved in tumour cell proliferation and growth.

ATF4 is also involved in upregulation of other transcription factors including ATF3, ATF5 and ATF6 (Zhou et al., 2008, Teske et al., 2011, Lee et al., 2013). When analysing ATF4 knockdown cells in comparison to controls, ATF3, ATF5 and ATF6 were downregulated in fast growing cancer cell lines tested. These data described in chapter 6 are in agreement with the literature and suggest that ATF4 regulates ATF3, ATF5 and ATF6 expression in NSCLC and colorectal cancer cell lines tested. In some tumours ATF3 is involved in cell growth, migration and metastasis (Thompson et al., 2009, Hai et al., 2011). ATF5, in some cancers types, activates anti-apoptotic genes, induces transcription of mTOR and reduces autophagy as pro-survival mechanisms and also is involved with tumour invasiveness (Nukuda et al., 2016, Deng and Haynes, 2017, Sheng et al., 2011). ATF6 is activated when unfolded proteins accumulate in ER during stress conditions, such as amino acid deprivation, and then regulates genes involved in autophagy and protein-folding (Sano and Reed, 2013, Notte et al., 2015). Thus, the influence of ATF4 on other ATFs could have contributed to its effect in the tumour cell proliferation observed in this study.

Under stress conditions, such as amino acid deprivation and oxidative stress, ATF4 also activates the transcription of amino acid transporters and synthesising enzymes as an attempt to restore nutrient levels and recover homeostasis (Wortel et al., 2017). ATF4 upregulates expression of amino acid transporters such as LAT1 and GLYT1, and increases intracellular expression of non-essential amino acid synthetic pathway enzymes, such as asparagine synthetase and enzymes of the SSP, such as PHGDH, PSAT1, PSPH and SHMT2 (Harding et al., 2003, Ye et al., 2010, Ding et al., 2013). In agreement with Harding and collaborators, data described in this thesis (chapter 6) demonstrated that GLYT1 transcription was also regulated by ATF4 in all cells tested. Additionally, as predicted, ATF4 regulated SHMT2 mRNA in all cells in this study, thus, also supporting intracellular glycine synthesis. These data suggest that under stress conditions, increased uptake of extracellular glycine by GLYT1 or increase in glycine intercellular synthesis might be necessary to overcome stress and maintain proliferation.

The mRNA expression of other amino acid transporters able to transport glycine were also affected by ATF4, although to a lesser degree than GLYT1. SNAT2 mRNA in the renal cancer cell line and PAT1 and $ATB^{0,+}$ mRNAs in the colorectal cancer cell line were downregulated following ATF4 knockdown. As the effect of ATF4 on

transcription of other amino acid transporters able to transport glycine is not uniform for all cells tested, is possible to speculate that ATF4 influence on PAT1, SNAT2 and ATB^{0+} might be a consequence of other metabolic changes in ATF4 knockdown cells and not a direct regulation. As discussed in Chapter 1, ATF4 is upregulated under stress by eIF2α, which also reduces total protein expression. ATF4 then activates the transcription of genes to recover cellular homeostasis. In ATF4 knockdown experiments, cells were cultured for 72 hours without medium change; this could lead to depletion in nutrient levels. Once ATF4 levels are depleted, a possible increase in cellular stress and induction of eIF2α phosphorylation might occur leading to a reduction in total cellular protein expression that might have affected these amino acid transporters mRNA expression. Experiments analysing eIF2α phosphorylation and total protein synthesis following 72 hours of ATF4 knockdown experiment might elucidate this hypothesis.

Interestingly, ATF4 downregulation had only a small influence on glycine uptake of NSCLC and renal cell lines, and had no effect in the colorectal cancer cell line. Possibly, changes in transcription do not reflect changes in GLYT1 protein levels in cell membrane over the timescale that the experiments were conducted. Even though GLYT1 half-life at the plasma membrane is about four hours (Barrera et al., 2015), in contrast with GLYT1 knockdown experiments, downregulation of GLYT1 protein expression following ATF4 knockdown might require longer time, since more processes are involved in the transcriptional regulation. Additionally, while ATF4 proteins are easily degraded and require post-translational mechanisms for activity, ATF4 mRNA seems to be more stable and is constitutively expressed in tissues (Yang and Karsenty, 2004). Therefore, ATF4 knockdown might require longer time than GLYT1 knockdown to reveal a functional effect on glycine transport, or indeed an effect on glycine transporter protein expression. Further experiments analysing protein abundance of amino acid transporters are required to test this hypothesis. However, GLYT1 antibodies available are not efficient in western blotting assay, as discussed in Chapter 4, so to analyse of GLYT1 protein level would be challenging.

ATF4 influenced GSH levels and its synthesising enzymes. It is known that ATF4 regulates genes involved in redox chemistry (Harding et al., 2003, Rutkowski and Kaufman, 2003). ATF4 activates the transcription of xCT and GLYT1, cystine and glycine transporters, respectively (Harding et al., 2003). Both amino acids are precursors of GSH, the major cellular antioxidant as described in Chapter 1. ATF4 also activates the transcription of Mthfd that converts meTHF to 10,formyl-THF that can be

utilised in purine synthesis (Harding et al., 2003). Interestingly, in mitochondria, GCS generates meTHF that is then converted by the enzyme Mthfd2 to 10,formyl-THF, which is fully oxidised to CO_2 producing NADPH, important in redox defence (Fan et al., 2014). So, as predicted, when ATF4 was downregulated, there was a reduction in GSH levels and also in xCT, GCLC and GCLM mRNA abundance. One study observed that under cysteine deprivation GCL subunits are upregulated indirectly by GCN2/ATF4 pathway (Sikalidis et al., 2014). It was suggested that ATF4 regulates proteins involved in GCLC mRNA expression and GCLM mRNA stabilisation (Sikalidis et al., 2014). Therefore, in agreement with the literature, data from the present study suggest that ATF4 controls multiple factors in GSH synthesis, such as availability of cysteine and glycine, through regulation of xCT and GLYT1, respectively, and indirectly expression of GCLC and GCLM subunits of GCL enzyme resulting in a reduction of GSH levels in tumour cells. Additionally, ATF4 may contribute to redox reactions increasing NADPH formation as consequence of upregulation of mthfd2 in mitochondria. ATF4 may also contribute to purine synthesis through regulation of SHMT2, producing meTHF, and also mthfd, converting meTHF in 10,formyl-THF. ATF4 also upregulates GLYT1, increasing intracellular levels of glycine, which then are able to be utilised in purine synthesis.

Conclusion

Glycine uptake mediated by GLYT1 is crucial in maintaining the rapid proliferating profile of fast growing NSCLC and colorectal cancer cells, especially when cells are growing under stressed conditions. In contrast, no such effect was evident in slow growing renal cancer and non-transformed endothelial cell lines. GLYT1 downregulation resulted in reduced glutathione levels in all tumour cells utilised in this study, and had a great effect on DNA replication of rapidly proliferating tumour cells, possibly as a result of reduced purine synthesis, in comparison to the slowly proliferative one (Figure 7.3). GLYT1 knockdown reduced PAT1 and SNAT2 transcription and this might also contribute to a reduction in glycine uptake and reduction in proliferation in rapidly proliferating cancer cells. An upregulation of SHMT2 following GLYT1 knockdown indicates that increased glycine synthesis is required in fast growing tumour cells, but wasn't enough to maintain the rapid proliferative profile. However, GLYT1 inhibitor ALX-5407 influence on cell proliferation becomes relevant only when fast growing tumour cells are under stress conditions. Additionally, the effect of ATF4 knockdown on reducing SHMT2, GLYT1, xCT and GCL mRNA levels

contributes to a reduction in GSH levels and suggests an important role of GLYT1 during cellular stress. Thus, GLYT1 inhibition may reduce cell proliferation of highly proliferative tumour cells by inhibiting DNA synthesis and increasing cell susceptibility to oxidative stress. Also, it is possible to speculate that GLYT1 inhibition may increase extracellular levels of glycine over time that could inhibit angiogenesis via glycine interaction with GlyR, but further *in vivo* investigation is required to substantiate this speculation. Therefore, glycine uptake and GLYT1 may be considered a possible target in a novel therapeutic approach to reduce tumours and this study encourages further *in vivo* investigation of GLYT1 effects in animal models for cancer. The evidence that a specific GLYT1 inhibitor ALX-5407 had similar effects to GLYT1kd, suggests that simple pharmacological tools might be effective therapies or adjuvants in the therapy of rapidly proliferating tumours, providing a novel approach to improving cancer treatments and prognosis.

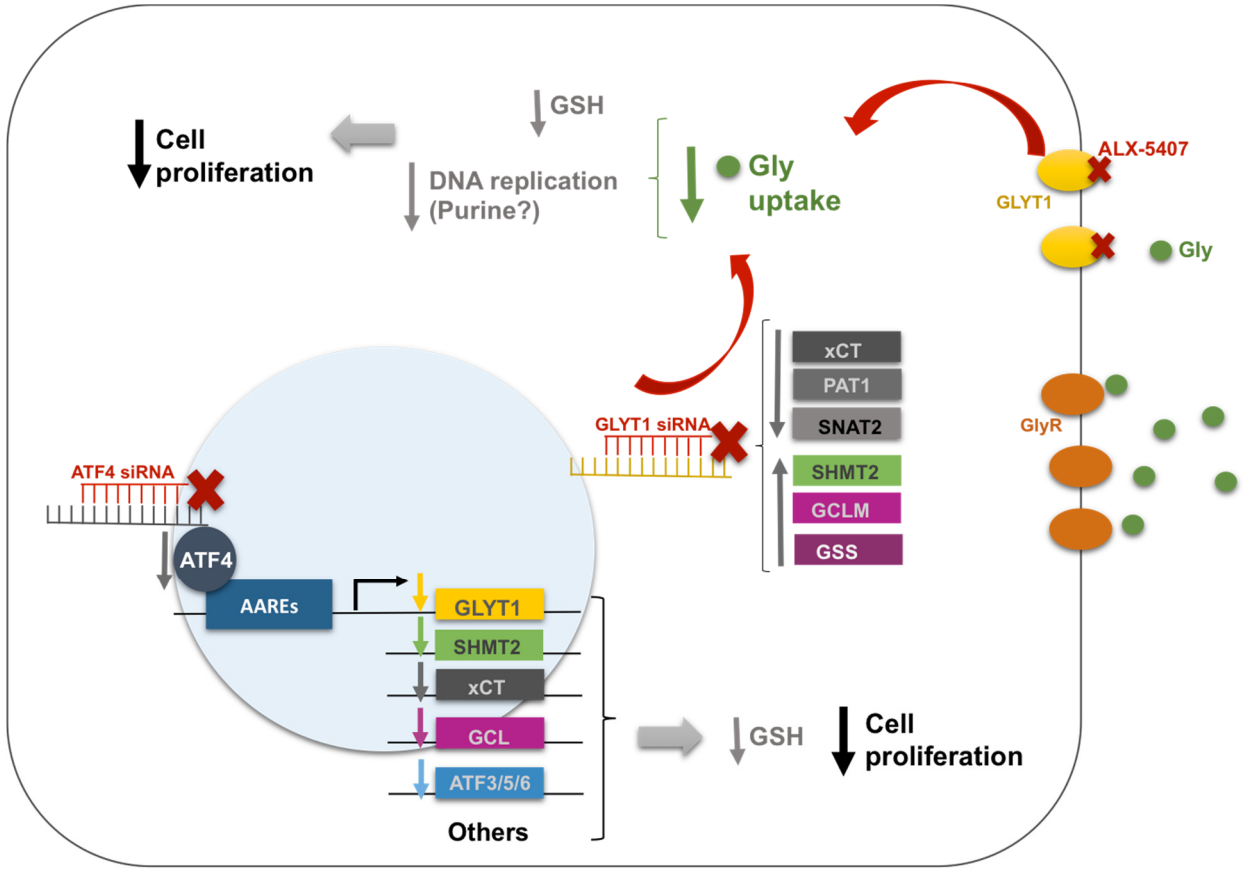

Figure 7.3: GLYT1 influence on cell metabolism of rapid proliferating colorectal and NSCLC cell lines. Effects of GLYT1kd and ALX-5407 treatment in DNA replication and glutathione (GSH) synthesis and its possible effects increasing extracellular glycine and facilitating glycine interaction with GlyR and consequent reduction in angiogenesis, which may all contribute to a reduction in cell proliferation in fast growing tumour cells. GLYT1kd also lead to a reduction in other amino acid transporters (SNAT2, PAT1 and xCT) that support tumour cell proliferation and an increase in SHMT2, and GSH synthesising enzymes (GCLM and GSS) possibly as an attempt to restore intracellular levels of glycine and GSH. ATF4kd reduced GLYT1, SHMT2, xCT and GCL mRNA expression, which may have contributed to a reduction in intracellular glycine and GSH synthesis, thus affecting cell proliferation. ATF4kd also reduced ATF3, ATF5 and ATF6 transcription, which have been implicated to tumour cell survival.

8. References

ABRAHAMSEN, H. & STENMARK, H. 2011. Cell biology. Growth signaling from inside. *Science,* 334**,** 611-2.

ADAMS, C. M. 2007. Role of the transcription factor ATF4 in the anabolic actions of insulin and the anti-anabolic actions of glucocorticoids. *J Biol Chem,* 282**,** 16744-53.

AKSAMITIENE, E., KIYATKIN, A. & KHOLODENKO, B. N. 2012. Cross-talk between mitogenic Ras/MAPK and survival PI3K/Akt pathways: a fine balance. *Biochem Soc Trans,* 40**,** 139-46.

ALBERTS, B., JOHNSON, A., LEWIS, J., RAFF, M., ROBERTS, K. & WALTER, P. 2002. The Cell Cycle and Programmed Cell Death. *In:* GIBBS, S. (ed.) *Molecular Biology of The Cell.* Fourth Edition ed. New York, USA: Garland Science.

AMELIO, I., CUTRUZZOLÁ, F., ANTONOV, A., AGOSTINI, M. & MELINO, G. 2014. Serine and glycine metabolism in cancer. *Trends Biochem Sci,* 39**,** 191-8.

AMIN, K., LI, J., CHAO, W. R., DEWHIRST, M. W. & HAROON, Z. A. 2003. Dietary glycine inhibits angiogenesis during wound healing and tumor growth. *Cancer Biol Ther,* 2**,** 173-8.

ATCC®. *A-498 (ATCC ® HTB-44 ™) general information* [Online]. Available: https://www.lgcstandards-atcc.org/Products/All/HTB-44.aspx-generalinformation [Accessed]. in July 2017

ATCC® A549 (ATCC ® CCL-185 ™) characteristics.

ATCC® HT-29 (ATCC ® HTB-38 ™) characteristics

ATKINSON, B. N., BELL, S. C., DE VIVO, M., KOWALSKI, L. R., LECHNER, S. M., OGNYANOV, V. I., THAM, C. S., TSAI, C., JIA, J., ASHTON, D. & KLITENICK, M. A. 2001. ALX 5407: a potent, selective inhibitor of the hGlyT1 glycine transporter. *Mol Pharmacol,* 60**,** 1414-20.

AUBREY, K. R. & VANDENBERG, R. J. 2001. N[3-(4'-fluorophenyl)-3-(4'-phenylphenoxy)propyl]sarcosine (NFPS) is a selective persistent inhibitor of glycine transport. *Br J Pharmacol,* 134**,** 1429-36.

B., K. R. J. & M.W., R. 2006a. Growth: a balance of cell proliferation, death and differentiation. *Cancer Biology* 3rd ed.: Pearson Education Limited.

B., K. R. J. & M.W., R. 2006b. Natural history: the life of a cancer. *Cancer Biology.* 3rd ed.: Pearson Education Limited.

BAGGOTT, J. E., GORMAN, G. S. & TAMURA, T. 2007. 13C enrichment of carbons 2 and 8 of purine by folate-dependent reactions after [13C]formate and [2-13C]glycine dosing in adult humans. *Metabolism,* 56**,** 708-15.

BAIRD FE, PINILLA-TENAS JJ, OGILVIE WL, GANAPATHY V, HUNDAL HS, TAYLOR PM. 2006. Evidence for allosteric regulation of pH-sensitive System A (SNAT2) and System N (SNAT5) amino acid transporter activity involving a conserved histidine residue. *Biochem J.*, 397(2), 369-75.

BANERJEE, A., LANG, J. Y., HUNG, M. C., SENGUPTA, K., BANERJEE, S. K., BAKSI, K. & BANERJEE, D. K. 2011. Unfolded protein response is required in nu/nu mice microvasculature for treating breast tumor with tunicamycin. *J Biol Chem,* 286**,** 29127-38.

BAR-PELED, L. & SABATINI, D. M. 2014. Regulation of mTORC1 by amino acids. *Trends Cell Biol,* 24**,** 400-6.

BARRERA, S. P., CASTREJON-TELLEZ, V., TRINIDAD, M., ROBLES-ESCAJEDA, E., VARGAS-MEDRANO, J., VARELA-RAMIREZ, A. & MIRANDA, M. 2015. PKC-Dependent GlyT1 Ubiquitination Occurs Independent of Phosphorylation: Inespecificity in Lysine Selection for Ubiquitination. *PLoS One,* 10**,** e0138897.

BARTHEL, F., URBAN, A., SCHLÖSSER, L., EULENBURG, V., WERDEHAUSEN, R., BRANDENBURGER, T., ARAGON, C., BAUER, I. & HERMANNS, H. 2014. Long-term application of glycine transporter inhibitors acts antineuropathic and modulates spinal N-methyl-D-aspartate receptor subunit NR-1 expression in rats. *Anesthesiology,* 121**,** 160-9.

BETZ, H., GOMEZA, J., ARMSEN, W., SCHOLZE, P. & EULENBURG, V. 2006. Glycine transporters: essential regulators of synaptic transmission. *Biochem Soc Trans,* 34**,** 55-8.

BEYOĞLU, D. & IDLE, J. R. 2012. The glycine deportation system and its pharmacological consequences. *Pharmacol Ther,* 135**,** 151-67.

BI, M., NACZKI, C., KORITZINSKY, M., FELS, D., BLAIS, J., HU, N., HARDING, H., NOVOA, I., VARIA, M., RALEIGH, J., SCHEUNER, D., KAUFMAN, R. J., BELL, J., RON, D., WOUTERS, B. G. & KOUMENIS, C. 2005. ER stress-regulated translation increases tolerance to extreme hypoxia and promotes tumor growth. *EMBO J,* 24**,** 3470-81.

BOLL, M., FOLTZ, M., RUBIO-ALIAGA, I., KOTTRA, G. & DANIEL, H. 2002. Functional characterization of two novel mammalian electrogenic proton-dependent amino acid cotransporters. *J Biol Chem,* 277**,** 22966-73.

BOROWSKY, B. & HOFFMAN, B. J. 1998. Analysis of a gene encoding two glycine transporter variants reveals alternative promoter usage and a novel gene structure. *J Biol Chem,* 273**,** 29077-85.

BOROWSKY, B., MEZEY, E. & HOFFMAN, B. J. 1993. Two glycine transporter variants with distinct localization in the CNS and peripheral tissues are encoded by a common gene. *Neuron,* 10**,** 851-63.

BRODACZEWSKA, K. K., SZCZYLIK, C., FIEDOROWICZ, M., PORTA, C. & CZARNECKA, A. M. 2016. Choosing the right cell line for renal cell cancer research. *Mol Cancer,* 15**,** 83.

BRÖER, S., BAILEY, C. G., KOWALCZUK, S., NG, C., VANSLAMBROUCK, J. M., RODGERS, H., AURAY-BLAIS, C., CAVANAUGH, J. A., BRÖER, A. & RASKO, J. E. 2008. Iminoglycinuria and hyperglycinuria are discrete human phenotypes resulting from complex mutations in proline and glycine transporters. *J Clin Invest,* 118**,** 3881-92.

BRÖER, S. & BRÖER, A. 2017. Amino acid homeostasis and signalling in mammalian cells and organisms. *Biochem J,* 474**,** 1935-1963.

BRUNS, H., KAZANAVICIUS, D., SCHULTZE, D., SAEEDI, M. A., YAMANAKA, K., STRUPAS, K. & SCHEMMER, P. 2016. Glycine inhibits angiogenesis in colorectal cancer: role of endothelial cells. *Amino Acids,* 48**,** 2549-2558.

BRUNS, H., PETRULIONIS, M., SCHULTZE, D., AL SAEEDI, M., LIN, S., YAMANAKA, K., AMBRAZEVIČIUS, M., STRUPAS, K. & SCHEMMER, P. 2014. Glycine inhibits angiogenic signaling in human hepatocellular carcinoma cells. *Amino Acids,* 46**,** 969-76.

CAO, M. D., GISKEØDEGÅRD, G. F., BATHEN, T. F., SITTER, B., BOFIN, A., LØNNING, P. E., LUNDGREN, S. & GRIBBESTAD, I. S. 2012. Prognostic value of metabolic response in breast cancer patients receiving neoadjuvant chemotherapy. *BMC Cancer,* 12**,** 39.

CHANETON, B., HILLMANN, P., ZHENG, L., MARTIN, A. C., MADDOCKS, O. D., CHOKKATHUKALAM, A., COYLE, J. E., JANKEVICS, A., HOLDING, F. P., VOUSDEN, K. H., FREZZA, C., O'REILLY, M. & GOTTLIEB, E. 2012. Serine is a natural ligand and allosteric activator of pyruvate kinase M2. *Nature,* 491**,** 458-62.

CHEN, D., FAN, Z., RAUH, M., BUCHFELDER, M., EYUPOGLU, I. Y. & SAVASKAN, N. 2017. ATF4 promotes angiogenesis and neuronal cell death and confers ferroptosis in a xCT-dependent manner. *Oncogene,* 36**,** 5593-5608.

CHEN, Z., KENNEDY, D. J., WAKE, K. A., ZHUANG, L., GANAPATHY, V. & THWAITES, D. T. 2003. Structure, tissue expression pattern, and function of the amino acid transporter rat PAT2. *Biochem Biophys Res Commun,* 304**,** 747-54.

CHRISTIE, G. R., FORD, D., HOWARD, A., CLARK, M. A. & HIRST, B. H. 2001. Glycine supply to human enterocytes mediated by high-affinity basolateral GLYT1. *Gastroenterology,* 120**,** 439-48.

DAVID, C. J., CHEN, M., ASSANAH, M., CANOLL, P. & MANLEY, J. L. 2010. HnRNP proteins controlled by c-Myc deregulate pyruvate kinase mRNA splicing in cancer. *Nature,* 463**,** 364-8.

DAVIDSON, S. M., JONAS, O., KEIBLER, M. A., HOU, H. W., LUENGO, A., MAYERS, J. R., WYCKOFF, J., DEL ROSARIO, A. M., WHITMAN, M., CHIN, C. R., CONDON, K. J., LAMMERS, A., KELLERSBERGER, K. A., STALL, B. K., STEPHANOPOULOS, G., BAR-SAGI, D., HAN, J., RABINOWITZ, J. D., CIMA, M. J., LANGER, R. & VANDER HEIDEN, M. G. 2017. Direct evidence for cancer-cell-autonomous extracellular protein catabolism in pancreatic tumors. *Nat Med,* 23**,** 235-241.

DE LUCA, A., MAIELLO, M. R., D'ALESSIO, A., PERGAMENO, M. & NORMANNO, N. 2012. The RAS/RAF/MEK/ERK and the PI3K/AKT signalling pathways: role in cancer pathogenesis and implications for therapeutic approaches. *Expert Opin Ther Targets,* 16 Suppl 2**,** S17-27.

DEBERARDINIS, R. J., LUM, J. J., HATZIVASSILIOU, G. & THOMPSON, C. B. 2008. The biology of cancer: metabolic reprogramming fuels cell growth and proliferation. *Cell Metab,* 7**,** 11-20.

DEBERARDINIS, R. J., MANCUSO, A., DAIKHIN, E., NISSIM, I., YUDKOFF, M., WEHRLI, S. & THOMPSON, C. B. 2007. Beyond aerobic glycolysis: transformed cells can engage in glutamine metabolism that exceeds the requirement for protein and nucleotide synthesis. *Proc Natl Acad Sci U S A,* 104**,** 19345-50.

DENG, P. & HAYNES, C. M. 2017. Mitochondrial dysfunction in cancer: Potential roles of ATF5 and the mitochondrial UPR. *Semin Cancer Biol,* 47**,** 43-49.

DI CIAULA, A., GARRUTI, G., LUNARDI BACCETTO, R., MOLINA-MOLINA, E., BONFRATE, L., WANG, D. Q. & PORTINCASA, P. 2017. Bile Acid Physiology. *Ann Hepatol,* 16**,** s4-s14.

DI PIETRO, E., SIROIS, J., TREMBLAY, M. L. & MACKENZIE, R. E. 2002. Mitochondrial NAD-dependent methylenetetrahydrofolate dehydrogenase-methenyltetrahydrofolate cyclohydrolase is essential for embryonic development. *Mol Cell Biol,* 22**,** 4158-66.

DI SALVO, M. L., CONTESTABILE, R., PAIARDINI, A. & MARAS, B. 2013. Glycine consumption and mitochondrial serine hydroxymethyltransferase in cancer cells: the heme connection. *Med Hypotheses,* 80**,** 633-6.

DING, J., LI, T., WANG, X., ZHAO, E., CHOI, J. H., YANG, L., ZHA, Y., DONG, Z., HUANG, S., ASARA, J. M., CUI, H. & DING, H. F. 2013. The histone H3 methyltransferase G9A epigenetically activates the serine-glycine synthesis pathway to sustain cancer cell survival and proliferation. *Cell Metab,* 18**,** 896-907.

DTP, D. T. P. N. N. *NCI60: Cell Lines In The In Vitro Screen* [Online]. Available: http://dtp.nci.nih.gov/docs/misc/common_files/cell_list.html [Accessed]. in September 2017

DUCKER, G. S. & RABINOWITZ, J. D. 2017. One-Carbon Metabolism in Health and Disease. *Cell Metab,* 25**,** 27-42.

DURKIN, J. T., SPAIS, C. M., SCHREIBER, J., KOPEC, K. & MEYER, S. L. 2011. Amino-terminal isoforms of the human glycine transporter GlyT1 exhibit similar pharmacology. *Brain Res,* 1374**,** 1-7.

DYACHOK, J., EARNEST, S., ITURRARAN, E. N., COBB, M. H. & ROSS, E. M. 2016. Amino Acids Regulate mTORC1 by an Obligate Two-step Mechanism. *J Biol Chem,* 291**,** 22414-22426.

EHREN, J. L. & MAHER, P. 2013. Concurrent regulation of the transcription factors Nrf2 and ATF4 mediates the enhancement of glutathione levels by the flavonoid fisetin. *Biochem Pharmacol,* 85**,** 1816-26.

EIGENBRODT, E., LEIB, S., KRĂMER, W., FRIIS, R. R. & SCHONER, W. 1983. Structural and kinetic differences between the M2 type pyruvate kinases from lung and various tumors. *Biomed Biochim Acta,* 42**,** S278-82.

EIGENBRODT, E., REINACHER, M., SCHEEFERS-BORCHEL, U., SCHEEFERS, H. & FRIIS, R. 1992. Double role for pyruvate kinase type M2 in the expansion of phosphometabolite pools found in tumor cells. *Crit Rev Oncog,* 3**,** 91-115.

ESTRELA, J. M., ORTEGA, A. & OBRADOR, E. 2006. Glutathione in cancer biology and therapy. *Crit Rev Clin Lab Sci,* 43**,** 143-81.

EULENBURG, V., ARMSEN, W., BETZ, H. & GOMEZA, J. 2005. Glycine transporters: essential regulators of neurotransmission. *Trends Biochem Sci,* 30**,** 325-33.

FAN, J., YE, J., KAMPHORST, J. J., SHLOMI, T., THOMPSON, C. B. & RABINOWITZ, J. D. 2014. Quantitative flux analysis reveals folate-dependent NADPH production. *Nature,* 510**,** 298-302.

FERNANDEZ, J., LOPEZ, A. B., WANG, C., MISHRA, R., ZHOU, L., YAMAN, I., SNIDER, M. D., HATZOGLOU, M. & HATZOLGOU, M. 2003. Transcriptional control of the arginine/lysine transporter, cat-1, by physiological stress. *J Biol Chem,* 278**,** 50000-9.

FOLTZ, M., OECHSLER, C., BOLL, M., KOTTRA, G. & DANIEL, H. 2004. Substrate specificity and transport mode of the proton-dependent amino acid transporter mPAT2. *Eur J Biochem,* 271**,** 3340-7.

FOX, S. I. 2004. *Human Physiology, Cell Structure and Genetic Control,* New York, NY, McGraw-Hill.

FRANKS, L. M. & KNOWLES, M. A. 2005. What is Cancer? *Introduction to the Cellular and Molecular Biology of Cancer.* 4th Edition ed. United States: Oxford University Press.

FRØLUND, S., LANGTHALER, L., KALL, M. A., HOLM, R. & NIELSEN, C. U. 2012. Intestinal drug transport via the proton-coupled amino acid transporter PAT1 (SLC36A1) is inhibited by Gly-X(aa) dipeptides. *Mol Pharm,* 9**,** 2761-9.

FU, L. & KILBERG, M. S. 2013. Elevated cJUN expression and an ATF/CRE site within the ATF3 promoter contribute to activation of ATF3 transcription by the amino acid response. *Physiol Genomics,* 45**,** 127-37.

GACCIOLI, F., HUANG, C. C., WANG, C., BEVILACQUA, E., FRANCHI-GAZZOLA, R., GAZZOLA, G. C., BUSSOLATI, O., SNIDER, M. D. & HATZOGLOU, M. 2006. Amino acid starvation induces the SNAT2 neutral amino acid transporter by a mechanism that involves eukaryotic initiation factor 2alpha phosphorylation and cap-independent translation. *J Biol Chem,* 281**,** 17929-40.

GANAPATHY, M. E. & GANAPATHY, V. 2005. Amino Acid Transporter ATB0,+ as a delivery system for drugs and prodrugs. *Curr Drug Targets Immune Endocr Metabol Disord,* 5**,** 357-64.

GANAPATHY, V., THANGARAJU, M. & PRASAD, P. D. 2009. Nutrient transporters in cancer: relevance to Warburg hypothesis and beyond. *Pharmacol Ther,* 121**,** 29-40.

GENEVESTIGATOR. Available: https://genevestigator.com/gv/index.jsp [Accessed]. in Sptember 2017

GERDES, J., SCHWAB, U., LEMKE, H. & STEIN, H. 1983. Production of a mouse monoclonal antibody reactive with a human nuclear antigen associated with cell proliferation. *Int J Cancer,* 31**,** 13-20.

GJYMISHKA, A., PALII, S. S., SHAN, J. & KILBERG, M. S. 2008. Despite increased ATF4 binding at the C/EBP-ATF composite site following activation of the unfolded protein response, system A transporter 2 (SNAT2) transcription activity is repressed in HepG2 cells. *J Biol Chem,* 283**,** 27736-47.

GOBERDHAN, D. C. 2010. Intracellular amino acid sensing and mTORC1-regulated growth: new ways to block an old target? *Curr Opin Investig Drugs,* 11**,** 1360-7.

GOMEZA, J., ARMSEN, W., BETZ, H. & EULENBURG, V. 2006. Lessons from the knocked-out glycine transporters. *Handb Exp Pharmacol*, 457-83.

GONZÁLEZ, A. & HALL, M. N. 2017. Nutrient sensing and TOR signaling in yeast and mammals. *EMBO J,* 36, 397-408.

GORRINI, C., HARRIS, I. S. & MAK, T. W. 2013. Modulation of oxidative stress as an anticancer strategy. *Nat Rev Drug Discov,* 12, 931-47.

GOUT, P. W., BUCKLEY, A. R., SIMMS, C. R. & BRUCHOVSKY, N. 2001. Sulfasalazine, a potent suppressor of lymphoma growth by inhibition of the x(c)- cystine transporter: a new action for an old drug. *Leukemia,* 15, 1633-40.

GUHA, P., KAPTAN, E., GADE, P., KALVAKOLANU, D. V. & AHMED, H. 2017. Tunicamycin induced endoplasmic reticulum stress promotes apoptosis of prostate cancer cells by activating mTORC1. *Oncotarget,* 8, 68191-68207.

GUO, D., MURDOCH, C. E., XU, H., SHI, H., DUAN, D. D., AHMED, A. & GU, Y. 2017. Vascular endothelial growth factor signaling requires glycine to promote angiogenesis. *Sci Rep,* 7, 14749.

GUPTA, N., PRASAD, P. D., GHAMANDE, S., MOORE-MARTIN, P., HERDMAN, A. V., MARTINDALE, R. G., PODOLSKY, R., MAGER, S., GANAPATHY, M. E. & GANAPATHY, V. 2006. Up-regulation of the amino acid transporter ATB(0,+) (SLC6A14) in carcinoma of the cervix. *Gynecol Oncol,* 100, 8-13.

HACKL, C., LANG, S. A., MOSER, C., MORI, A., FICHTNER-FEIGL, S., HELLERBRAND, C., DIETMEIER, W., SCHLITT, H. J., GEISSLER, E. K. & STOELTZING, O. 2010. Activating transcription factor-3 (ATF3) functions as a tumor suppressor in colon cancer and is up-regulated upon heat-shock protein 90 (Hsp90) inhibition. *BMC Cancer,* 10, 668.

HAHN, W. C. & WEINBERG, R. A. 2002. Modelling the molecular circuitry of cancer. *Nat Rev Cancer,* 2, 331-41.

HAI, T., JALGAONKAR, S., WOLFORD, C. C. & YIN, X. 2011. Immunohistochemical detection of activating transcription factor 3, a hub of the cellular adaptive-response network. *Methods Enzymol,* 490, 175-94.

HANAHAN, D. & WEINBERG, R. A. 2000. The hallmarks of cancer. *Cell,* 100, 57-70.

HANAHAN, D. & WEINBERG, R. A. 2011. Hallmarks of cancer: the next generation. *Cell,* 144, 646-74.

HARDING, H. P., NOVOA, I., ZHANG, Y., ZENG, H., WEK, R., SCHAPIRA, M. & RON, D. 2000. Regulated translation initiation controls stress-induced gene expression in mammalian cells. *Mol Cell,* 6**,** 1099-108.

HARDING, H. P., ZHANG, Y., ZENG, H., NOVOA, I., LU, P. D., CALFON, M., SADRI, N., YUN, C., POPKO, B., PAULES, R., STOJDL, D. F., BELL, J. C., HETTMANN, T., LEIDEN, J. M. & RON, D. 2003. An integrated stress response regulates amino acid metabolism and resistance to oxidative stress. *Mol Cell,* 11**,** 619-33.

HARSING, L. G. & MATYUS, P. 2013. Mechanisms of glycine release, which build up synaptic and extrasynaptic glycine levels: the role of synaptic and non-synaptic glycine transporters. *Brain Res Bull,* 93**,** 110-9.

HARVEY, R. J. & YEE, B. K. 2013. Glycine transporters as novel therapeutic targets in schizophrenia, alcohol dependence and pain. *Nat Rev Drug Discov,* 12**,** 866-85.

HATANAKA, T., HARAMURA, M., FEI, Y. J., MIYAUCHI, S., BRIDGES, C. C., GANAPATHY, P. S., SMITH, S. B., GANAPATHY, V. & GANAPATHY, M. E. 2004. Transport of amino acid-based prodrugs by the Na+- and Cl(-) -coupled amino acid transporter ATB0,+ and expression of the transporter in tissues amenable for drug delivery. *J Pharmacol Exp Ther,* 308**,** 1138-47.

HEASLEY, L. E., THALER, S., NICKS, M., PRICE, B., SKORECKI, K. & NEMENOFF, R. A. 1997. Induction of cytosolic phospholipase A2 by oncogenic Ras in human non-small cell lung cancer. *J Biol Chem,* 272**,** 14501-4.

HEUBLEIN, S., KAZI, S., OGMUNDSDÓTTIR, M. H., ATTWOOD, E. V., KALA, S., BOYD, C. A., WILSON, C. & GOBERDHAN, D. C. 2010. Proton-assisted amino-acid transporters are conserved regulators of proliferation and amino-acid-dependent mTORC1 activation. *Oncogene,* 29**,** 4068-79.

HIRSCH, I., WEIWAD, M., PRELL, E. & FERRARI, D. M. 2014. ERp29 deficiency affects sensitivity to apoptosis via impairment of the ATF6-CHOP pathway of stress response. *Apoptosis,* 19**,** 801-15.

HLATKY, L. & HAHNFELDT, P. 2014. Beyond the cancer cell: progression-level determinants highlight the multiscale nature of carcinogenesis risk. *Cancer Res,* 74**,** 659-64.

HOWARD, A. & HIRST, B. H. 2011. The glycine transporter GLYT1 in human intestine: expression and function. *Biol Pharm Bull,* 34**,** 784-8.

HOWARD, A., TAHIR, I., JAVED, S., WARING, S. M., FORD, D. & HIRST, B. H. 2010. Glycine transporter GLYT1 is essential for glycine-mediated protection of human intestinal epithelial cells against oxidative damage. *J Physiol,* 588**,** 995-1009.

HSU, P. P. & SABATINI, D. M. 2008. Cancer cell metabolism: Warburg and beyond. *Cell,* 134**,** 703-7.

HUANG, B., XIE, Q., LU, X., QIAN, T., LI, S., ZHU, R., YU, W., CHEN, G., CHEN, Z., XU, X., WANG, T. & LI, L. 2016. GlyT1 Inhibitor NFPS Exerts Neuroprotection via GlyR Alpha1 Subunit in the Rat Model of Transient Focal Cerebral Ischaemia and Reperfusion. *Cell Physiol Biochem,* 38**,** 1952-62.

HUANG, Y., DAI, Z., BARBACIORU, C. & SADÉE, W. 2005. Cystine-glutamate transporter SLC7A11 in cancer chemosensitivity and chemoresistance. *Cancer Res,* 65**,** 7446-54.

HUGGINS, C. J., MAYEKAR, M. K., MARTIN, N., SAYLOR, K. L., GONIT, M., JAILWALA, P., KASOJI, M., HAINES, D. C., QUIÑONES, O. A. & JOHNSON, P. F. 2015. C/EBPγ Is a Critical Regulator of Cellular Stress Response Networks through Heterodimerization with ATF4. *Mol Cell Biol,* 36**,** 693-713.

HUSSAIN, S. P., HOFSETH, L. J. & HARRIS, C. C. 2003. Radical causes of cancer. *Nat Rev Cancer,* 3**,** 276-85.

IARC, I. A. F. R. O. C. *GLOBOCAN 2012: Estimated Cancer Incidence, Mortality and Prevalence Worldwide in 2012* [Online]. Available: http://globocan.iarc.fr/Pages/fact_sheets_cancer.aspx [Accessed]. in January 2015

IGARASHI, T., IZUMI, H., UCHIUMI, T., NISHIO, K., ARAO, T., TANABE, M., URAMOTO, H., SUGIO, K., YASUMOTO, K., SASAGURI, Y., WANG, K. Y., OTSUJI, Y. & KOHNO, K. 2007. Clock and ATF4 transcription system regulates drug resistance in human cancer cell lines. *Oncogene,* 26**,** 4749-60.

INVITROGEN AlamarBlue® Assay (U.S. Patent No. 5,501,959) manufacturer specifications PI-DAL1025/1100Rev 1.0.

ISHIHARA, S. & HAGA, H. 2015. ATF5: development of oncogenic resistance to radiotherapy. *Aging (Albany NY),* 7**,** 453-4.

JAIN, M., NILSSON, R., SHARMA, S., MADHUSUDHAN, N., KITAMI, T., SOUZA, A. L., KAFRI, R., KIRSCHNER, M. W., CLISH, C. B. & MOOTHA, V. K. 2012. Metabolite profiling identifies a key role for glycine in rapid cancer cell proliferation. *Science,* 336**,** 1040-4.

JIANG, H. Y., WEK, S. A., MCGRATH, B. C., LU, D., HAI, T., HARDING, H. P., WANG, X., RON, D., CAVENER, D. R. & WEK, R. C. 2004. Activating transcription factor 3 is integral to the eukaryotic initiation factor 2 kinase stress response. *Mol Cell Biol,* 24**,** 1365-77.

JONES, H. N., ASHWORTH, C. J., PAGE, K. R. & MCARDLE, H. J. 2006. Cortisol stimulates system A amino acid transport and SNAT2 expression in a human placental cell line (BeWo). *Am J Physiol Endocrinol Metab,* 291**,** E596-603.

JU, P., AUBREY, K. R. & VANDENBERG, R. J. 2004. Zn2+ inhibits glycine transport by glycine transporter subtype 1b. *J Biol Chem,* 279**,** 22983-91.

KALHAN, S. C. & HANSON, R. W. 2012. Resurgence of serine: an often neglected but indispensable amino Acid. *J Biol Chem,* 287**,** 19786-91.

KANAI, Y. & ENDOU, H. 2003. Functional properties of multispecific amino acid transporters and their implications to transporter-mediated toxicity. *J Toxicol Sci,* 28**,** 1-17.

KANAI, Y., SEGAWA, H., MIYAMOTO, K., UCHINO, H., TAKEDA, E. & ENDOU, H. 1998. Expression cloning and characterization of a transporter for large neutral amino acids activated by the heavy chain of 4F2 antigen (CD98). *J Biol Chem,* 273**,** 23629-32.

KANDIL, S., BRENNAN, L. & MCBEAN, G. J. 2010. Glutathione depletion causes a JNK and p38MAPK-mediated increase in expression of cystathionine-gamma-lyase and upregulation of the transsulfuration pathway in C6 glioma cells. *Neurochem Int,* 56**,** 611-9.

KARUNAKARAN, S., RAMACHANDRAN, S., COOTHANKANDASWAMY, V., ELANGOVAN, S., BABU, E., PERIYASAMY-THANDAVAN, S., GURAV, A., GNANAPRAKASAM, J. P., SINGH, N., SCHOENLEIN, P. V., PRASAD, P. D., THANGARAJU, M. & GANAPATHY, V. 2011. SLC6A14 (ATB0,+) protein, a

highly concentrative and broad specific amino acid transporter, is a novel and effective drug target for treatment of estrogen receptor-positive breast cancer. *J Biol Chem,* 286**,** 31830-8.

KARUNAKARAN, S., UMAPATHY, N. S., THANGARAJU, M., HATANAKA, T., ITAGAKI, S., MUNN, D. H., PRASAD, P. D. & GANAPATHY, V. 2008. Interaction of tryptophan derivatives with SLC6A14 (ATB0,+) reveals the potential of the transporter as a drug target for cancer chemotherapy. *Biochem J,* 414**,** 343-55.

KIKUCHI, G., MOTOKAWA, Y., YOSHIDA, T. & HIRAGA, K. 2008. Glycine cleavage system: reaction mechanism, physiological significance, and hyperglycinemia. *Proc Jpn Acad Ser B Phys Biol Sci,* 84**,** 246-63.

KILBERG, M. S., SHAN, J. & SU, N. 2009. ATF4-dependent transcription mediates signaling of amino acid limitation. *Trends Endocrinol Metab,* 20**,** 436-43.

KIM KM, KINGSMORE SF, HAN H, YANG-FENG TL, GODINOT N, SELDIN MF, CARON MG, GIROS B. 1994. Cloning of the human glycine transporter type 1: molecular and pharmacological characterization of novel isoform variants and chromosomal localization of the gene in the human and mouse genomes. *Mol Pharmacol*, 45(4), 608-17.

KIM, D., FISKE, B. P., BIRSOY, K., FREINKMAN, E., KAMI, K., POSSEMATO, R. L., CHUDNOVSKY, Y., PACOLD, M. E., CHEN, W. W., CANTOR, J. R., SHELTON, L. M., GUI, D. Y., KWON, M., RAMKISSOON, S. H., LIGON, K. L., KANG, S. W., SNUDERL, M., VANDER HEIDEN, M. G. & SABATINI, D. M. 2015. SHMT2 drives glioma cell survival in ischaemia but imposes a dependence on glycine clearance. *Nature,* 520**,** 363-7.

KIM, S. K., JUNG, W. H. & KOO, J. S. 2014. Differential expression of enzymes associated with serine/glycine metabolism in different breast cancer subtypes. *PLoS One,* 9**,** e101004.

KING, R. J. & ROBINS, M. W. 2006a. Epidemiology: Identifying Causes for Human Cancers. *In:* LIMITED, P. E. (ed.) *Cancer Biology* 3rd ed.

KING, R. J. & ROBINS, M. W. 2006b. Growth: a balance of cell proliferation, death and differentiation. *Cancer Biology* 3rd ed.: Pearson Education Limited.

KING, R. J. & ROBINS, M. W. 2006c. Natural history: the life of a cancer. *Cancer Biology.* 3rd ed.: Pearson Education Limited.

KOMATSU, H., FURUYA, Y., SAWADA, K. & ASADA, T. 2015. Involvement of the strychnine-sensitive glycine receptor in the anxiolytic effects of GlyT1 inhibitors on maternal separation-induced ultrasonic vocalization in rat pups. *Eur J Pharmacol,* 746**,** 252-7.

KOUMENIS, C. 2006. ER stress, hypoxia tolerance and tumor progression. *Curr Mol Med,* 6**,** 55-69.

KROKOWSKI, D., JOBAVA, R., GUAN, B. J., FARABAUGH, K., WU, J., MAJUMDER, M., BIANCHI, M. G., SNIDER, M. D., BUSSOLATI, O. & HATZOGLOU, M. 2015. Coordinated Regulation of the Neutral Amino Acid Transporter SNAT2 and the Protein Phosphatase Subunit GADD34 Promotes Adaptation to Increased Extracellular Osmolarity. *J Biol Chem,* 290**,** 17822-37.

KUME, A., KOYATA, H., SAKAKIBARA, T., ISHIGURO, Y., KURE, S. & HIRAGA, K. 1991. The glycine cleavage system. Molecular cloning of the chicken and human glycine decarboxylase cDNAs and some characteristics involved in the deduced protein structures. *J Biol Chem,* 266**,** 3323-9.

LABUSCHAGNE, C. F., VAN DEN BROEK, N. J., MACKAY, G. M., VOUSDEN, K. H. & MADDOCKS, O. D. 2014. Serine, but not glycine, supports one-carbon metabolism and proliferation of cancer cells. *Cell Rep,* 7**,** 1248-58.

LAIN, S. & LANE, D. P. 2005. Tumour Supressor genes. *Introduction to the Cellular and Molecular*

Biology of Cancer Fourth Edition ed. New York, USA: Oxford University Press.

LAMERS, Y., WILLIAMSON, J., GILBERT, L. R., STACPOOLE, P. W. & GREGORY, J. F. 2007. Glycine turnover and decarboxylation rate quantified in healthy men and women using primed, constant infusions of [1,2-(13)C2]glycine and [(2)H3]leucine. *J Nutr,* 137**,** 2647-52.

LARSSON, A. & MATTSSON, B. 1976. On the mechanism of 5-oxoproline overproduction in 5-oxoprolinuria. *Clin Chim Acta,* 67**,** 245-53.

LASSOT, I., ESTRABAUD, E., EMILIANI, S., BENKIRANE, M., BENAROUS, R. & MARGOTTIN-GOGUET, F. 2005. p300 modulates ATF4 stability and

transcriptional activity independently of its acetyltransferase domain. *J Biol Chem,* 280**,** 41537-45.

LASSOT, I., SÉGÉRAL, E., BERLIOZ-TORRENT, C., DURAND, H., GROUSSIN, L., HAI, T., BENAROUS, R. & MARGOTTIN-GOGUET, F. 2001. ATF4 degradation relies on a phosphorylation-dependent interaction with the SCF(betaTrCP) ubiquitin ligase. *Mol Cell Biol,* 21**,** 2192-202.

LEE, G. Y., HAVERTY, P. M., LI, L., KLJAVIN, N. M., BOURGON, R., LEE, J., STERN, H., MODRUSAN, Z., SESHAGIRI, S., ZHANG, Z., DAVIS, D., STOKOE, D., SETTLEMAN, J., DE SAUVAGE, F. J. & NEVE, R. M. 2014. Comparative oncogenomics identifies PSMB4 and SHMT2 as potential cancer driver genes. *Cancer Res,* 74**,** 3114-26.

LEE, J. I., KANG, J. & STIPANUK, M. H. 2006. Differential regulation of glutamate-cysteine ligase subunit expression and increased holoenzyme formation in response to cysteine deprivation. *Biochem J,* 393**,** 181-90.

LEE, S. H., MIN, K. W., ZHANG, X. & BAEK, S. J. 2013. 3,3'-diindolylmethane induces activating transcription factor 3 (ATF3) via ATF4 in human colorectal cancer cells. *J Nutr Biochem,* 24**,** 664-71.

LEWERENZ, J., HEWETT, S. J., HUANG, Y., LAMBROS, M., GOUT, P. W., KALIVAS, P. W., MASSIE, A., SMOLDERS, I., METHNER, A., PERGANDE, M., SMITH, S. B., GANAPATHY, V. & MAHER, P. 2013. The cystine/glutamate antiporter system x(c)(-) in health and disease: from molecular mechanisms to novel therapeutic opportunities. *Antioxid Redox Signal,* 18**,** 522-55.

LI, H., LI, J., YU, X., ZHENG, H., SUN, X., LU, Y., ZHANG, Y., LI, C. & BI, X. 2017. The incidence rate of cancer in patients with schizophrenia: A meta-analysis of cohort studies. *Schizophr Res*.

LIU, B., CHEN, P., XI, D., ZHU, H. & GAO, Y. 2017. ATF4 regulates CCL2 expression to promote endometrial cancer growth by controlling macrophage infiltration. *Exp Cell Res,* 360**,** 105-112.

LIU, L. N., FU, T. T., XU, X. F., FU, C., FANG, M. J., LIU, Y., XU, P. X. & ZHAO, Y. F. 2015. Tracing the nitrogen metabolites of glycine using (15)N-glycine and mass spectrometry. *Rapid Commun Mass Spectrom,* 29**,** 645-53.

LOCASALE, J. W. 2013. Serine, glycine and one-carbon units: cancer metabolism in full circle. *Nat Rev Cancer,* 13**,** 572-83.

LOCASALE, J. W., GRASSIAN, A. R., MELMAN, T., LYSSIOTIS, C. A., MATTAINI, K. R., BASS, A. J., HEFFRON, G., METALLO, C. M., MURANEN, T., SHARFI, H., SASAKI, A. T., ANASTASIOU, D., MULLARKY, E., VOKES, N. I., SASAKI, M., BEROUKHIM, R., STEPHANOPOULOS, G., LIGON, A. H., MEYERSON, M., RICHARDSON, A. L., CHIN, L., WAGNER, G., ASARA, J. M., BRUGGE, J. S., CANTLEY, L. C. & VANDER HEIDEN, M. G. 2011. Phosphoglycerate dehydrogenase diverts glycolytic flux and contributes to oncogenesis. *Nat Genet,* 43**,** 869-74.

LONZA. *HUVEC information at*

https://www.lonza.com/products-services/bio-research/primary-cells/human-cells-and-media/endothelial-cells-and-media/huvec-human-umbilical-vein-endothelial-cells.aspx [Online]. [Accessed]. in September 2017

LÓPEZ-FONTANALS, M., RODRÍGUEZ-MULERO, S., CASADO, F. J., DÉRIJARD, B. & PASTOR-ANGLADA, M. 2003. The osmoregulatory and the amino acid-regulated responses of system A are mediated by different signal transduction pathways. *J Gen Physiol,* 122**,** 5-16.

LU, P. D., HARDING, H. P. & RON, D. 2004. Translation reinitiation at alternative open reading frames regulates gene expression in an integrated stress response. *J Cell Biol,* 167**,** 27-33.

LU, S. C. 2013. Glutathione synthesis. *Biochim Biophys Acta,* 1830**,** 3143-53.

LUO, H., ZHAO, L., JI, X., ZHANG, X., JIN, Y. & LIU, W. 2017. Glycosylation affects the stability and subcellular distribution of human PAT1 protein. *FEBS Lett,* 591**,** 613-623.

LUO, J. Q., CHEN, D. W. & YU, B. 2013. Upregulation of amino acid transporter expression induced by L-leucine availability in L6 myotubes is associated with ATF4 signaling through mTORC1-dependent mechanism. *Nutrition,* 29**,** 284-90.

MACKENZIE, B. & ERICKSON, J. D. 2004. Sodium-coupled neutral amino acid (System N/A) transporters of the SLC38 gene family. *Pflugers Arch,* 447**,** 784-95.

MADDOCKS, O. D., BERKERS, C. R., MASON, S. M., ZHENG, L., BLYTH, K., GOTTLIEB, E. & VOUSDEN, K. H. 2013. Serine starvation induces stress and p53-dependent metabolic remodelling in cancer cells. *Nature,* 493**,** 542-6.

MADDOCKS, O. D. K., ATHINEOS, D., CHEUNG, E. C., LEE, P., ZHANG, T., VAN DEN BROEK, N. J. F., MACKAY, G. M., LABUSCHAGNE, C. F., GAY, D., KRUISWIJK, F., BLAGIH, J., VINCENT, D. F., CAMPBELL, K. J., CETECI, F., SANSOM, O. J., BLYTH, K. & VOUSDEN, K. H. 2017. Modulating the therapeutic response of tumours to dietary serine and glycine starvation. *Nature,* 544**,** 372-376.

MALLORGA, P. J., WILLIAMS, J. B., JACOBSON, M., MARQUES, R., CHAUDHARY, A., CONN, P. J., PETTIBONE, D. J. & SUR, C. 2003. Pharmacology and expression analysis of glycine transporter GlyT1 with [3H]-(N-[3-(4'-fluorophenyl)-3-(4'phenylphenoxy)propyl])sarcosine. *Neuropharmacology,* 45**,** 585-93.

MAUDSLEY, A. A., GUPTA, R. K., STOYANOVA, R., PARRA, N. A., ROY, B., SHERIFF, S., HUSSAIN, N. & BEHARI, S. 2014. Mapping of glycine distributions in gliomas. *AJNR Am J Neuroradiol,* 35**,** S31-6.

MAZUREK, S. 2011. Pyruvate kinase type M2: a key regulator of the metabolic budget system in tumor cells. *Int J Biochem Cell Biol,* 43**,** 969-80.

MAZUREK, S., BOSCHEK, C. B., HUGO, F. & EIGENBRODT, E. 2005. Pyruvate kinase type M2 and its role in tumor growth and spreading. *Semin Cancer Biol,* 15**,** 300-8.

MCCRACKEN, A. N. & EDINGER, A. L. 2015. Targeting cancer metabolism at the plasma membrane by limiting amino acid access through SLC6A14. *Biochem J,* 470**,** e17-9.

MCCUBREY, J. A., STEELMAN, L. S., KEMPF, C. R., CHAPPELL, W. H., ABRAMS, S. L., STIVALA, F., MALAPONTE, G., NICOLETTI, F., LIBRA, M., BÄSECKE, J., MAKSIMOVIC-IVANIC, D., MIJATOVIC, S., MONTALTO, G., CERVELLO, M., COCCO, L. & MARTELLI, A. M. 2011. Therapeutic resistance resulting from mutations in Raf/MEK/ERK and PI3K/PTEN/Akt/mTOR signaling pathways. *J Cell Physiol,* 226**,** 2762-81.

MENDOZA, M. C., ER, E. E. & BLENIS, J. 2011. The Ras-ERK and PI3K-mTOR pathways: cross-talk and compensation. *Trends Biochem Sci,* 36**,** 320-8.

MILKEREIT, R., PERSAUD, A., VANOAICA, L., GUETG, A., VERREY, F. & ROTIN, D. 2015. LAPTM4b recruits the LAT1-4F2hc Leu transporter to lysosomes and promotes mTORC1 activation. *Nat Commun,* 6**,** 7250.

MIYAMOTO, N., IZUMI, H., MIYAMOTO, R., BIN, H., KONDO, H., TAWARA, A., SASAGURI, Y. & KOHNO, K. 2011. Transcriptional regulation of activating transcription factor 4 under oxidative stress in retinal pigment epithelial ARPE-19/HPV-16 cells. *Invest Ophthalmol Vis Sci,* 52**,** 1226-34.

MOBASHERI, A., RICHARDSON, S., MOBASHERI, R., SHAKIBAEI, M. & HOYLAND, J. A. 2005. Hypoxia inducible factor-1 and facilitative glucose transporters GLUT1 and GLUT3: putative molecular components of the oxygen and glucose sensing apparatus in articular chondrocytes. *Histol Histopathol,* 20**,** 1327-38.

MORGAN, D. O. 2007a. The Cell Cycle in Cancer. *In:* LAWRENCE, E. (ed.) *The Cell Cycle: Principle of Control.* London, UK: New Science Press.

MORGAN, D. O. 2007b. *The Cell Cycle: Principles of Control,*

Chapter 3 The cell Cycle Control System, London, UK, New Science Press Ltd.

MOTOYAMA, N., MORITA, K., SHIRAISHI, S., KITAYAMA, T., KANEMATSU, T., UEZONO, Y. & DOHI, T. 2014. Relief of cancer pain by glycine transporter inhibitors. *Anesth Analg,* 119**,** 988-95.

NCI. *NCI60 data of doubling times at* https://dtp.cancer.gov/discovery_development/nci-60/cell_list.htm [Online]. Available: https://dtp.cancer.gov/discovery_development/nci-60/cell_list.htm [Accessed]. in July 2017

NELSON, D. L. & COX, M. M. 2005. Biosynthesis of Amino Acids, Nucleotides, and Related Molecules. *In:* COMPANY, W. H. F. A. (ed.) *Lehninger Principles of Biochesmestry.* 4th ed.

NOH, S., KIM, D. H., JUNG, W. H. & KOO, J. S. 2014. Expression levels of serine/glycine metabolism-related proteins in triple negative breast cancer tissues. *Tumour Biol,* 35**,** 4457-68.

NOTTE, A., REBUCCI, M., FRANSOLET, M., ROEGIERS, E., GENIN, M., TELLIER, C., WATILLON, K., FATTACCIOLI, A., ARNOULD, T. & MICHIELS, C. 2015. Taxol-induced unfolded protein response activation in breast cancer cells exposed to hypoxia: ATF4 activation regulates autophagy and inhibits apoptosis. *Int J Biochem Cell Biol,* 62**,** 1-14.

NUKUDA, A., ENDOH, H., YASUDA, M., MIZUTANI, T., KAWABATA, K. & HAGA, H. 2016. Role of ATF5 in the invasive potential of diverse human cancer cell lines. *Biochem Biophys Res Commun,* 474**,** 509-514.

NÚÑEZ, E., MARTÍNEZ-MAZA, R., GEERLINGS, A., ARAGÓN, C. & LÓPEZ-CORCUERA, B. 2005. Transmembrane domains 1 and 3 of the glycine transporter GLYT1 contain structural determinants of N[3-(4'-fluorophenyl)-3-(4'-phenylphenoxy)-propyl]sarcosine specificity. *Neuropharmacology,* 49**,** 922-34.

O'BRIEN, M. L. & TEW, K. D. 1996. Glutathione and related enzymes in multidrug resistance. *Eur J Cancer,* 32A**,** 967-78.

O'CONNOR, P. M., JACKMAN, J., BAE, I., MYERS, T. G., FAN, S., MUTOH, M., SCUDIERO, D. A., MONKS, A., SAUSVILLE, E. A., WEINSTEIN, J. N., FRIEND, S., FORNACE, A. J. & KOHN, K. W. 1997. Characterization of the p53 tumor suppressor pathway in cell lines of the National Cancer Institute anticancer drug screen and correlations with the growth-inhibitory potency of 123 anticancer agents. *Cancer Res,* 57**,** 4285-300.

ODA, K., HOSODA, N., ENDO, H., SAITO, K., TSUJIHARA, K., YAMAMURA, M., SAKATA, T., ANZAI, N., WEMPE, M. F., KANAI, Y. & ENDOU, H. 2010. L-type amino acid transporter 1 inhibitors inhibit tumor cell growth. *Cancer Sci,* 101**,** 173-9.

OKUDAIRA, H., SHIKANO, N., NISHII, R., MIYAGI, T., YOSHIMOTO, M., KOBAYASHI, M., OHE, K., NAKANISHI, T., TAMAI, I., NAMIKI, M. & KAWAI, K. 2011. Putative transport mechanism and intracellular fate of trans-1-amino-3-18F-fluorocyclobutanecarboxylic acid in human prostate cancer. *J Nucl Med,* 52**,** 822-9.

OLIVARES, L., ARAGÓN, C., GIMÉNEZ, C. & ZAFRA, F. 1995. The role of N-glycosylation in the targeting and activity of the GLYT1 glycine transporter. *J Biol Chem,* 270**,** 9437-42.

PELENGARIS, S. & KAN, M. 2006a. Introduction. *The molecular Biology of Cancer.* Wiley-Blackwell.

PELENGARIS, S. & KAN, M. 2006b. Oncogenes *The molecular Biology of Cancer.* Wiley-Blackwell.

PELENGARIS, S. & KAN, M. 2006c. Regulation of Growth: Growth factors, Receptors and Signalling Pathways. *The molecular Biology of Cancer.* Wiley-Blackwell.

PINILLA, J., ALEDO, J. C., CWIKLINSKI, E., HYDE, R., TAYLOR, P. M. & HUNDAL, H. S. 2011. SNAT2 transceptor signalling via mTOR: a role in cell growth and proliferation? *Front Biosci (Elite Ed),* 3**,** 1289-99.

POLLARI, S., KÄKÖNEN, S. M., EDGREN, H., WOLF, M., KOHONEN, P., SARA, H., GUISE, T., NEES, M. & KALLIONIEMI, O. 2011. Enhanced serine production by bone metastatic breast cancer cells stimulates osteoclastogenesis. *Breast Cancer Res Treat,* 125**,** 421-30.

POSSEMATO, R., MARKS, K. M., SHAUL, Y. D., PACOLD, M. E., KIM, D., BIRSOY, K., SETHUMADHAVAN, S., WOO, H. K., JANG, H. G., JHA, A. K., CHEN, W. W., BARRETT, F. G., STRANSKY, N., TSUN, Z. Y., COWLEY, G. S., BARRETINA, J., KALAANY, N. Y., HSU, P. P., OTTINA, K., CHAN, A. M., YUAN, B., GARRAWAY, L. A., ROOT, D. E., MINO-KENUDSON, M., BRACHTEL, E. F., DRIGGERS, E. M. & SABATINI, D. M. 2011. Functional genomics reveal that the serine synthesis pathway is essential in breast cancer. *Nature,* 476**,** 346-50.

RAZAK, M. A., BEGUM, P. S., VISWANATH, B. & RAJAGOPAL, S. 2017. Multifarious Beneficial Effect of Nonessential Amino Acid, Glycine: A Review. *Oxid Med Cell Longev,* 2017**,** 1716701.

REDALEN, K. R., SITTER, B., BATHEN, T. F., GRØHOLT, K. K., HOLE, K. H., DUELAND, S., FLATMARK, K., REE, A. H. & SEIERSTAD, T. 2016. High tumor glycine concentration is an adverse prognostic factor in locally advanced rectal cancer. *Radiother Oncol,* 118**,** 393-8.

ROSE, M. L., MADREN, J., BUNZENDAHL, H. & THURMAN, R. G. 1999. Dietary glycine inhibits the growth of B16 melanoma tumors in mice. *Carcinogenesis,* 20**,** 793-8.

ROUSSEL, M. 2006. Tumor Supressors *In:* PELENGARIS, S. & KAN, M. (eds.) *The molecular Biology of Cancer.* Wiley-Blackwell.

ROUX, M. J. & SUPPLISSON, S. 2000. Neuronal and glial glycine transporters have different stoichiometries. *Neuron,* 25**,** 373-83.

RUTKOWSKI, D. T. & KAUFMAN, R. J. 2003. All roads lead to ATF4. *Dev Cell,* 4**,** 442-4.

SALCEDA, R. 2006. Pharmacological properties of glycine uptake in the developing rat retina. *Neurochem Int,* 49**,** 342-6.

SAMLUK, Ł., CZEREDYS, M. & NAŁĘCZ, K. A. 2010. Regulation of amino acid/carnitine transporter B 0,+ (ATB 0,+) in astrocytes by protein kinase C: independent effects on raft and non-raft transporter subpopulations. *J Neurochem,* 115**,** 1386-97.

SANO, R. & REED, J. C. 2013. ER stress-induced cell death mechanisms. *Biochim Biophys Acta,* 1833**,** 3460-3470.

SASAKI, H., SATO, H., KURIYAMA-MATSUMURA, K., SATO, K., MAEBARA, K., WANG, H., TAMBA, M., ITOH, K., YAMAMOTO, M. & BANNAI, S. 2002. Electrophile response element-mediated induction of the cystine/glutamate exchange transporter gene expression. *J Biol Chem,* 277**,** 44765-71.

SATO, H., NOMURA, S., MAEBARA, K., SATO, K., TAMBA, M. & BANNAI, S. 2004. Transcriptional control of cystine/glutamate transporter gene by amino acid deprivation. *Biochem Biophys Res Commun,* 325**,** 109-16.

SATO, H., SHIIYA, A., KIMATA, M., MAEBARA, K., TAMBA, M., SAKAKURA, Y., MAKINO, N., SUGIYAMA, F., YAGAMI, K., MORIGUCHI, T., TAKAHASHI, S. & BANNAI, S. 2005. Redox imbalance in cystine/glutamate transporter-deficient mice. *J Biol Chem,* 280**,** 37423-9.

SATO, H., TAMBA, M., KURIYAMA-MATSUMURA, K., OKUNO, S. & BANNAI, S. 2000. Molecular cloning and expression of human xCT, the light chain of amino acid transport system xc-. *Antioxid Redox Signal,* 2**,** 665-71.

SCHIÖTH, H. B., ROSHANBIN, S., HÄGGLUND, M. G. & FREDRIKSSON, R. 2013. Evolutionary origin of amino acid transporter families SLC32, SLC36 and SLC38 and physiological, pathological and therapeutic aspects. *Mol Aspects Med,* 34**,** 571-85.

SCHOLZEN, T. & GERDES, J. 2000. The Ki-67 protein: from the known and the unknown. *J Cell Physiol,* 182**,** 311-22.

SEO, J., FORTUNO, E. S., SUH, J. M., STENESEN, D., TANG, W., PARKS, E. J., ADAMS, C. M., TOWNES, T. & GRAFF, J. M. 2009. Atf4 regulates obesity, glucose homeostasis, and energy expenditure. *Diabetes,* 58**,** 2565-73.

SHENG, Z., MA, L., SUN, J. E., ZHU, L. J. & GREEN, M. R. 2011. BCR-ABL suppresses autophagy through ATF5-mediated regulation of mTOR transcription. *Blood,* 118**,** 2840-8.

SHI, Z. Z., HABIB, G. M., RHEAD, W. J., GAHL, W. A., HE, X., SAZER, S. & LIEBERMAN, M. W. 1996. Mutations in the glutathione synthetase gene cause 5-oxoprolinuria. *Nat Genet,* 14**,** 361-5.

SHOEMAKER, R. H. 2006. The NCI60 human tumour cell line anticancer drug screen. *Nat Rev Cancer,* 6**,** 813-23.

SIKALIDIS, A. K., MAZOR, K. M., LEE, J. I., ROMAN, H. B., HIRSCHBERGER, L. L. & STIPANUK, M. H. 2014. Upregulation of capacity for glutathione synthesis in response to amino acid deprivation: regulation of glutamate-cysteine ligase subunits. *Amino Acids,* 46**,** 1285-96.

SIKDER, M. O. F., YANG, S., GANAPATHY, V. & BHUTIA, Y. D. 2017. The Na+/Cl--Coupled, Broad-Specific, Amino Acid Transporter SLC6A14 (ATB0,+): Emerging Roles in Multiple Diseases and Therapeutic Potential for Treatment and Diagnosis. *AAPS J,* 20**,** 12.

SINGLETON, D. C. & HARRIS, A. L. 2012. Targeting the ATF4 pathway in cancer therapy. *Expert Opin Ther Targets,* 16**,** 1189-202.

SITTER, B., BATHEN, T. F., SINGSTAD, T. E., FJØSNE, H. E., LUNDGREN, S., HALGUNSET, J. & GRIBBESTAD, I. S. 2010. Quantification of metabolites in breast cancer patients with different clinical prognosis using HR MAS MR spectroscopy. *NMR Biomed,* 23**,** 424-31.

SLOAN, J. L. & MAGER, S. 1999. Cloning and functional expression of a human Na(+) and Cl(-)-dependent neutral and cationic amino acid transporter B(0+). *J Biol Chem,* 274**,** 23740-5.

SOOD, R., PORTER, A. C., OLSEN, D. A., CAVENER, D. R. & WEK, R. C. 2000. A mammalian homologue of GCN2 protein kinase important for translational

control by phosphorylation of eukaryotic initiation factor-2alpha. *Genetics,* 154**,** 787-801.

SREEKUMAR, A., POISSON, L. M., RAJENDIRAN, T. M., KHAN, A. P., CAO, Q., YU, J., LAXMAN, B., MEHRA, R., LONIGRO, R. J., LI, Y., NYATI, M. K., AHSAN, A., KALYANA-SUNDARAM, S., HAN, B., CAO, X., BYUN, J., OMENN, G. S., GHOSH, D., PENNATHUR, S., ALEXANDER, D. C., BERGER, A., SHUSTER, J. R., WEI, J. T., VARAMBALLY, S., BEECHER, C. & CHINNAIYAN, A. M. 2009. Metabolomic profiles delineate potential role for sarcosine in prostate cancer progression. *Nature,* 457**,** 910-4.

STEELMAN, L. S., CHAPPELL, W. H., ABRAMS, S. L., KEMPF, R. C., LONG, J., LAIDLER, P., MIJATOVIC, S., MAKSIMOVIC-IVANIC, D., STIVALA, F., MAZZARINO, M. C., DONIA, M., FAGONE, P., MALAPONTE, G., NICOLETTI, F., LIBRA, M., MILELLA, M., TAFURI, A., BONATI, A., BÄSECKE, J., COCCO, L., EVANGELISTI, C., MARTELLI, A. M., MONTALTO, G., CERVELLO, M. & MCCUBREY, J. A. 2011. Roles of the Raf/MEK/ERK and PI3K/PTEN/Akt/mTOR pathways in controlling growth and sensitivity to therapy-implications for cancer and aging. *Aging (Albany NY),* 3**,** 192-222.

STRATTON, M. R., CAMPBELL, P. J. & FUTREAL, P. A. 2009. The cancer genome. *Nature,* 458**,** 719-24.

SUN, K., WU, Z., JI, Y. & WU, G. 2016. Glycine Regulates Protein Turnover by Activating Protein Kinase B/Mammalian Target of Rapamycin and by Inhibiting MuRF1 and Atrogin-1 Gene Expression in C2C12 Myoblasts. *J Nutr,* 146**,** 2461-2467.

SURYAWAN, A., NGUYEN, H. V., ALMONACI, R. D. & DAVIS, T. A. 2013. Abundance of amino acid transporters involved in mTORC1 activation in skeletal muscle of neonatal pigs is developmentally regulated. *Amino Acids,* 45**,** 523-30.

TEDESCHI, P. M., MARKERT, E. K., GOUNDER, M., LIN, H., DVORZHINSKI, D., DOLFI, S. C., CHAN, L. L., QIU, J., DIPAOLA, R. S., HIRSHFIELD, K. M., BOROS, L. G., BERTINO, J. R., OLTVAI, Z. N. & VAZQUEZ, A. 2013. Contribution of serine, folate and glycine metabolism to the ATP, NADPH and purine requirements of cancer cells. *Cell Death Dis,* 4**,** e877.

TERASHIMA, J., TACHIKAWA, C., KUDO, K., HABANO, W. & OZAWA, S. 2013. An aryl hydrocarbon receptor induces VEGF expression through ATF4 under glucose deprivation in HepG2. *BMC Mol Biol,* 14**,** 27.

TESKE, B. F., FUSAKIO, M. E., ZHOU, D., SHAN, J., MCCLINTICK, J. N., KILBERG, M. S. & WEK, R. C. 2013. CHOP induces activating transcription factor 5 (ATF5) to trigger apoptosis in response to perturbations in protein homeostasis. *Mol Biol Cell,* 24**,** 2477-90.

TESKE, B. F., WEK, S. A., BUNPO, P., CUNDIFF, J. K., MCCLINTICK, J. N., ANTHONY, T. G. & WEK, R. C. 2011. The eIF2 kinase PERK and the integrated stress response facilitate activation of ATF6 during endoplasmic reticulum stress. *Mol Biol Cell,* 22**,** 4390-405.

THELWALL, P. E., SIMPSON, N. E., RABBANI, Z. N., CLARK, M. D., POURDEYHIMI, R., MACDONALD, J. M., BLACKBAND, S. J. & GAMCSIK, M. P. 2012. In vivo MR studies of glycine and glutathione metabolism in a rat mammary tumor. *NMR Biomed,* 25**,** 271-8.

THELWALL, P. E., YEMIN, A. Y., GILLIAN, T. L., SIMPSON, N. E., KASIBHATLA, M. S., RABBANI, Z. N., MACDONALD, J. M., BLACKBAND, S. J. & GAMCSIK, M. P. 2005. Noninvasive in vivo detection of glutathione metabolism in tumors. *Cancer Res,* 65**,** 10149-53.

THOMPSON, M. R., XU, D. & WILLIAMS, B. R. 2009. ATF3 transcription factor and its emerging roles in immunity and cancer. *J Mol Med (Berl),* 87**,** 1053-60.

THUL PJ, ÅKESSON L, WIKING M, MAHDESSIAN D, GELADAKI A, AIT BLAL H, ALM T, ASPLUND A, BJÖRK L, BRECKELS LM, BÄCKSTRÖM A, DANIELSSON F, FAGERBERG L, FALL J, GATTO L, GNANN C, HOBER S, HJELMARE M, JOHANSSON F, LEE S, LINDSKOG C, MULDER J, MULVEY CM, NILSSON P, OKSVOLD P, ROCKBERG J, SCHUTTEN R, SCHWENK JM, SIVERTSSON Å, SJÖSTEDT E, SKOGS M, STADLER C, SULLIVAN DP, TEGEL H, WINSNES C, ZHANG C, ZWAHLEN M, MARDINOGLU A, PONTÉN F, VON FEILITZEN K, LILLEY KS, UHLÉN M, LUNDBERG E. 2017. A subcellular map of the human proteome. *Science.* 356(6340):eaal3321

THWAITES, D. T. & ANDERSON, C. M. 2011. The SLC36 family of proton-coupled amino acid transporters and their potential role in drug transport. *Br J Pharmacol,* 164**,** 1802-16.

THWAITES, D. T., MCEWAN, G. T., BROWN, C. D., HIRST, B. H. & SIMMONS, N. L. 1993. Na(+)-independent, H(+)-coupled transepithelial beta-alanine absorption by human intestinal Caco-2 cell monolayers. *J Biol Chem,* 268**,** 18438-41.

TIBBETTS, A. S. & APPLING, D. R. 2010. Compartmentalization of Mammalian folate-mediated one-carbon metabolism. *Annu Rev Nutr,* 30**,** 57-81.

TOYODA, M., KAIRA, K., OHSHIMA, Y., ISHIOKA, N. S., SHINO, M., SAKAKURA, K., TAKAYASU, Y., TAKAHASHI, K., TOMINAGA, H., ORIUCHI, N., NAGAMORI, S., KANAI, Y., OYAMA, T. & CHIKAMATSU, K. 2014. Prognostic significance of amino-acid transporter expression (LAT1, ASCT2, and xCT) in surgically resected tongue cancer. *Br J Cancer,* 110**,** 2506-13.

TRAVERSO, N., RICCIARELLI, R., NITTI, M., MARENGO, B., FURFARO, A. L., PRONZATO, M. A., MARINARI, U. M. & DOMENICOTTI, C. 2013. Role of glutathione in cancer progression and chemoresistance. *Oxid Med Cell Longev,* 2013**,** 972913.

UHLÉN, M., BJÖRLING, E., AGATON, C., SZIGYARTO, C. A., AMINI, B., ANDERSEN, E., ANDERSSON, A. C., ANGELIDOU, P., ASPLUND, A., ASPLUND, C., BERGLUND, L., BERGSTRÖM, K., BRUMER, H., CERJAN, D., EKSTRÖM, M., ELOBEID, A., ERIKSSON, C., FAGERBERG, L., FALK, R., FALL, J., FORSBERG, M., BJÖRKLUND, M. G., GUMBEL, K., HALIMI, A., HALLIN, I., HAMSTEN, C., HANSSON, M., HEDHAMMAR, M., HERCULES, G., KAMPF, C., LARSSON, K., LINDSKOG, M., LODEWYCKX, W., LUND, J., LUNDEBERG, J., MAGNUSSON, K., MALM, E., NILSSON, P., ODLING, J., OKSVOLD, P., OLSSON, I., OSTER, E., OTTOSSON, J., PAAVILAINEN, L., PERSSON, A., RIMINI, R., ROCKBERG, J., RUNESON, M., SIVERTSSON, A., SKÖLLERMO, A., STEEN, J., STENVALL, M., STERKY, F., STRÖMBERG, S., SUNDBERG, M., TEGEL, H., TOURLE, S., WAHLUND, E., WALDÉN, A., WAN, J., WERNÉRUS, H., WESTBERG, J., WESTER, K., WRETHAGEN, U., XU, L. L., HOBER, S. & PONTÉN, F. 2005. A human protein atlas for normal and cancer tissues based on antibody proteomics. *Mol Cell Proteomics,* 4**,** 1920-32.

UHLÉN, M., FAGERBERG, L., HALLSTRÖM, B. M., LINDSKOG, C., OKSVOLD, P., MARDINOGLU, A., SIVERTSSON, Å., KAMPF, C., SJÖSTEDT, E., ASPLUND, A., OLSSON, I., EDLUND, K., LUNDBERG, E., NAVANI, S., SZIGYARTO, C. A., ODEBERG, J., DJUREINOVIC, D., TAKANEN, J. O., HOBER, S., ALM, T., EDQVIST, P. H., BERLING, H., TEGEL, H., MULDER, J., ROCKBERG, J., NILSSON, P., SCHWENK, J. M., HAMSTEN, M., VON FEILITZEN, K., FORSBERG, M., PERSSON, L., JOHANSSON, F., ZWAHLEN, M., VON HEIJNE, G., NIELSEN, J. & PONTÉN, F. 2015. Proteomics. Tissue-based map of the human proteome. *Science,* 347**,** 1260419.

UHLÉN, M., OKSVOLD, P., FAGERBERG, L., LUNDBERG, E., JONASSON, K., FORSBERG, M., ZWAHLEN, M., KAMPF, C., WESTER, K., HOBER, S., WERNERUS, H., BJÖRLING, L. & PONTEN, F. 2010. Towards a knowledge-based Human Protein Atlas. *Nat Biotechnol,* 28**,** 1248-50.

UHLÉN, M., ZHANG, C., LEE, S., SJÖSTEDT, E., FAGERBERG, L., BIDKHORI, G., BENFEITAS, R., ARIF, M., LIU, Z., EDFORS, F., SANLI, K., VON FEILITZEN, K., OKSVOLD, P., LUNDBERG, E., HOBER, S., NILSSON, P., MATTSSON, J., SCHWENK, J. M., BRUNNSTRÖM, H., GLIMELIUS, B., SJÖBLOM, T., EDQVIST, P. H., DJUREINOVIC, D., MICKE, P., LINDSKOG, C., MARDINOGLU, A. & PONTEN, F. 2017. A pathology atlas of the human cancer transcriptome. *Science,* 357.

VANDER HEIDEN, M. G., CANTLEY, L. C. & THOMPSON, C. B. 2009. Understanding the Warburg effect: the metabolic requirements of cell proliferation. *Science,* 324**,** 1029-33.

VANDER HEIDEN, M. G., LOCASALE, J. W., SWANSON, K. D., SHARFI, H., HEFFRON, G. J., AMADOR-NOGUEZ, D., CHRISTOFK, H. R., WAGNER, G., RABINOWITZ, J. D., ASARA, J. M. & CANTLEY, L. C. 2010. Evidence for an alternative glycolytic pathway in rapidly proliferating cells. *Science,* 329**,** 1492-9.

VANDESOMPELE, J., DE PRETER, K., PATTYN, F., POPPE, B., VAN ROY, N., DE PAEPE, A. & SPELEMAN, F. 2002. Accurate normalization of real-time quantitative RT-PCR data by geometric averaging of multiple internal control genes. *Genome Biol,* 3**,** RESEARCH0034.

VAZQUEZ, A., LIU, J., ZHOU, Y. & OLTVAI, Z. N. 2010. Catabolic efficiency of aerobic glycolysis: the Warburg effect revisited. *BMC Syst Biol,* 4**,** 58.

VAZQUEZ, A. & OLTVAI, Z. N. 2011. Molecular crowding defines a common origin for the Warburg effect in proliferating cells and the lactate threshold in muscle physiology. *PLoS One,* 6**,** e19538.

VERMEERSCH, K. A. & STYCZYNSKI, M. P. 2013. Applications of metabolomics in cancer research. *J Carcinog,* 12**,** 9.

WANG, D. W., WU, L., CAO, Y., YANG, L., LIU, W., E, X. Q., JI, G. & BI, Z. G. 2017. A novel mechanism of mTORC1-mediated serine/glycine metabolism in osteosarcoma development. *Cell Signal,* 29**,** 107-114.

WANG, W., WU, Z., DAI, Z., YANG, Y., WANG, J. & WU, G. 2013a. Glycine metabolism in animals and humans: implications for nutrition and health. *Amino Acids,* 45**,** 463-77.

WANG, Y., ALAM, G. N., NING, Y., VISIOLI, F., DONG, Z., NÖR, J. E. & POLVERINI, P. J. 2012. The unfolded protein response induces the angiogenic switch in human tumor cells through the PERK/ATF4 pathway. *Cancer Res,* 72**,** 5396-406.

WANG, Y., NING, Y., ALAM, G. N., JANKOWSKI, B. M., DONG, Z., NÖR, J. E. & POLVERINI, P. J. 2013b. Amino acid deprivation promotes tumor angiogenesis through the GCN2/ATF4 pathway. *Neoplasia,* 15**,** 989-97.

WARBURG, O. 1956. On the origin of cancer cells. *Science,* 123**,** 309-14.

WEST, K. L., CASTELLINI, M. A., DUNCAN, M. K. & BUSTIN, M. 2004. Chromosomal proteins HMGN3a and HMGN3b regulate the expression of glycine transporter 1. *Mol Cell Biol,* 24**,** 3747-56.

WHO. Available: http://www.who.int/mediacentre/factsheets/fs297/en/ [Accessed]. January 2015

WILLARD HH, MERRITT LL & JA., D. 1965. Ultraviolet and visible absorption methods. . *In:* PRINCETON, N. (ed.) *Instrumental Methods of Analysis* D Van Norstrand.

WORTEL, I. M. N., VAN DER MEER, L. T., KILBERG, M. S. & VAN LEEUWEN, F. N. 2017. Surviving Stress: Modulation of ATF4-Mediated Stress Responses in Normal and Malignant Cells. *Trends Endocrinol Metab,* 28**,** 794-806.

WREDEN, C. C., JOHNSON, J., TRAN, C., SEAL, R. P., COPENHAGEN, D. R., REIMER, R. J. & EDWARDS, R. H. 2003. The H+-coupled electrogenic lysosomal amino acid transporter LYAAT1 localizes to the axon and plasma membrane of hippocampal neurons. *J Neurosci,* 23**,** 1265-75.

WU, G., FANG, Y. Z., YANG, S., LUPTON, J. R. & TURNER, N. D. 2004. Glutathione metabolism and its implications for health. *J Nutr,* 134**,** 489-92.

WU, X., ZHAO, L., CHEN, Z., JI, X., QIAO, X., JIN, Y. & LIU, W. 2016. FLCN Maintains the Leucine Level in Lysosome to Stimulate mTORC1. *PLoS One,* 11**,** e0157100.

WU, Y., WU, B., CHEN, R., ZHENG, Y. & HUANG, Z. 2014. High ATF5 expression is a favorable prognostic indicator in patients with hepatocellular carcinoma after hepatectomy. *Med Oncol,* 31**,** 269.

YADAV, S., KALRA, N., GANJU, L. & SINGH, M. 2017. Activator protein-1 (AP-1): a bridge between life and death in lung epithelial (A549) cells under hypoxia. *Mol Cell Biochem,* 436**,** 99-110.

YAMASHINA, S., IKEJIMA, K., RUSYN, I. & SATO, N. 2007. Glycine as a potent anti-angiogenic nutrient for tumor growth. *J Gastroenterol Hepatol,* 22 Suppl 1**,** S62-4.

YAMASHINA, S., KONNO, A., WHEELER, M. D., RUSYN, I., RUSYN, E. V., COX, A. D. & THURMAN, R. G. 2001. Endothelial cells contain a glycine-gated chloride channel. *Nutr Cancer,* 40**,** 197-204.

YANG, X. & KARSENTY, G. 2004. ATF4, the osteoblast accumulation of which is determined post-translationally, can induce osteoblast-specific gene expression in non-osteoblastic cells. *J Biol Chem,* 279**,** 47109-14.

YAO D, MACKENZIE B, MING H, VAROQUI H, ZHU H, HEDIGER MA, ERICKSON JD. 2000. A novel system A isoform mediating Na+/neutral amino acid cotransport. *J Biol Chem*. 275(30), 22790-7.

YE, J., KUMANOVA, M., HART, L. S., SLOANE, K., ZHANG, H., DE PANIS, D. N., BOBROVNIKOVA-MARJON, E., DIEHL, J. A., RON, D. & KOUMENIS, C. 2010. The GCN2-ATF4 pathway is critical for tumour cell survival and proliferation in response to nutrient deprivation. *EMBO J,* 29**,** 2082-96.

YE, J., MANCUSO, A., TONG, X., WARD, P. S., FAN, J., RABINOWITZ, J. D. & THOMPSON, C. B. 2012. Pyruvate kinase M2 promotes de novo serine synthesis to sustain mTORC1 activity and cell proliferation. *Proc Natl Acad Sci U S A,* 109**,** 6904-9.

YE, P., MIMURA, J., OKADA, T., SATO, H., LIU, T., MARUYAMA, A., OHYAMA, C. & ITOH, K. 2014. Nrf2- and ATF4-dependent upregulation of xCT modulates the sensitivity of T24 bladder carcinoma cells to proteasome inhibition. *Mol Cell Biol,* 34**,** 3421-34.

YIN, X., DEWILLE, J. W. & HAI, T. 2008. A potential dichotomous role of ATF3, an adaptive-response gene, in cancer development. *Oncogene,* 27**,** 2118-27.

ZHANG Z, GREWER C. 2007. The sodium-coupled neutral amino acid transporter SNAT2 mediates an anion leak conductance that is differentially inhibited by transported substrates. *Biophys J.*, 92(7), 2621-32.

ZHANG, W. C., SHYH-CHANG, N., YANG, H., RAI, A., UMASHANKAR, S., MA, S., SOH, B. S., SUN, L. L., TAI, B. C., NGA, M. E., BHAKOO, K. K., JAYAPAL, S. R., NICHANE, M., YU, Q., AHMED, D. A., TAN, C., SING, W. P., TAM, J., THIRUGANANAM, A., NOGHABI, M. S., PANG, Y. H., ANG, H. S., MITCHELL, W., ROBSON, P., KALDIS, P., SOO, R. A., SWARUP, S., LIM, E. H. & LIM, B. 2012. Glycine decarboxylase activity drives non-small cell lung cancer tumor-initiating cells and tumorigenesis. *Cell,* 148**,** 259-72.

ZHAO, Q., CAO, Y., WANG, Y., HU, C., HU, A., RUAN, L., BO, Q., LIU, Q., CHEN, W., TAO, F., REN, M., GE, Y., CHEN, A. & LI, L. 2014. Plasma and tissue free amino acid profiles and their concentration correlation in patients with lung cancer. *Asia Pac J Clin Nutr,* 23**,** 429-36.

ZHENG, L., ZHANG, W., ZHOU, Y., LI, F., WEI, H. & PENG, J. 2016. Recent Advances in Understanding Amino Acid Sensing Mechanisms that Regulate mTORC1. *Int J Mol Sci,* 17.

ZHOU, D., PALAM, L. R., JIANG, L., NARASIMHAN, J., STASCHKE, K. A. & WEK, R. C. 2008. Phosphorylation of eIF2 directs ATF5 translational control in response to diverse stress conditions. *J Biol Chem,* 283**,** 7064-73.

ZHU, H., CHEN, X., CHEN, B., SONG, W., SUN, D. & ZHAO, Y. 2014. Activating transcription factor 4 promotes esophageal squamous cell carcinoma invasion

and metastasis in mice and is associated with poor prognosis in human patients. *PLoS One,* 9**,** e103882.

ZONCU, R., BAR-PELED, L., EFEYAN, A., WANG, S., SANCAK, Y. & SABATINI, D. M. 2011a. mTORC1 senses lysosomal amino acids through an inside-out mechanism that requires the vacuolar H(+)-ATPase. *Science,* 334**,** 678-83.

ZONCU, R., EFEYAN, A. & SABATINI, D. M. 2011b. mTOR: from growth signal integration to cancer, diabetes and ageing. *Nat Rev Mol Cell Biol,* 12**,** 21-35.